



NATIONAL TECHNICAL UNIVERSITY OF ATHENS

School of Mechanical Engineering

Manufacturing Technology Section

Diploma Thesis

Design and Simulation of a Flexible Robotic System for Biotechnology Experiment Production

Angelidou Charikleia

Supervisors

G. - C. Vosniakos

Professor, NTUA

P. Benardos

Assistant Professor, NTUA

Athens, October 2019

“The best preparation for tomorrow is doing your best today”

H. Jackson Brown Jr, (b. 1941)

ACKNOWLEDGEMENTS

This project and the work that came with it wouldn't have been realized without the support and guidance of many great people.

First of all I would like to thank professor Georgios C. Vosniakos for giving me the opportunity to be part of his team and for turning this experience into more than a simple academic project. Having been given the chance to collaborate directly with the industry, I acquired valuable knowledge and skills. The interest and trust from his behalf have been major factors towards the completion of this diploma thesis. His advisory and guidance meant a lot for me and I highly appreciate it.

Moreover, I am grateful to have met and worked with assistant professor Panorios Benardos, who was always keen on helping me overcome the difficulties that I encountered throughout the project. His drive and his fresh view of things were very pleasant and enlightening.

I would also like to address a sincere thank you towards the people of *experoment*, a team of young innovators, for trusting me with a project of their start-up and especially thank Imperial College PhD candidate Francesco Cursi, for devoting his time to helping, advising and supporting me throughout my work, even though he was not obliged to.

Beside the people in academia, I would like to wholeheartedly thank my friends who have always been supportive and helpful in their own unique way. I wouldn't have been the person I am without them.

Finally, I would like to express my gratitude to my parents for always believing in me and for providing me with their valuable support and love throughout my studies, as well as to my siblings, who are always there for me, even though distance keeps us apart, and to whom I want to dedicate this diploma thesis.

ABSTRACT

The intent to accelerate scientific research on biotechnology has been increasing for the last few decades drastically. Investing in novel ways of advancing this sector, utilizing the most up-to-date technological equipment, has therefore been in the center of attention. This is why researchers and companies have started directing their attention towards automation and its branches. Robotic cloud biotechnology laboratories constitute one of these branches, which aim is to change the way research is done, dramatically offsetting the ever-increasing costs of clinical trials, automating tedious lab work, and accelerating research by running experiments in parallel, by making scientific testing efficient and programmable for all. An overview of the design and function of such a robotic system is the central theme of the current project.

In the current thesis, studied are the methodology and tools for developing the virtual equivalent of a real biotechnology laboratory for pharmaceutical experiments. Specifically, a SCARA type robot, the Stäubli TX2-90XL robotic arm, as well as the lab environment, are modeled using the 3D application development software VREP by Coppelia Robotics. The goal is to investigate the offline programming of the arm in a virtual reality environment, as well as to fully design a suitable lab layout that can be extrapolated on real-life laboratory settings.

As part of the design process, introduced are the components for the creation of the laboratory set up, including equipment and consumables. Different laboratory layouts are then created and compared, concluding to two specific set ups that are finally simulated.

For the modeling and simulation, the robot models are introduced and their respective kinematic chains are developed. The forward and inverse kinematics of the arm are analyzed and developed in Matlab, using different approaches and inverse algorithm methods such as inverse and pseudo-inverse Jacobian, as well as the Damped Least Squares Method. The trajectory of both robotic arms is planned so as to create a motion plan that can be used for any experiment within the laboratory set ups. Additionally, a User Interface (UI) is created for the communication of the experiment protocols between the researcher and the robotic arms. Finally, two experiments are simulated for both robots and layouts.

Table of Contents

1	INTRODUCTION	1
1.1	What is a Robotic Biotechnology Cloud Lab?.....	1
1.2	Digital Factory Technologies.....	2
1.3	Efforts towards automated biotechnology labs.....	3
1.3.1	Existent Robotic Cloud Platforms.....	3
1.4	Objectives and Goals of the Thesis Project.....	4
2	V-REP AND MATLAB INTERFACING	6
2.1	Virtual Robot Experimentation Platform (V-REP).....	6
2.1.1	Scene Object Types and Properties.....	6
2.1.2	Coordinate Systems.....	8
2.1.3	3D Model Import and Neutral File Formats.....	10
2.2	Communication between MATLAB and the V-REP platform.....	11
2.3	Enabling the remote API.....	12
2.3.1	Client side activation.....	13
2.3.2	Server side activation.....	15
2.3.3	Basic Remote-API functions for MATLAB client.....	16
3	THE ROBOTS	17
3.1	The custom SCARA robot of Experiment.....	17
3.1.1	Description.....	17
3.1.2	Advantages and limitations of SCARA robots.....	19
3.2	Stäubli TX2-90XL.....	19
3.2.1	Description.....	19
3.2.2	Advantages and limitations of 6-axis robots.....	21
3.3	Robot 3D Model Import.....	21
3.3.1	Unified Robot Description Format (URDF).....	22
3.3.2	Robot Coordinate Systems.....	23
3.3.3	Scaling Factor.....	24
3.3.4	URDF and MATLAB Robotics Toolbox.....	24
3.4	Gripper Choice.....	25
3.4.1	Parallel Grippers.....	26
4	LABORATORY EQUIPMENT	28
4.1	Machines.....	28

4.1.1	Liquid Handler	28
4.1.2	Centrifuge	29
4.1.3	Freezer	29
4.1.4	Incubator	30
4.1.5	Plate Reader	30
4.2	Consumables.....	31
5	LABORATORY STRUCTURE AND LAYOUTS	32
5.1	Flexible Manufacturing Systems (FMS).....	32
5.2	Production line layouts for FMS.....	32
5.2.1	Linear layout	33
5.2.2	Island (or Circular) Layout	33
5.2.3	Vertical Ladder Layout.....	34
5.3	Laboratory Structure.....	35
6	KINEMATIC ANALYSIS OF MANIPULATORS.....	39
6.1	Introduction.....	39
6.2	Kinematics.....	39
6.2.1	Forward Kinematics	40
6.2.2	Joint Space and Operational Space	41
6.2.3	Inverse Kinematics.....	42
6.3	Differential Kinematics.....	42
6.3.1	Geometric Jacobian	43
6.3.2	Inverse Differential Kinematics.....	44
6.3.3	Kinematic Singularities	44
6.4	Inverse Kinematics Algorithms.....	45
6.4.1	Inverse Jacobian	45
6.4.2	Pseudo-Inverse Jacobian	46
6.4.3	Damped Least Squares (DLS).....	46
6.5	Trajectory Planning.....	47
6.6	Implementation on Robotic Manipulators.....	50
7	SIMULATION	55
7.1	Visual Simulation Models.....	55
7.1.1	Robots.....	55
7.1.2	Lab Equipment.....	56
7.1.3	Safe Positions.....	57
7.1.4	Parameterization of the simulation.....	57
7.2	Experiment Protocols.....	58

7.3	User Interface (UI).....	59
7.4	Simulation of Experiment with SCARA and STAUBLI.....	60
7.4.1	SCARA	60
7.4.2	STAUBLI TX2-90XL.....	62
7.5	Collision Detection.....	64
8	RESULTS	66
8.1	General Remarks.....	66
8.2	SCARA.....	67
8.3	STAUBLI RX-90.....	74
9	CONCLUSIONS AND FUTURE WORK	78
9.1	Contribution.....	78
9.2	Advantages of virtual environments.....	78
9.3	Suggestions for future development.....	79
10	BIBLIOGRAPHY	80
	APPENDIX	82
	A URDF Template[22].....	- 1 -
	B TECHNICAL SPECIFICATIONS OF EQUIPMENT AND CONSUMABLES	- 6 -
	C MATLAB CODE.....	- 13 -
	SCARA FILES	- 13 -
	STAUBLI FILES	- 42 -

Figure Inventory

Figure 1: Section of web page of the experoment platform.....	4
Figure 2: Clockwise coordinate system	9
Figure 3: V-REP communication framework[8].....	11
Figure 4: Remote API functionality overview[8]	12
Figure 5: MATLAB code for establishing and terminating communication with V-REP platform	14
Figure 6: LUA code for server-side activation	15
Figure 7: Workspace of SCARA type robot.....	18
Figure 8: Stäubli TX2-90XL Robot	19
Figure 9: Working space of Staubli TX2-90XL <small>[Source: Staubli]</small>	20
Figure 10: Different mounting positions for Staubli TX2-90XL	21
Figure 11: Link and joint representation	22
Figure 12: Matlab code for importing URDF file	24
Figure 13: Details for SCARA robot	25
Figure 14: Details for Staubli TX2-90XL	25
Figure 15: Cell-carrier 96 on the left and Cell-carrier 384 on the right.....	31
Figure 16: Linear layout for production	33
Figure 17: Island (or circular) layout for production	34
Figure 18: Vertical Ladder layout for production.....	35
Figure 19: Conventional representations of joints[17]	40
Figure 20: Description of the position and orientation of the end-effector frame[17].....	40
Figure 21: Calculation of Homogenous Transform T with Matlab Robotics Toolbox	50
Figure 22: Calculation of Geometric Jacobian with Matlab Robotics Toolbox	52
Figure 23: Calculation of damping factor λ with SVD.....	52
Figure 24: Quadrating programming and solving of Inverse Kinematics with Matlab Robotics Toolbox	53
Figure 25: Validation flowchart of kinematic model[21]	54
Figure 26: Robotic manager architecture	54
Figure 27: Experiment protocol examples	58
Figure 28: User interface flowchart	60

Table Inventory

Table 1: Enabling the remote API-client side, Matlab documentation for simxStart function.	14
Table 2: Enabling the remote API-client side, Matlab documentation for simxFinish function	15
Table 3: Enabling the remote API –server side, LUA documentation for simRemoteApi.start function	15
Table 4: Translational Joint Limits of the SCARA type robot.....	18
Table 5: Rotary Joint Limits of the SCARA type robot.....	18
Table 6: Joint Limits of the Stäubli TX90XL.....	20

Diagram Inventory

Diagram 1: EE position of SCARA with FK- Home to Safe Position	67
Diagram 2: Joint angles of SCARA with FK-Home to Safe Position	67
Diagram 3: Joint velocities of SCARA with FK- Home to Safe Position	67
Diagram 4: Desired vs Actual EE position of SCARA during IK- Safe to Input Position	68
Diagram 5: Joint angles of SCARA during IK- Safe to Input Position	68
Diagram 6: Desired vs Actual EE velocity of SCARA during IK- Safe to Input Position	68
Diagram 7: Desired vs Actual EE position of SCARA during IK- Home to Safe Position	69
Diagram 8: Joint angles of SCARA during IK- Home to Safe Position	69
Diagram 9: EE velocity of SCARA during IK- Home to Safe Position	69
Diagram 10: Desired vs Actual EE position of SCARA during IK- Safe Position to Plate	70
Diagram 11: Joint angles of SCARA during IK- Safe position to Plate	70
Diagram 12: Desired vs Actual EE velocity of SCARA during IK- Safe position to Plate	70
Diagram 13: Desired vs Actual EE position of SCARA during IK – Machine to Machine	71
Diagram 14: Joint angles of SCARA during IK- Machine to Machine	71
Diagram 15: Desired vs Actual EE velocity of SCARA during IK- Machine to Machine	71
Diagram 16: EE position of SCARA with FK- Home to Safe Position	72
Diagram 17: Joint angles of SCARA with FK- Home to Safe Position	72
Diagram 18: Joint velocities of SCARA with FK- Home to Safe Position	72
Diagram 19: Desired vs Actual EE position of SCARA during IK - Safe to Output Position	73
Diagram 20: Joint angles of SCARA during IK- Safe to Output Position	73
Diagram 21: Desired vs Actual EE velocity of SCARA during IK- Safe to Output Position	73
Diagram 22: Desired vs Actual EE position of STAUBLI during IK- Home to Input Position	74
Diagram 23: Joint angles of STAUBLI during IK - Home to Input Position	74

Diagram 24: Desired vs Actual EE velocity of STAUBLI during IK- Home to Input Position	74
Diagram 25: Desired vs Actual EE position of STAUBLI during IK- Home to Machine	75
Diagram 26: Joint angles of STAUBLI during IK- Home to Machine	75
Diagram 27: Desired vs Actual EE velocity of SCARA during IK- Home to Machine.....	75
Diagram 28: EE position of STAUBLI with FK- Machine to Home	76
Diagram 29: Joint angles of STAUBLI with FK- Machine to Home	76
Diagram 30: Joint velocities of STAUBLI with FK- Machine to Home	76
Diagram 31: Desired vs Actual EE position of STAUBLI during IK- Home to Output Position.	77
Diagram 32: Joint angles of STAUBLI during IK- Home to Output Position	77
Diagram 33: Desired vs Actual EE velocity for STAUBLI- Home to Output Position	77

1

INTRODUCTION

1.1 What is a Robotic Biotechnology Cloud Lab?

When we think of automation and productivity improvements, industrial robots are the first things to come into our mind. But there is much more to it. Most researchers, both in academia and industry, are still using handwritten lab notes and Excel spreadsheets to record their findings. For many of these labs entering into the 21st century of automation, sensors and Internet of Things (IoT) is nearly impossible without major financial investment for hiring expert staff and buying equipment.

One of the most 'hot' and developing, to this respect, sectors is biotechnology. However, innovation in biotechnology is hindered by the lack of two major factors. The first is reproducibility. Most of the experiments in scientific publications are difficult to reproduce. The second is accessibility. Very few people have access to the equipment or capital required to start a lab. Even if someone does, it can take many months or even years of research before having even a single product in the pipeline.

The main concept hidden behind a robotic biotechnology cloud lab, is an API-driven (Application Programming Interface) and robot-operated molecular and cell biology research facility. It's use? Letting scientists manage a fully-fledged biotech facility automatically and remotely. The drudge work of pipetting and transferring liquids between machines is automated, with robotic arms having the primer role in fulfilling experiments with little human intervention. Clients submit work orders via a user interface or an API call, and receive data feedback at each step of the experiment. The underlying idea is that many experiments in biology use the same basic operations on different material and in a different sequence. A typical experiment involves centrifugation, plate reading and a small number of other operations that can be handled in sequence and be fully automated.[1]

The aim is to change the way research is done, dramatically offsetting the ever-increasing costs of clinical trials, automating tedious lab work, and accelerating research by running experiments in parallel. In particular, this novel approach opens up the possibility of cheaply and efficiently reproducing past scientific experiments, which is a perplexing problem in the field. It also promises to drastically reduce the time and cost of getting new pharmaceutical drugs on the market. More specifically, the number of new drugs being approved per billion dollars of money spent is decreasing, as much as by half every nine years. The inefficiency of research and development ensures that drug development remains the polity of the big, multinational corporations and that most life-saving drugs remain unaffordable for the

majority of people in the world. [2] This is why the current drug development model needs to give way to a more democratic approach — and why the cloud and open source models hold so much promise. Cloud labs remove the requirement of large capital expenditures from the drug development process and in doing so enable a wider swath of people to design and test new scientific ideas.

It will also likely change the way scientists plan experiments, since with human-operated science, every additional step in a lab process incurs exponential cost and increases the likelihood of human error and deviance from the protocol, something which is prevented by a fully automatized approach.

In other words, there are multiple advantages to cloud labs, remote, real-time access being just one of them. The labs allow researchers to more easily reproduce results. They make documentation and standardization of the experimental process easier. Researchers can more efficiently analyze knowledge from all experiments stored on the cloud. All of this can translate to massively increased productivity.

1.2 Digital Factory Technologies

Industry 4.0 is focused on the adoption of new computing and Internet-based technologies, including internet of things, cyber-physical systems, cloud manufacturing, digital/virtual reality, etc., as Key Enabling Technologies to meet new challenges.[3], [4] The main features of Industry 4.0 include interoperability, decentralisation, real-time capability, service orientation and virtualisation, i.e. linking real factory data with virtual plant models and simulation models to create a virtual copy of the Smart Factory. Its purpose is to lead to increased flexibility in production, e.g. via the use of configurable robots and machineries that may produce a variety of different products, mass customisation, e.g. allowing the production even of small lots adapted to customer specifications due the ability to rapidly configure machines, process speed up, since digital design and virtual modelling of manufacturing processes and systems can reduce time between design and start of production, allowing to substantially decrease the time needed to deliver orders and the time to get products to market. [5]

Accordingly, the fourth industrial revolution is not only represented by Internet-enabled interaction between machines, robot, computer, and data, but also by the increased use of digital manufacturing and software tools, allowing for the digital representation of the real production environment, including all levels from the entire production plant, a single machine, a specific process or operation or just the design and the development of new products. [6] In this framework, Digital Factory technologies, based on the employment of digital methods and tools, such as numerical simulation, 3D modelling and Virtual Reality to examine a complex manufacturing system and evaluate different configurations for optimal decision-making with a relatively low cost and fast analysis instrument, are an essential part of the continuous effort towards the reduction in a product's development time and cost, as well as towards the increase in customization options. [4], [7] Simulation-based technologies are central in the Digital Factory approach, since they allow for the experimentation and validation of different product, process and manufacturing system configurations [8]

The shared digital data and models within the Smart Factory should be adaptive, in the sense that they should always represent the current status of the physical manufacturing system. For this reason, they should be regularly updated with information coming from the physical manufacturing system as well as based on user input. As the models are updated and valid, they can be effectively used to carry out decision-making through the employment of valid optimization methods. A fundamental issue is therefore represented by the adaptation of shared data and models realizing a tight coupling between the physical and the digital world.[4]

In this respect, the importance of developing cutting-edge production methods for pharmaceuticals utilizing the digital factory technologies is evident. Start-up companies, among others, may be the biggest beneficiaries of these technologies, since the costs and the risk in building, in our case, a biotechnology laboratory, are minimized thanks to simulation-based technologies, on which the current project is also heavily dependent on.

1.3 Efforts towards automated biotechnology labs

Most pharma and biotech companies, and in part also academic labs, have automated sections of their processes and make use of liquid-handling systems, especially those pursuing high-throughput screenings, while the first laboratory science application programming interfaces (APIs) are already available. Science-as-a-Service (SciAAS) companies have started popping up, with the intent to accelerate scientific research and improvements in biotechnology. By letting researchers outsource the expensive work of conducting experiments, teams save time and money without compromising the quality of scientific research, thus reducing the barrier to entry for biotech startups. Making scientific testing efficient and programmable will enable anyone with the needs and ideas, but lacking the resources to turn their experiments into a reality.

Currently common experimental protocols like Polymerase Chain Reaction (PCR) for genotyping animal samples, DNA/RNA synthesis, and protein extraction are offered. More complex or custom experiments are still better delegated to a Contract Research Organization (CRO), but in the future all experiments may be conducted in this way. APIs will liberate researchers from compromises, such as human error and lack of reproducibility, and will lead to many more experiments.

1.3.1 Existent Robotic Cloud Platforms

The self-proclaimed first robotic cloud lab for on-demand life science research was developed by a start-up company called *Transcriptic*. Founded in 2012, and backed by Google Ventures and the founders behind Pay Pal, the company now numbers 40 people and occupies a 22,000 square-foot facility in the heart of Silicon Valley. The company builds and manages Plexiglas-enclosed robotic biology labs, or “workcells” that house about 20 devices each, including pipetting systems. The workcells are operated by computers, which receive experiment work orders and run the assemblage of machines. A robot on a gantry runs the length of the workcell, transferring plates from machine to machine to carry out the experiments. [Source:

[Transcriptic](#)]

A platform that has recently also emerged is *Arctoris*. The Arctoris cloud lab specializes in the automation of cell-based and biochemical experiments, with an emphasis on complex in vitro models, augmented by machine learning-driven analytics. The start-up company aims mostly at fundamental biology, target identification and validation, toxicology, phenotypic screening and compound profiling for drug discovery and preclinical R&D. [Source: [Arctoris](#)]

Various efforts towards this respect have been made, among which also the effort of the start-up *experoment*, in collaboration with which this project has been completed and which aims mainly at immuno-oncology experiments, some of which will be recreated and virtually simulated for the purposes of the current thesis.

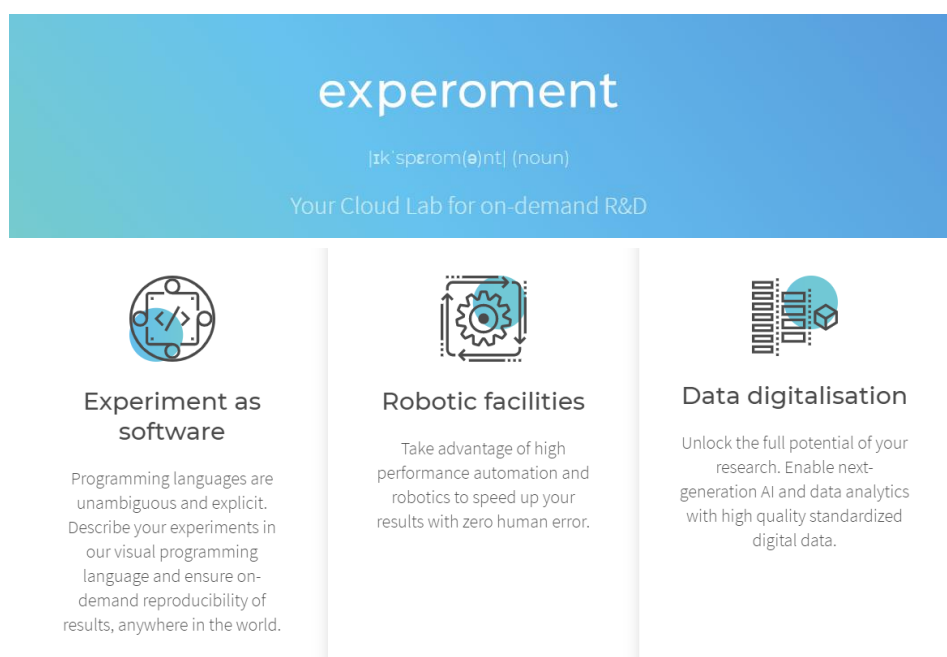


Figure 1: Section of web page of the experoment platform

1.4 Objectives and Goals of the Thesis Project

The subject of the current research is the trajectory planning and remote operation of a robotic arm in a biotechnology laboratory, using a virtual simulation environment, and also the design of a Flexible Manufacturing System (FMS), which can alternatively be characterized as a Flexible Experiment Production System (FEPS), aiming at introducing new items with a low overhead and increasing productivity of the cell. The system should be able to process any mix of experiments or continuous batches of experiments at any time window.

The technology studied consists of a software interface connecting hardware and wetware in a robotic biotechnology laboratory to automate simple workflows of experimentation. It allows a researcher to build a protocol and then communicate it to their lab equipment. Researchers can access it through a cloud platform in order to remotely execute experiments without the need of physical access to the laboratory. The user selects the experiment to execute from the designed platform and has the freedom to change a few parameters, with

respect to the experiments that are to be conducted. The experiments can be categorized into:

- I. pre-optimized experiments and
- II. custom-designed experiments

Researchers describe their experiment parameters in a user-friendly visual language and then the plan is uploaded in the remote wet lab, offering execution transparency as researchers have continuous remote supervision, while the user can download the results of the experiments after their finalization.

Specifically, in the frameworks of this study, attempted is:

- Modeling of a custom SCARA type robotic arm and of the robotic arm Stäubli TX2-90XL, as well as the environment of the wet lab, using the Virtual Robot Experimentation Platform (V-REP).
- Development of the kinematic chain between the links of the robots and of their inverse kinematics.
- Programming of the robot's trajectory for tending each of the instruments and for linking them, too.
- Choice of mechanical interfaces between the robots and the instruments and their entry into the simulation model.
- Simulating experiments and assessing the behavior of the robots in different laboratory settings.

The goals of the above mentioned study are:

- Simplification of the robot's trajectory scheduling task, if the operator controls the end-effector point and the values of the joint angles are derived from the inverse kinematics.
- Reducing errors in physical production, as errors in a virtual environment do not have physical consequences and can be corrected, saving time and preventing machine damage or costly failures during production.
- Ability to monitor and modify the operation of the robotic arm without an individual required in the robot space. The latter eliminates the possibility of injury to the human factor by moving mechanical parts.
- Offering a low cost alternative to impedance control or visual servoing of the robot or to expensive high-accuracy robots, especially since in this case all consumable items are moved between known, predefined positions and orientations and the robotic arm is responsible of transferring pre-defined in shape and size objects from one workstation to another.

2

V-REP AND MATLAB INTERFACING

2.1 Virtual Robot Experimentation Platform (V-REP)

Used in the current study is the Virtual Robot Experimentation Platform (V-REP), a physical simulator which provides an easy and intuitive environment to create your own virtual platform and to include robots, objects, structures, actuators and sensors.

Virtual Robot Experimental Platform (V-REP) is the product of Coppelia Robotics that was developed for general purpose robot simulation. A customized user interface and a modular structure integrated development environment are the main characteristics of the simulator. Modularity is in high level both for the simulation objects and control methods. The easy development of a custom environment inside the simulator provides the user with the ability to create various different simulation cases. This feature can be used in cases of fast prototyping, algorithm design and implementation. During simulation, this area acts as real 3D world and gives real time feedback according to the behavior of models. The objects that compose the scene, the control mechanism and the computing modules are the three main functionalities of the simulator.

2.1.1 Scene Object Types and Properties

The function of V-REP is based on the philosophy of the existence of a "scene", in which there are objects that are either independent of each other, or are linked to each other by parent-child relationships, have specific behaviors and interact with each other in various ways. These objects are called Scene Objects. The following object types compose the V-REP simulation scene or model:

- Shapes: Shapes are triangular faced rigid mesh objects. These objects can be used in collision detections against other collidable objects and minimum distance calculations with other measurable objects. Shapes can also be detected by proximity.
- Joints: Joints are used for building mechanisms and moving objects, which have at least one Degree of Freedom (DOF). There are three types of joints: revolute, prismatic and spherical.

- Proximity sensors: From ultrasonic to infrared nearly all type of proximity sensors can be modeled to simulate proximity sensors. They do an exact distance calculation between their sensing point and any detectable entity that interferes with their detection volume.
- Vision sensors: They will render all renderable objects in simulation scene (colors, objects sizes, depth maps, etc.) and extract complex image information. Built-in filters and image processing functions ease the use of vision sensors in simulation.
- Force sensors: Force sensors are objects that measure transmitted force and torque values between two or more objects. The force sensor working principle can be modeled as in reality, so that they can even break in overshoot force and torque values.
- Graphs: Graphs are objects for recording, visualizing and exporting data from a simulation.
- Cameras: Cameras are objects that can monitor the simulation from different viewpoints. There is the ability to add multi view windows in one view window or attach each view to separate windows.
- Lights: Lights are the objects that light the simulation scene and directly influence camera and vision sensors.
- Paths: Paths are objects that define a rotational, translational or combined path or trajectory in space.
- Dummies: A dummy is a type of object that can be defined as a reference frame or point of orientation attached to the object. They are useful especially for path-trajectory planning and following a specific path. Dummies are generally defined as a multipurpose helper object in combination with other objects. It must be noticed that alone they are not so useful.

The behavior of each Scene Object in the scene depends on its Properties, the simplest of which are Object/Item Shift for translating the object to a different position and Object/Item Rotate for rotating the object and changing its orientation. These changes in position and orientation of the objects can take place with respect to the world, parent or own frame that will be analyzed in following chapters.

Some of above objects can have special properties allowing other objects or calculation modules to interact with them. Objects can be:

- Collidable: Collidable objects can be tested for collision against other collidable objects.
- Measurable: measurable objects can have the minimum distance between them and other measurable objects calculated.
- Detectable: detectable objects can be detected by proximity sensors.
- Renderable: Renderable objects can be seen or detected by vision sensors.

- **Viewable:** viewable objects can be looked through, looked at, or their image content can be visualized in views.

The combination of above described scene objects allow the creation of complex sensors and complex models of manipulators and many different types of robots. There is a wide, fully customizable sensor and robot model library in the V-REP environment that can be easily dragged and added to the scene. Additionally, the library offers an amplitude of models that can be used as surroundings for the simulation environment, such as furniture, obstacles, rendered sceneries etc.

Previously there was a reference for parent-child relationships between Scene Objects. Firstly, it is to notice that any object within the created scene appears on the left tab of the project called Scene Hierarchy. The hierarchy is like a tree, representing the relationships between the different objects of the Scene. Let's see how the hierarchy in V-REP works by looking at the example of **Image 1**. The image shows part of the horizontal configuration of the lab that will be assessed in the following chapters. It represents the frame on which the lab machines will be located and in this particular image, there is only one machine, the centrifuge. As shown in the Hierarchy, the Centrifuge and its components are children of the "FRAME" parent. The Scene Object "FRAME" in this case is the metallic base on which the centrifuge is located, meaning that changes in the position and orientation of the "FRAME" will influence the children as well.

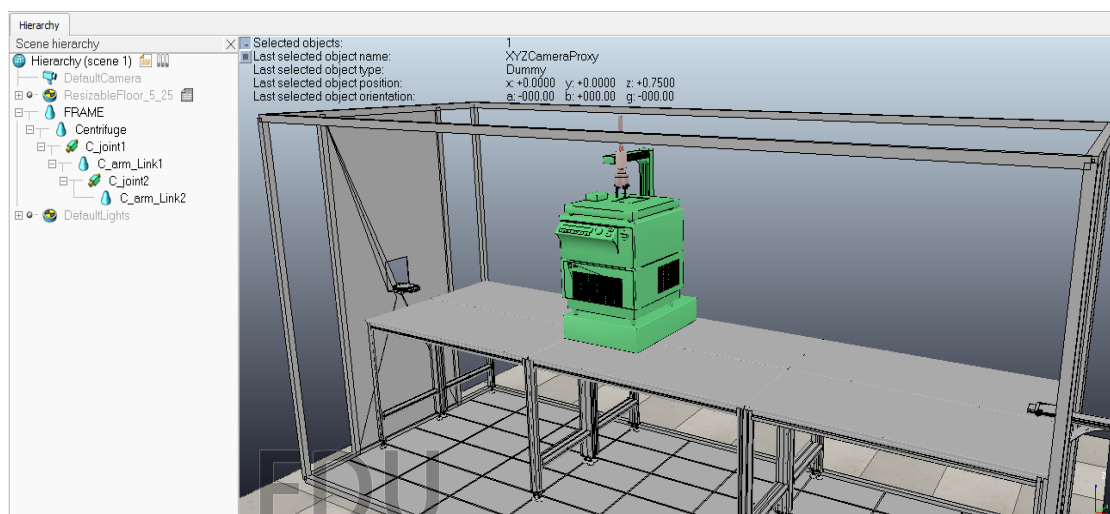


Image 1: Scene Hierarchy inside of V-REP

The user has of course the ability to modify each object individually, even if it is the child of another object. However, in case that the user wants to modify the parent, for example to resize or move him, his children will be enlarged or moved accordingly, without changing the relative size or relative position of the parent-child. That is, there is the concept of inheritance that dominates object-oriented programming.

2.1.2 Coordinate Systems

The coordinate systems used by V-REP are two, the World and the Parent frames, which are clockwise, meaning that they follow the rule of the right hand that is depicted in **Figure 2**.

The world frame $[x, y, z] = [0, 0, 0]$ position is its origin in V-REP. Any movement of an object along the three axes is measured with respect to this point. If we wish to move an object at the origin of the world frame, all of the position values with respect to the "World" should be set to zero. In order to better monitor movements and rotations, the axes of the global coordinate system (world frame) always appear in the lower right corner of the screen. Color coding is set accordingly to R (Red), G (Green), B (Blue) \rightarrow X, Y, Z and is used to facilitate the recognition of the axes.

The local coordinate system, referring to the parent, shows the position and rotation of an object with respect to its parent's coordinate system respectively.

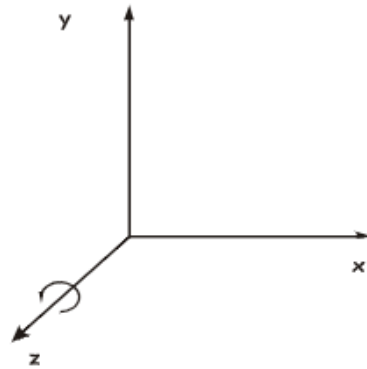


Figure 2: Clockwise coordinate system

If the user wishes to translate or rotate an object in the simulation scene, an additional option is given, specifically the option to move the object with respect to its own frame, meaning that the object does not take into consideration the position or orientation of the world frame or of the parent frame of the object, but rather it is handled as a solo standing entity in the simulation scene. To better understand the way that the local reference frame works, **Image 2** and **Image 3** are attached.

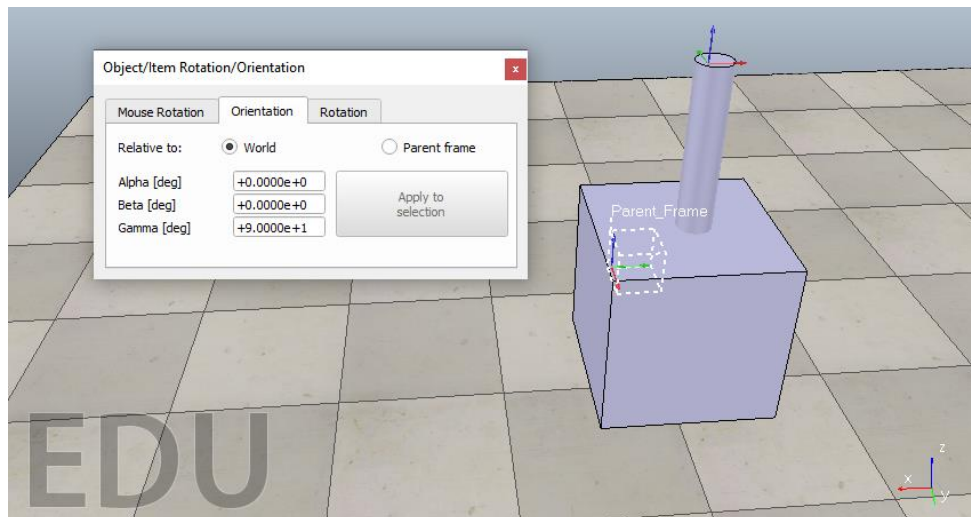


Image 2: Orientation of Parent_Frame with respect to the World Frame

In **Image 2** the cylinder is child of the cube. Comparing the cube coordinate system (Parent_Frame) with the global coordinate system of VREP, we observe a 90° rotation around the Z axis, which is also written in the orientation window of the cube.

Looking now at the cylinder coordinate system (Child_Frame) in **Image 3**, we observe a rotation of 180° around the Z axis of the global frame, but the orientation window shows a rotation of 90° . This is because the cylinder has rotated 90° with respect to its parent, but has also adopted the rotation of the cube to the global system. Therefore, in its sum, the rotation of the Child_Frame with respect to the World coordinate system equals 180° .

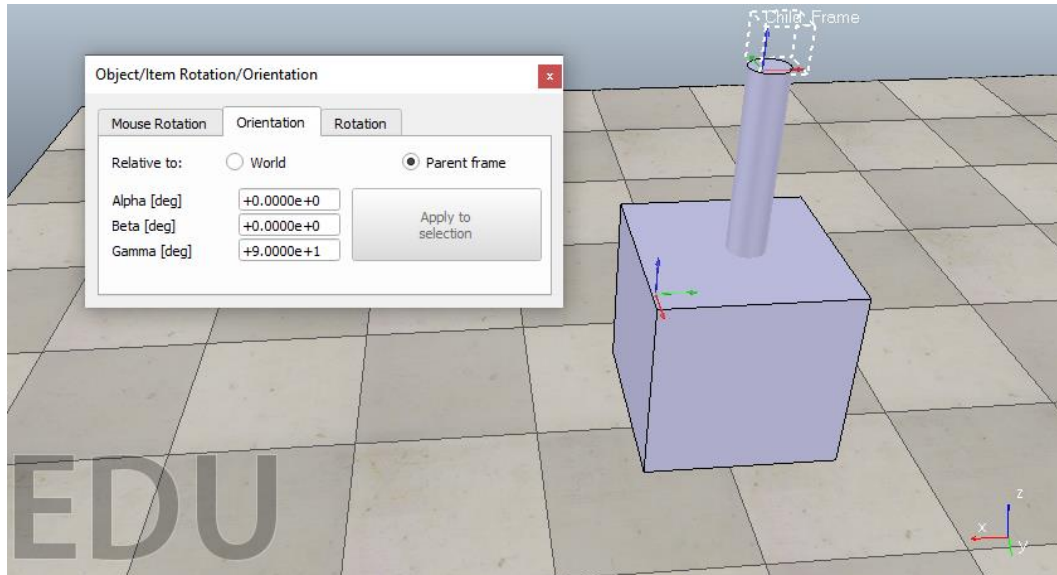


Image 3: Orientation of the Child_Frame with respect to its Parent Frame

2.1.3 3D Model Import and Neutral File Formats

Computer Aided Design (CAD) technology for engineering, and manufacturing is now playing an increasingly important role in production industry. The importance of this technology to increase productivity in engineering design has been widely recognized. These technologies make it possible to shorten the time and lower the cost of development. Additionally, the reliability and the quality of the product can be improved. CAD systems have therefore been used in various fields of industry including automobile and aircraft manufacture, architecture and shipbuilding, and there are currently many commercial systems available. SolidWorks, Catia and Inventor are examples of available systems using CAD technology. With the existence of a great diversity of CAD tools emerge the demand to import/export files between different CAD software. The emergence of neutral format files and neutral format file interfaces in order to exchange product data between CAD systems solve this problem. The most widely accepted formats have been the Initial Graphics Exchange Standard (IGES), the Standard d'Echange et de Transfert (SET), the STandard for the Exchange of Product model data (STEP) and the Standard Transform Language (STL).[9]

The simulator V-REP does offer some basic geometrical shapes, as mentioned previously, that can be used to model basic objects and structures. Yet, to model more difficult geometries, these basic 3D Objects the software offers are not sufficient and are rather time consuming if used for this case. V-REP therefore provides the ability to import 3D models from other design programs. V-REP uses triangular meshes to describe and display shapes and for this reason it only imports formats that describe objects as triangular meshes. If however importing objects

described as parametric surfaces for example (e.g. IGES, etc.) is desired, then first conversion of the file to an appropriate triangular mesh format should be done. V-REP supports following file-formats for shape import ([Menu bar --> File --> Import --> Mesh...]):

- OBJ: Wavefront Technologies file format. This is currently the only format that allows importing of textured meshes in V-REP.
- DXF: AutoCAD file format (Autodesk). Non-3D information that might be contained in the file is ignored.
- STL (ASCII or binary): 3D Systems file format. ASCII and binary files are supported.
- COLLADA
- URDF

2.2 Communication between MATLAB and the V-REP platform

Concerning the control of the behavior of the simulation objects, there is a wide range of mechanisms used for this purpose, which characterize the V-REP framework that is schematically presented in **Figure 3**. These controllers can be implemented not only inside of the simulation environment, but also outside of it.

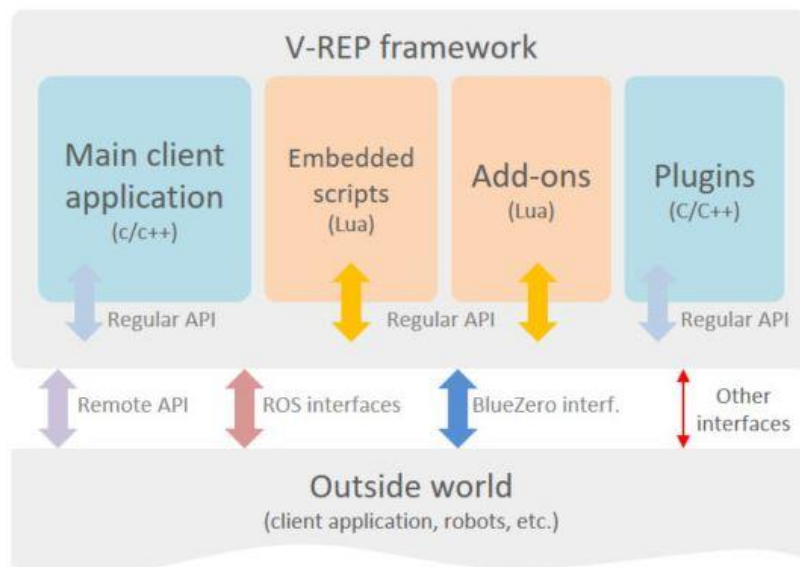


Figure 3: V-REP communication framework[10]

The main internal control mechanism is the use of child scripts, which can be associated with any element in the scene. The child scripts handle a specific part of the simulation and they are an integral part of their associated object. Due to that property they can be duplicated and serialized, together with them. Therefore, they are a single package containing the model parameters together with its control which makes them portable and scalable. Child scripts have two execution modes. Non-threaded child scripts are pass-through scripts which means every time they are called they execute some task and then return to control. Threaded child scripts launch in thread and are handled by the main script code. The latter require more advanced programming knowledge compared to non-threaded child scripts, while they take

up more processing power and time, causing lagging in response to simulation commands. The main script handles both threaded and non-threaded child scripts. These embedded scripts open and handle communication lines, start remote API servers, launch executables, load and unload plugins.

V-REP also offers a method to control the simulation from outside the simulator by externally applied controller algorithms. The remote API interface in V-REP communicates with the simulation scene using socket communication. It is composed by remote API server services and remote API clients. The client side can be developed in C/C++, Python, Java, Matlab or other languages, also embedded in any software running on remote control hardware or real robots, and it allows remote function calling, as well as fast and bidirectional data streaming. Functions support two calling methods to adapt to any configuration: blocking, waiting until the server replies, or non-blocking, reading streamed commands from a buffer.

On the client side, which is the application the user is running, at least 2 threads will be running: the main thread -the one from which remote API functions are called-, and the communication thread -the one that is handling data transfers behind the scenes. There can be as many communication threads as needed on the client side. The server side, which is implemented with a V-REP plugin, operates in a similar way. **Figure 4** illustrates the remote API modus operandi.

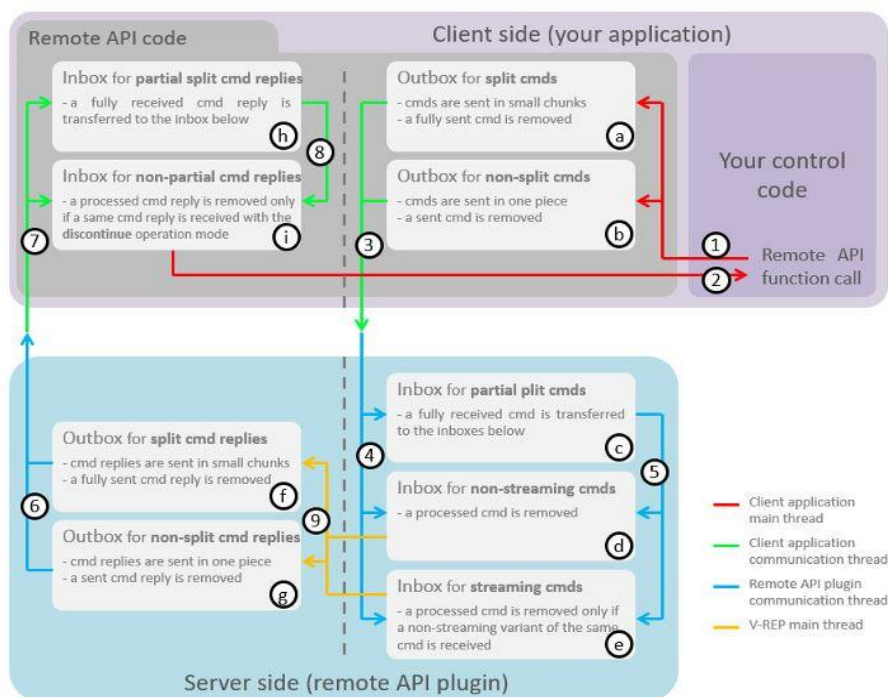


Figure 4: Remote API functionality overview[10]

2.3 Enabling the remote API

To enable the remote API on the server side, in other words on V-REP's side, the remote API plugin must be successfully loaded at V-REP start-up. The remote API plugin can start as many server services as needed and each service will be listening/communicating on a different port. A server service can be started in two different ways:

1. At V-REP start-up (**continuous remote API server service**). The remote API plugin will try reading a configuration file named *remoteApiConnections.txt* and according to its content, start appropriate server services. With this method remote API functions will always be executed on the server side, even if simulation is not running, which is not always the case with next method.
2. From within a script (**temporary remote API server service**). This is most of the time the preferred method of starting a remote API server service. The user is in control when the service is started or stopped. When a temporary remote API server service is started from a simulation script however, the service will automatically be stopped at simulation end. A temporary remote API server service can be started with custom Lua function: *simRemoteApi.start*.

2.3.1 Client side activation

For the needs of the current project, the interface used is this of the remote API and the client side is developed in Matlab. To use the remote API functionality in the Matlab program, Matlab must use the same bit-architecture as the remoteApi library, as 64bit Matlab with 32bit remoteApi library will not work, and vice-versa, and also following 3 items, which are located in V-REP's installation directory, under *programming/remoteApiBindings/matlab*, are needed:

- remoteApiProto.m
- remApi.m
- remoteApi.dll, remoteApi.dylib or remoteApi.so (depending on the target platform)

In order to initiate the desired application, *vrep=remApi ('remoteApi')* is used to build the object and load the library via Matlab. The V-REP remote API is composed by approximately one hundred functions supported by Matlab which can easily be recognized from their "simx"-prefix and that can be used to control the objects and the scenes simulated in VREP. To enable the remote API on the client side, *vrep.simxStart* is called. Respectively, the *vrep.simxFinish* function is used to terminate the connection with the server. Shortly, the description and the syntax of the *simx.Start* and *simxFinish* commands are presented in

Table 1 and **Table 2**.

The chunk of code illustrated in **Figure 5** must always be used if establishing a connection between our application and VREP is wished, with the aim of withdrawing information from the simulator scene and utilize them in the kinematic analysis and trajectory planning of the robots.

```

%start simulation
%connect to VREP
disp('Program started');
% vrep=remApi('remoteApi','extApi.h'); % using the header (requires a compiler)
vrep=remApi('remoteApi'); % using the prototype file (remoteApiProto.m)
vrep.simxFinish(-1); % just in case, close all opened connections
clientID =vrep.simxStart('127.0.0.1',19999,true,true,5000,5);

if (clientID>-1)
    disp('Connected ');
else
    disp('Failed connecting to remote API server');
end

% call the destructor!
vrep.simxFinish(clientID);
vrep.delete();

```

Figure 5: MATLAB code for establishing and terminating communication with V-REP platform

simxStart	
Description	Starts a communication thread with the server (i.e. V-REP). A same client may start several communication threads (but only one communication thread for a given IP and port). This should be the very first remote API function called on the client side. Make sure to start an appropriate remote API server service on the server side that will wait for a connection. See also simxFinish. This is a remote API helper function.
Matlab synopsis	[number clientID]=simxStart(string connectionAddress,number connectionPort,boolean waitUntilConnected,boolean doNotReconnectOnceDisconnected,number timeOutInMs,number commThreadCycleInMs)
Matlab parameters	<p>connectionAddress: the ip address where the server is located (i.e. V-REP)</p> <p>connectionPort: the port number where to connect. Specify a negative port number in order to use shared memory, instead of socket communication.</p> <p>waitUntilConnected: if true, then the function blocks until connected (or timed out).</p> <p>doNotReconnectOnceDisconnected: if true, then the communication thread will not attempt a second connection if a connection was lost.</p> <p>timeOutInMs: if positive: the connection time-out in milliseconds for the first connection attempt. In that case, the time-out for blocking function calls is 5000 milliseconds. if negative: its positive value is the time-out for blocking function calls. In that case, the connection time-out for the first connection attempt is 5000 milliseconds.</p> <p>commThreadCycleInMs: indicates how often data packets are sent back and forth. Reducing this number improves responsiveness, and a default value of 5 is recommended.</p>
Matlab return values	clientID: the client ID, or -1 if the connection to the server was not possible (i.e. a timeout was reached). A call to simxStart should always be followed at the end with a call to simxFinish if simxStart didn't return -1

Table 1: Enabling the remote API-client side, Matlab documentation for simxStart function

simxFinish	
Description	Ends the communication thread. This should be the very last remote API function called on the client side. <code>simxFinish</code> should only be called after a successful call to <code>simxStart</code> . This is a remote API helper function.
Matlab synopsis	<code>simxFinish(number clientID)</code>
Matlab parameters	clientID : the client ID. refer to <code>simxStart</code> . Can be -1 to end all running communication threads.
Matlab return values	None

Table 2: Enabling the remote API-client side, Matlab documentation for `simxFinish` function

2.3.2 Server side activation

To enable the remote API on the server side, utilized is the temporary remote API server service, via the command `simRemoteApi.start`, which in our case is called from a non-threaded child script attached to the Base Arm Link of the robotic arm, which is the parent of all links of the robot. Shortly, the description and the syntax of the `simRemoteApi.start` command is presented in **Table 3** :

simRemoteApi.start	
Description	Starts a temporary remote API server service on the specified port. When started from a simulation script, the service will automatically end when the simulation finishes
Lua synopsis	<code>number result=simRemoteApi.start(number portNumber,number maxPacketSize=1300,Boolean debug=false,Boolean preEnableTrigger=false)</code>
Lua parameters	<p>portNumber: port where to install the server service. Ports above 20000 are preferred. Negative port numbers can be specified in order to use shared memory, instead of socket communication.</p> <p>maxPacketSize: the maximum size of a socket send-packet. Make sure to keep the value at 1300, unless the client side has a different setting.</p> <p>Debug: if true, a window will display the data traffic on that port.</p> <p>preEnableTrigger: if true, the server service will be pre-enabled for synchronous trigger signals from the client.</p>
Lua return values	-1 if operation was not successful. In a future release, a more differentiated return value might be available

Table 3: Enabling the remote API –server side, LUA documentation for `simRemoteApi.start` function

The server side activation has following structure as shown in **Figure 6**, which was extracted from the VREP environment.

```

Non-threaded child script (BaseArm_Link)
1 function sysCall_init()
2     -- server side activation
3     -- port number 19999
4     simRemoteApi.start(19999)
5
6 end
7

```

Figure 6: LUA code for server-side activation

2.3.3 Basic Remote-API functions for MATLAB client

In order for the user to be able to effectively communicate with the V-REP platform via the chosen client, which in our case is MATLAB, there is a list of remote API functions specifically designed for each client and which facilitate the procedure. Some of the most basic function that were also used throughout this project are mentioned and briefly explained below.

- [simxGetObjectHandle](#)
Retrieves an object handle based on its name. If the client application is launched from a child script, then you could also let the child script figure out what handle correspond to what objects, and send the handles as additional arguments to the client application during its launch.
- [simxGetObjectOrientation](#)
Retrieves the orientation (Euler angles¹) of an object.
- [simxGetObjectPosition](#)
Retrieves the position of an object.
- [simxGetJointPosition](#)
Retrieves the intrinsic position of a joint. This function cannot be used with spherical joints (use `simxGetJointMatrix` instead).
- [simxSetJointPosition](#)
Sets the intrinsic position of a joint. May have no effect depending on the joint mode. This function cannot be used with spherical joints (use `simxSetSphericalJointMatrix` instead). If you want to set several joints that should be applied at the exact same time on the V-REP side, then use `simxPauseCommunication`.
- [simxPauseCommunication](#)
Allows to temporarily halt the communication thread from sending data. This can be useful if you need to send several values to V-REP that should be received and evaluated at the same time. This is a remote API helper function.

There are many more functions that can be used according to the needs of the user and the desired tasks that are assigned to the objects in the V-REP scene, however for the needs of the current project the above mentioned functions are sufficient. All of the functions can be found in the official help files of Coppelia Robotics. [10]

In order for the functions to be correctly incorporated in the MATLAB code, they must always be accompanied with the prefix 'vrep.', i.e. `vrep.simxGetObjectHandle`, and then followed by their respective input parameters and have the correct synopsis.

¹ $Q = R_x(\alpha) \cdot R_y(\beta) \cdot R_z(\gamma)$ [Euler angles convention in V-REP]

3

THE ROBOTS

3.1 The custom SCARA robot of Experiment

3.1.1 Description

SCARA robots were first developed in the 1980's in Japan and the name SCARA stands for *Selective Compliance Assembly Robot Arm*. The main feature of the SCARA robot is that it has a jointed two-link arm which in some ways imitates the human arm, hence the often used term articulated. It operates on a single plane, allowing the arm to extend into confined areas and then retract or “fold up” out of the way, which makes it suitable for reaching inside enclosures or pick-and-place from one location to another. [11]

The custom arm used in this study has 5 degrees of freedom, which depict the joints of the robot. Of them, three (3) are revolute and two (2) prismatic joints. The arm is mounted on a horizontal rail above the machines of the lab, for the needs of this study. The structure of the SCARA robot studied in the current thesis is shown in **Image 4**.

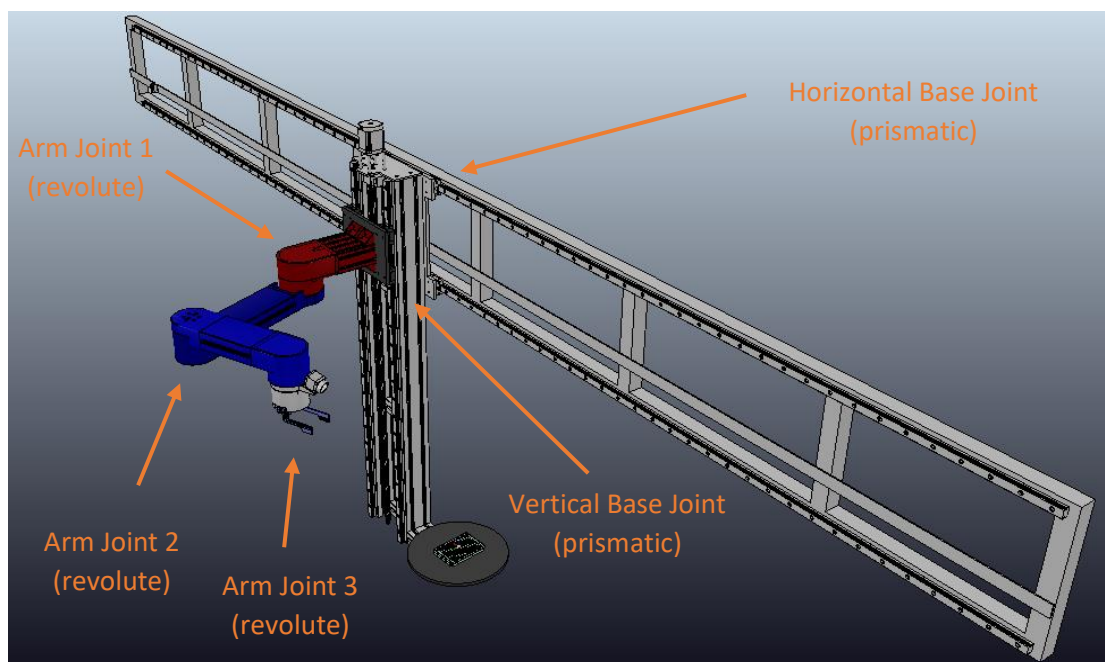


Image 4: Structure of custom SCARA robot

Each joint has its own stand-alone motor that allows it to move independently, within some boundaries, which are shown in **Table 4** and **Table 5**, and to move the second link between every two that it connects. The robotic arm can be separated into two sections:

1. the translational joints (prismatic) → movements of the robot vertically and horizontally on the rails
2. the rotary joints (revolute) → rotation of the robot to its vertical axis

Therefore, the limits of the two tables are expressed in different units, since in the 1st case we are referring to translation, which equals meters, and in the 2nd case to rotation, which equals degrees.

Translational Joints	1	2
Range(m)	3.7	1.9
Limits(m)	-1.9, 1.8	0, 1.9

Table 4: Translational Joint Limits of the SCARA type robot

Rotary Joints	3	4	5
Range(°)	240	286	180
Limits(°)	-120, 120	-143, 143	-90,90

Table 5: Rotary Joint Limits of the SCARA type robot

The boundaries of the joints determine the working space of the arm that is defined as the space that the end-effector can reach in any orientation. For the SCARA robot, the working space is shown in **Figure 7**. In our case however, some restrictions apply as to the reach of the workspace, since it has to be taken into consideration that the robot is hang from a rail, which should not interfere with the movement of the arm. Therefore, the workspace for the SCARA type robot used in the current thesis is smaller than the actual workspace, something which is depicted in by the black line which represents the rail from which the arm is hung.

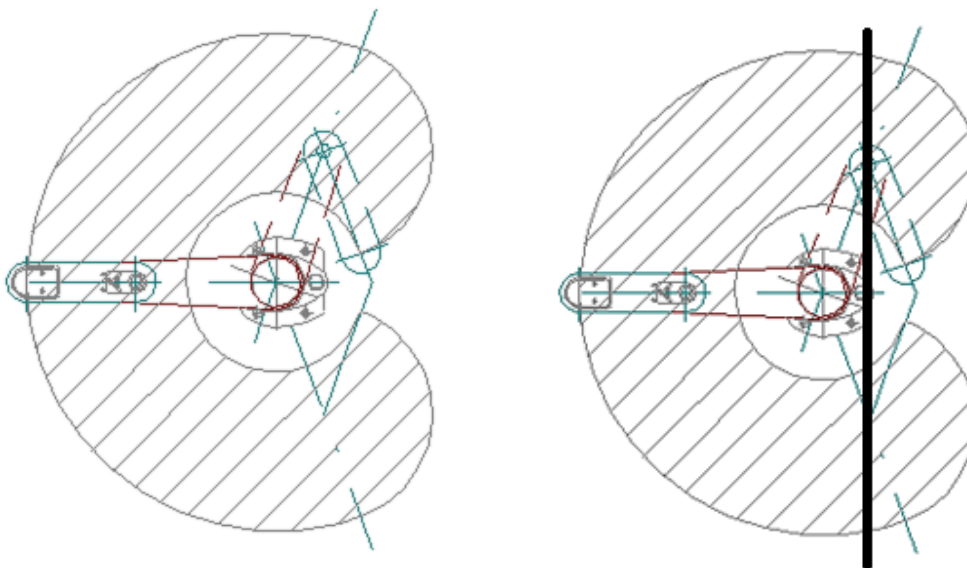


Figure 7: Workspace of SCARA type robot

3.1.2 Advantages and limitations of SCARA robots

The SCARA robot is most commonly used for pick-and-place or assembly operations where high speed and high accuracy is required. Generally a SCARA robot can operate at higher speed and with optional cleanroom specification. In terms of repeatability, currently available SCARA robots can achieve tolerances lower than 10 microns, compared to 20 microns for a six-axis robot. By design, the SCARA robot suits applications with a smaller field of operation and where floor space is limited, the compact layout also making them more easily re-allocated in temporary or remote applications.

On the other side, due to their configuration, the SCARA robots are typically only capable of carrying a relatively light payload, typically up to 2 kg nominal (10 kg maximum). The envelope of a SCARA robot is typically circular, which does not suit all applications, and the robot has limited dexterity and flexibility compared to the full 3D capability of other types of robot. For example, following a 3D contour is something that will be more likely fall within the capabilities of a six-axis robot. [12]

3.2 Stäubli TX2-90XL

3.2.1 Description

The second robot used to run simulations of the experiments is the Stäubli TX2-90XL Robot. The TX designation indicates a low payload, while the XL refers to the length of the arm. For the purposes of the current study, the extra-long arm will be used. This arm is sufficiently flexible and is able to perform a great variety of applications, such as:

- Handling of loads
- Assembly, process, application of adhesive beads
- Control check
- Clean room applications

The arm consists of six links, which are connected in pairs of two, by six rotary joints. The links of the robot are shown in **Figure 8** and are named accordingly and are each represented with a capital letter. The links of the Stäubli TX2-90XL are named after human body parts, because of its anthropomorphic form.

- A – Base
- B – Shoulder
- C – Arm
- D – Elbow
- E – Forearm
- F – Wrist

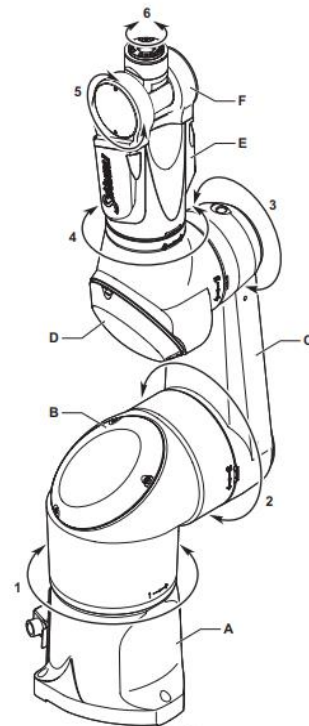


Figure 8: Stäubli TX2-90XL Robot

Movements on the arm joints are generated by servomotors coupled with position sensors. Each of these motors is equipped with a parking break. The motors allow for each joint to rotate independently, within some boundaries, which are shown in **Table 6**, and to move the second link between every two that it connects. For example, joint 1 moves link B and joint 2 moves link C.

Joint Limits						
Joint	1	2	3	4	5	6
Range(°)	360	277.5	280	540	255	540
Limits(°)	±180	-130, +147.5	±145	±270	-115, 140	±270

Table 6: Joint Limits of the Stäubli TX90XL

The boundaries of the joints determine the working space of the arm that is defined as the space that the end-effector can reach in any orientation. For the Stäubli TX2-90XL, the working space is shown in **Figure 9**.

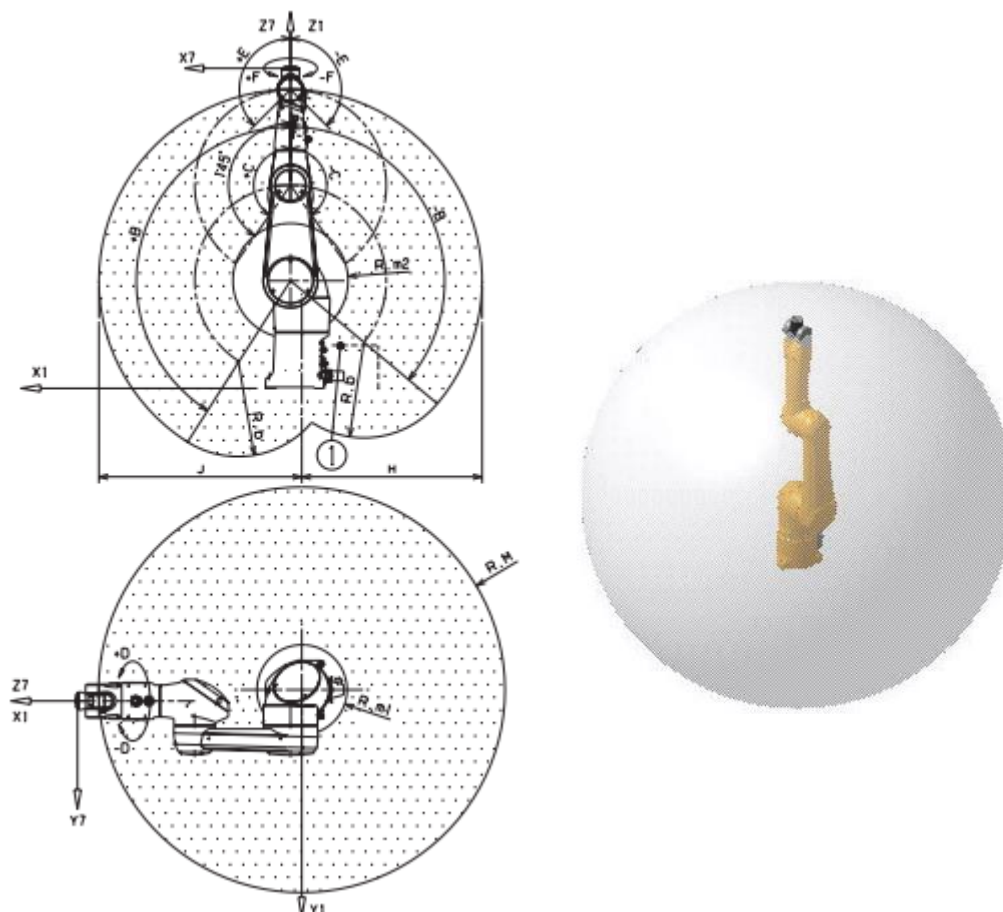


Figure 9: Working space of Staubli TX2-90XL [Source: [Staubli](#)]

The Stäubli robot has multiple mounting configurations (floor/wall/ceiling) to make its integration into the production line easier. **Figure 10** shows four different ways that the Staubli TX2-90XL Robot can be mounted, while more information on the technical specifications of the model can be found in **Appendix B**.

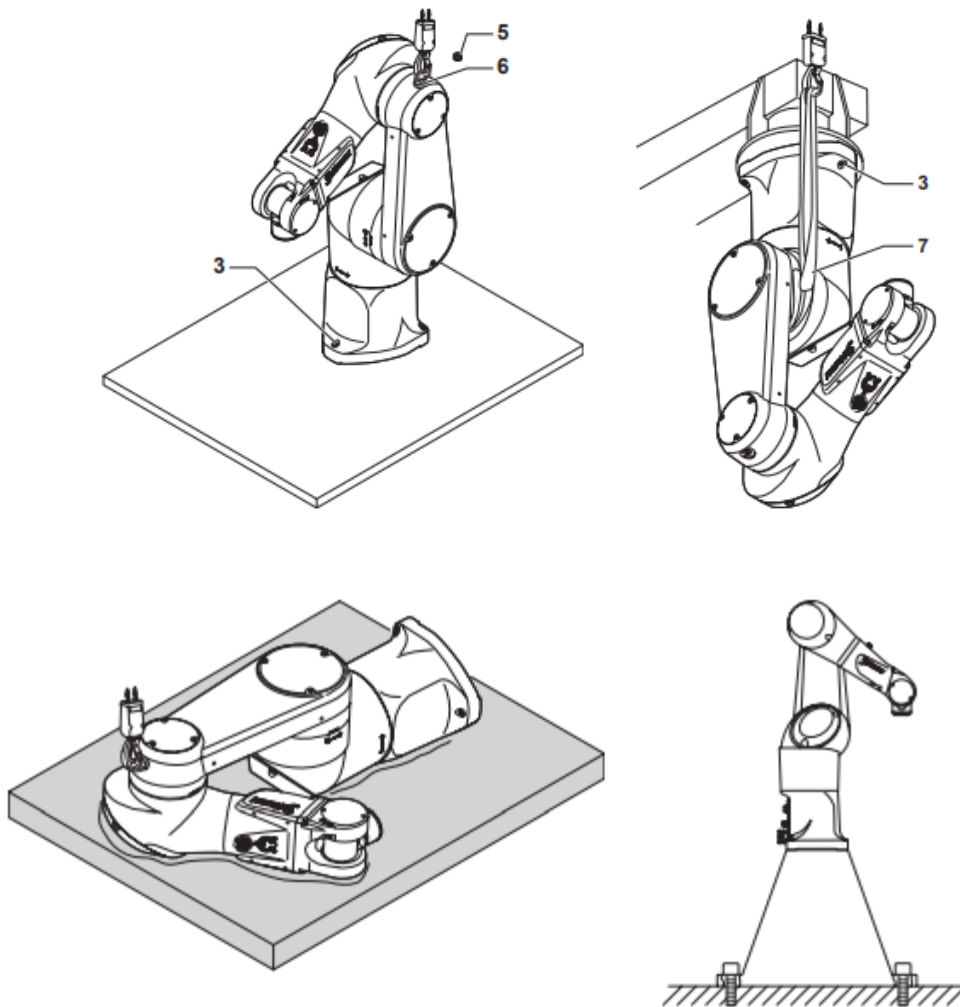


Figure 10: Different mounting positions for Staubli TX2-90XL

3.2.2 Advantages and limitations of 6-axis robots

Articulated robots, or 6-axis robots, are easier to align to multiple planes, simple to operate and maintain, and easily redeployed for automation applications and for a wide range of upstream and downstream applications. They present high repeatability and accuracy, while being able to reach orientations and positions, which are not possible by other robots. At the same time however, they have greater demands as far as their working space and cost is concerned.

3.3 Robot 3D Model Import

In the present work, the design of the Staubli robot was downloaded from the official CAD Library of Staubli, whereas the design of the custom robotic arm was done in Autodesk's AutoCAD and was received as ready file from the experement team. The robot models were exported in URDF, a file format mentioned in previous chapters, and then entered in the simulation scene.

3.3.1 Unified Robot Description Format (URDF)

The URDF format expresses the kinematic tree structure of the robot and the order of the properties in the file does not affect the results.

A URDF consists of attributes and elements, some of which are required for the file to be a valid representation of the robot and some of which are optional and are used to provide extra information that can be useful for the simulation. A graphic representation of these elements is offered in **Figure 11**, whereas a general template of a URDF file is presented in **Appendix A**, followed by some explanatory comments for each section. For the purposes of this research, only some basic optional elements are included.

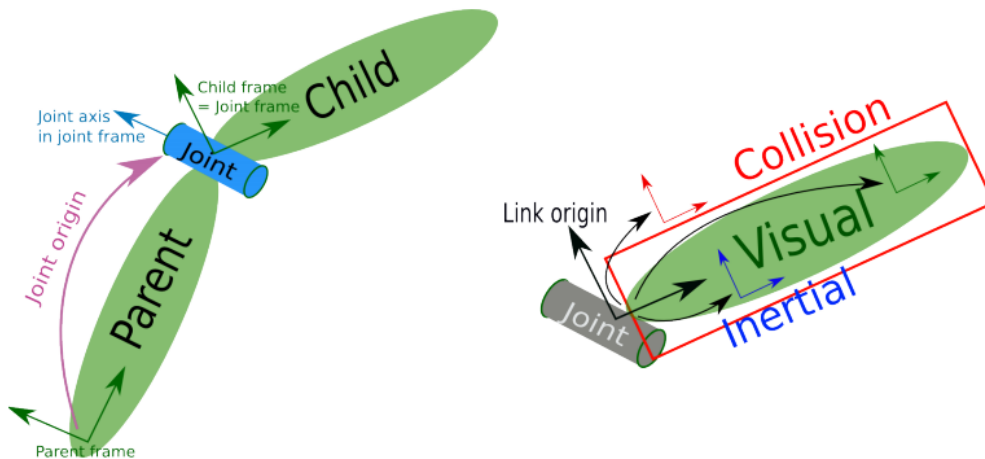


Figure 11: Link and joint representation

If we want the URDF model to be permanently attached to the world frame (the ground plane), we must create a "world" link and a joint that fixes it to the base of the model. In both our robot models, this is desired, since the "world" link will work as the reference frame with respect to which the kinematics and all other components of the simulation scene will be expressed. Therefore, we need a link attached to a specific position, which is the base of the SCARA and the Staubli models respectively. It is worth noticing that even though the SCARA robot has a mobile base and it is free to move vertically and horizontally on the attached rail, as also seen in previous chapters, the world link remains fixed to its initial position. The same happens with the Staubli model, if it is mounted on a rail. The chunk of code for this action presented below is written according to the URDF template of **Appendix A** and is the same for both robots used for the purposes of the current thesis.

```
<link name="world">
</link>
<joint
  name="world_joint"
  type="fixed">
  <origin
    xyz="0 0 0"
    rpy="0 0 0" />
  <parent
    link="world" />
  <child
```

```

    link="First_link_of_robot_model" />
</joint>

```

Respectively, an additional link is fixed to the last link of the robot model, representing the end-effector frame that will be the part following the trajectory, which will be calculated in the kinematics chapter. The origin attributes `xyz` and `rpy` depend on the position and orientation of the parent link and are added in a way so that the `ee_link` is located approximately at the edge of the parent link, which is usually the tool flange of the robot or the edge of the gripper.

```

<link name="ee_link">
</link>
  <joint
    name="ee_joint"
    type="fixed">
    <origin
      xyz="x y z"
      rpy="r p y" />
    <parent
      link="Last_link_of_robot_model" />
    <child
      link="ee_link" />
  </joint>

```

It is worth noting that in the case that the `ee_link` is located on the tool flange, a suitable offset to the actual gripping edge should be taken into consideration, since the position where the gripper is attached differs from the part which actually follows the trajectory and which is no other but the gripper fingers. Usually, a *dummy* is utilized in the simulation to represent the finger edge which will be grabbing the product, with respect to which the offset to the `ee_link` is set.

For every URDF file, its name is mentioned in the beginning with the name attribute:

```

<robot
  name>
</robot>

```

and the file is saved with the same name as 'name.urdf'.

3.3.2 Robot Coordinate Systems

For the expression of the position and the orientation of the links of a robotic arm, utilized are usually the three (3) following coordinate systems. [13]

1. Global Coordinate System: A Cartesian coordinate system is located on the base of the robot and all the positions of its distinct links are expressed with respect to this frame.
2. Coordinates of End-Effector: The cartesian coordinate system is located on the edge of the robotic arm, always taking it's rotation into consideration.

3. Joint Coordinate Frames: The position of each joint, for example the angle of a rotational joint, is used for describing the position and configuration of the robot at all times.

It is crucial that these coordinate frames are the same, in orientation and position, both in the URDF file as well as in the VREP simulator. Otherwise, the results may diverge from the actual positions and orientations that the robotic manipulators should acquire.

3.3.3 Scaling Factor

Upon importing the URDF file in the simulation environment, of the many options available, one that is of interest and on which the accuracy of the research result depends is the Scale Factor, which the user has to adjust in order to get realistic results. The question is now: why is it so important to have realistic results rather than something nearly accurate?

The purpose of the current project is to virtually move the robots in the 3 dimensions of space and to read the position and rotation of the end-effector point (EE) on the 3 axes. From these 6 numbers, the inverse kinematics (see **Chapter 6**) will result in the values of the angles of the joints, which can then be loaded onto the real robot and set up a physical simulation. Since the mathematics of the robot's kinematic chain depend on its physical dimensions, if the dimensions of the simulation model are not exactly the same as those of the real robot, the results will not only be inaccurate, but they may not correspond to the actual movement of the robot at all. In our case, both robots and all machinery have been designed according to their real dimensions and the transformation of the units from millimeters [mm] of the SolidWorks and Creo files to meters [m] in VREP takes place automatically upon import. Therefore, the scale factor of all components of the simulation scenes is 1. By setting different values to the scale factor, the respective size is multiplied by the respective scaling factor.

3.3.4 URDF and MATLAB Robotics Toolbox

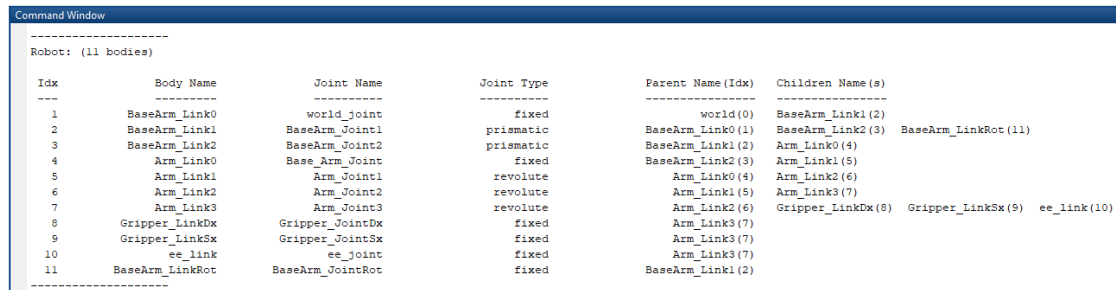
The URDF format is however not only useful for importing 3D representations of the robotic arms in V-REP, but also for expressing the kinematic tree structure of the robot inside of MATLAB. Specifically, importing a URDF file using the `importrobot()` function of the MATLAB Robotics Toolbox, MATLAB can read and analyze the kinematic structure of the imported robotic arm, an asset which facilitates the forward and inverse kinematic analysis of the robots that will take place in the next chapters. The Robotics Toolbox consists of functions that prevent the user from consuming time in analytically extracting the kinematic analysis of a robot and is ideal for the purposes of the current project that deals with simulations using two different robotic arms.

Figure 12 shows the chunk of code used to import the URDF file in MATLAB and print in the MATLAB Command Window the details of the kinematic chain which is to be studied.

```
%import URDF file of arm- define kinematic matrix and show details
robot= importrobot('name.urdf');
showdetails(robot);
```

Figure 12: Matlab code for importing URDF file

The details that are presented using the `showdetails()` function for each robot in the Command Window are shown in **Figure 13** and **Figure 14**.

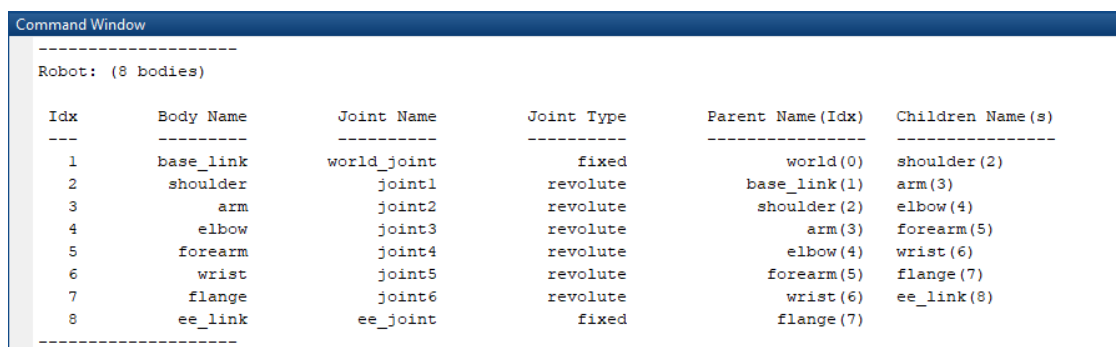


```

Command Window
-----
Robot: (11 bodies)
-----
Idx      Body Name      Joint Name      Joint Type      Parent Name (Idx)  Children Name (s)
-----
1        BaseArm_Link0   world_joint     fixed           world(0)           BaseArm_Link1(2)
2        BaseArm_Link1   BaseArm_Joint1  prismatic      BaseArm_Link0(1)  BaseArm_Link2(3) BaseArm_LinkRot(11)
3        BaseArm_Link2   BaseArm_Joint2  prismatic      BaseArm_Link1(2)  Arm_Link0(4)
4        Arm_Link0       Base_Arm_Joint  fixed          BaseArm_Link2(3)  Arm_Link1(5)
5        Arm_Link1       Arm_Joint1      revolute       Arm_Link0(4)      Arm_Link2(6)
6        Arm_Link2       Arm_Joint2      revolute       Arm_Link1(5)      Arm_Link3(7)
7        Arm_Link3       Arm_Joint3      revolute       Arm_Link2(6)      Gripper_LinkDx(8) Gripper_LinkSx(9) ee_link(10)
8        Gripper_LinkDx  Gripper_JointDx fixed          Arm_Link3(7)
9        Gripper_LinkSx  Gripper_JointSx fixed          Arm_Link3(7)
10       ee_link         ee_joint        fixed          Arm_Link3(7)
11       BaseArm_LinkRot BaseArm_JointRot fixed          BaseArm_Link1(2)
-----

```

Figure 13: Details for SCARA robot



```

Command Window
-----
Robot: (8 bodies)
-----
Idx      Body Name      Joint Name      Joint Type      Parent Name (Idx)  Children Name (s)
-----
1        base_link      world_joint     fixed           world(0)           shoulder(2)
2        shoulder       joint1          revolute       base_link(1)       arm(3)
3        arm            joint2          revolute       shoulder(2)        elbow(4)
4        elbow         joint3          revolute       arm(3)             forearm(5)
5        forearm       joint4          revolute       elbow(4)           wrist(6)
6        wrist         joint5          revolute       forearm(5)        flange(7)
7        flange        joint6          revolute       wrist(6)           ee_link(8)
8        ee_link       ee_joint        fixed          flange(7)
-----

```

Figure 14: Details for Staubli TX2-90XL

3.4 Gripper Choice

The gripper of a robot has to be adapted according to the tasks it is asked to fulfill. In the current study, the goal is the handling of standardized plates and racks in microplate format. In the frameworks of a biotechnology laboratory, sometimes also non-standardized equipment such as syringes, filters and many more need to be handled, thus demanding a different finger gripper form. [14] However, for the needs of the current study we will choose grippers that are suitable for the former goal, namely carrying microplates.

The gripper that can be incorporated in a laboratory setting has to be specifically developed for application in clean rooms. Needed is a precise, fine-tuned construction that can ensure a nearly particle-free performance of all movements. Also, since the object that will be carried along the laboratory setting is a microplate, one of the most important prerequisites is a stable parallel gripping ability. Since the microplates have liquids in them, desired is that these liquids remain in their respective wells of the plate and at the same do not spill out of it. Therefore, attention should be focused on parallel grippers.



Image 5: Example of parallel servo-gripper [Source: [Applied Robotics](#)]

3.4.1 Parallel Grippers

A parallel gripper for handling multiwell plates in an automated analysis system, moves individual multiwell plates between workstations, for example from a plate storage array unit to an imaging station. More particularly, the gripper has two parallel plate-gripping arms that move in equal, but opposite linear directions, and are controlled using a stepper motor. Each of the arms has a shelf that provides support for the corresponding side edge of a multiwell plate. [16]

1. SCARA

For the Scara type robot, the gripper choice is quite simple, since the robot itself moves in a planar way, rotating only around the z axis. Therefore, a parallel gripper is sure to maintain the desired orientation of the well plate – parallel to the lab floor – and fulfill its task. Along with the 3D CAD models of the SCARA robot, incorporated is a custom made parallel gripper, whose design drawing is provided in **Appendix B**. The difference to common grippers is that it includes a rotating base for the fingers, an addition that contributes to the change of orientation during loading or unloading the well-plates, if necessary. For simplification purposes, the gripper in the simulation of the SCARA remained as it is.

Alternatively, if the rotating base for the fingers is not deemed necessary, a good alternative would be LGR Electric Servo Gripper “The Gripster”. More information on the LGR Electric Servo Gripper can be found in **Appendix B**.

2. STAUBLI TX2-90XL

For the Stäubli model which is an articulated robot, the gripper choice is vast and can be done in many different ways, always according to the needs of the respective laboratory and the tasks at hand. Due to its 6-dof nature, the tool-flange can acquire multiple different positions and orientations along and around the x, y and z axis. The need for the microplate to remain parallel to the ground is vital in this case.

For this robot model, the LGR Electric Servo Gripper can be a suitable solution, since it can be easily mounted on the Stäubli and is fully compatible with the Stäubli model series, while at the same time providing a stable parallel grip for the desired tasks. PTM Präzisionstechnik also offers good alternatives to the gripper choice.

ROBOTIQ provides an alternative gripper solution. Though it is suitable for industrial purposes and factory work, it can also be used inside a biotechnology laboratory and be either vertically or horizontally located. More information can be found under **Appendix B**.

This gripper choice was also used for the simulation purposes, since it was of the few gripper designs that were provided online as 3D CAD models. Unfortunately, the CAD files are for visual purposes only and are not thus functional, in the sense that the gripping for the case of the Staubli model will not be simulated.



Image 6: ROBOTIQ 2F-140 Gripper [Source: [ROBOTIQ](#)]

The general idea, no matter the choice of company, remains the same. The objective is to incorporate grippers that have a stroke of at least the greatest dimensions of the well-plates that will be used. Smaller stroke grippers will not be able to grab the plate in both portrait and landscape orientations, since they will not have an opening wide enough to clamp the microplate.

The grippers that will be used for the simulations are thus:

- ✓ The custom made gripper by experiment for the SCARA
- ✓ The 2F-140 gripper by ROBOTIQ for the Staubli.

4

LABORATORY EQUIPMENT

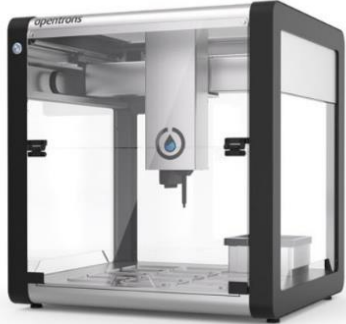
4.1 Machines

The machines that may be included in a Biotechnology Lab vary according to the experiments that are to be conducted. Some demand few steps in order to be completed, however others are extremely complicated and demand specific conditions and treatment, something that equals the need for more specialized equipment in the lab. Therefore, there is no standard when it comes to how many and which machines will be added in one lab, but it all depends on the experimentation demands of the people running the laboratory and of course, the cost margin that each company wants to abide by.

For the needs of the current project, included in the lab simulation, are following machines, accompanied by their basic specifications. They are all compatible with automation solutions so that they can be used in a robotic biotech lab. More on their dimensions and form can be found in **Appendix B**.


4.1.1 Liquid Handler

Multipurpose liquid handling automated workstations are tools designed to do much of the sampling, mixing, and combining of liquid samples automatically. Liquid handlers can measure out samples, add reagents, and make sure liquids are added to bioassays in a uniform fashion. The volume of sample the liquid handling automated workstation can handle is one feature to consider when making a purchase. Other features to consider include how large a footprint the workstation makes and the ease of use of its software interface. For our simulation, used is the robotic Liquid Handler of *Opentrons*.

Rendered Visualization [Source: Opentrons]	Specification (Biochem)	Specification (Mechanical / Automation)
	Handles 96 & 384 standard well plates	Includes internal robotic arm to move plates between decks
	Dispense range [0.5-250µL]	Has a hand-off position which is unobstructable and easily accessible by external robotic arms
	Cooling deck	Has the ability to be fed (by external robotic arm) pipette tips
	Orbital shake deck	Has the ability to remove waste (by handing it off to the external robotic arm)


4.1.2 Centrifuge

A centrifuge is a laboratory device that is used for the separation of fluids, gas or liquid, based on density. Separation is achieved by spinning a vessel containing material at high speed; the centrifugal force pushes heavier materials to the outside of the vessel. This apparatus is found in most laboratories from academic to clinical to research and used to purify cells, subcellular organelles, viruses, proteins, and nucleic acids. There are multiple types of centrifuge, which can be classified by intended use or by rotor design. In addition to its basic form presented below, a robotic gripper can be mounted externally above the insertion opening for the plate, so that the plate can be grabbed directly from the centrifuge. The latter will be the case for the needs of the current project. For our simulation, used is ROTANTA 460 Robotic, a centrifuge by *Hettich*.

Rendered Visualization [Source: Hettich]	Specification (Biochem)	Specification (Mechanical / Automation)
	1000g max centrifugal force	Has the ability to be fed a well plate from the external robotic arm


4.1.3 Freezer

Laboratory refrigerators are used to cool samples or specimens for preservation. They include refrigeration units for storing blood plasma and other blood products, as well as vaccines and other medical or pharmaceutical supplies. They differ from standard refrigerators used in homes or restaurant because they need to be totally hygienic and completely reliable. Laboratory refrigerators need to maintain a consistent temperature in order to minimize the risk of bacterial contamination and explosions of volatile materials. For our simulation, used is STR44, a freezer of *Liconic*.

Rendered Visualization [Source: Liconic]	Specification (Biochem)	Specification (Mechanical / Automation)
	-20 °C	Has the ability to be fed a well plate from the external robotic arm
		~50 well plate capacity


4.1.4 Incubator

Incubator is a device used to grow and maintain microbiological cultures or cell cultures. The incubator maintains optimal temperature, humidity and other conditions such as the CO (CO₂) and oxygen content of the atmosphere inside. Incubators are essential for a lot of experimental work in cell biology, microbiology and molecular biology and are used to culture both bacterial as well as eukaryotic cells. For our simulation, used is STR240, an incubator of *Liconic*.

Rendered Visualization <small>[Source: Liconic]</small>	Specification (Biochem)	Specification (Mechanical / Automation)
	37 °C	Has a hand-off position which is unobstructable and easily accessible by external robotic arms
	95% CO ₂	~50 well plate capacity

4.1.5 Plate Reader

Plate readers, also known as microplate readers or microplate photometers, are instruments which are used to detect biological, chemical or physical events of samples in microtiter plates. They are widely used in research, drug discovery, bioassay validation, quality control and manufacturing processes in the pharmaceutical and biotechnological industry and academic organizations. Common detection modes for microplate assays are absorbance, fluorescence intensity, luminescence, time-resolved fluorescence, and fluorescence polarization. Microplate readers come in two main forms: Those that detect a single type of signal (single-mode readers) and those that can detect multiple types (multimode readers). For our simulation, used is EnVision by *Perkin Elmer*.

Rendered Visualization <small>[Source: Perkin Elmer]</small>	Specification (Biochem)	Specification (Mechanical / Automation)
	Multimode reader	Has the ability to be fed a well plate from the external robotic arm

The models of the simulation environment, incorporating all machines, were done in Catia and Autodesk's AutoCAD and were received as ready files from the experoment team.

4.2 Consumables

Sample reactions can be assayed in 1 - to -1536 well format microtiter plates. The most common microplate format used in academic research laboratories or clinical diagnostic laboratories is 96-well , which is an 8 x 12 matrix, with a typical reaction volume between 100 and 200 μL per well. Higher density microplates, with 384 (16 x 24 matrix) or 1536 wells, are typically used for screening applications, when the number of samples processed per day, in other words the throughput, and assay cost per sample become critical parameters, with a typical assay volume between 5 and 50 μL per well. A 96- and 384- wellplate are presented in **Figure 14**.



Figure 15: Cell-carrier 96 on the left and Cell-carrier 384 on the right

Irrespective of the number of wells, the dimensions of the microplates usually remain the same, a fact that facilitates their handling by the robotic arm. The dimensions and drawings of the microplates can be found in **Appendix B**, where basic elements of the well plates are mentioned. In general, the well plates follow a specific standardization, therefore dimensions remain the same among different production companies.

5

LABORATORY STRUCTURE AND LAYOUTS

5.1 Flexible Manufacturing Systems (FMS)

A flexible manufacturing system is a manufacturing system that contains enough flexibility to allow the system to rapidly react to production changes. This flexibility is generally considered to fall into two categories. The first is machine flexibility. This allows the system to be changed to produce new product types and to change the order of operations executed on a part. The second is routing flexibility. This consists of the ability to use multiple machines to perform the same operation on a part as well as the system's ability to absorb large-scale changes, such as in volume, capacity, or capability.[17]

Most FMS systems consist of three main systems: a material handling system to optimize the flow of parts, a central control computer that controls material movement, and the working machines, which are often automated machines or robots.

Control optimization, material flow efficiency, setup efficiency, and data flow efficiency can be achieved by using Flexible Manufacturing Systems. Economical machining is achieved by:

- Exploiting the flexibility and productivity of numerically controlled machine tools for the production of smaller and medium sized lots
- Utilizing costly production equipment more effectively through the reduction or elimination of setups
- Changing parts, tools, and machining programs automatically.[18]

5.2 Production line layouts for FMS

The analogies of FEPS to FMS are obvious and therefore layouts used for Flexible Manufacturing can also be applied in the current project.

There are alternatives to setting up a robotic production cell for a biotechnology laboratory, which vary according to the needs and the restrictions that apply each time. Some of these needs and restrictions can be:

- Limited working space, narrow aisles and floor obstructions
- Number and position of machines in the cell

- Desired production rates and times
- Flexibility in production for implementing low cost alternatives inside the cell
- Aesthetics

Depending on these parameters, there is a range of different set-up alternatives to choose from. Modelled and analyzed for the purposes of the thesis will be 3 of the most popular layouts, namely:

1. Linear layout
2. Island (or Circular) layout
3. Ladder layout

5.2.1 Linear layout

The linear layout constitutes a very common production layout, which offers flexibility and possibilities for extension. Specifically, scaling-up production is easier with this kind of format, since increasing the number of machines in a cell, would mean elongation of the production line to the wished extend, without any problem. The only restriction for its implementation are the dimensions of the space available. This layout is ideal for narrow, but long spaces, where a robot can be mounted on a rail and easily move along the lab space and to the machines. For the needs of this layout, a SCARA type robot is sufficient, since the movements of the robot are specific and restricted to planar movements in space. SCARA robots offer an ergonomic alternative to more complex types of robots, in an economic as well as in a controls respect.

However, as flexible as this layout can be, its implementation may result in unnecessary motion between the workstations.[19] For example, if an experiment, in our case, consists of a two-step procedure between two workstations that are each located on opposite sides, then the translation times of the robot between the machines increases with the length of the production line and results in unnecessary motion, since the whole production line has to be run through, in order for only two machines to communicate.

A representation of this layout is presented in **Figure 16**.

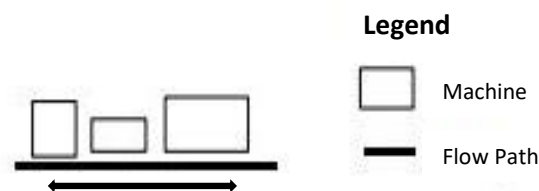


Figure 16: Linear layout for production

5.2.2 Island (or Circular) Layout

The island layout, which could also be described as circular, involves the concept of a robot centered cell, meaning that the machines are organized in a circular manner around the robot. This format constitutes an effective layout when considering product movement as all the

necessary operations to produce a component or subassembly are performed in close proximity, resulting in near zero operation-to-operation transfer times.[19] At the same time, this layout is suitable for limited space availability. In contrast to the linear layout, it also facilitates access in the lab, since human interference might be deemed necessary at some point.

On the other side of things, the islands are isolated with respect to each other, since the formation is circular and does not allow communication between the robots, which are located in the middle of each cell. This layout also offers finite possibilities of extension, a factor that constricts flexibility since the number of additional machines that can be incorporated in the cell is restricted. More specifically, the possible reaching area for the robotic arm reaches a maximum, which cannot be overcome, no matter how much the diameter of the cyclic layout is increased in order for more machines to be added. As for the robot that can be used for this type of layout, recommended is a 6-DOF (Degrees Of Freedom) robot to ensure maximum flexibility, since in this case wished is achieving any position and orientation in the lab space. This equals increased cost and more complex robot control strategies.

A representation of this layout is presented in **Figure 17**.

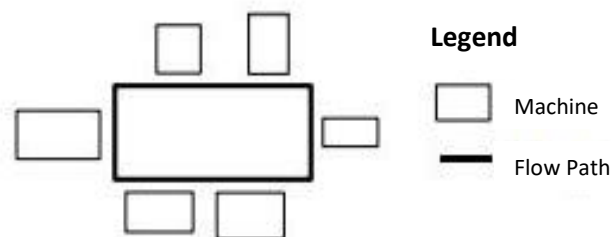


Figure 17: Island (or circular) layout for production

5.2.3 Vertical Ladder Layout

The vertical ladder layout is a differentiation to the ladder layout implemented for horizontal production cells. The machines in the vertical ladder layout are located in levels above each other, creating a ladder formation, which resembles the design of library shelves, each of which is basically a different machine. This layout can be used in combination with either the linear or island layouts in order to increase their extension possibilities, having the same advantages and disadvantages as mentioned before in each case respectively.

The linear production can be thus extended in length and height, if the machines are organized according to the ladder layout, by using a longer vertical rail that can help the robot reach both the lowest and highest positions of the machines in the lab, always with respect to the dimension restrictions of the lab space. Accordingly, the same is valid for the circular layout, where no modifications are needed, since a 6-DOF can reach all the positions and orientations in space that fall within its capabilities and working space.

A representation of this layout is presented in **Figure 18**.

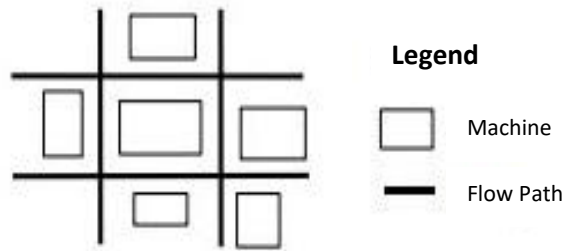


Figure 18: Vertical Ladder layout for production

5.3 Laboratory Structure

Following the above mentioned guidelines, as far as production organization and layouts are concerned, we can now create possible structures for the robotic biotechnology cloud lab analyzed in this thesis, taking into consideration specific restrictions and facts concerning our case and modelling demands. Some of these factors are analyzed below.

I. Available robotic arms

As already mentioned in previous chapters, we have two alternatives as to what kind of robots will be used to simulate the experiment production flow. The one is the custom SCARA robot provided by experoment and the second one the 6-DOF robotic arm Staubli TX2-90XL.

SCARA: As mentioned previously, the SCARA robot is ideal, due to its smaller weight, cost and easier control, when compared to a 6-DOF robot, for implementing a linear layout in the production line. Therefore, mounting it on a vertical rail, which is then connected to a horizontal rail hung on the lab wall, covering in that way translations of the robot along the height and the length of the lab respectively, while organizing the machines in a linear fashion.

STAUBLI: The Staubli can also be mounted in the same way from the ceiling of the lab, covering a bigger work space than the SCARA, which in the case of the linear layout does not actually offer any more benefits to the structure, since the movements are very simple. Therefore, the Staubli in the linear layout increases the cost and complexity of the system, without essentially increasing production flexibility. In the contrary, the Staubli would be ideal for the island layout, reaching positions in space that the SCARA cannot.

II. Available working space

The available lab space for the experoment team for now has following dimensions:

Length: 4,96 m | Width: 1,84 m | Height: 2,24 m

This equals a very narrow but long laboratory that restricts the possible layouts of the lab to linear, since this is the only way for the machines and the robot to fit in this space.

However, when considering scaling up a start-up, space should not be restrictive of testing new configurations for future implementation and development. Therefore, supposing that we want the lab to at least take up no more area in square meters [m²] than the already available space, which equals 9,13 m², and keep its height to 2,24 m, we could utilize a space with following dimensions:

Length: 3,02 m | Width: 3,02 m | Height: 2,24 m

to set up an island layout, where the robot will be located in the middle of the lab and the rest of the machines around it in a circular fashion.

III. Number and position of machines in the cell

For the needs of the current project the number of machines that will be used to simulate the experiments is five (5) and includes all of the machines that were thoroughly mentioned in **Chapter 4**. This number does not constitute a restrictive parameter for any of the available layouts. However, an increase in the number of machines should be dealt with thoroughly.

In the same manner, the position of the machines does not play a decisive role in structuring the lab, because all of the machines are used in the different experiments without a specific order, thus there is no optimal position for each of the machines.

IV. Desired production rates and times

The experiments conducted in the platform are very time-consuming in the sense that each step of an experiment might have a duration between 2 and even 24 hours. Therefore the translation times of the robot from workstation to workstation is not a decisive factor in setting up the laboratory. In spite of that, in case of very long linear production lines, this should be taken into consideration, since it could add up to disproportionate translation times to average experiment completion times.

Taking all of these factors into consideration, we can now visualize the two most beneficial possible layouts for our laboratory, which are no other than the:

- ✓ Linear layout with the SCARA robot (**Image 7, Image 8**)
- ✓ Island layout with the Staubli TX2-90XL (**Image 9, Image 10, Image 11**)

It is worth mentioning that in the frameworks of this project, the ladder layout will not be analyzed, since the number of machines does not demand such formation and for the purposes of this study the two other layouts are sufficient. In case of an increase in the number of machines or due to other factors which may demand the ladder layout, it can be formed through simple modifications, such as lengthening the vertical rail in the linear lineout and adjusting the heights of the machines in the circular layout.

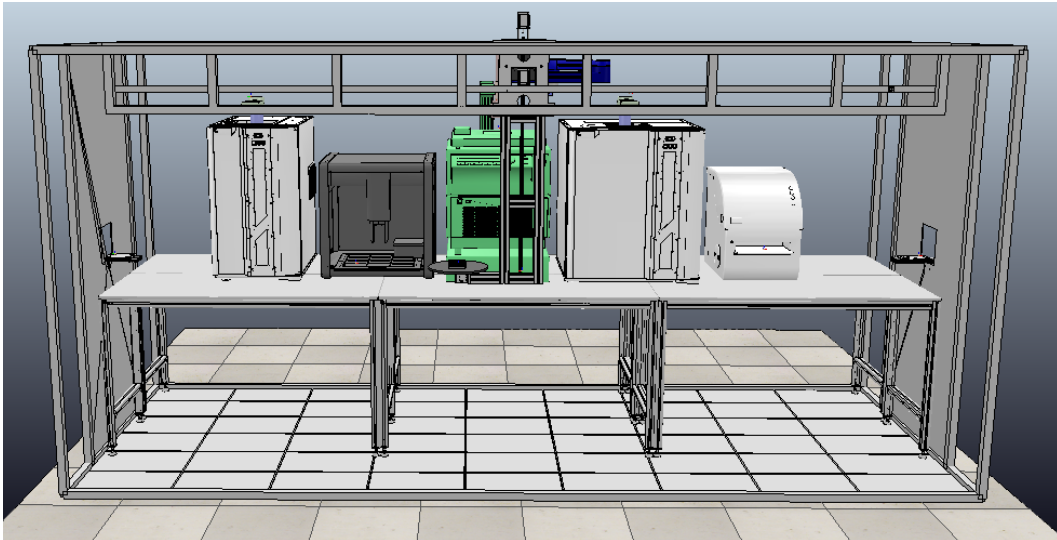


Image 7: Front view of linear layout for biotechnology lab

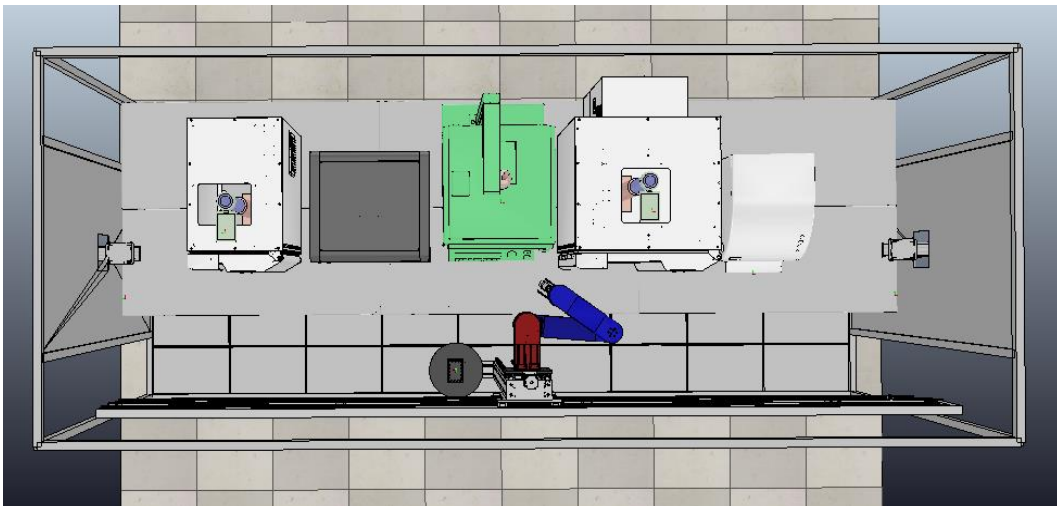


Image 8: Top view of linear layout for biotechnology laboratory

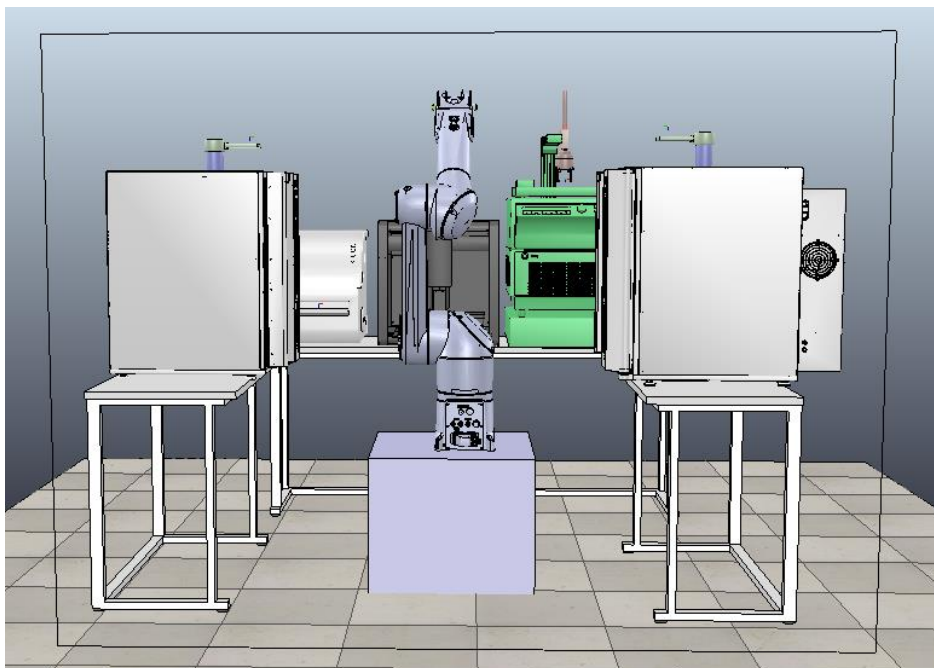


Image 9: Front view of island layout for biotechnology laboratory

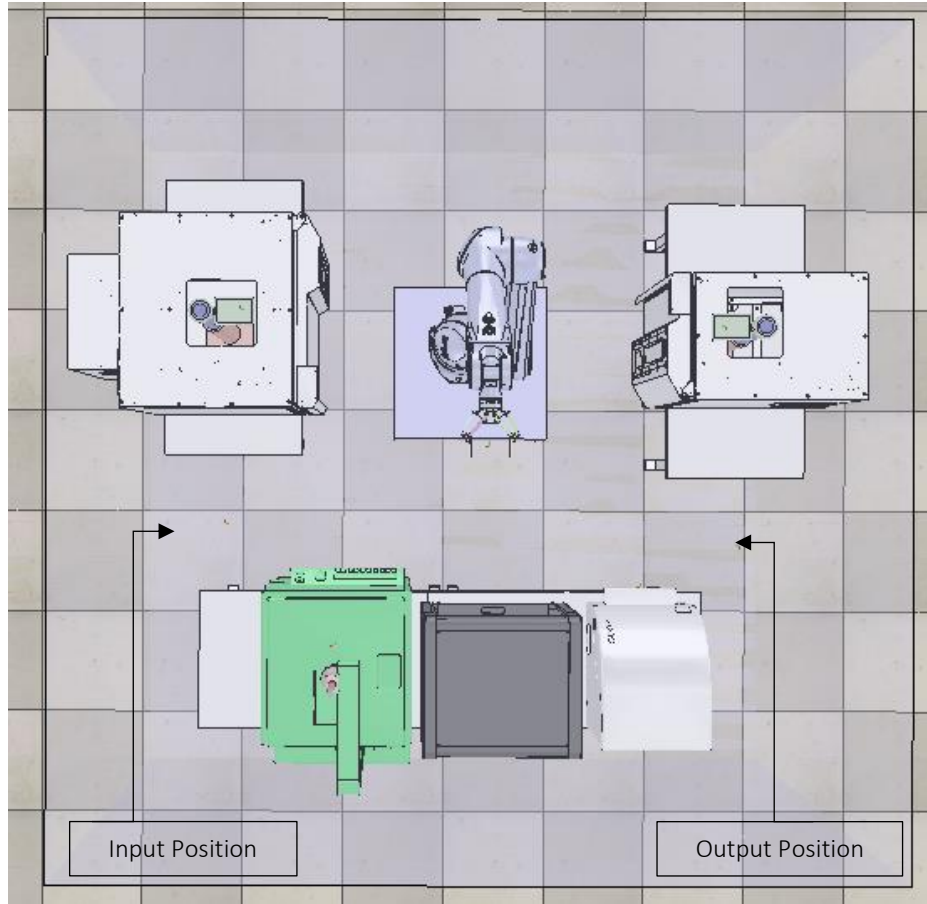


Image 10: Top view of island layout for biotechnology laboratory with possible Input and Output Positions²

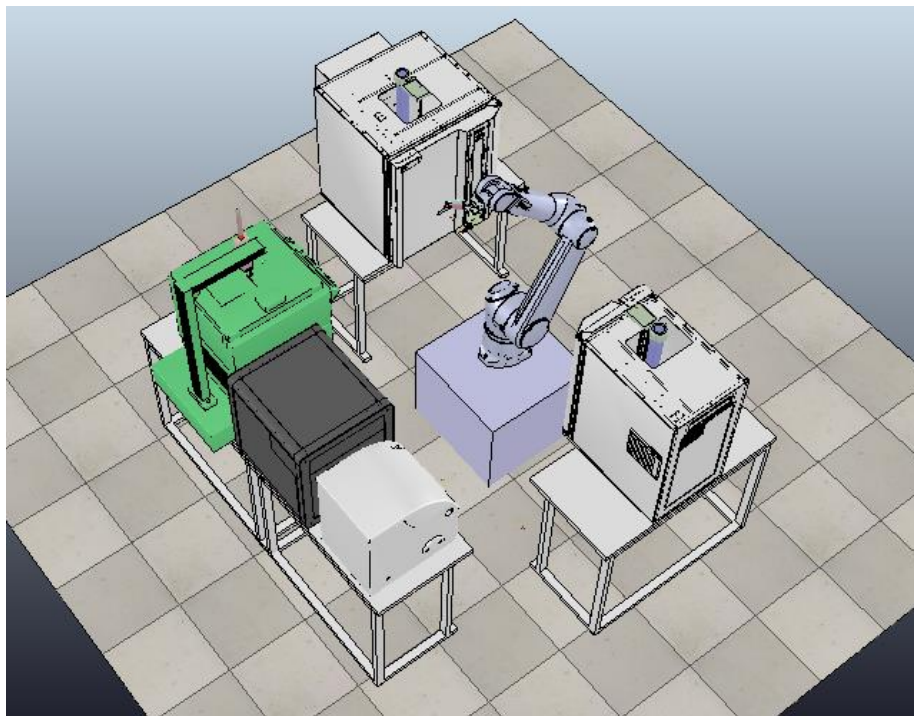


Image 11: Diagonal view of the island layout for biotechnology laboratory

² The gray cube represents the frame of the lab, in other words its limits. We could think of it as a metallic structure, similar to the case with the linear layout.

6

KINEMATIC ANALYSIS OF MANIPULATORS

6.1 Introduction

In this chapter, the most basic details about the kinematics of manipulators will be mentioned and thorough calculations and relationship derivations will be omitted, since for the needs of the current project and for modelling two different robotic structures, the Robotics System Toolbox [17] of MATLAB was utilized to facilitate the procedure and prevent unnecessary long and complex mathematical calculations. This toolbox provides many features that are useful for the study and simulation of classic type robotic arm, for example things like kinematics, dynamics and trajectory generation. The toolbox also provides functions for handling and converting data types, such as vectors, as well as homogeneous and unit-quaternions, axis-angle transformations that are necessary to represent the position and orientation respectively in the 3 dimensions.

It is crucial however that there is a solid background and knowledge of the kinematic analysis of a robotic manipulator, so that the functions offered by the Robotics System Toolbox can be used correctly.

6.2 Kinematics

Kinematics is the science of motion that treats the subject without regard to the forces that cause it. Within the science of kinematics, one studies the position, the velocity, the acceleration, and all higher order derivatives of the position variables -with respect to time or any other variable(s). Hence, the study of the kinematics of manipulators refers to all the geometrical and time-based properties of the motion. The relationships between these motions and the forces and torques that cause them constitute the problem of dynamics. [20] In order to deal with the complex geometry of a manipulator, we affix frames to the links of the mechanism, and then describe the relationships between these frames. The study of manipulator kinematics involves, among other things, how the locations of these frames change as the mechanism articulates.

The central topic of this chapter is a method to compute the position and orientation of the manipulator's end-effector relative to the base of the manipulator as a function of the joint variables. In order to fulfill this goal, there are two problems that need to be solved: the direct or forward kinematics problem and the inverse kinematics problem.

6.2.1 Forward Kinematics

A manipulator consists of a series of rigid bodies (links) connected by means of kinematic pairs or joints. Joints can be essentially of two types: revolute and prismatic. Conventional representations of the two types of joints are sketched in **Figure 19**. The whole structure forms a kinematic chain. One end of the chain is constrained to a base. An end-effector (gripper, tool) is connected to the other end allowing manipulation of objects in space. From a topological viewpoint, the kinematic chain is termed open, when there is only one sequence of links connecting the two ends of the chain. Alternatively, a manipulator contains a closed kinematic chain, when a sequence of links forms a loop. The mechanical structure of a manipulator is characterized by a number of degrees of freedom (DOFs) which uniquely determine its posture. Each DOF is typically associated with a joint articulation and constitutes a joint variable. The aim of forward, or else direct, kinematics is to compute the pose of the end-effector as a function of the joint variables.

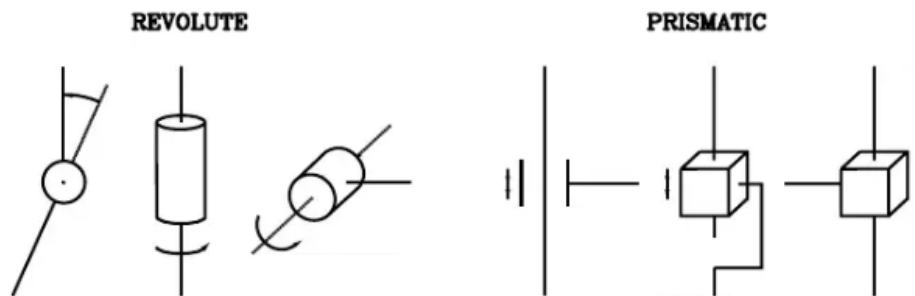


Figure 19: Conventional representations of joints[21]

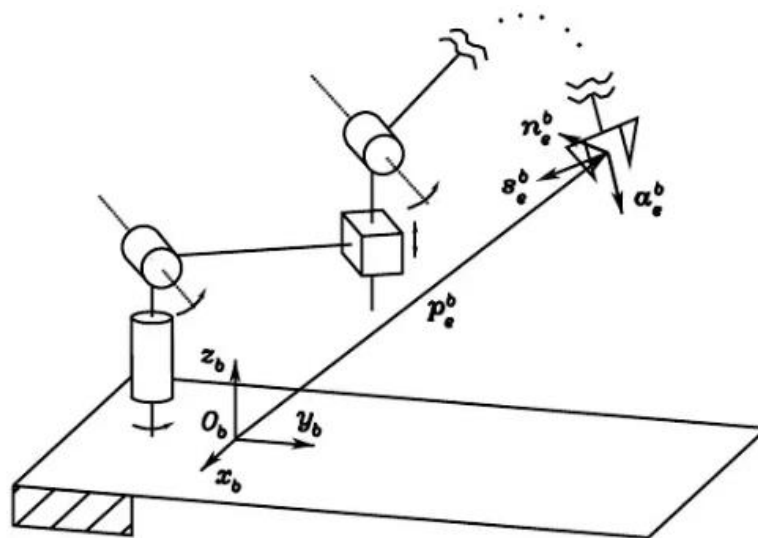


Figure 20: Description of the position and orientation of the end-effector frame[21]

The pose of a body with respect to a reference frame is described by the position vector of the origin and the unit vectors of a frame attached to the body. The transformation describing the position of the end-effector relative to the base is obtained by simply concatenating transformations between frames fixed in adjacent links of the chain. This leads to finding an equivalent 4x4 homogeneous transformation matrix that relates the spatial displacement of the end-effector coordinate frame to the base frame. Hence, with respect to a reference

frame $O_b-x_b y_b z_b$, the direct kinematics function is expressed by the homogeneous 4x4 transformation matrix:

$$T_e^b(q) = \begin{bmatrix} n_e^b(q) & s_e^b(q) & a_e^b(q) & p_e^b(q) \\ 0 & 0 & 0 & 1 \end{bmatrix}$$

, where q is the $(n \times 1)$ vector of joint variables, n_e, s_e, a_e are the unit vectors of a frame attached to the end-effector, and p_e is the position vector of the origin of such a frame with respect to the origin of the base frame $O_b-x_b y_b z_b$ (**Figure 20**). n_e, s_e, a_e and p_e are a function of q . The frame $O_b-x_b y_b z_b$ is termed base frame. The frame attached to the end-effector is termed end-effector frame and is conveniently chosen according to the particular task geometry. If the end-effector is a gripper, the origin of the end-effector frame is located at the centre of the gripper, the unit vector a_e is chosen in the approach direction to the object, the unit vector s_e is chosen normal to a_e in the sliding plane of the jaws, and the unit vector n_e is chosen normal to the other two so that the frame (n_e, s_e, a_e) is right-handed. [21]

6.2.2 Joint Space and Operational Space

As described in the previous sections, the direct kinematics equation of a manipulator allows the position and orientation of the end-effector frame to be expressed as a function of the joint variables with respect to the base frame. If a task is to be specified for the end-effector, it is necessary to assign the end-effector position and orientation, eventually as a function of time (trajectory). This is quite easy for the position. On the other hand, specifying the orientation through the unit vector triplet (n_e, s_e, a_e) is quite difficult, since their nine components must be guaranteed to satisfy the orthonormality constraints imposed before at each time instant. This problem will be resumed in the Differential Kinematics section.

The problem of describing end-effector orientation admits a natural solution if one of the above minimal representations is adopted. In this case, indeed, a motion trajectory can be assigned to the set of angles chosen to represent orientation. Therefore, the position can be given by a minimal number of coordinates with regard to the geometry of the structure, and the orientation can be specified in terms of a minimal representation (Euler angles) describing the rotation of the end-effector frame with respect to the base frame. In this way, it is possible to describe the end-effector pose by means of the $(m \times 1)$ vector, with $m \leq n$,

$$x_e = \begin{bmatrix} p_e \\ \varphi_e \end{bmatrix}$$

, where p_e describes the end-effector position and φ_e its orientation.

This representation of position and orientation allows the description of an end-effector task in terms of a number of inherently independent parameters. The vector x_e is defined in the space in which the manipulator task is specified. Hence, this space is typically called operational space. On the other hand, the joint space (configuration space) denotes the space in which the $(n \times 1)$ vector of joint variables

$$q = \begin{bmatrix} q_1 \\ \vdots \\ q_n \end{bmatrix}$$

, is defined. It is $q_i = \vartheta_i$ for a revolute joint and $q_i = d_i$ for a prismatic joint. Accounting for dependence of position and orientation from the joint variables, the direct kinematics equation can be written in following form:

$$x_e = k(q)$$

The $(m \times 1)$ vector function $k(\cdot)$ — nonlinear in general — allows computation of the operational space variables from the knowledge of the joint space variables. It is worth noticing that the dependence of the orientation components of the function $k(q)$ on the joint variables is not easy to express except for simple cases. In fact, in the most general case of a six-dimensional operational space ($m = 6$), the computation of the three components of the function $\varphi_e(q)$ cannot be performed in closed form but goes through the computation of the elements of the rotation matrix, i.e., $n_e(q)$, $s_e(q)$, $a_e(q)$. The equations that allow the determination of the Euler angles from the triplet of unit vectors n_e, s_e, a_e were given before. [21]

6.2.3 Inverse Kinematics

The direct kinematics establish the functional relationship between the joint variables and the end-effector position and orientation. The inverse kinematics problem consists of the determination of the joint variables corresponding to a given end-effector position and orientation. The solution to this problem is of fundamental importance in order to transform the motion specifications, assigned to the end-effector in the operational space, into the corresponding joint space motions that allow execution of the desired motion.

As regards the direct kinematics equation with the transformation matrixes, the end-effector position and rotation matrix are computed in a unique manner, once the joint variables are known. On the other hand, the inverse kinematics problem is much more complex for the following reasons:

- The equations to solve are in general nonlinear, and thus it is not always possible to find a closed-form solution
- Multiple solutions may exist.
- Infinite solutions may exist, e.g., in the case of a kinematically redundant manipulator.
- There might be n admissible solutions, in view of the manipulator kinematic structure. The existence of solutions is guaranteed only if the given end-effector position and orientation belong to the manipulator dexterous workspace.

The existence of mechanical joint limits may eventually reduce the number of admissible multiple solutions for the real structure. In cases where solutions do exist, they often cannot be presented in closed form, so numerical methods are required. [21]

6.3 Differential Kinematics

In the previous section, direct and inverse kinematics equations establishing the relationship between the joint variables and the end-effector pose were derived. In this section,

differential kinematics is presented which gives the relationship between the joint velocities and the corresponding end-effector linear and angular velocity. This mapping is described by a matrix, termed geometric Jacobian, which depends on the manipulator configuration. Alternatively, it is possible to compute the Jacobian matrix via differentiation of the direct kinematics function with respect to the joint variables, if the end-effector pose is expressed with reference to a minimal representation in the operational space. The resulting Jacobian, termed analytical Jacobian, in general differs from the geometric one. The Jacobian matrix depends on the –current- configuration of the robot. The Jacobian constitutes one of the most important tools for manipulator characterization. In fact, it is useful for finding singularities, analyzing redundancy, determining inverse kinematics algorithms, describing the mapping between forces applied to the end-effector and resulting torques at the joints (statics) and deriving dynamics equations of motion and designing operational space control schemes. [21]

6.3.1 Geometric Jacobian

Consider an n-DOF manipulator. The direct kinematics equation can be written in the form

$$T_e(q) = \begin{bmatrix} R_e(q) & p_e(q) \\ 0^T & 1 \end{bmatrix}$$

Where $q = [q_1 \dots q_n]^T$ is the vector of joint variables. Both end-effector position and orientation vary as q varies.

The goal of the differential kinematics is to find the relationship between the joint velocities and the end-effector linear and angular velocities. In other words, it is desired to express the end-effector linear velocity \dot{p}_e and angular velocity ω_e as a function of the joint velocities \dot{q} . As will be seen afterwards, the sought relations are both linear in the joint velocities, i.e.,

$$\begin{aligned} \dot{p}_e &= J_p(q)\dot{q} \\ \omega_e &= J_o(q)\dot{q} \end{aligned}$$

J_p is the (3×n) matrix relating the contribution of the joint velocities \dot{q} to the end-effector linear velocity \dot{p}_e while in J_o is the (3×n) matrix relating the contribution of the joint velocities \dot{q} to the end-effector angular velocity ω_e . In compact form, the two above relationships can be written as:

$$\dot{x}_e = v_e = \begin{bmatrix} \dot{p}_e \\ \omega_e \end{bmatrix} = J(q)\dot{q}$$

, which represents the manipulator differential kinematics equation. The (6×n) matrix J is the manipulator geometric Jacobian:

$$J = \begin{bmatrix} J_p \\ J_o \end{bmatrix}$$

, which in general is a function of the joint variables. [21]

6.3.2 Inverse Differential Kinematics

Previously, it was shown how the inverse kinematics problem admits closed-form solutions only for manipulators having a simple kinematic structure. Problems arise whenever the end-effector attains a particular position and/or orientation in the operational space, or the structure is complex and it is not possible to relate the end-effector pose to different sets of joint variables, or else the manipulator is redundant. These limitations are caused by the highly non-linear relationship between joint space variables and operational space variables. On the other hand, the differential kinematics equation represents a linear mapping between the joint velocity space and the operational velocity space, although it varies with the current configuration. This fact suggests the possibility to utilize the differential kinematics equations to tackle the inverse kinematics problem. Suppose that a motion trajectory is assigned to the end-effector in terms of v_e and the initial conditions on position and orientation. The aim is to determine a feasible joint trajectory $(q(t), \dot{q}(t))$ that reproduces the given trajectory. By considering the relationship found above:

$$v_e = J(q)\dot{q}$$

, the joint velocities can be obtained via simple inversion of the Jacobian matrix

$$\dot{q} = J^{-1}(q)v_e$$

If the initial manipulator posture $q(0)$ is known, joint positions can be computed by integrating velocities over time, i.e.

$$q(t) = \int_0^t \dot{q}(\zeta) d\zeta + q(0).$$

The integration can be performed in discrete time by resorting to numerical techniques. The simplest technique is based on the Euler integration method, which is that given an integration interval Δt , if the joint positions and velocities at time t_k are known, the joint positions at time $t_{k+1} = t_k + \Delta t$ can be computed as

$$q(t_k + 1) = q(t_k) + \dot{q}(t_k)\Delta t$$

This technique for inverting kinematics is independent of the solvability of the kinematic structure. Nonetheless, it is necessary that the Jacobian be square and of full rank .[21]

6.3.3 Kinematic Singularities

Kinematic singularities have long been recognized as causing one of the most serious problems in programming and control of robotic manipulators. It is well-known that when a manipulator is at-or is in the neighborhood of-a singular configuration, severe restrictions may occur on its motion. Avoiding or reducing the effects of singularities has been an attractive topic which has captured the attention of many researchers in robotics during the last decade. A remarkable number of methods and/or algorithms aimed at computing well-behaved or robust inverse kinematics solutions have been proposed in the literature, and many papers in the past have presented simulation results. Close to a kinematic singularity, the usual inverse differential kinematics solutions based on Jacobian (pseudo-) inverse become ill-conditioned,

and this is experienced in the form of very high joint velocities and large control deviations. Nonetheless, when a pre-programmed reference end-effector trajectory is to be tracked, it is possible either to interpolate in joint coordinates close to singular configurations or to plan motions so that singularities are avoided. On the other hand, in real-time and sensory control of robotic manipulators, the reference trajectory is not known a priori and some remedies must be taken in order to counteract the unexpected occurrence of singularities. The same kind of problem is encountered in joy-stick control of a robot if the operator attempts to lead the robot through-or nearby-a singularity using end-effector motion increments.[22]

6.4 Inverse Kinematics Algorithms

Computation of joint velocities is obtained by using the inverse of the Jacobian evaluated with the joint variables at the previous instant of time

$$q(t_k + 1) = q(t_k) + J^{-1}(q(t_k))v_e(t_k)\Delta t$$

It follows that the computed joint velocities \dot{q} do not coincide with those satisfying

$$\dot{q} = J^{-1}(q)v_e$$

in the continuous time. Therefore, reconstruction of joint variables q is entrusted to a numerical integration. As a consequence, the end-effector pose corresponding to the computed joint variables differs from the desired one. This inconvenience can be overcome by resorting to a solution scheme that accounts for the error between the desired and the actual end-effector position and orientation. Let

$$e = x_d - x_e$$

be the expression of such error.

Considering its derivative, we get:

$$\dot{e} = \dot{x}_d - \dot{x}_e = \dot{x}_d - J(q)\dot{q}$$

For this equation to lead to an inverse kinematics algorithm, it is worth relating the computed joint velocity vector \dot{q} to the error e so that a differential equation describing error evolution over time can be given. Nonetheless, it is necessary to choose a relationship between \dot{q} and e that ensures convergence of the error to zero.

6.4.1 Inverse Jacobian

The inversion of the Jacobian, which was mentioned before, can represent a serious inconvenience not only at a singularity but also in the neighborhood of a singularity. For instance, for the Jacobian inverse it is well known that its computation requires the computation of the determinant. In the neighborhood of a singularity, the determinant takes on a relatively small value which can cause large joint velocities. [21]

6.4.2 Pseudo-Inverse Jacobian

For kinematically redundant robots, the Jacobian matrix is non-square and its inverse can be obtained using a pseudo-inverse J^+ . Specifically, if the Jacobian matrix J has a size of m rows and n columns ($m \neq n$), i.e., J is a non-square matrix, its inverse matrix cannot be computed. In order to solve inverse kinematics task for this case, pseudoinverse of Jacobian matrix is used, which is expressed as:

$$J^+ = (J^T J)^{-1} J^T$$

Pseudoinverse J^+ , also called Moore-Penrose inverse of Jacobian matrix, gives the best possible solution in the sense of least squares.

However, by using the pseudoinverse, the problems of singularities in the Jacobian still remain. These singularities might occur for instance, when multiple links become aligned in the same direction and subsequently, identical derivatives for several joints of the robot arm are obtained. Inversion of nearly singular matrices results in excessively large velocities and causes unrealistic behavior with oscillations around a singular configuration. In addition to that, the limits of the robots are not taken into consideration and may lead to false and inaccurate results.[23]

6.4.3 Damped Least Squares (DLS)

An effective strategy that allows motion control of manipulators in the neighborhood of kinematic singularities is the damped least-squares technique, which is also the method that was used within this study. The method corresponds to solving the equation:

$$J^T(q) \dot{x}_r = (J^T(q)J(q) + \lambda^2 I) \dot{q}$$

$\lambda \geq 0$ is the damping factor and I is the $(n \times n)$ identity matrix, which depends on the dimensions of the Jacobian and thus on the DOF of the respective robot. Also,

$$\dot{x}_r = \dot{x}_d + Ke$$

is the reference value vector with \dot{x}_d that is the time derivative of the desired task function, K is a positive definite (usually diagonal) matrix and e is the task-space error, to which the orientation error can also be incorporated .[24]

It can be easily shown that the equation above can be formally written as

$$\dot{q} = (J^T(q)J(q) + \lambda^2 I)^{-1} J^T(q) \dot{x}_r$$

It is worth noting that when $\lambda = 0$, the damped least-squares solution reduces to a regular matrix inversion which is ill-conditioned close to a singularity. So, it is essential to select suitable values for the damping factor. Small values of λ give accurate solutions, but low robustness to the occurrence of singular and near-singular configurations. Large values of λ result in low tracking accuracy even when a feasible and accurate solution would be possible.

The damping factor λ determines the degree of approximation introduced with respect to the pure least-squares solution. In the same manner, using a constant value for λ may turn out to

be inadequate for obtaining good performance over the entire manipulator workspace. An effective choice is to adjust λ as a function of some measure of closeness to the singularity at the current configuration of the manipulator. To this purpose manipulability measures or estimates of the smallest singular value can be adopted. A singular region can be defined on the basis of the estimate of the smallest singular value of J . Outside the region the exact solution is used, while inside the region a configuration varying damping factor is introduced to obtain the desired approximate solution. The factor must be chosen so that continuity of joint velocity q is ensured in the transition at the border of the singular region. We have selected the damping factor according to the following law:

$$\lambda^2 = \left\{ \begin{array}{ll} 0 & , \sigma \geq \varepsilon \\ (1 - (\frac{\sigma}{\varepsilon})^2) \lambda_{max}^2 & , otherwise \end{array} \right\}$$

, where σ : the estimate of the smallest singular value of J

ε : a threshold that defines the size of the singular region

The value of λ_{max} is at the user's disposal to suitably shape the solution in the neighborhood of a singularity. Utilizing the singular value decomposition method, we can find an estimate of the smallest singular value of J . [22]

6.5 Trajectory Planning

The goal of trajectory planning is to generate the reference inputs to the motion control system which ensures that the manipulator executes the planned trajectories. The user typically specifies a number of parameters to describe the desired trajectory. Planning consists of generating a time sequence of the values attained by an interpolating function, typically a polynomial, of the desired trajectory.

The minimal requirement for a manipulator is the capability to move from an initial posture to a final assigned posture. The transition should be characterized by motion laws requiring the actuators to exert joint generalized forces which do not violate the saturation limits and do not excite the typically modelled resonant modes of the structure. It is then necessary to devise planning algorithms that generate suitably smooth trajectories. In order to avoid confusion between terms often used as synonyms, the difference between a path and a trajectory is to be explained. A path denotes the locus of points in the joint space, or in the operational space, which the manipulator has to follow in the execution of the assigned motion; a path is then a pure geometric description of motion. On the other hand, a trajectory is a path on which a timing law is specified, for instance in terms of velocities and/or accelerations at each point.

In principle, it can be conceived that the inputs to a trajectory planning algorithm are the path description, the path constraints, and the constraints imposed by manipulator dynamics, whereas the outputs are the end-effector trajectories in terms of a time sequence of the values attained by position, velocity and acceleration. [21]

Whenever it is desired that the end-effector motion follows a geometrically specified path in the operational space, it is necessary to plan trajectory execution directly in the same space. Planning can be done either by interpolating a sequence of prescribed path points or by generating the analytical motion primitive and the relative trajectory in a punctual way. In

both cases, the time sequence of the values attained by the operational space variables is utilized in real time to obtain the corresponding sequence of values of the joint space variables, via an inverse kinematics algorithm.

To that respect, it is convenient to refer to the parametric description of paths in space. Then let p be a (3×1) vector and $f(\sigma)$ a continuous vector function defined in the interval $[\sigma_i, \sigma_f]$. Consider the equation

$$p = f(\sigma)$$

With reference to its geometric description, the sequence of values of p with σ varying in $[\sigma_i, \sigma_f]$ is termed path in space. The equation above defines the parametric representation of the path Γ and the scalar σ is called parameter. As σ increases, the point p moves on the path in a given direction. This direction is said to be the direction induced on Γ by the parametric representation $p = f(\sigma)$. A path is closed when $p(\sigma_f) = p(\sigma_i)$, otherwise it is open.

Let p_i be a point on the open path Γ on which a direction has been fixed. The arc length s of the generic point p is the length of the arc of Γ with extremes p and p_i if p follows p_i , the opposite of this length if p precedes p_i . The point p_i is said to be the origin of the arc length ($s = 0$). From the above presentation it follows that to each value of s a well-determined path point corresponds, and then the arc length can be used as a parameter in a different parametric representation of the path Γ

$$p = f(s), s \in [0, L]$$

, where $s = \frac{\sigma}{L}, \sigma \in [0, L]$, with L representing the current length of the path.

The range of variation of the parameter s will be the sequence of arc lengths associated with the points of Γ . Consider a path Γ represented by the relationship $p = f(s)$. Let p be a point corresponding to the arc length s . Except for special cases, p allows the definition of three unit vectors characterizing the path. The orientation of such vectors depends exclusively on the path geometry, while their direction depends also on the direction induced on the path. [21]

Considering the simplest case, which is connection of the initial and final points of a path with line segments, the parametric representation of the path is expressed as following:

$$p(s) = p_i + s(p_f - p_i)$$

The velocity of point p is given by the time derivative of p :

$$\dot{p}(s) = \frac{dp}{ds} \dot{s} = (p_f - p_i) \dot{s}$$

Then, \dot{s} represents the magnitude of the velocity vector relative to point p , taken with the positive or negative sign depending on the direction of \dot{p} along t . The magnitude of \dot{p} starts from zero at $t = 0$, then it varies with a parabolic profile as the above choice of linear segments for $s(t)$, and finally it returns to zero at $t = t_f$.

Let x_e be the vector of operational space variables expressing the pose of the manipulator's end-effector. Generating a trajectory in the operational space means to determine a function $x_e(t)$ taking the end-effector frame from the initial to the final pose in a time t_f along a given

path with a specific motion timing law. First, consider end-effector position. Let $p_e = f(s)$ be the (3×1) vector of the parametric representation of the path Γ as a function of the arc length s . The origin of the end-effector frame moves from p_i to p_f in a time t_f . For simplicity, suppose that the origin of the arc length is at p_i and the direction induced on Γ is that going from p_i to p_f . The arc length then goes from the value $s = 0$ at $t = 0$ to the value $s = s_f$ (path length) at $t = t_f$. The timing law along the path is described by the function $s(t)$. In order to find an analytic expression for $s(t)$, either a cubic polynomial or a sequence of linear segments with parabolic blends can be chosen. [21]

The choice of a third-order polynomial function to generate a timing law represents a valid solution for the problem at issue. Therefore, the cubic polynomial and its derivative presented below can be chosen.

$$s(t) = a_3 t^3 + a_2 t^2 + a_1 t^1 + a_0$$

$$\dot{s}(t) = 3a_3 t^2 + 2a_2 t + a_1$$

Usually, $t_i = 0$ and $t_f = T$, which is the total time assigned by the user to traverse the path. Since four coefficients are available, it is possible to impose, besides the initial and final position values $s(0)$ and $s(T)$, the initial and final magnitudes of the velocity vector relative to point p , $\dot{s}(0)$ and $\dot{s}(T)$, which are $\dot{s}(0) = 0$, $\dot{s}(T) = 0$ as it was already mentioned. Determination of a specific trajectory is given by the solution to the following system of equations:

$$a_0 = 0$$

$$a_1 = 0$$

$$a_3 t_f^3 + a_2 t_f^2 = 1$$

$$3a_3 t_f^2 + 2a_2 t_f = 0$$

However, in the case where the trajectory is more stringent and the constraint condition is increased, the cubic polynomial interpolation cannot satisfy the requirement, and a high order polynomial is used for interpolation. For example, when the starting point and the ending point of a certain path are specified for the position, velocity and acceleration of their joints, a quintic polynomial can be used for interpolation. The functional equation of the joint angle, velocity and acceleration is as follows:

$$s(t) = a_5 t^5 + a_4 t^4 + a_3 t^3 + a_2 t^2 + a_1 t^1 + a_0$$

$$\dot{s}(t) = 5a_5 t^4 + 4a_4 t^3 + 3a_3 t^2 + 2a_2 t^1 + a_1$$

$$\ddot{s}(t) = 20a_5 t^3 + 12a_4 t^2 + 6a_3 t^1 + 2a_2$$

Usually, $t_i = 0$ and $t_f = T$, which is the total time assigned by the user to traverse the path. Since six coefficients are available, it is possible to impose, similar to before the values $s(0) = 0$, $s(T) = 1$, $\dot{s}(0) = 0$, $\dot{s}(T) = 0$, $\ddot{s}(0) = 0$, $\ddot{s}(T) = 0$. Determination of a specific trajectory is given by the solution to the following system of equations:

$$a_0 = 0$$

$$a_1 = 0$$

$$a_2 = 0$$

$$a_5 t^5 + a_4 t^4 + a_3 t^3 = 1$$

$$5a_5 t^4 + 4a_4 t^3 + 3a_3 t^2 = 0$$

$$20a_5 t^3 + 12a_4 t^2 + 6a_3 t = 0$$

The same approach is also valid for the creation of joint trajectories, but instead of points in space, specified are the joint values q . In the case of joint trajectories, there is no need for solving the inverse kinematics. [25]

6.6 Implementation on Robotic Manipulators

For the purposes of the current study, two robotic manipulators are modeled and analyzed as to their kinematics, in order to be incorporated into the environment of the biotechnology laboratory that is set up. The methodology followed in both cases is similar and only few things change throughout. In general, the steps that follow are according to the respective theory analyzed above.

I. Forward Kinematics (FK)

The theory used for the trajectory planning in the cartesian space can also be extrapolated in the joint space, where the timing law can basically remain the same, and the only things that change in the trajectory is that instead of the initial and final desired position p and the velocity of point \dot{p} , we use the initial and final desired joint angles q and their respective velocities \dot{q} . In the current thesis, there are two ways of expressing the forward kinematics.

- a. When the desired task is to retrieve the current position of the end-effector, which is used for the trajectory planning in the cartesian space, then the position is expressed as the homogenous transformation from the basis of the robot to its tip (end-effector). Used for this task is the built-in function of Matlab `getTransform`.

```

17 | %offset between visual EE and actual EE
18 - | T_dummy_e=[1 0 0 0.071004;0 1 0 0.029014 ; 0 0 1 0 ;0 0 0 1];
19 |
20 | %homogenous transformation for robot chain
21 - | Trans= getTransform(robot,double(q),'ee_link');
22 |
23 | %Transformation from visual EE to actual EE
24 - | T_fi= Trans* T_dummy_e;
25 - | P_o= T_fi(1:3,4);

```

Figure 21: Calculation of Homogenous Transform T with Matlab Robotics Toolbox

If there is an offset between the end-effector as it is expressed in the URDF, and the end-effector as it is expressed in the visual environment, it should always be taken into consideration when expressing the final position of the

end-effector. For example, this offset could be presented when a new gripper part is tested on a robot.

- b. When the desired task is to bring the robot arm to a specific configuration and when the position of the end-effector is of no importance, then the forward kinematics are expressed with the help of the trajectory planning in the joint space. For example, if we want the robot to always return to a fixed “Home” configuration, then by setting the final configuration as q_f to specific values for each joint, and by retrieving the current configuration q_i of the robot, the trajectory can be planned. In this case there is no need for inverse kinematics to be solved, since the final position of the end-effector does not play a significant role. q_f and q_i are vectors of length (5x1) for the SCARA and (6x1) for the STAUBLI. It is also possible to create separate programs that each controls only a specific number of joints each time, if that is desired.

II. Trajectory Planning

For the trajectory planning, the simplest approaches possible have been adopted for each separate case. Namely:

a. SCARA

Taking into account the structure of the SCARA type robot, which allows movements along the x,y and z axis, however rotation only around one axis- in our case the z axis-, the form of the trajectory does not need to be more complicated than movements along linear segments. To that respect, the cubic polynomial is used for the time law. The SCARA robot therefore translates from one position to the next, following a straight line. The intermediate points must thus be carefully selected, so as to abide by this convention and receive better simulation results.

b. STAUBLI

As for the Staubli, which is a 6-axis robot, the trajectory is more stringent and the constraints are increased. In that case the cubic polynomial interpolation cannot satisfy the requirements, and a fifth order polynomial is used for interpolation. The quantic polynomial ensures smoother transition between the different positions when compared to the cubic polynomial and is preferred for articulated robots, like the STAUBLI.

III. Jacobian

The Jacobian depends on the current configuration of the robot, it therefore changes every time, since the orientation and position of the end-effector change accordingly. In order to facilitate its calculation at every time step, the built-in function of Matlab `geometricJacobian` is used. However, the Jacobian calculated by Matlab has its rows reversed. Therefore, it is necessary to reverse their order before proceeding further. The Jacobian retrieves the position and orientation of the end-effector to the base frame of the robot.

```

85     %%%% JACOBIAN %%%%
86     %calculate geometric jacobian
87 -   Jac_rev = geometricJacobian(robot,double(q),'ee_link');
88
89     %reverse rows
90     %Matlab default (first rotation, second transaltion)
91 -   Jac= [Jac_rev(4:6,:);Jac_rev(1:3,:)] ;
92

```

Figure 22: Calculation of Geometric Jacobian with Matlab Robotics Toolbox

- a. **SCARA**: Only the three first and the last one rows are useful in the case of the Jacobian for the SCARA type robot. This is due to the fact that SCARA robots can only rotate around one axis, which in our case is the z-axis. Therefore, we do not need the whole Jacobian matrix.
- b. **STAUBLI**: The Staubli on the other hand, as a 6-axis robot, can move, as well as rotate around all of the axis. Therefore, the whole Jacobian matrix is maintained.

IV. Damping factor λ

The damping factor that is used for the DLS algorithm is calculated according to the respective theory. SVD is utilized to retrieve the singular configuration matrix of the Jacobian and to find in that way an estimate of the smallest singular value. λ_{\max} was chosen to equal 0.04 in our case. This value depends on the user and the robot at hand. This number in our case was retrieved based on the robot models and the bibliography recommendations. The threshold ϵ was calculated for the singular case where the robot arms had all of their links aligned, which is a singular position for both of the robots.

```

97     %damping factor  $\lambda$  via SVD
98 -   [~,S,~] = svd(J);
99 -   sigma=min(S(S>0));
100 -   lamdamax=0.04;
101 -   eps= 10e-4;
102
103 -   if sigma >= eps
104 -       lamda = 0;
105 -   else
106 -       lamda= sqrt((1- ((sigma/eps)^2)*(lamdamax^2)));
107 -   end

```

Figure 23: Calculation of damping factor λ with SVD

V. DLS

As mentioned before, the inverse kinematics algorithm that is used is expressed in the equation below, which calculates the joint velocities of the robot.

$$\dot{q} = (J^T(q)J(q) + \lambda^2 I)^{-1} J^T(q)(v_d + Ke) \quad (I)$$

Incorporating the joint limits that apply in reality for a robotic manipulator can be tricky. In order to include the limits that may already be specified for the robot, we must reformulate the problem using quadratic programming.

Matlab has the built in function `quadprog` that is a solver for quadratic objective functions with linear constraints. `quadprog` finds a minimum for a problem specified by

$$\min_x \frac{1}{2} x^T H x + f^T x \text{ such that } \begin{cases} A \cdot x \leq b, \\ Aeq \cdot x = beq, \\ lb \leq x \leq ub. \end{cases} \quad (II)$$

, where $H, A,$ and Aeq are matrices, and $f, b, beq, lb, ub,$ and x are vectors. $x = \text{quadprog}(H, f, A, b, Aeq, beq, lb, ub)$ solves the preceding problem subject to the additional restrictions $lb \leq x \leq ub$. The inputs lb and ub are vectors of doubles, and the restrictions hold for each x component. If no equalities exist, set $Aeq = []$ and $beq = []$ and similarly if no $A \cdot x \leq b$ restrictions exist, the respective arguments are set to $[]$. Taking into account that the robots have a joint range and limits that have been mentioned previously and that the manipulators need to abide by, in the case studied the existing restrictions take the form $lb \leq x \leq ub$, where lb the minimum and ub the maximum limits for each joint.

Combining the relationships (I) and (II), it is apparent that

$$\begin{aligned} x &= \dot{q} \\ H &= J^T(q)J(q) + \lambda^2 I \\ f &= -(v_d + Ke)^T J(q) \end{aligned}$$

We can now find the values for \dot{q} , which will be used to compute the new configuration of the robot joints at each time instant dt , which will be then fed to the VREP platform for every time step dt , updating thus the position of the joints and making the robot move according to the planned trajectory, until the final time T is reached.

```

110     %%%% QUADRATIC PROGRAMMING %%%%
111     %set lower-upper bounds for quadprog
112 -   q_min=[-1.9;0;-2.1;-2.5;0];
113 -   q_max= [1.75;1.9;2.1;2.5;0];
114 -   lb=(q_min-q)/dt;
115 -   ub=(q_max-q)/dt;
116
117     %Solving IK
118     %quadratic programming
119 -   H=(J'*J + ((lamda)^2)*eye(5,5));
120 -   b=([v;wd(3)]+ e);
121 -   f=- (b')*J ;
122 -   qd = quadprog(double(H),double(f), [], [], [], [], double(lb), double(ub));
123
124 -   q= q+qd*dt; %joint position at t+dt

```

Figure 24: Quadratic programming and solving of Inverse Kinematics with Matlab Robotics Toolbox

VI. Update configuration of manipulators and end-effector pose

After calculating the desired trajectory and solving the inverse kinematics at hand, the visualization of each iteration step is needed so that the robotic arm can smoothly move to the desired end-point and acquire a new pose in space. For this purpose, the VREP remote API functions for MATLAB client are used. These functions are fed with

the new values of q that are calculated at each time step dt and are translated into commands in the VREP environment, where the robot moves accordingly. The smaller the time step dt is, the smoother and more accurate the final motion of the manipulators is. This procedure from the beginning of the kinematic analysis to the final visualization is shown in **Figure 25**.

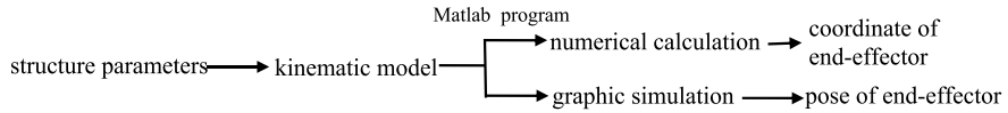


Figure 25: Validation flowchart of kinematic model[26]

The robotic manager architecture, incorporating sensors and cameras for the live localization of the machinery, the robotic arms and the well-plates is presented in **Figure 26** schematically for comprehension.

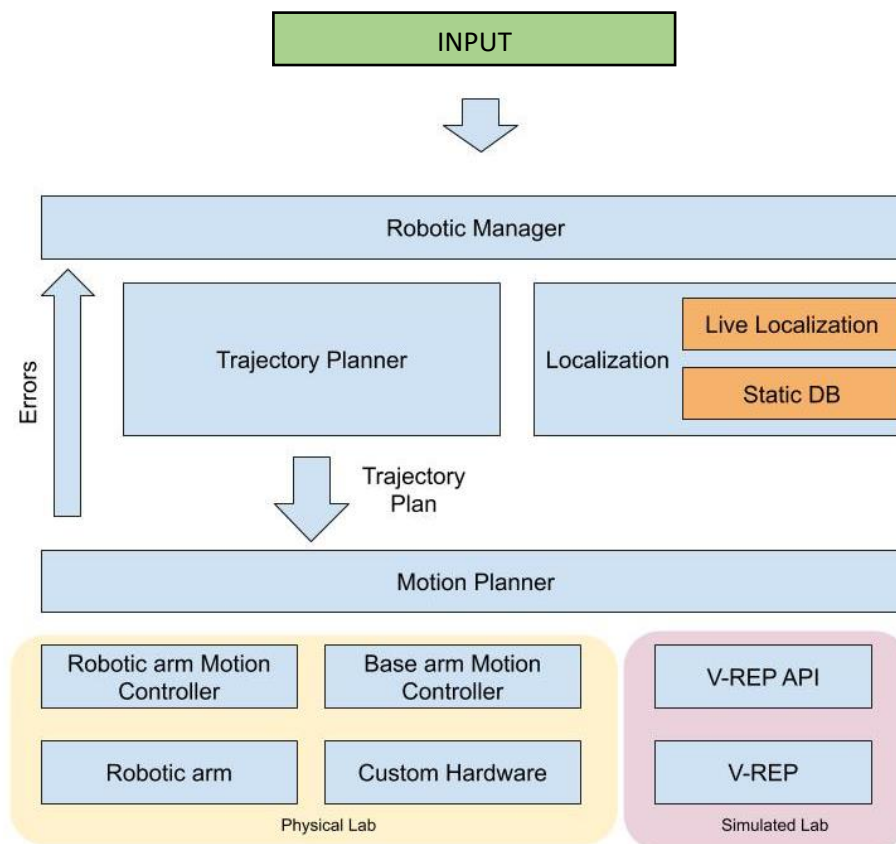


Figure 26: Robotic manager architecture

It is thus easily understood that the above mentioned approach, which is applied on two different robotic manipulators, can also be applied on other various robotic arms with small adjustments that mainly concern the robot itself, such as the number of DOF's, the range and limits of its joints as well as the lab settings that the robot is found in. However, it should be noted that this methodology is followed for the case where the machinery has predefined positions in space and also the consumables have predefined shapes and sizes. The behavior of the system under different circumstances is unknown and will not be analyzed within the frameworks of the current thesis.

7

SIMULATION

7.1 Visual Simulation Models

According to the information provided in the previous chapters, the simulation models that will be tested can be finalized. The most important factor of the simulation that has been stressed throughout the current project is to provide flexibility to the researcher and to be parameterized in a way that any experiment protocol can be brought through, regardless of the number or type of machines, the order of their use during an experiment or even regardless of the background of the user.

7.1.1 Robots

After expressing the kinematic chain of each robot as URDF file the models are inserted in the simulation scene. Each robot consists of its own links and joints, while in the URDF files two more entities were added, namely the `ee_link` and the `world`, which were mentioned in the respective chapter, as well.

The role of the `world` entity, which will be referred to as the robot's world frame and is by no means to be confused with the global frame of VREP, is to provide a reference frame for everything that happens in the simulation scene. Since the robotic arms constitute the central theme for the function of the robotic systems at hand, it is logical that not only the position and orientation of the robotic links, but also the position and orientation of all the components of a scene are expressed with reference to this frame. The `world` entity is fixed in the laboratory space, which is mandatory to have uniformity in the expression of different objects in the lab.

Respectively, the `ee_link` represents the actual final end-effector position, which is always approximately the middle of the gripper and the point where the microplate is attached. However, it is possible that the `ee_link` of the URDF file does not represent the actual gripping point, but rather the base of the gripper or the final joint of a robot. In that case, a visual `ee_link_dummy` is added in the VREP scene. The visual gripping point `ee_link_dummy` is then expressed with respect to the `ee_link` of the URDF, via the respective offset and this is later expressed with respect to the `world`. Maintaining a homogenous expression of position and orientation is the key to a successful and accurate simulation.

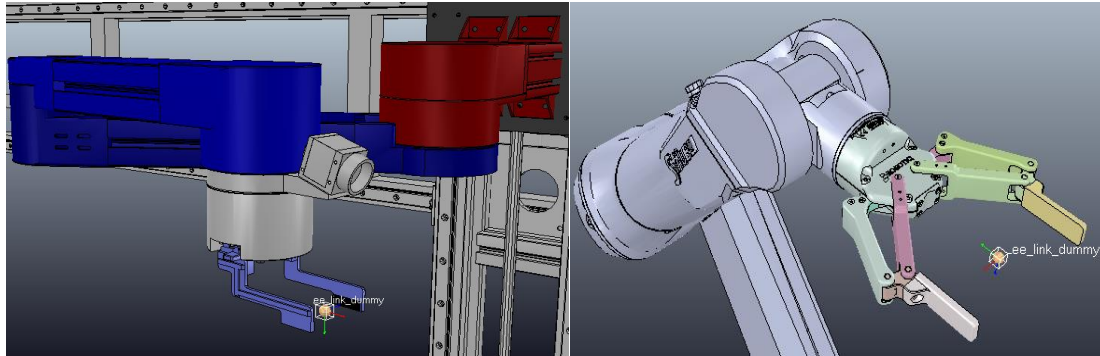


Image 12: ee_link_dummy for SCARA (left) and STAUBLI (right) robots

7.1.2 Lab Equipment

The lab equipment, including the machines, the input and output positions from which the microplates are received and returned to at the beginning and the end of each experiment respectively, as well as the consumables, are inserted in the scene according to the desired layout. The goal is to create an environment, where the robot will be able to spot the loading and unloading points of each machine with respect to its world frame. In order for the robot to understand, which machines it should visit during an experiment, dummy objects are set in the loading-unloading positions of each machine and are named after their machines. It is important that the orientation of these dummy points is the same as the orientation of the ee_link_dummy so that the robotic arm may be able to approach the right position with the correct orientation. The positions where the robotic arms should unload and load a microplate in the machines and the surroundings of the lab are presented in **Image 13**.

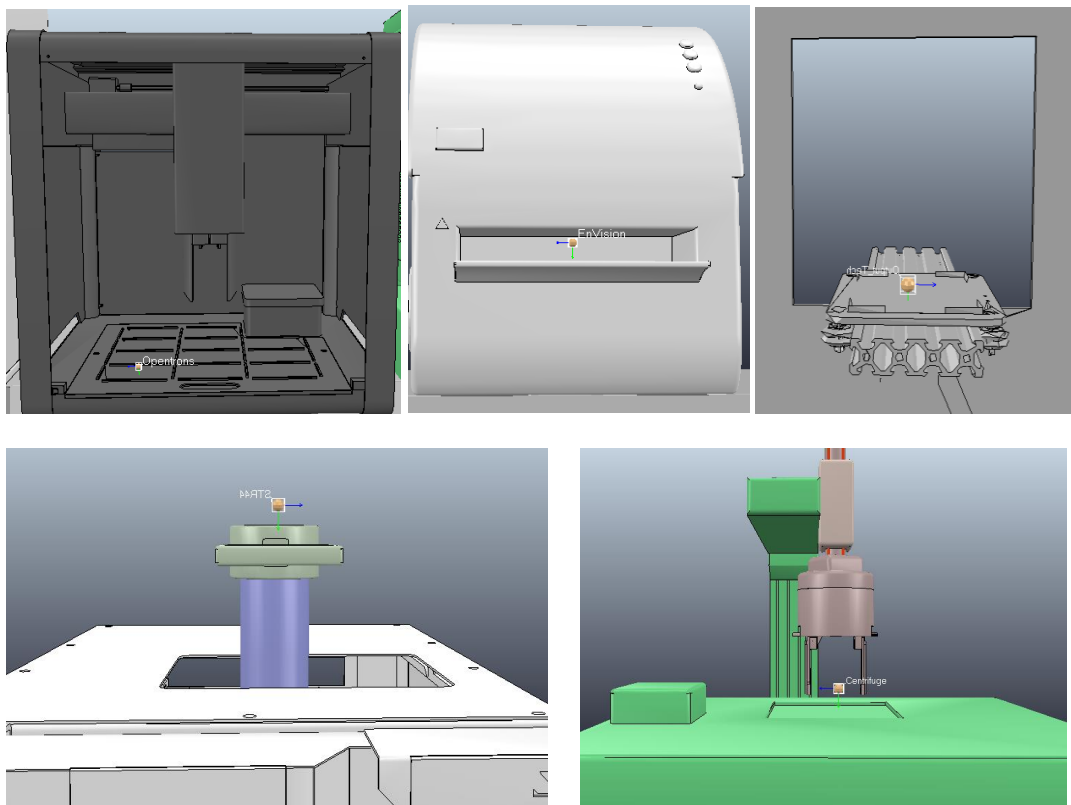


Image 13: Loading- unloading points of laboratory machines

7.1.3 Safe Positions

These dummies are not only used to express the position and orientation of an object with respect to the world frame of the robot, but are also used as references to describe some other positions in space, which are necessary for the robot in order to plan its trajectory smoothly.

For example it is highly recommended that intermediate points are used between the robot Home position and any Machine Position. Defining a Machine Safe Position helps eliminate collisions of the robot with the lab equipment. Such a machine position can be defined as the (Machine Position +/- an offset). The offset can represent a distance from the actual loading-unloading position which is deemed safe for the robot to approach, before completing its task.

Safe Positions in the experiments to follow are defined for following cases:

- Before the SCARA robotic arm approaches the rotary base on which the microplates change orientation to avoid collision with the machines during folding/ unfolding of the arm and with itself
- Before the SCARA robotic arm approaches the Input/ Output positions to avoid collisions with the frame of the laboratory
- Before the SCARA and the STAUBLI robotic arms approach the Loading/ Unloading positions of each machine to avoid irregular arm movements and collisions with the machines

In real-life experiments, this procedure is accomplished with the use of a live localization system, which gives feedback to the robot as to its end-effector position with the use of cameras and vision sensors.

7.1.4 Parameterization of the simulation

In our case, once the simulation environment is set and the dummies are defined, VREP stores this information and communicates it to Matlab. So, for example, by giving a command to Matlab for the robot to reach the Centrifuge, VREP having the machine's position and orientation stored, may parse this information to Matlab, where the code is responsible for the rest. Therefore, parameterizing the problem at hand is easy.

The existence of multiple intermediate points makes it necessary for the trajectory to be recalculated every time between two different points. More specifically, the trajectory is computed every time that the robot needs to move between two points A and B. Matlab requests from VREP the position and orientation of point A, which is the initial current position P_o of the end-effector, as well as the position and orientation of point B, which is the final desired position P_f the end-effector has to reach. After the robots moves from A to B, then the new position A' is basically the position B of the previous trajectory. In order for the robot to start a new movement between A' and C, a new trajectory with the updated positions has to be recalculated. The trajectory is then followed by the robotic manipulator according to its inverse kinematics programming and the position of the end-effector is updated in VREP at every time step dt .

Among other parameters that can be controlled by the user is the resolution of the results and the smoothness of the robot's movements. It is apparent that the smaller the time step dt is, the more accurate and smooth the movement of the robot will be, since the interpolation number is higher and more points of the trajectory are calculated.

7.2 Experiment Protocols

An experiment protocol describes the necessary actions for an experiment to be conducted, from its beginning to its end. Examples of experimental protocols are provided below for two experiments, which are dependent on each other, since Experiment 02 needs material from Experiment 01.

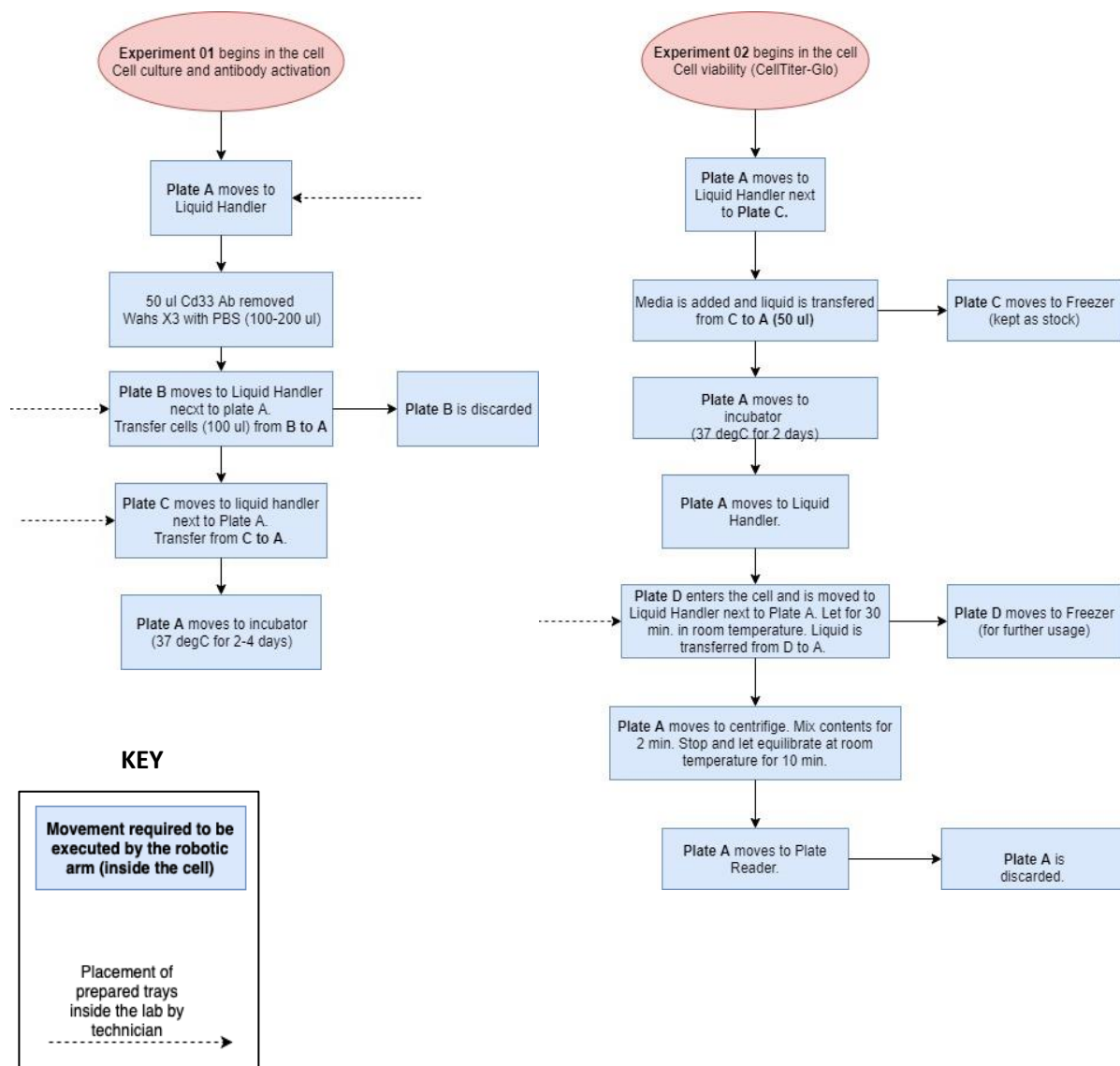


Figure 27: Experiment protocol examples

7.3 User Interface (UI)

The facilitation of the communication between the user (researcher) and the simulation environment is of major importance, since the platform must be accessible enough to people, who do not have deep robotics knowledge. The goal is to simply communicate an experiment protocol as presented above, with the least effort possible, thus building a UI friendly to its user is the first step towards a successful simulation.

Upon starting the programs `main_SCARA.m` and `main_STAUBLI.m`, which are the two Matlab programs responsible for everything that happens inside each lab, the user is asked to

```
Input working station:
```

At this point, the user can input the name of the workstations – laboratory machines – which are included in the experiment and in the order that the user wishes each machine to be used, along with the time that the user wishes for the test specimen to remain in each machine. The available machine options that the user can type for the laboratories at hand are:

- Opentrans
- Centrifuge
- EnVision
- STR44
- STR240

Each machine can be used more than once, if the experiment demands that a specific workstation is visited multiple times. After including all the machines and respective times in the correct order the user can type `stop` to indicate that the experiment protocol is complete and that all the necessary equipment have already been referred to.

For the needs of the current study, the times have not been taken into consideration, since they can even reach two days of waiting in a specific machine. Thus, this procedure is represented by pausing the arm movements for a few seconds.

After the protocol is input in the platform, the program checks if the robot is located in its Home position , which is a safe position for the robot to start any experiment. If it is, the user is prompted with the notification:

```
Robot is in Home Position-Ready to start experiment
```

Otherwise, the robot moves to its Home position and then the user is asked for one last if he/she wishes to proceed with the experiment. The default answer is set to YES.

```
Do you wish to continue to experiment? Y/N [Y]:
```

If the user types `N`, then the experiment is interrupted. If the user types `Y`, the experiment starts according to its protocol.

After completion of the experiment, the user is notified accordingly:

```
Experiment successfully completed!
```

Below, a flowchart is provided, representing the interaction of the user with the platform.

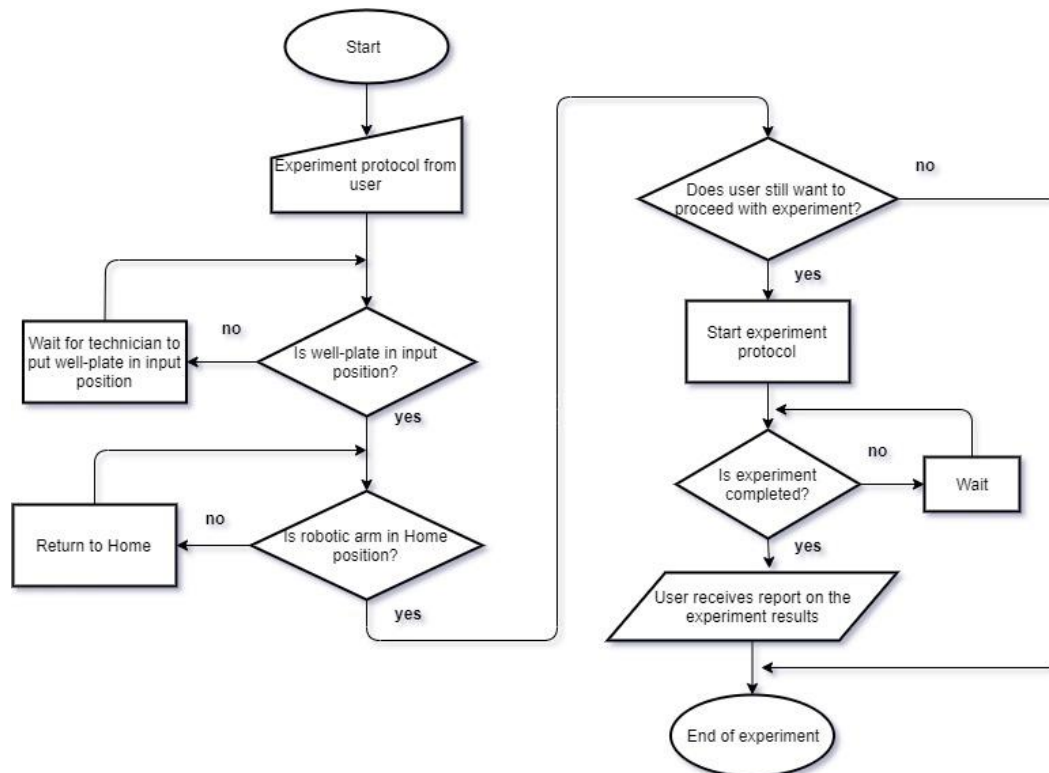


Figure 28: User interface flowchart

7.4 Simulation of Experiment with SCARA and STAUBLI

After the start of the experiment, the robot acquires different positions and configurations in space, which depend on its final destination and the constraints that are imposed. Below, a series of images is presented, showing a series of changes in the position and orientation of the robotic arm for both the SCARA and the STAUBLI.

7.4.1 SCARA

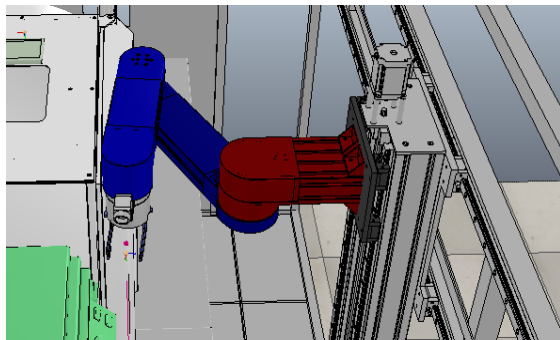


Image 14: Home position of SCARA robot (input position)

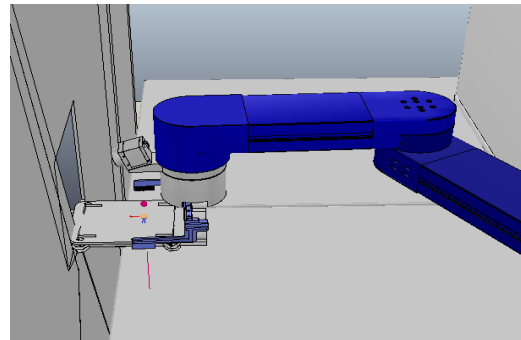


Image 15: SCARA grabbing plate from technician

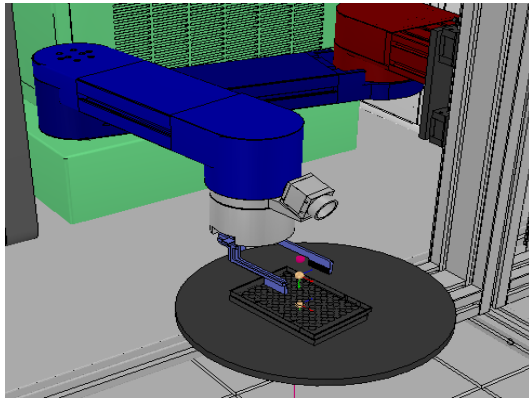


Image 16: SCARA above well-plate on rotating base (used to change plate orientation if needed)

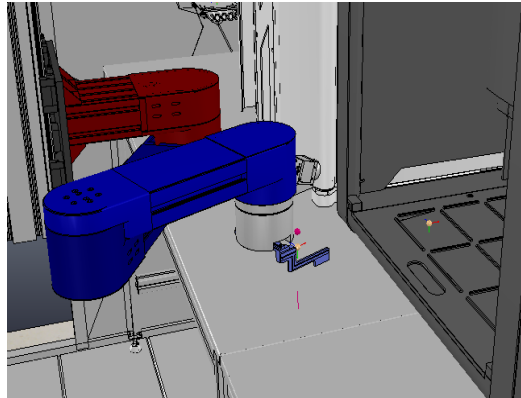


Image 17: Safe distance from machines for SCARA

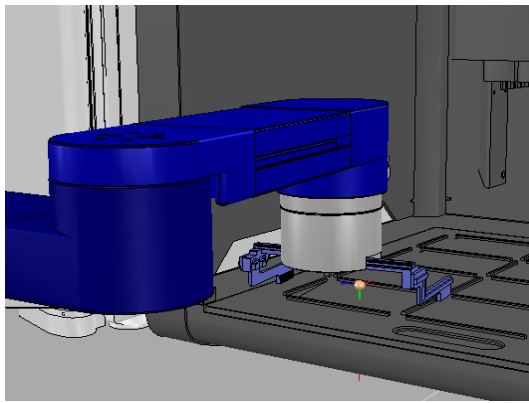


Image 18: Gripper is open ready to leave/grab plate for SCARA

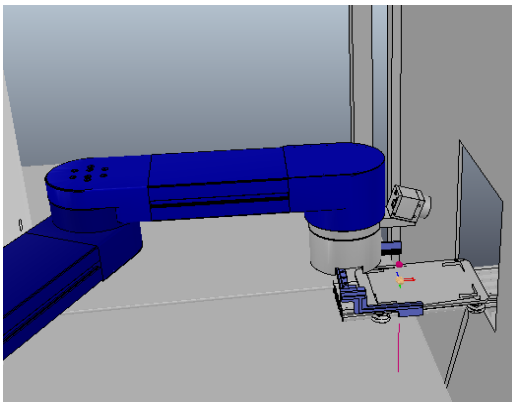


Image 19: SCARA returning plate to technician (output position)

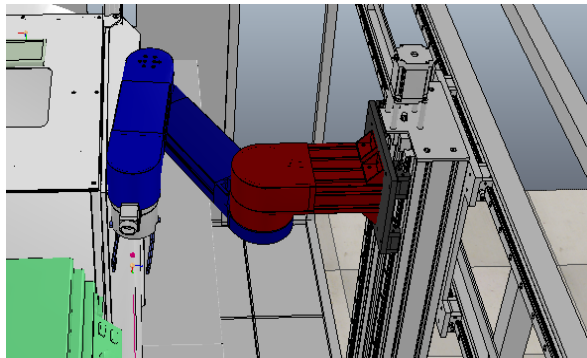


Image 20: Return of SCARA to Home

7.4.2 STAUBLI TX2-90XL

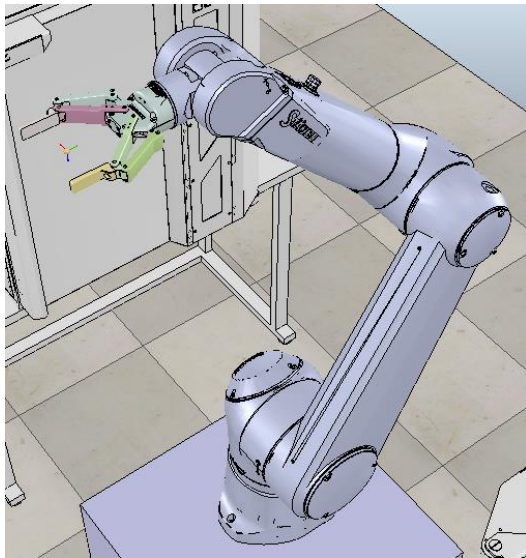


Image 21: Home position of STAUBLI

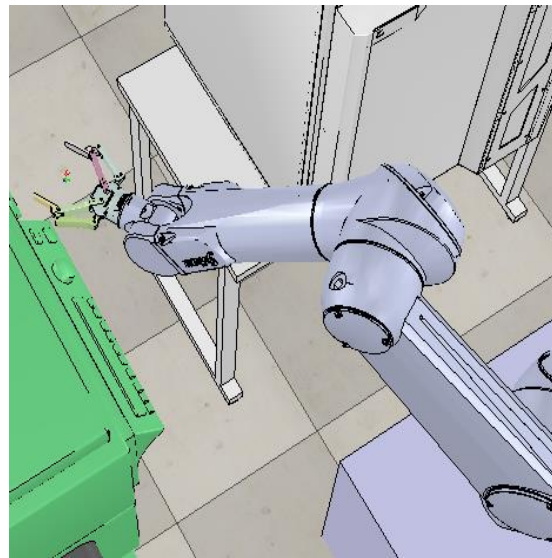


Image 22: STAUBLI grabbing plate from technician

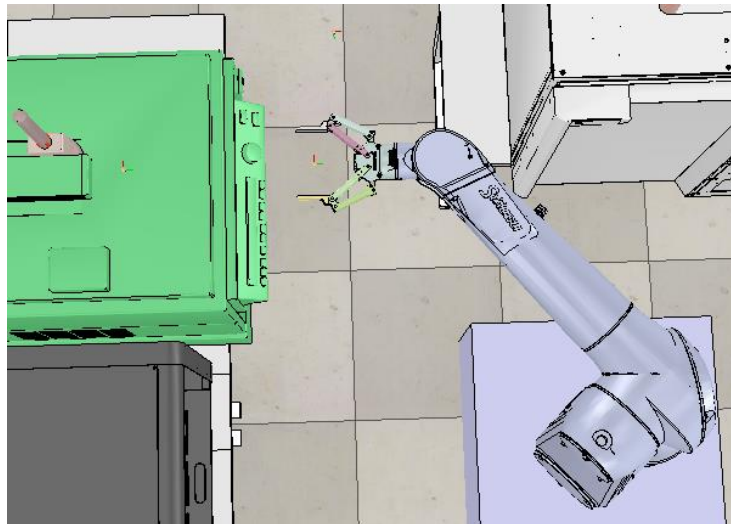


Image 23 : Safe distance from machine for STAUBLI

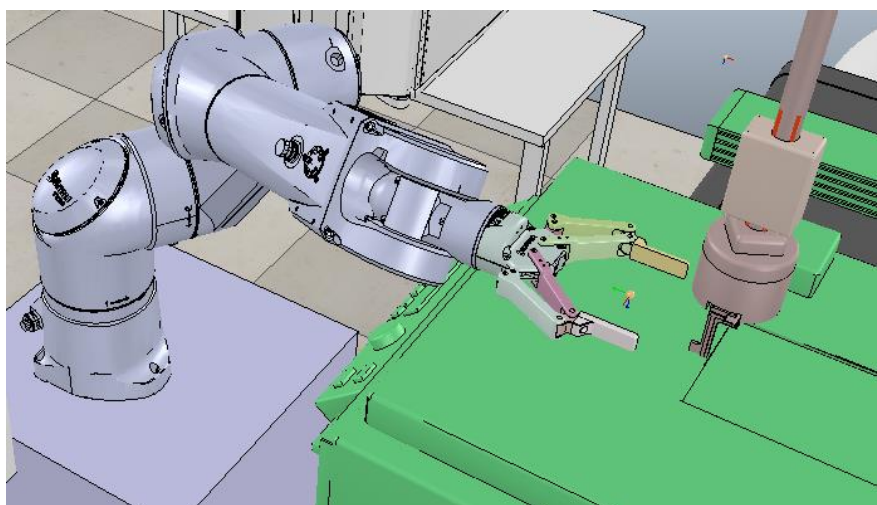


Image 24: STAUBLI ready to leave/grab plate from machine

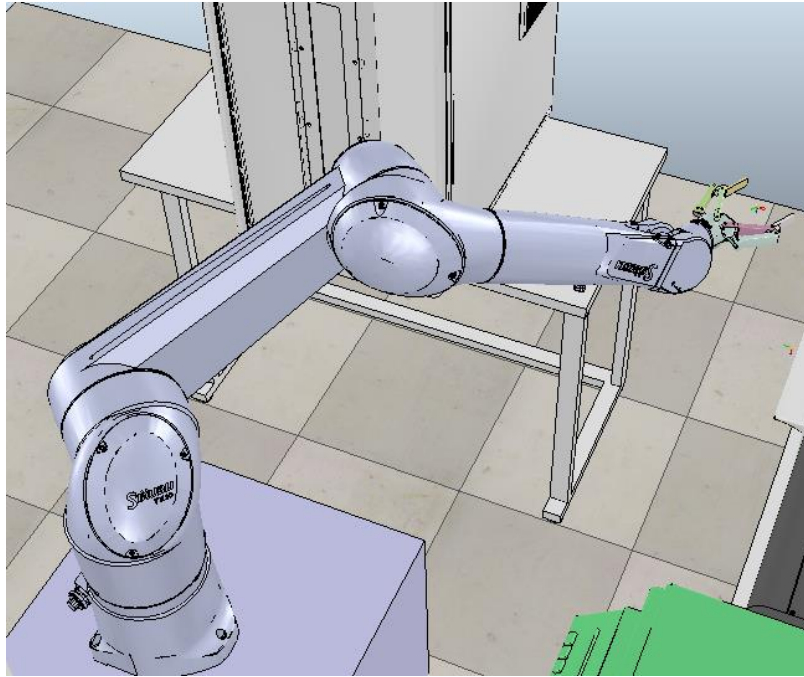


Image 25: STAUBLI returning plate to technician

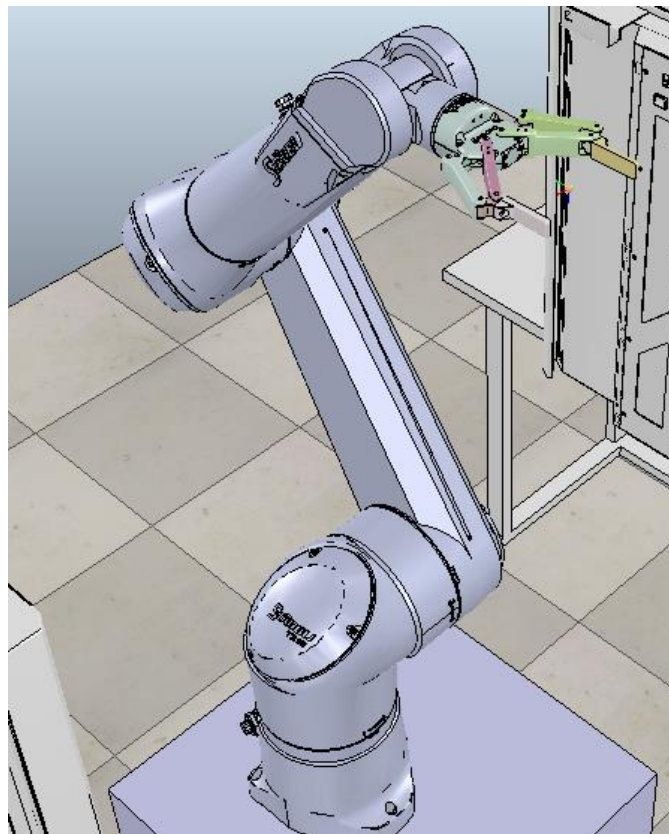


Image 26: Return of STAUBLI to Home

7.5 Collision Detection

Collisions of the robotic arm with the surrounding area can cause significant damage both to the robot itself and to the work being done. In the virtual environment, unlike the real one, conflicts have no consequence and their purpose is to warn the user. In this way, the operator can program the arm's trajectory, preventing collisions before they can occur.

V-REP can detect collisions between two collidable entities in a very flexible way. The calculation is an exact interference calculation. The collision detection module will only detect collisions, it does however not directly react to them, something which depends on the dynamic modeling of the scene that exceeds the purposes of this thesis.

More specifically, a colliding property, also mentioned before, was added to both the robots and all objects in the surrounding environment. This option helps recognize the collision between two objects, while allowing for overlap. The collision detection module allows registering collision objects which are collidable entity-pairs consisting of a collider entity and collidEE entity. During simulation, the collision state of each registered collision object can then be visualized with a different coloring.

In order to define the collidable entity-pairs that we want to be detected during simulation, utilized is the "collection" function of provided by VREP, which is a user-defined collection of scene objects. V-REP supports calculations based not only on objects, but also on collections. For instance the collision detection module allows registering following collision pair: (collection A; object B). The collision checking algorithm will then check whether the collection A (any object composing it) collides with object B. In our case we set three different collections which refer respectively to:

COLLECTION A: All objects of which a robotic arm consists (chain, tip included)

COLLECTION B: The "body" of the robotic arms.

COLLECTION C: The rest of the components of the robotic arms (including tip and gripper).

The goal is to check for collisions between the robots and the surrounding objects of the scene (COLLECTION A; All other entities-machines, frame, objects in scene) and to check for collisions between the robotic arms and their "bodies", since it is possible that a robot may collide with itself as well. (COLLECTION B; COLLECTION C). When the two objects, between which the collision is checked, stop contacting each other, the color of the entities is reset to its initial state. The following pictures show some cases of robot collisions with other objects.

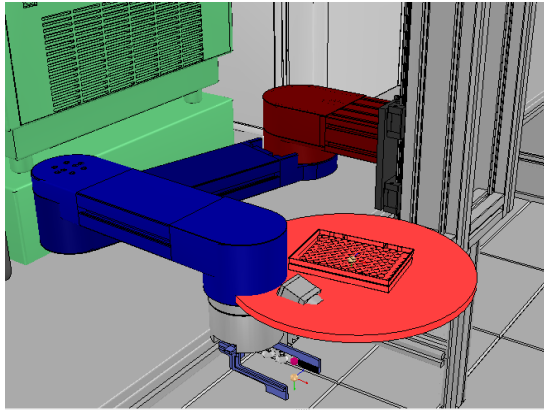


Image 27: Collision of SCARA with rotating base

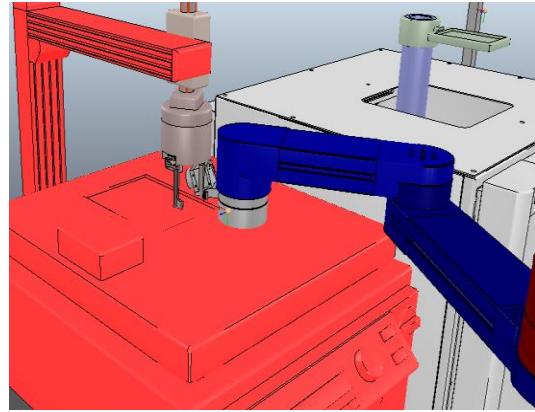


Image 28: Collision of SCARA robot with Centrifuge

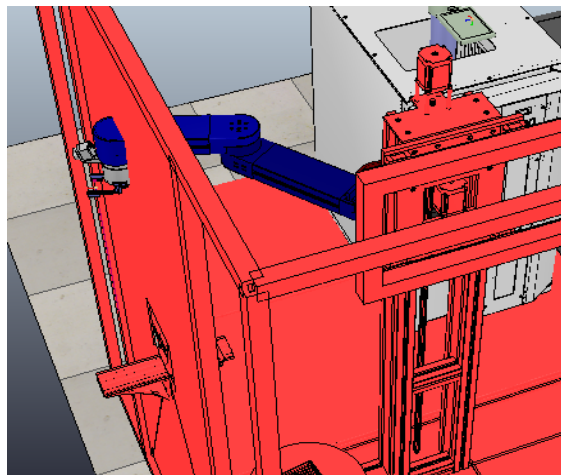


Image 29: Collision of SCARA robot with laboratory frame

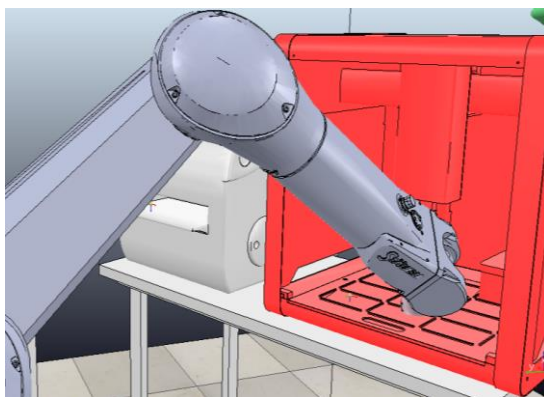


Image 30: Collision of STAUBLI robot with Liquid Handler

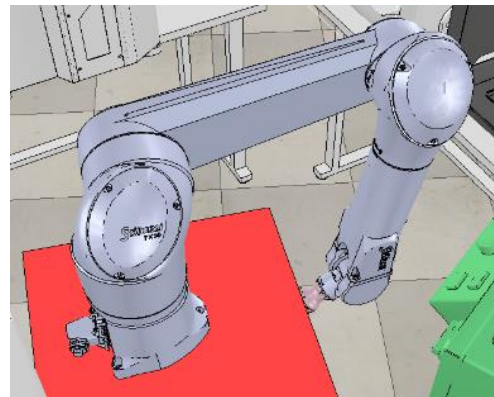
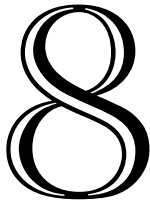


Image 31: Collision of STAUBLI robot with base



RESULTS

8.1 General Remarks

Following diagrams are the results of the simulations during different experiments. Only the most basic movements of each robot are included in these diagrams for the sake of brevity, however the behaviors of the robots do not change dramatically between movements. It is important to note and pay attention to the scale of the axis of each diagram. Specifically, in some cases the graphs may seem to diverge or present important errors, but this is usually due to the scale of the axis whose magnitude might represent changes to the 10^{-3} .

For the SCARA it is worth noting that the 5th joint, namely the joint of the gripper, which rotates it, is set to 0 for all the simulations at hand. This is due to the fact that since the machines are all in a row there is no need for the gripper to rotate. If that is needed, then the respective joint can be “activated” by setting its upper and lower limits in the `SCARAp1atetraj.m` program.

The same approach can also be utilized for the STAUBLI robot. In the simulations below the joints of the robot are all activated and work according to their limits, as they are set by the company and which were mentioned in previous chapters. If however the robot behaves unexpectedly, in the sense that it does not keep the well-plate parallel to the ground, the 4th and 6th joints can be set to 0. The fourth controls the rotation of the forearm, meanwhile the sixth controls the rotation of the tool flange. Keeping these two still, then the problem can be addressed accordingly.

Overall, the resulting graphs are very satisfying, showing that the methods and algorithms used achieved the expected, which was the control of the robotic arms, according to their own and their environment’s specifications. More specifically:

- ✓ The movements of the robots are always within their predefined limits and never exceed them, as the *Joint Angles* diagrams represent.
- ✓ The velocities have the expected curve form in both cases of the simulation.
- ✓ The position error is eliminated in most cases with the exception of the Home-Plate movement of the SCARA. This most probably happens because the translational joint (1st joint of SCARA) is inactive, because we want the move to be stationary, while at the same time the points that are fed to the robotic arm are not fully linear, which makes it a little more difficult for the arm to follow. This is also why errors are observed, but still not big enough to disrupt the experiment and influence its accuracy

The results of the SCARA and the STAUBLI will be presented separately. The diagrams refer to simulations with $T=1$ and $dt=0.01$.

8.2 SCARA

A. From **Home** position to **safe position** before Input position via FK

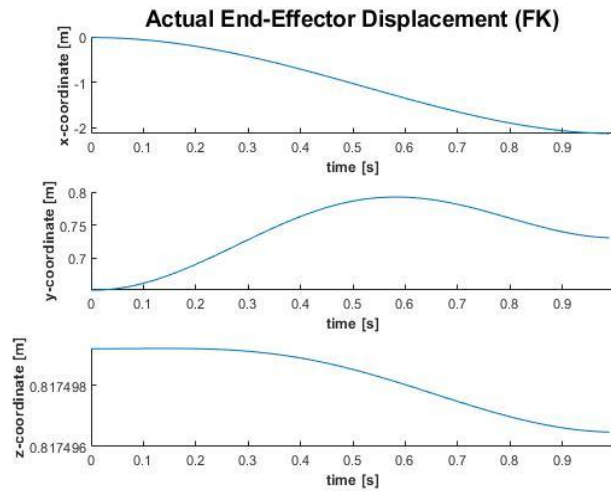


Diagram 1: EE position of SCARA with FK- Home to Safe Position

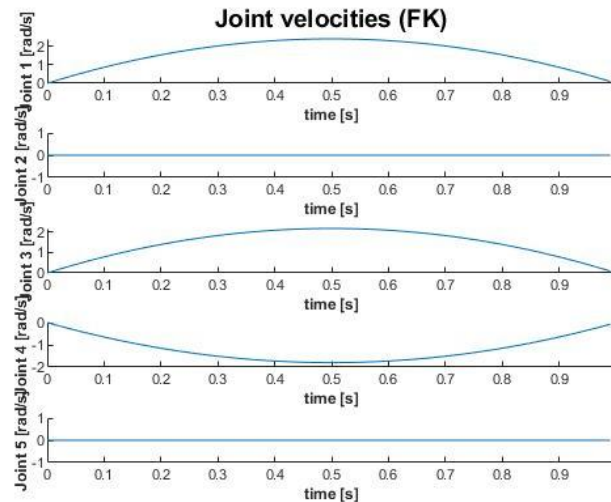


Diagram 2: Joint angles of SCARA with FK-Home to Safe Position

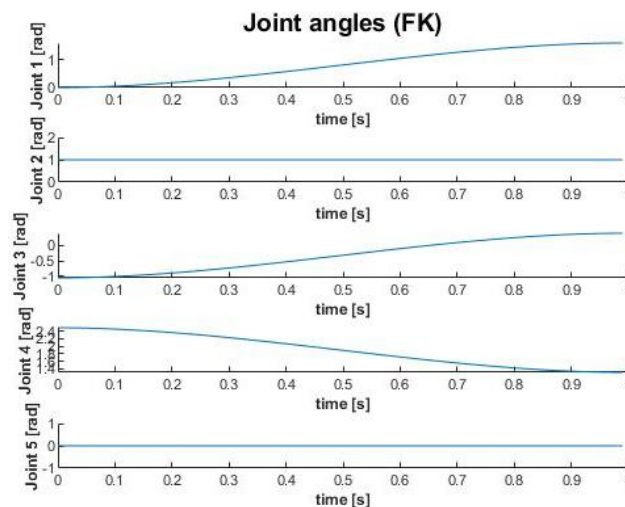


Diagram 3: Joint velocities of SCARA with FK- Home to Safe Position

B. From **safe position** before Input position to **Input** via IK

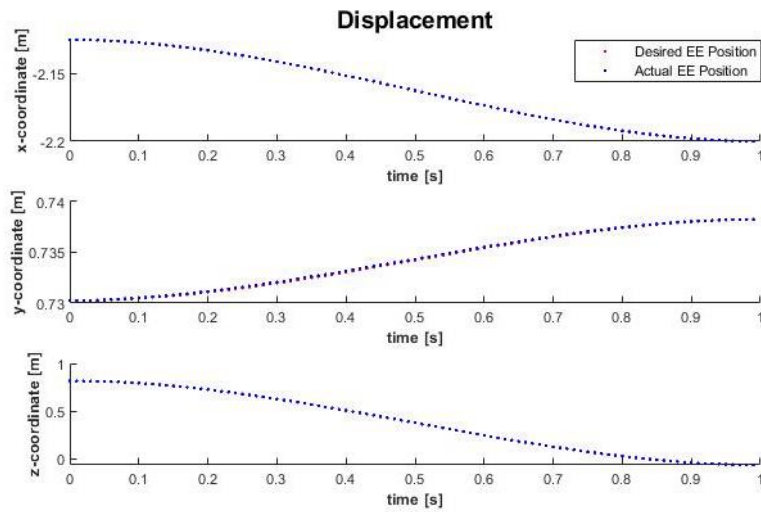


Diagram 4: Desired vs Actual EE position of SCARA during IK- Safe to Input Position

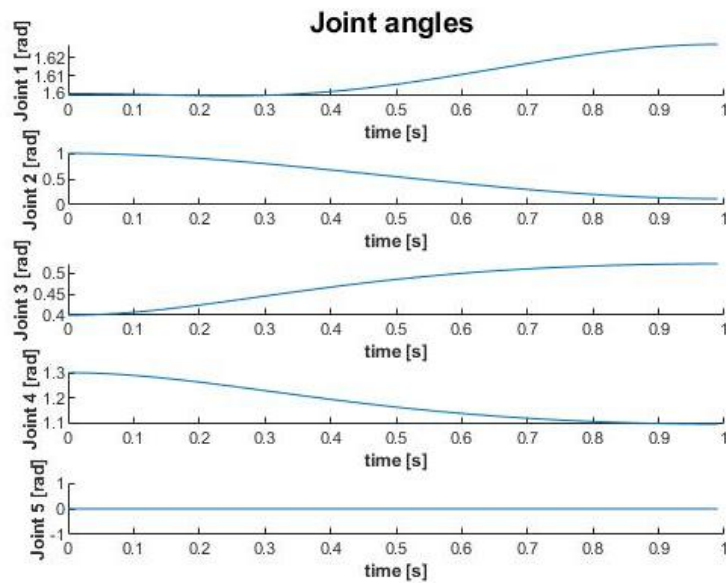


Diagram 5: Joint angles of SCARA during IK- Safe to Input Position

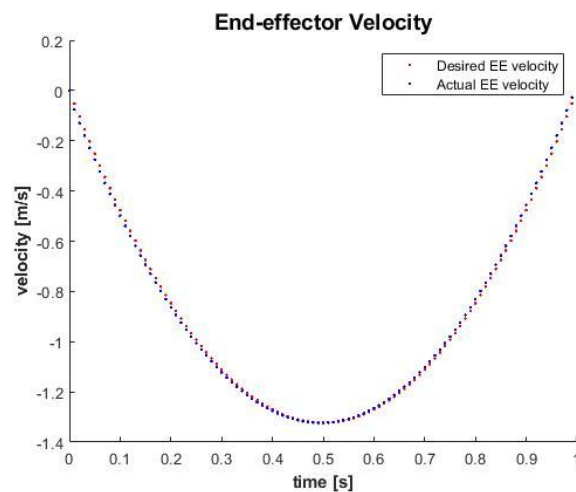


Diagram 6: Desired vs Actual EE velocity of SCARA during IK- Safe to Input Position

C. From **Home** position to **safe position** above Plate on rotating base via IK

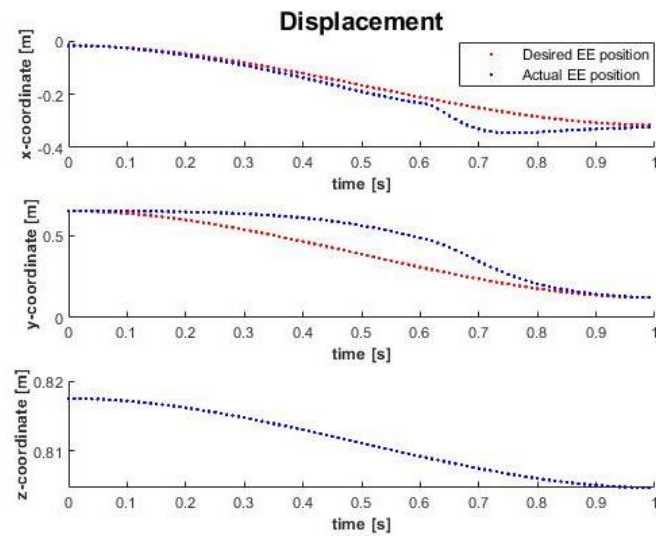


Diagram 7: Desired vs Actual EE position of SCARA during IK- Home to Safe Position

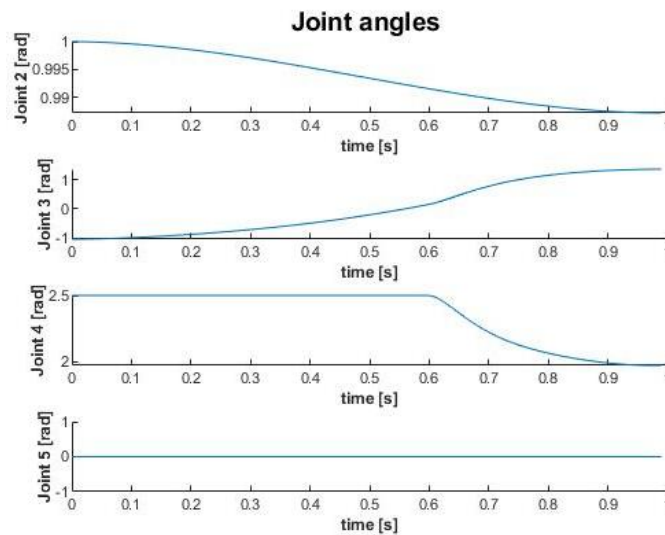


Diagram 8: Joint angles of SCARA during IK- Home to Safe Position

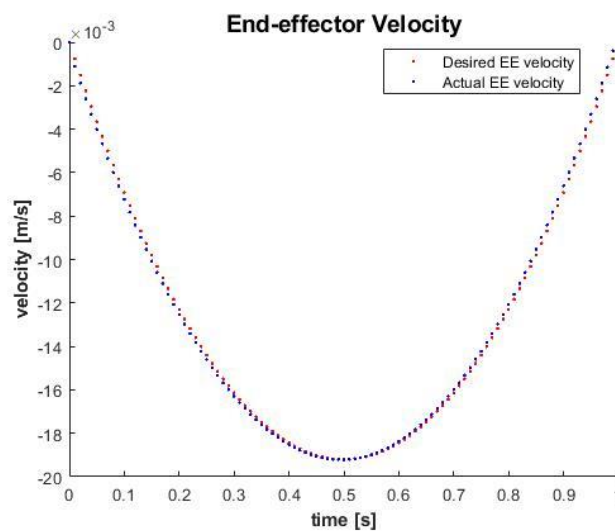


Diagram 9: EE velocity of SCARA during IK- Home to Safe Position

D. From **safe position** above Plate to **Plate** on rotating base via IK

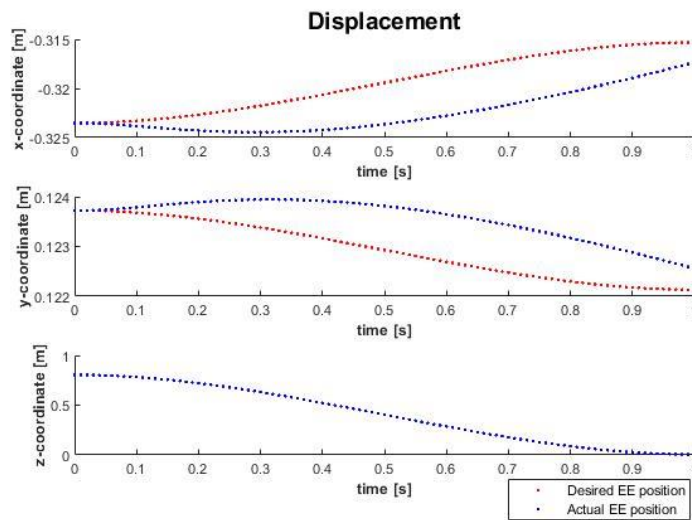


Diagram 10: Desired vs Actual EE position of SCARA during IK- Safe Position to Plate

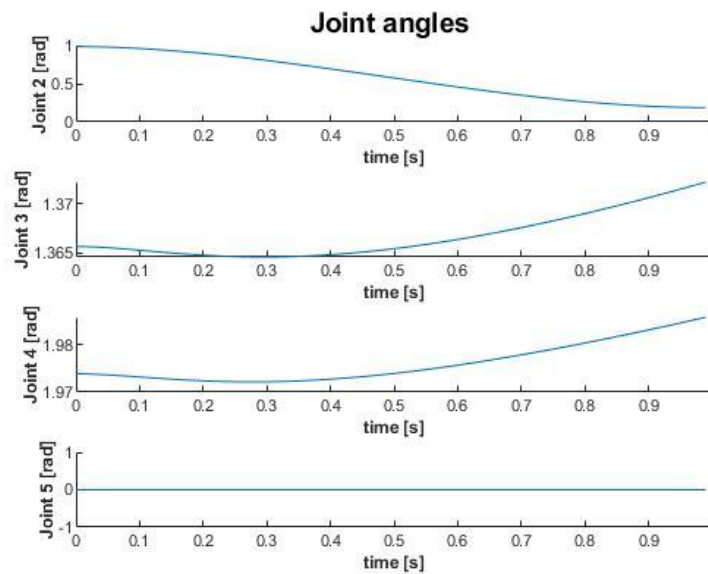


Diagram 11: Joint angles of SCARA during IK- Safe position to Plate

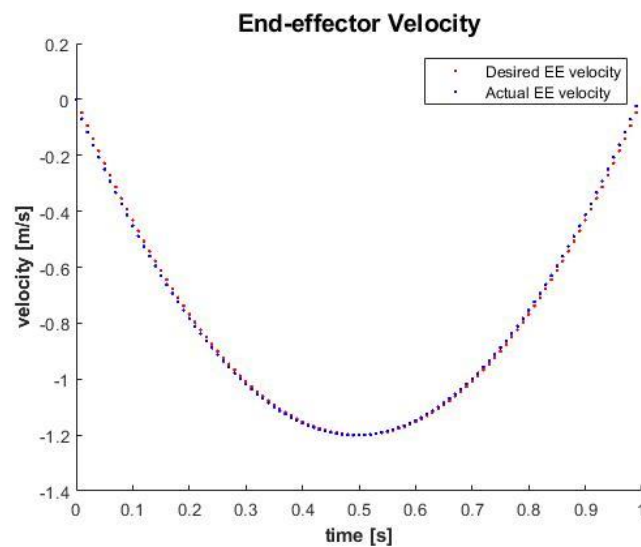


Diagram 12: Desired vs Actual EE velocity of SCARA during IK- Safe position to Plate

E. From Machine 1 to Machine 2 via IK

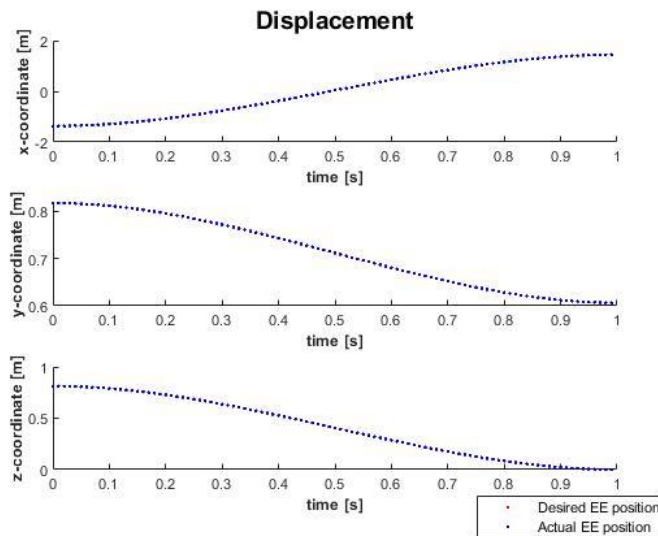


Diagram 13: Desired vs Actual EE position of SCARA during IK – Machine to Machine

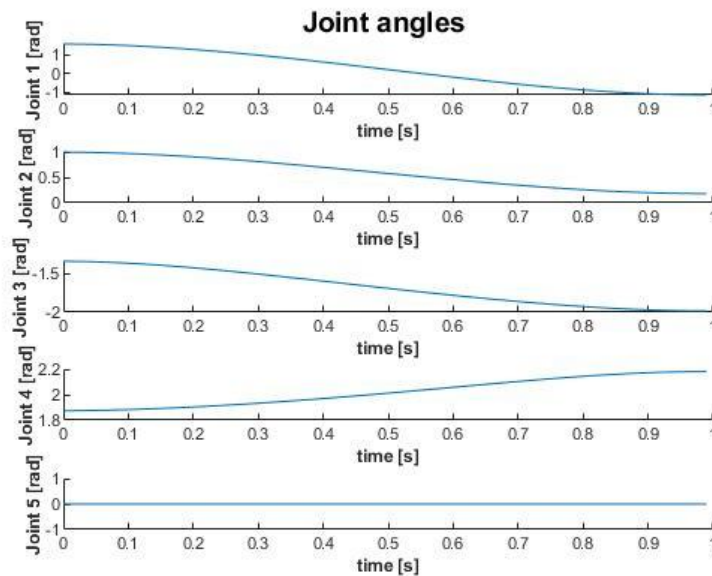


Diagram 14: Joint angles of SCARA during IK- Machine to Machine

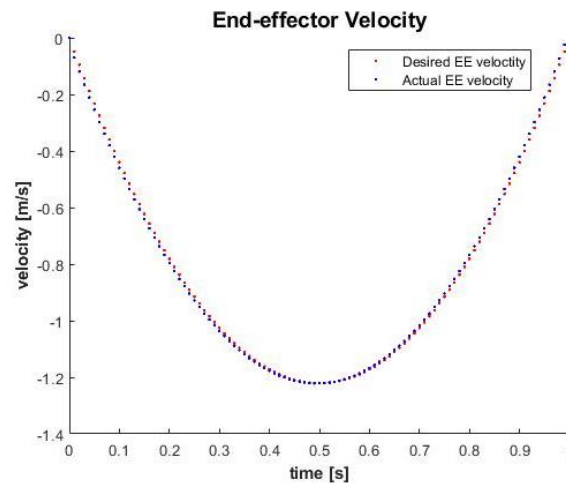


Diagram 15: Desired vs Actual EE velocity of SCARA during IK- Machine to Machine

F. From **Home** position to **safe** position before Output position via FK

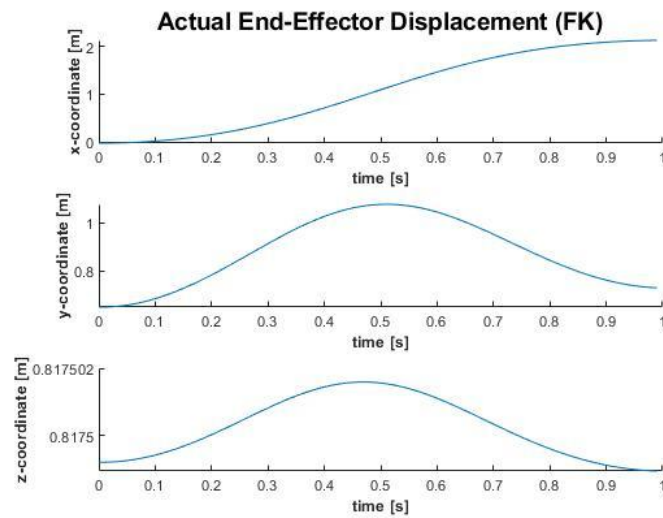


Diagram 16: EE position of SCARA with FK- Home to Safe Position

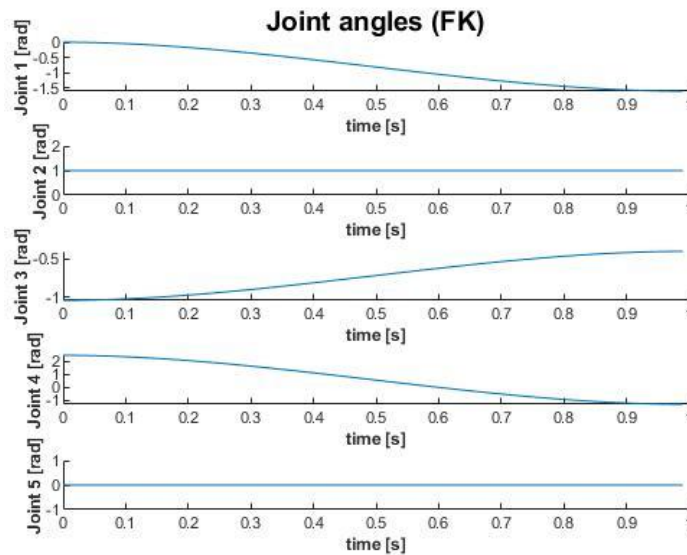


Diagram 17: Joint angles of SCARA with FK- Home to Safe Position

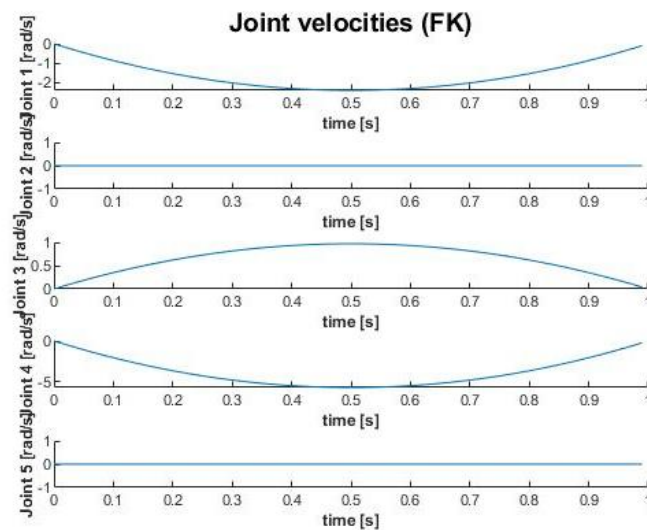


Diagram 18: Joint velocities of SCARA with FK- Home to Safe Position

G. From safe position before Output position to **Output** via IK

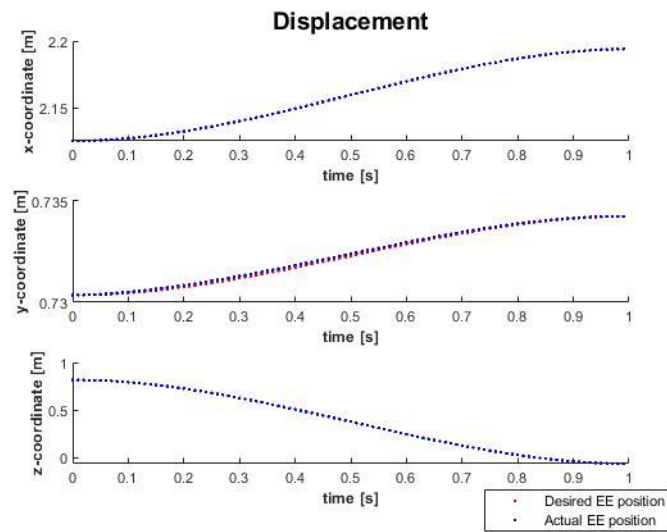


Diagram 19: Desired vs Actual EE position of SCARA during IK - Safe to Output Position

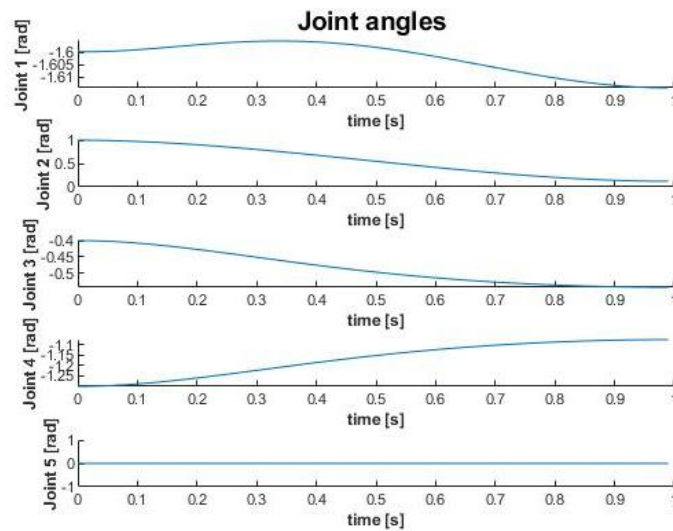


Diagram 20: Joint angles of SCARA during IK- Safe to Output Position

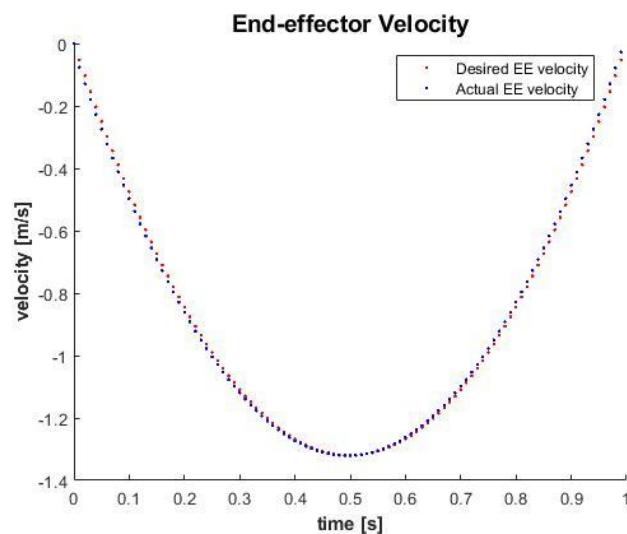


Diagram 21: Desired vs Actual EE velocity of SCARA during IK- Safe to Output Position

8.3 STAUBLI RX-90

A. From Home position to Input position via IK

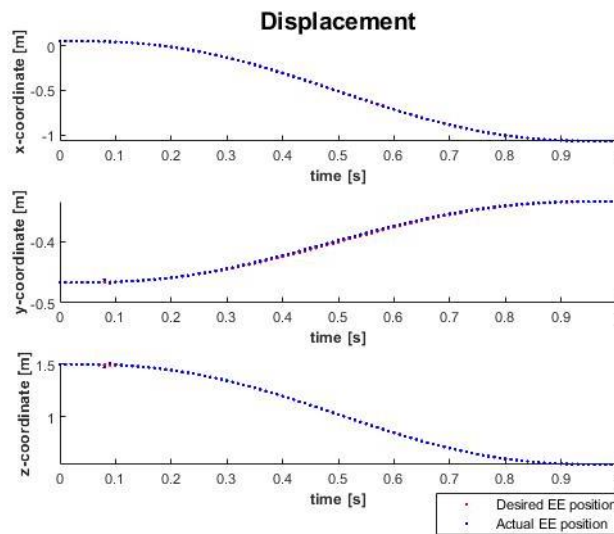


Diagram 22: Desired vs Actual EE position of STAUBLI during IK- Home to Input Position

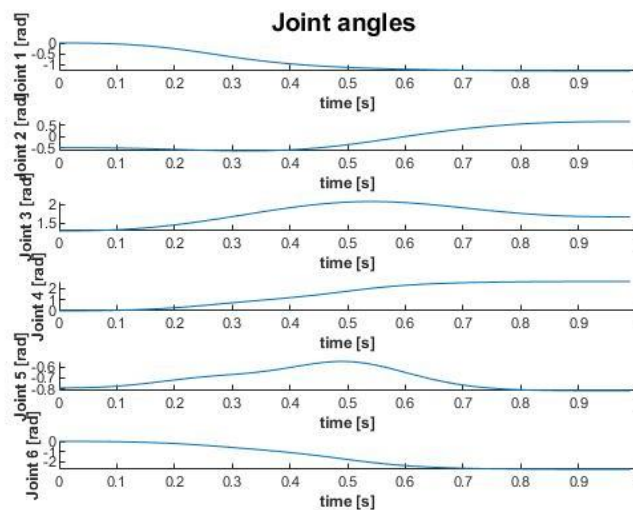


Diagram 23: Joint angles of STAUBLI during IK - Home to Input Position

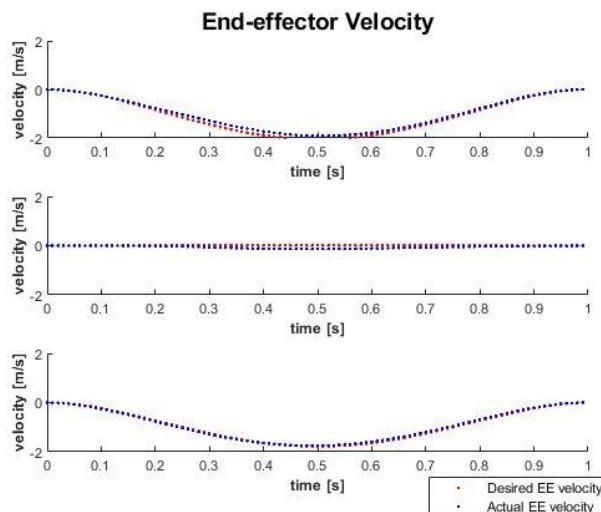


Diagram 24: Desired vs Actual EE velocity of STAUBLI during IK- Home to Input Position

B. From Home to Machine via IK

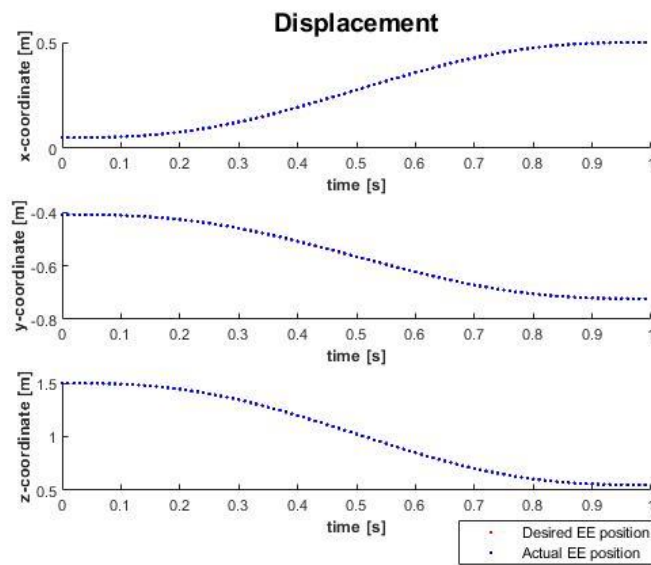


Diagram 25: Desired vs Actual EE position of STAUBLI during IK- Home to Machine

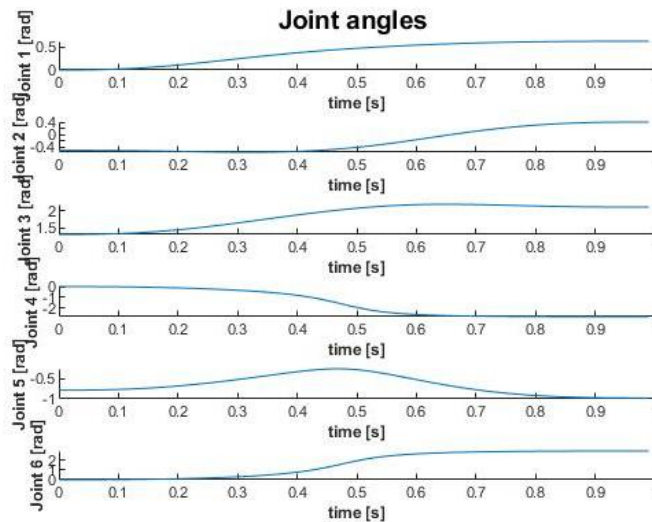


Diagram 26: Joint angles of STAUBLI during IK- Home to Machine

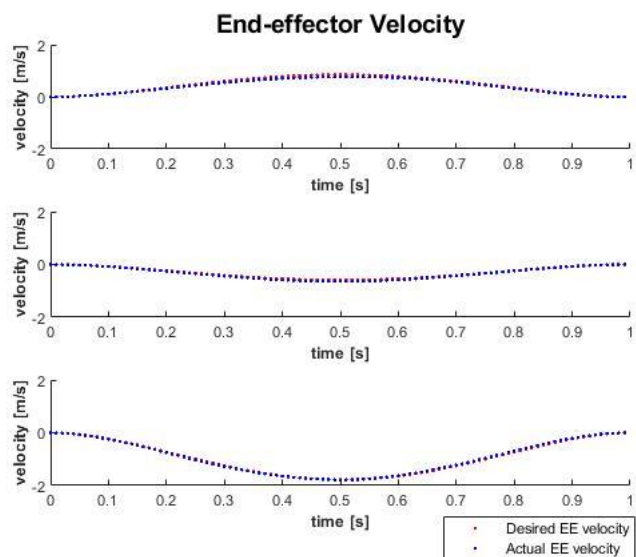


Diagram 27: Desired vs Actual EE velocity of STAUBLI during IK- Home to Machine

C. Machine to Home via FK

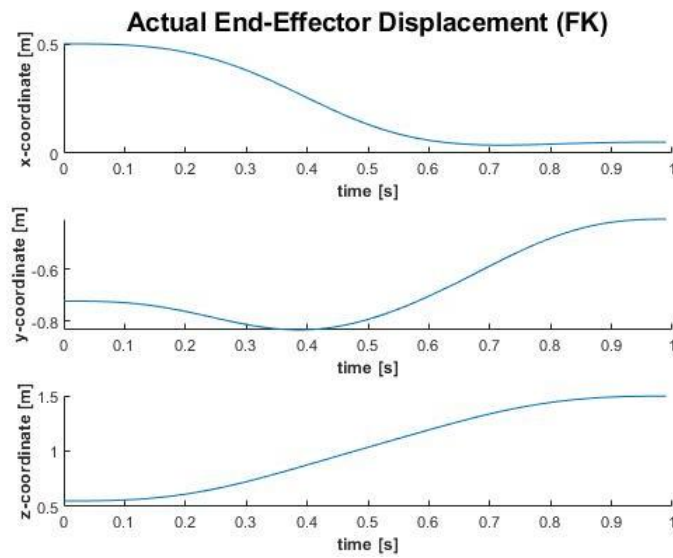


Diagram 28: EE position of STAUBLI with FK- Machine to Home

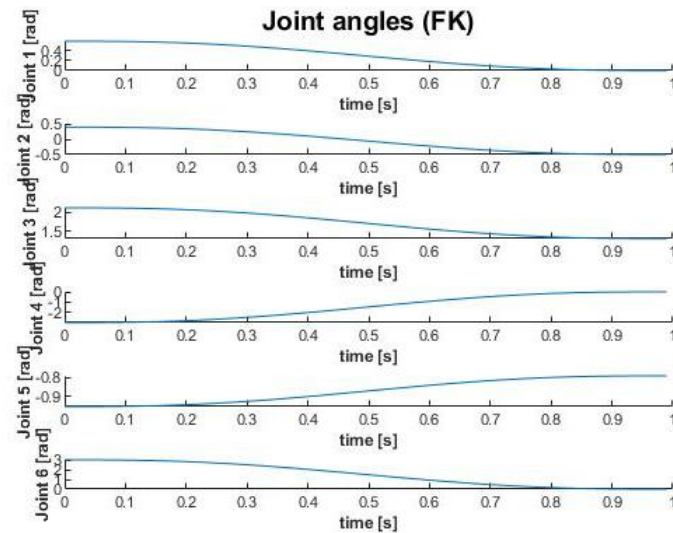


Diagram 29: Joint angles of STAUBLI with FK- Machine to Home

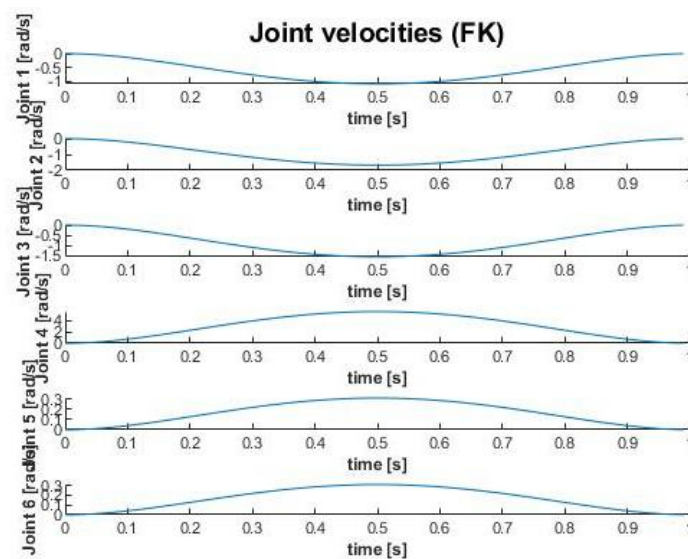


Diagram 30: Joint velocities of STAUBLI with FK- Machine to Home

D. From Home to Output Position via IK

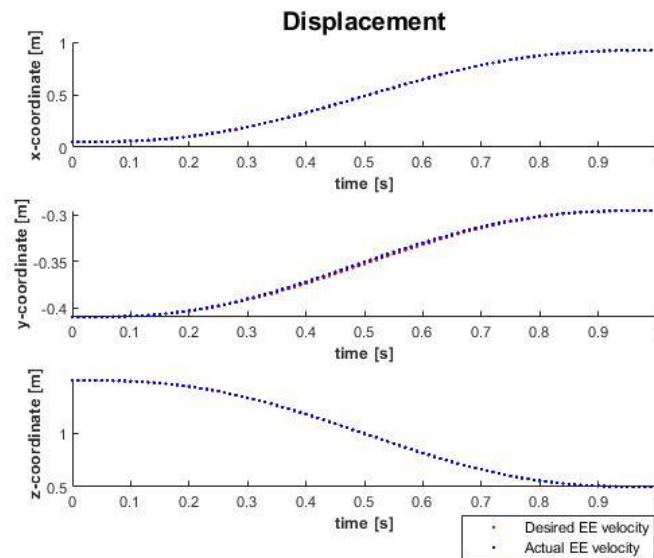


Diagram 31: Desired vs Actual EE position of STAUBLI during IK- Home to Output Position

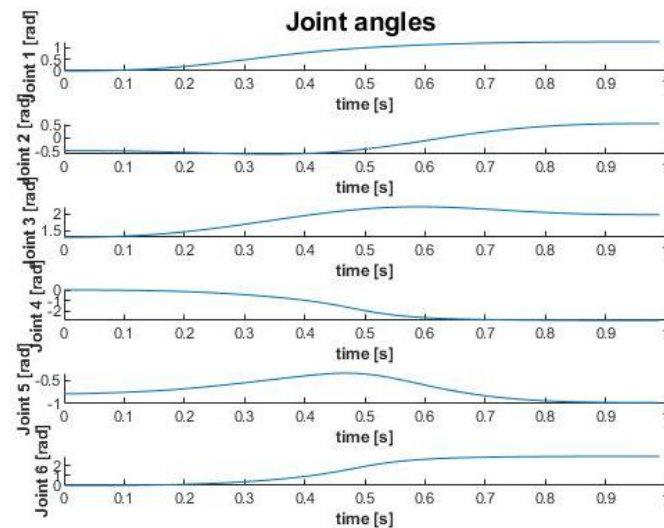


Diagram 32: Joint angles of STAUBLI during IK- Home to Output Position

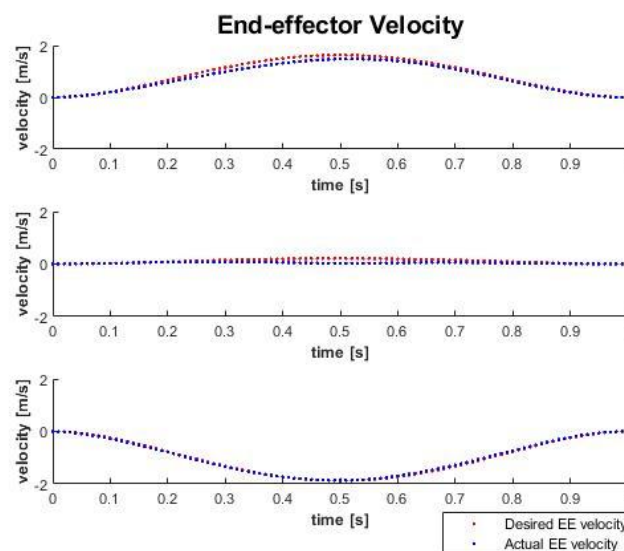
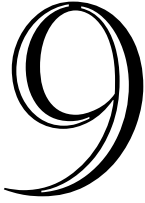


Diagram 33: Desired vs Actual EE velocity for STAUBLI- Home to Output Position



CONCLUSIONS AND FUTURE WORK

9.1 Contribution

This diploma thesis describes a methodology for developing a robotic biotechnology lab model in a virtual environment. The process involved both the introduction of 3D models for the representation of the physical space and their programming so that the moving parts –the robots –would gain "life" and interact with the rest.

The main contribution of this work is the development of a methodology towards the kinematical control of two different robots and two different system layouts, which can be used as a low cost alternative to impedance control or visual servoing of the robot or to expensive high-accuracy robots. The thesis can provide a background for expanding or even developing other related methodologies.

Specifically covered were:

1. Model of custom made SCARA type robotic arm with fully developed kinematic chain linkage.
2. Model of Stäubli TX2-90XL robotic arm with fully developed kinematic chain linkage.
3. Actual model of the biotechnology laboratory space with dimensions and layouts.
4. Direct and inverse kinematic analysis of the robotic arms at hand.
5. Simulation of complete experimental protocols in the virtual environment VREP.

9.2 Advantages of virtual environments

The conventional task scheduling of an industrial robot has always been based on the experience of the operator, who was planning his orbit while in operation. This way, besides being time consuming, it ran the risk of error, endangering the integrity of the operator, the industrial equipment as well as the work. Nowadays, young engineers and craftsmen are called upon to do the programming work. Due to their familiarity with virtual reality technologies, the use of the latter in this work gives fast, reliable and secure results.

There is an obvious economic benefit, as well. Money is saved because of reduced labor hours, failed efforts, and the damage caused by collisions. Also, such a system can be used to properly study the installation of additional mechanical equipment in an already existing environment.

9.3 Suggestions for future development

The development of the laboratory set up and the trajectory planning been successful, but there is still room for improvement.

As far as the laboratory set up is concerned:

- The experiment scenarios tested for the purposes of this thesis included only 5 machines – workstations, as part of the laboratory. These machines are the most common found in a biotechnology laboratory and most often used to conduct experiments. A possible extension could be to include more specialized machines in the same laboratory set ups for the conduction experiments. For example, a Flow Cytometer, a High-Content Screening and a Microplate Dispenser could be such additions.
- In the current project the experiments were also simulated one- by –one, meaning that a new experiment was planned to begin right after the previous experiment was completed. Implementing algorithms on the planning of Flexible Manufacturing could allow for multiple experiments to take place in the laboratory at the same time. Incorporating markers and vision systems to recognize the different microplates found in the lab at each instant, the robot could receive multiple experiment protocols and complete them simultaneously, increasing thus the productivity of the cell.

As far as the control of the robotic arms is concerned:

- The research focused on the kinematic analysis of the robotic arms, completely ignoring their dynamics. A dynamic simulation could be attempted to analyze the oscillations while the robots are in operation, as well as their effect on the accuracy of the trajectory.
- A live localization system with the addition of cameras can be implemented to ensure accuracy. An arm camera could be used to align the arm with the machine entry points and also one camera that can spot the position of the machines and the well-plate. These cameras can be utilized to correct position errors and give live feedback.
- Experimental results from the control of the Stäubli TX2-90XL robotic arm could be modeled on a physical level with the information provided from the virtual environment via the language V+. To that respect, Matlab-VREP output files concerning the position of the end-effector or the values of the joint angles at each configuration could be passed via a V+ controller to the actual model of the Stäubli to assess the actual behavior of the robot and if it coincides with the simulated one.

10

BIBLIOGRAPHY

- [1] R. Pauwels, H. Azijn, M. P. de Béthune, C. Claeys, and K. Hertogs, “Automated techniques in biotechnology,” *Curr. Opin. Biotechnol.*, vol. 6, no. 1, pp. 111–117, 1995.
- [2] A. Sertkaya, H. H. Wong, A. Jessup, and T. Beleche, “Key cost drivers of pharmaceutical clinical trials in the United States,” *Clin. Trials*, vol. 13, no. 2, pp. 117–126, Apr. 2016.
- [3] L. Monostori, “Cyber-physical production systems: Roots, expectations and R&D challenges,” in *Procedia CIRP*, 2014, vol. 17, pp. 9–13.
- [4] L. Monostori *et al.*, “Cyber-physical systems in manufacturing,” *CIRP Ann.*, vol. 65, no. 2, pp. 621–641, 2016.
- [5] M. Smith, J., Kreutzer, S., Moeller, C., & Carlberg, “Industry 4.0. Study for the ITRE committee,” 2016.
- [6] N. Shariatzadeh, T. Lundholm, L. Lindberg, and G. Sivard, “Integration of Digital Factory with Smart Factory Based on Internet of Things,” in *Procedia CIRP*, 2016, vol. 50, pp. 512–517.
- [7] U. Bracht and T. Masurat, “The Digital Factory between vision and reality,” *Comput. Ind.*, vol. 56, no. 4, pp. 325–333, May 2005.
- [8] D. Mourtzis, N. Papakostas, D. Mavrikios, and S. Makris, “Det 2011,” no. November 2017, 2011.
- [9] V. Bottazzi and J. Fonseca, “Off-line Programming Industrial Robots Based in the Information Extracted From Neutral Files Generated by the Commercial CAD Tools,” *Ind. Robot. Program. Simul. Appl.*, 2006.
- [10] Coppelia Robotics, “V-REP User Manual.” [Online]. Available: <http://www.coppeliarobotics.com/helpFiles/index.html>.
- [11] Wikipedia, “SCARA.” [Online]. Available: <https://en.wikipedia.org/wiki/SCARA>. [Accessed: 08-Aug-2019].
- [12] Cyan-Tec, “When to use a SCARA Robot.” [Online]. Available: <https://cyan-tec.com/laser-systems/when-to-use-a-scara-robot>.
- [13] Γ. Χ. Βοσνιάκος, *Συστήματα Κατεργασιών Ι, Πρόχειρες σημειώσεις*. .
- [14] H. Fleischer and K. Thurow, “Automation Solutions for Analytical Measurements: Concepts and Applications.” [Online]. Available: https://books.google.gr/books?id=Mlw6DwAAQBAJ&pg=PA171&lpg=PA171&dq=gripper+fingers+for+microplate&source=bl&ots=WlkBUNulqG&sig=ACfU3U24QXQ_rKo_7Q8UWz5Ui_lkVcCC_A&hl=el&sa=X&ved=2ahUKEwiotebAyrLIAhVOecAKHQI1D_oQ6AEwEXoECAgQAQ#v=onepage&q=gripper+fingers+f. [Accessed: 23-Oct-2019].

- [15] "PTM-Präzisionstechnik." [Online]. Available: <http://www.ptm-automation.de/HomePTMPräzisionstechnik/OurCompany/Products/ServoGripperLaboratoryAutomation.aspx>.
- [16] "PatentSwarm." [Online]. Available: <https://patentswarm.com/patents/US7670555B2>.
- [17] P. Kosky, R. Balmer, W. Keat, and G. Wise, "Manufacturing Engineering," in *Exploring Engineering*, Elsevier, 2013, pp. 205–235.
- [18] V. Manthou and M. Vlachopoulou, "Agile Manufacturing Strategic Options," in *Agile Manufacturing: The 21st Century Competitive Strategy*, Elsevier, 2001, pp. 685–702.
- [19] T. Yang, B. A. Peters, and M. Tu, "Layout design for flexible manufacturing systems considering single-loop directional flow patterns," *Eur. J. Oper. Res.*, vol. 164, no. 2, pp. 440–455, Jul. 2005.
- [20] J. J. Craig, *Introduction to ROBOTICS mechanics and control*, 3rd ed. Pearson Education International, 2005.
- [21] B. Siciliano, L. Sciavicco, L. Villani, and G. Oriolo, *Robotics : modelling, planning and control*. Springer, 2009.
- [22] S. Chiaverini, B. Siciliano, and O. Egeland, "Review of the Damped Least-Squares Inverse Kinematics with Experiments on an Industrial Robot Manipulator," *IEEE Trans. Control Syst. Technol.*, vol. 2, no. 2, pp. 123–134, 1994.
- [23] R. Krasňanský, P. Valach, D. Soós, and J. Zorbakhsh, "Reference trajectory tracking for a multi-DOF robot arm," *Arch. Control Sci.*, vol. 25, no. 4, pp. 513–527, 2015.
- [24] D. Di Vito, C. Natale, and G. Antonelli, "A Comparison of Damped Least Squares Algorithms for Inverse Kinematics of Robot Manipulators," *IFAC-PapersOnLine*, vol. 50, no. 1, pp. 6869–6874, 2017.
- [25] X. Zhao, M. Wang, N. Liu, and Y. Tang, "Trajectory Planning for 6-DOF Robotic Arm Based on Quintic Polynormial," vol. 134, no. Caai, pp. 115–118, 2017.
- [26] C. Feng, G. Gao, and Y. Cao, "Kinematic modeling and verification for a SCARA robot," no. Icmemtc, pp. 918–921, 2016.
- [27] "ROS URDF." [Online]. Available: <https://wiki.ros.org/urdf>.

APPENDIX



URDF Template[27]

- **Root element**

**<robot
name>**

- **Link element**

**<link
name>** (*required*)

- The name of the link itself.

<inertial> (*optional*)

- The inertial properties of the link.

<origin> (*optional: defaults to identity if not specified*)

- This is the pose of the inertial reference frame, relative to the link reference frame. The origin of the inertial reference frame needs to be at the center of gravity. The axes of the inertial reference frame do *not* need to be aligned with the principal axes of the inertia.

xyz (*optional: defaults to zero vector*)

- Represents the x,y,z offset.

rpy (*optional: defaults to identity if not specified*)

- Represents the fixed axis roll, pitch and yaw angles in radians.

</origin>

<mass>

- The mass of the link is represented by the value attribute of this element

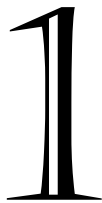
</mass>

<inertia>

- The 3x3 rotational inertia matrix, represented in the inertia frame. Because the rotational inertia matrix is symmetric, only 6 above-diagonal elements of this matrix are specified here, using the attributes *ixx*, *ixy*, *ixz*, *iyy*, *iyz*, *izz*.

</inertia>**</inertial>****<visual****name>** (*optional*)

- The visual properties of the link. This element specifies the shape of the object (box, cylinder, etc.) for visualization purposes. **Note:** multiple instances of **<visual>** tags can exist for the same link. The union of the geometry they define forms the visual representation of the link.
- Specifies a name for a part of a link's geometry. This is useful to be able to refer to specific bits of the geometry of a link.

<origin> (*optional: defaults to identity if not specified*)

The reference frame of the visual element with respect to the reference frame of the link.

xyz (*optional: defaults to zero vector*)

- Represents the x,y,z offset.

rpy (*optional: defaults to identity if not specified*)

- Represents the fixed axis roll, pitch and yaw angles in radians.

</origin>**<geometry>** (*required*)

- The shape of the visual object. This can be *one* of the following:
 - **<box size / >** attribute contains the three side lengths of the box. The origin of the box is in its center.
 - **<cylinder radius length/>** The origin of the cylinder is its center.
 - **<sphere radius/>** The origin of the sphere is in its center.

<mesh>

- A trimesh element specified by a **filename**, and an optional **scale** that scales the mesh's axis-aligned-bounding-box.

The recommended format for best texture and color support is Collada .dae files, though .stl files are also supported. The mesh file is not transferred between machines referencing the same model. It must be a local file.

</mesh>

<material

name> (*optional*)

- The material of the visual element. It is allowed to specify a material element outside of the 'link' object, in the top level 'robot' element. From within a link element you can then reference the material by name.

</material>

<color> (*optional*)

- **rgba** The color of a material specified by set of four numbers representing red/green/blue/alpha, each in the range of [0,1].

</color>

<texture> (*optional*)

- The texture of a material is specified by a **filename**

</texture>

</geometry>

</visual>

<collision

name> (*optional*)

- The collision properties of a link. Note that this can be different from the visual properties of a link, for example, simpler collision models are often used to reduce computation time. **Note:** multiple instances of <collision> tags can exist for the same link. The union of the geometry they define forms the collision representation of the link.
- Specifies a name for a part of a link's geometry. This is useful to be able to refer to specific bits of the geometry of a link.

<origin> (*optional: defaults to identity if not specified*)

- The reference frame of the collision element, relative to the reference frame of the link.

xyz (*optional: defaults to zero vector*)

- Represents the x,y,z offset.

rpy (*optional: defaults to identity if not specified*)

- Represents the fixed axis roll, pitch and yaw angles in radians.

</origin>

<geometry>

- See the geometry description in the above visual element.

</geometry>

</collision>

</link>

• Joint element

<joint

name *(required)*

- Specifies a unique name of the joint

type *>(required)*

- Specifies the type of joint, where type can be one of the following:
 - **revolute** - a hinge joint that rotates along the axis and has a limited range specified by the upper and lower limits.
 - **continuous** - a continuous hinge joint that rotates around the axis and has no upper and lower limits.
 - **prismatic** - a sliding joint that slides along the axis, and has a limited range specified by the upper and lower limits.
 - **fixed** - This is not really a joint because it cannot move. All degrees of freedom are locked. This type of joint does not require the axis, calibration, dynamics, limits or safety_controller.
 - **floating** - This joint allows motion for all 6 degrees of freedom.
 - **planar** - This joint allows motion in a plane perpendicular to the axis.

<origin> *(optional: defaults to identity if not specified)*

- This is the transform from the parent link to the child link. The joint is located at the origin of the child link, as shown in **Figure 11**.

xyz *(optional: defaults to zero vector)*

- Represents the x,y,z offset. All positions are specified in meters.

rpy *(optional: defaults 'to zero vector' if not specified)*

- Represents the rotation around fixed axis: first roll around x, then pitch around y and finally yaw around z. All angles are specified in radians.

</origin>

<parent

link> (*required*)

- Parent link name with mandatory attribute **link**.
- The name of the link that is the parent of this link in the robot tree structure.

</parent link>

<child

link> (*required*)

- Child link name with mandatory attribute **link**.
- The name of the link that is the child link.

</child link>

<axis> (*optional: defaults to (1,0,0)*)

- The joint axis specified in the joint frame. This is the axis of rotation for revolute joints, the axis of translation for prismatic joints, and the surface normal for planar joints. The axis is specified in the joint frame of reference. Fixed and floating joints do not use the axis field.

xyz (*required*)

- Represents the x,y,z components of a vector. The vector should be normalized.

</axis>

<limit> (*required only for revolute and prismatic joint*)

- An element can contain the following attributes:
 - **lower** (*optional, defaults to 0*): An attribute specifying the lower joint limit (radians for revolute joints, meters for prismatic joints). Omit if joint is continuous.
 - **upper** (*optional, defaults to 0*): An attribute specifying the upper joint limit (radians for revolute joints, meters for prismatic joints). Omit if joint is continuous.

</limit>

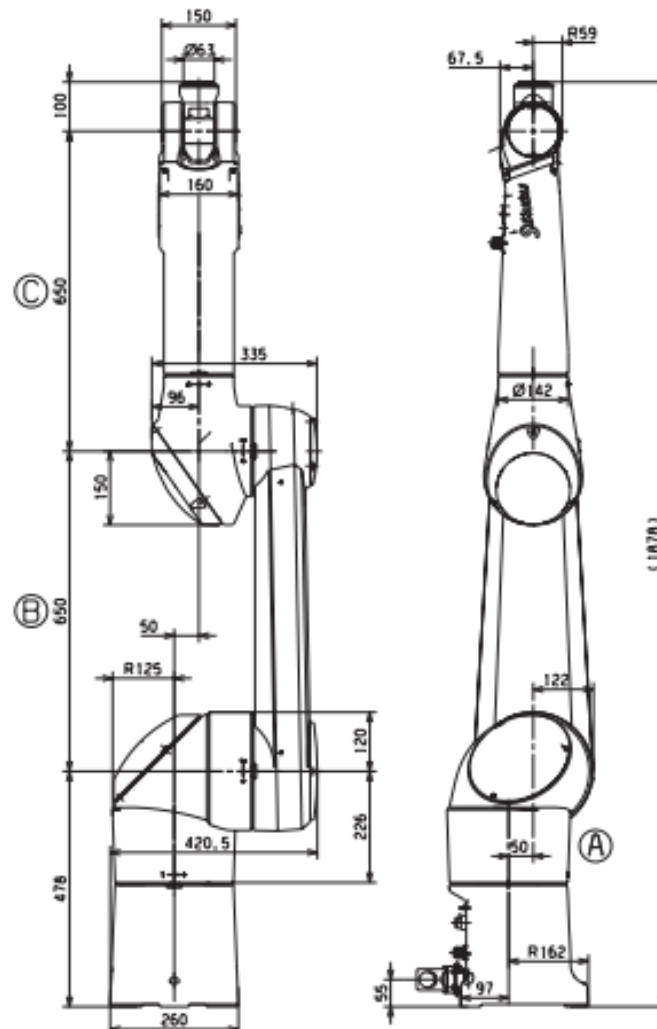
</joint>

</robot>

B

TECHNICAL SPECIFICATIONS OF EQUIPMENT AND CONSUMABLES

B1) Staubli TX2-90XL [Source: Staubli]



Nominal speed (°/s) TX90 XL	190	160	230	400	345	600
Maximum speed (°/s) ⁽²⁾	400	400	400	500	450	720
Angular resolution (°·10 ⁻³)	0.057	0.057	0.057	0.057	0.122	0.183

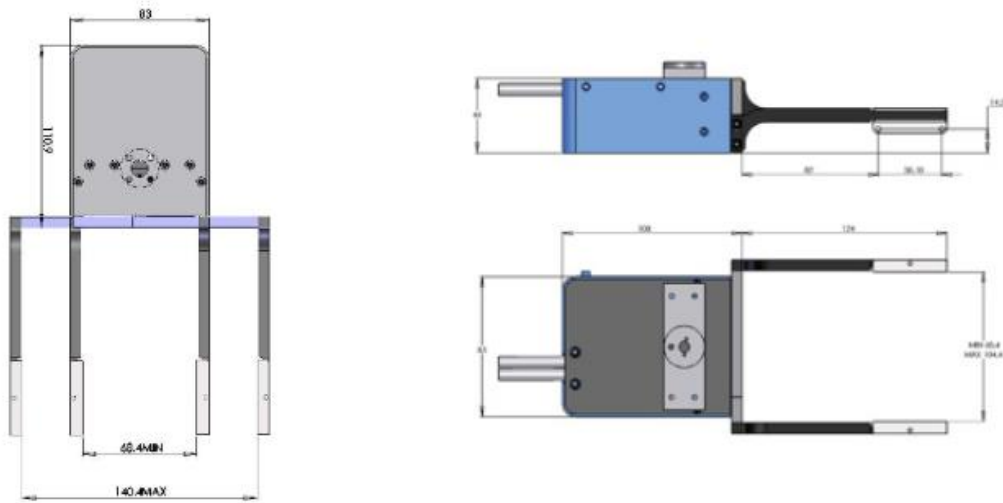
Arm XL	
Work envelope	
R.M max. reach between axis 1 and 5	1350 mm
R.M max. reach between axis 2 and 5	1300 mm
R.m1 min. reach between axis 1 and 5	327 mm
R.m2 min. reach between axis 2 and 5	391 mm
R.b reach between axis 3 and 5	650 mm
Maximum speed at load center of gravity	11.09 m/s
Repeatability at constant temperature	± 0.040 mm

B2) Custom experment Gripper

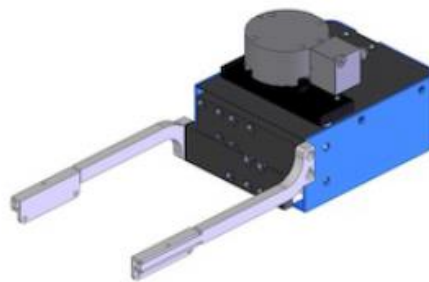
Parts List				
Item	Qty	Part Number	Description	Material
1	1	Flange		Steel
2	2	SSEBZ8-85		Generic
2	1	HTPA232M040-K-P4		Generic
3	1	Finger_dx		Steel
4	1	Finger_sx		Steel
5	2	TPCAT12Cy11		Generic
6	1	[Herkulex] DRS-01DX		Generic
7	1	Finger_frontal_plat e_dx		Steel
8	1	Finger_frontal_plat e_sx		Steel
9	1	RGEABLO_5N-50 v2 (1)		Generic
10	1	RGEABLO_5N-50 v2		Generic
11	1	Spur Gear (18 teeth)	Spur Gear, Module: 0.500000; Num Teeth: 18; Pressure Angle: 20.000000; Backlash: 0.00 mm	Steel
12	1	Shaft		Steel
13	2	_BR105ZZ		Steel
14	1	Belt		Steel

Drawn	Technical reference	Created by Andrea Fontanelli	Approved by 13/07/2018
		Document type	Document status
		Title	Draw No.
		Gripper	
		Rev.	Date of issue
			Sheet 1/1

B3) LGR Electric Servo Gripper [Source: [Let's Go Robotics.](#)]



*All dimensions in Millimeters (mm)



B4) ROBOTIQ 2F-140 Gripper [Source: [ROBOTIQ](#)]

Specifications

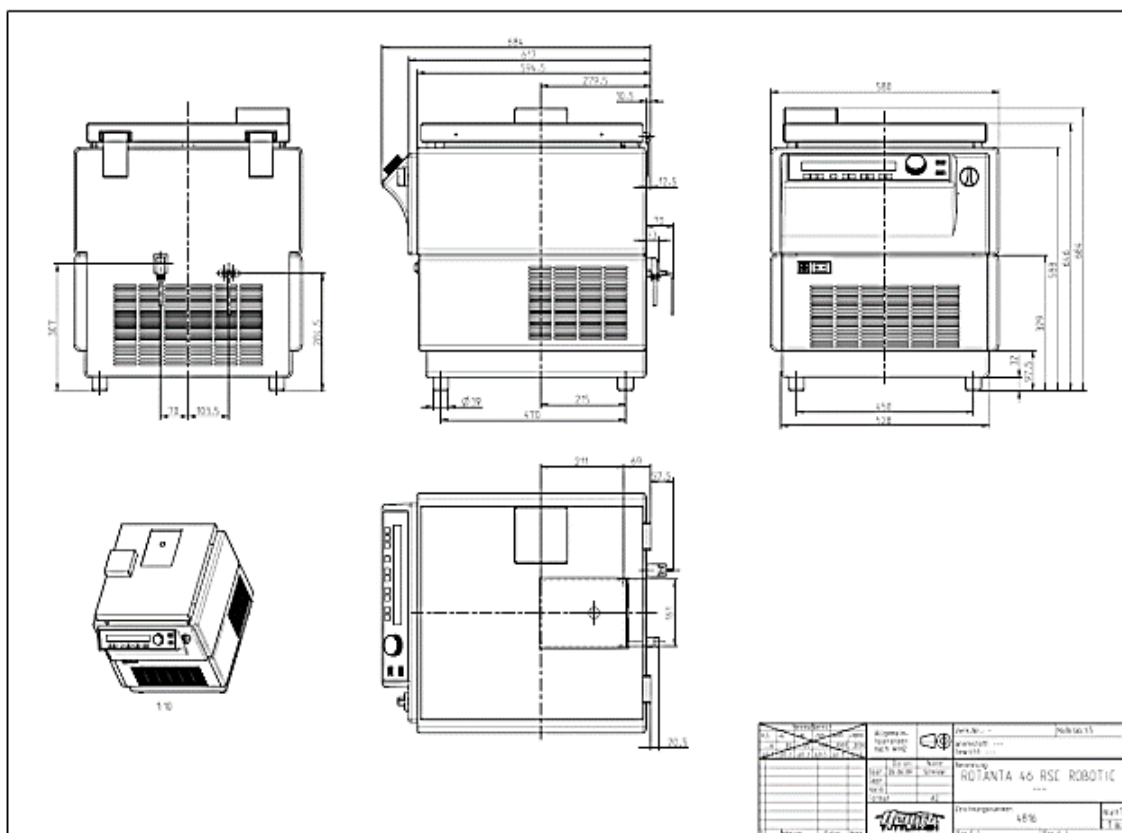
Stroke	140 mm	5.5 in
Grip Force	10 to 125 N	2 to 25 lbf
Form-fit Grip Payload	2.5 kg	5.5 lbs
Friction Grip Payload*	2.5 kg	5.5 lbs
Gripper Weight	1 kg	2 lbs
Closing speed	30 to 250 mm/s	1.2 to 9.8 in/s
Ingress protection (IP) rating	IP40	



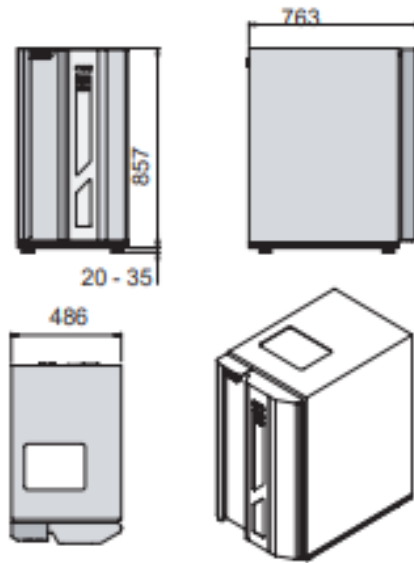
B5) Liquid Handler – Opentrons [Source: [Opentrons](#)]

Dimensions	[mm]
Height	630
Depth	570
Width	660

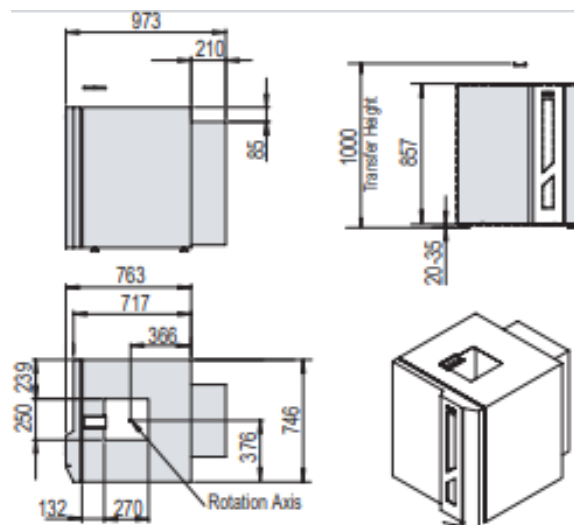
B6) Centrifuge - ROTANTA 460 Robotic [Source: [Hettich](#)]



B7) Freezer -STR44 [Source: [Liconic](#)]



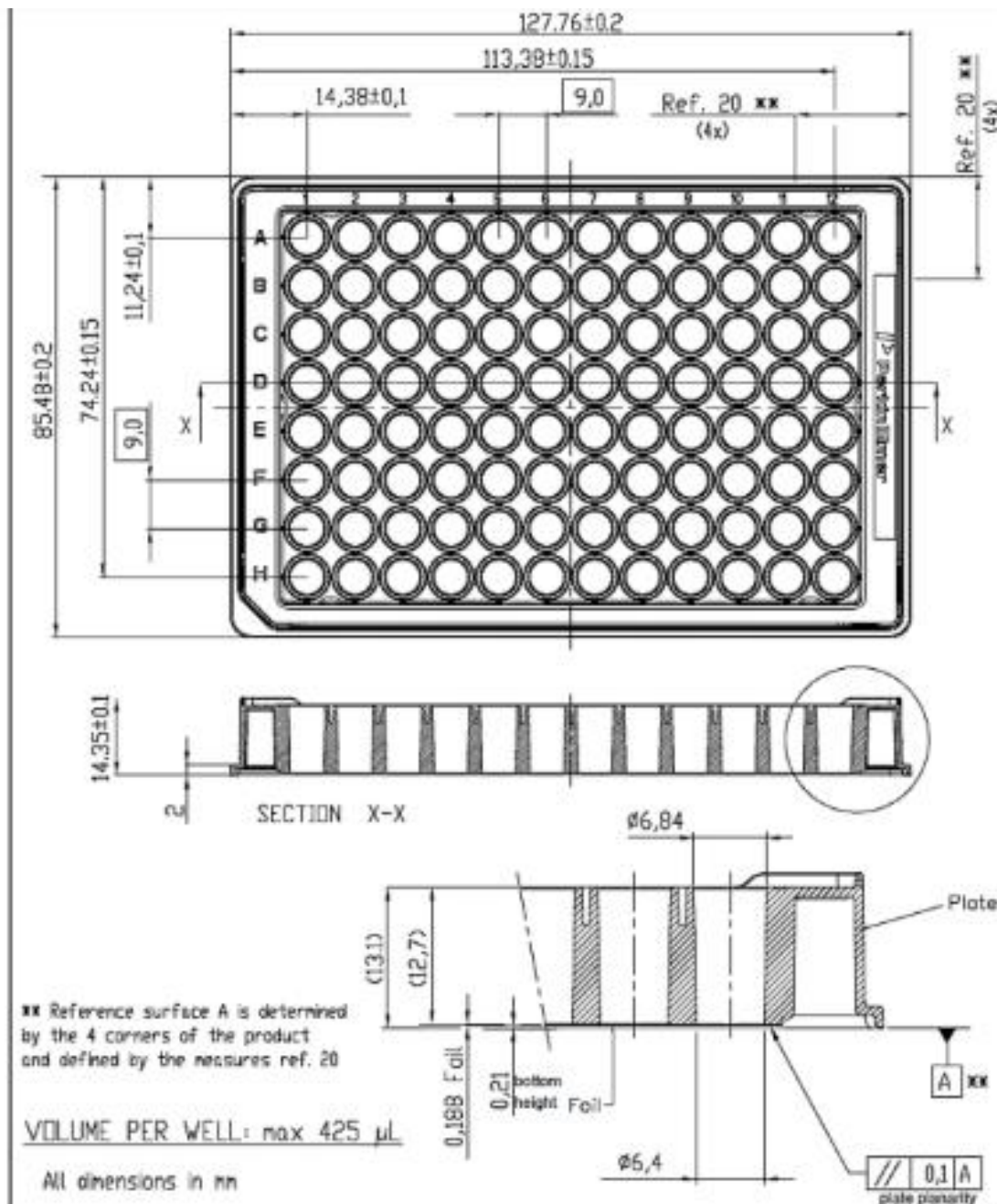
B8) Incubator- STR240 [Source: [Liconic](#)]



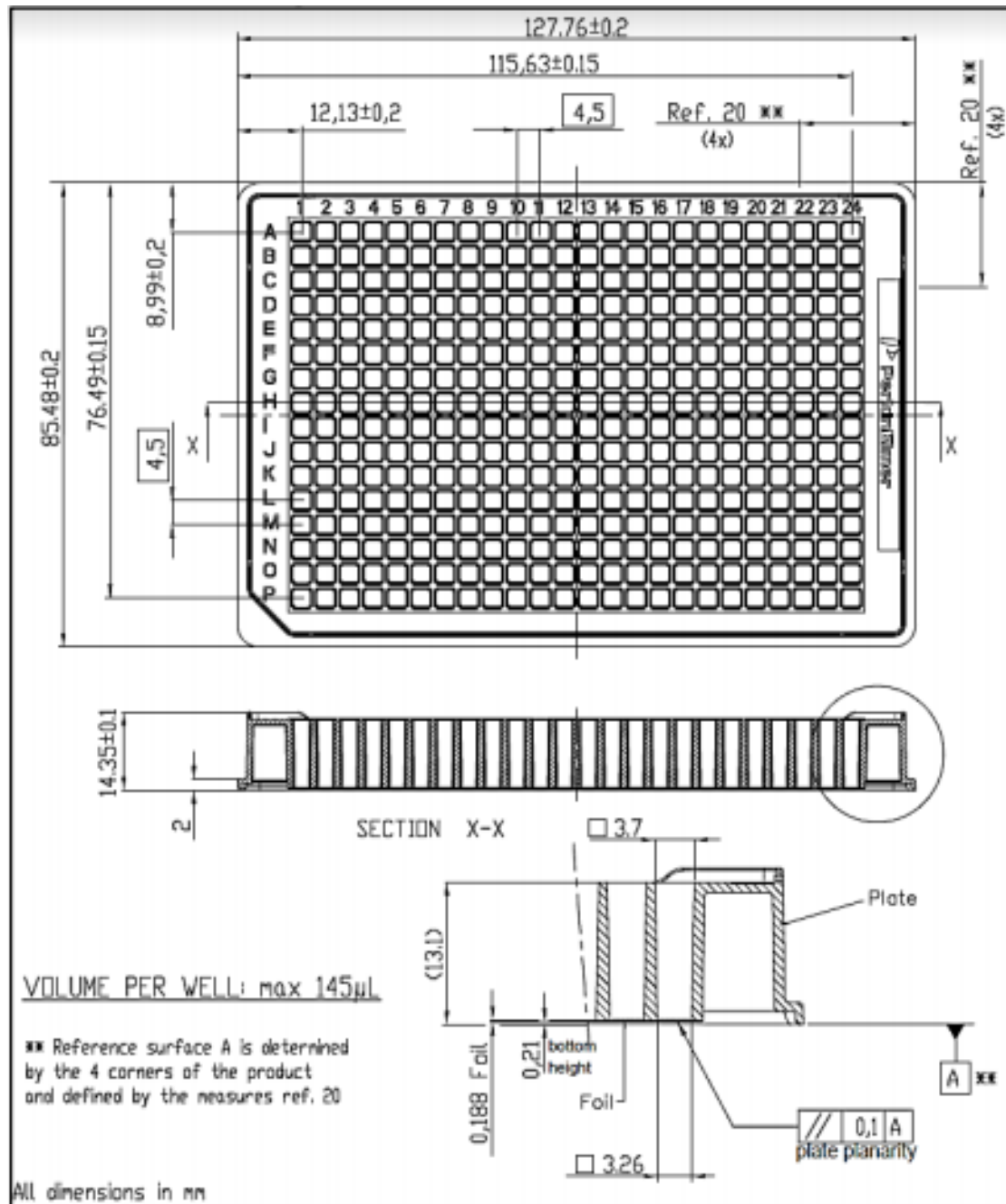
B9) Plate Reader- EnVision 2105 [Source: [Perkin Elmer](#)]

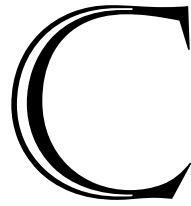
Dimensions	[mm]
Height	580
Depth	550
Width	420

B10) Cell-carrier 96 [Source: Perkin Elmer]



B11) Cell-carrier 384 [Source: Perkin Elmer]





MATLAB CODE

SCARA FILES

main_SCARA.m.....	14
USER_INPUT.m.....	15
TrajParam.m.....	15
Cartesian_Traj.m.....	16
Joint_Traj.m.....	16
SCENE_ELEMENTS.m.....	16
EXECUTE_EXPERIMENT.m.....	19
CHECK_HOME.m.....	20
Joint_Trajall.m.....	22
SCARAexetraj.m.....	26
SCARAplatetraj.m.....	31
OPEN_GRIPPER.m.....	36
CLOSE...GRIPPER.m.....	37
PLATE.m.....	38
TURN_PLATE.m.....	39
MACHINES.m.....	40
OUTPUT.m.....	41

main_SCARA.m

```

function main_SCARA()

%import URDF file of robot
robot= importrobot('Rob.urdf');
showdetails(robot); %show details about robot chain
robot.DataFormat='column';

%start simulation
%connect to VREP
disp('Program started');
    % vrep=remApi('remoteApi','extApi.h'); % using the header (requires a
    compiler)
    vrep=remApi('remoteApi'); % using the prototype file (remoteApiProto.m)
    vrep.simxFinish(-1); % just in case, close all opened connections
    clientID =vrep.simxStart('127.0.0.1',19999,true,true,5000,5);

if (clientID>-1)
    disp('Connected ');
else
    disp('Failed connecting to remote API server');
    % Now close the connection to V-REP:
    vrep.simxFinish(clientID);
end

%User defines experiment protocol
USER_INPUT;

%retrieve info from VREP for machines after user input
SCENE_ELEMENTS;

%define parameters for trajectory execution
T=1; %set time T
dt=0.01; %set time step dt, usually 10ms-1ms

%Execution of experiment according to protocol
EXECUTE_EXPERIMENT;

%Notify user that experiment was completed successfully
fprintf('Experiment successfully completed \n')

    % call the destructor!
    vrep.simxFinish(clientID);
    vrep.delete();

end

```

Published with MATLAB® R2018a

USER_INPUT.m

```

%%%%%%%%% USER INPUT %%%%%%%%%%%%%%
%ask user for machine input- experiment protocol
machine={};
    i=1;
while (1)
    prompt=input('Input working station \n', 's');

    if strcmp (prompt, 'stop')
        break
    end

    machine{i,1}=prompt;
    i=i+1;
end

```

Published with MATLAB® R2018a

TrajParam.m

```

function [x] = TrajParam(T)
% find time-law (3rd order polynomial), [a b c d] only need one time
computation
% s= a*t^3+ b*t^2+ c*t+d
% sd= 3*a*t^2+ 2*b*t+c

%define constraints
% s(0)=0 ; s(T)= 1;
% sd(0)= 0 ; sd(T)=0;

%x= [a b c d]
%Ax=b

A= [0 0 0 1;
    T^3 T^2 T 1;
    0 0 1 0;
    3*T^2 2*T 1 0];

B = [0; 1; 0; 0];

x= pinv(A) * B ;

end

```

Published with MATLAB® R2018a

Cartesian_Traj.m

```
function [P, v, theta, thetad]=Cartesian_Traj(P_o,P_f,theta_i, theta_f,t,x)

%calculate cartesian trajectory

s= x(1)*t^3 + x(2)*t^2+ x(3)*t+ x(4);
sd= 3*x(1)*t^2 + 2*x(2)*t+x(3);

P= (P_f-P_o)*s+P_o ;
v=(P_f-P_o)*sd ;

theta= (theta_f-theta_i)*s+theta_i ;
thetad=(theta_f-theta_i)*sd ;
end
```

Published with MATLAB® R2018a

Joint_Traj.m

```
function [q_d,qdot]=Joint_Traj(q_i,q_f,t,x)

%calculate joint trajectory

s= x(1)*t^3 + x(2)*t^2+ x(3)*t+ x(4);
sd= 3*x(1)*t^2 + 2*x(2)*t+x(3);

q_d= (q_f-q_i)*s+q_i ;
qdot=(q_f-q_i)*sd ;

end
```

Published with MATLAB® R2018a

SCENE_ELEMENTS.m

```
%%%%%%%%%%%%% HANDLES %%%%%%%%%%%%%%
%get handle for world frame-all machines are relative to this frame
[~,Base_frame]=vrep.simxGetObjectHandle(clientID,'world_visual',vrep.simx_op
mode_blocking);

%get handles for other necessary components of simulation
[~,Plate_frame]=vrep.simxGetObjectHandle(clientID,'Plate_frame',vrep.simx_op
mode_blocking);

[~,EE]=vrep.simxGetObjectHandle(clientID,'ee_link_dummy',vrep.simx_opmode_bl
ocking);
```

```

[~,ee]=vrep.simxGetObjectHandle(clientID,'ee_link_visual',vrep.simx_opmode_blocking);
[~,Input_Tech]=vrep.simxGetObjectHandle(clientID,'Input_Tech',vrep.simx_opmode_blocking);
[~,Output_Tech]=vrep.simxGetObjectHandle(clientID,'Output_Tech',vrep.simx_opmode_blocking);
[~,Turn]=vrep.simxGetObjectHandle(clientID,'BaseArm_JointRot',vrep.simx_opmode_blocking);
[~,ProxS]=vrep.simxGetObjectHandle(clientID,'ProxS',vrep.simx_opmode_blocking);

%get handles joints
[~,Joint1]=vrep.simxGetObjectHandle(clientID,'Arm_Joint1',vrep.simx_opmode_blocking);
[~,Joint2]=vrep.simxGetObjectHandle(clientID,'Arm_Joint2',vrep.simx_opmode_blocking);
[~,BaseJ1]=vrep.simxGetObjectHandle(clientID,'BaseArm_Joint1',vrep.simx_opmode_blocking);
[~,BaseJ2]=vrep.simxGetObjectHandle(clientID,'BaseArm_Joint2',vrep.simx_opmode_blocking);
[~,Joint3]=vrep.simxGetObjectHandle(clientID,'Arm_Joint3',vrep.simx_opmode_blocking);
[~,Grip1]=vrep.simxGetObjectHandle(clientID,'Gripper_JointDx',vrep.simx_opmode_blocking);
[~,Grip2]=vrep.simxGetObjectHandle(clientID,'Gripper_JointSx',vrep.simx_opmode_blocking);
[~,Turn]=vrep.simxGetObjectHandle(clientID,'BaseArm_JointRot',vrep.simx_opmode_blocking);

%get joint values from VREP

[~,J1]=vrep.simxGetJointPosition(clientID,BaseJ1,vrep.simx_opmode_blocking);

[~,J2]=vrep.simxGetJointPosition(clientID,BaseJ2,vrep.simx_opmode_blocking);

[~,J3]=vrep.simxGetJointPosition(clientID,Joint1,vrep.simx_opmode_blocking);

[~,J4]=vrep.simxGetJointPosition(clientID,Joint2,vrep.simx_opmode_blocking);

[~,J5]=vrep.simxGetJointPosition(clientID,Joint3,vrep.simx_opmode_blocking);

[~,GripR]=vrep.simxGetJointPosition(clientID,Grip1,vrep.simx_opmode_blocking);

[~,GripL]=vrep.simxGetJointPosition(clientID,Grip2,vrep.simx_opmode_blocking);

%INITIAL JOINT CONFIGURATION
q= [J1; J2;J3;J4;J5];

%set home configuration of robot-it always returns here

```

```

Home=[0;1;-1.0472; 2.5;0];

%%%%%%%%% POSITION %%%%%%%%%%%
%position of components
[~,Plate_Pose]=vrep.simxGetObjectPosition(clientID,Plate_frame,Base_frame,vr
ep.simx_opmode_blocking);
[~,BaseFrame_Pose]=vrep.simxGetObjectPosition(clientID,Base_frame,Base_frame
,vrep.simx_opmode_blocking);
[~,Input_Pose]=vrep.simxGetObjectPosition(clientID,Input_Tech,Base_frame,vre
p.simx_opmode_blocking);
[~,Output_Pose]=vrep.simxGetObjectPosition(clientID,Output_Tech,Base_frame,v
rep.simx_opmode_blocking);
[~,Home_eePose]=vrep.simxGetObjectPosition(clientID,EE,Base_frame,vrep.simx_
opmode_blocking);

%%%%%%%%% ORIENTATION %%%%%%%%%%%
%orientation of components
[~,Plate_Orient]=vrep.simxGetObjectOrientation(clientID,Plate_frame,Base_fra
me,vrep.simx_opmode_blocking);
[~,BaseFrame_Orient]=vrep.simxGetObjectOrientation(clientID,Base_frame,Base_
frame,vrep.simx_opmode_blocking);
[~,Input_Orient]=vrep.simxGetObjectOrientation(clientID,Input_Tech,Base_fram
e,vrep.simx_opmode_blocking);
[~,Output_Orient]=vrep.simxGetObjectOrientation(clientID,Output_Tech,Base_fr
ame,vrep.simx_opmode_blocking);

%rotation matrices of components
Rot_Input= eul2rotm(Input_Orient,'XYZ');
Rot_Output= eul2rotm(Output_Orient,'XYZ');

%%%%%%%%%% HANDLES | POSITION | ORIENTATION OF MACHINES%%%%%%%%%%
%only the machines used in the experiment each time
for i=1:length(machine)

    [~,Handles{i,1}] =
vrep.simxGetObjectHandle(clientID,machine{i,1},vrep.simx_opmode_blocking);

    [~,ObjPos{i,1}]=vrep.simxGetObjectPosition(clientID,Handles{i,1},Base_frame,
vrep.simx_opmode_blocking);

    [~,ObjOr{i,1}]=vrep.simxGetObjectOrientation(clientID,Handles{i,1},Base_fram
e,vrep.simx_opmode_blocking);
    Rot_machine{i,1} = eul2rotm(ObjOr{i,1},'XYZ');
    Pose=cell2mat(ObjPos);

    %set positions where robot will go
    Machine_Position{i,1}= ObjPos{i,1}' ;
    %set safe distance from each machine before arm approaches final goal
    MachSafe_Pose{i,1} = [Pose(i,1); (Pose(2)-0.5); Pose(i,3)];
end

```

Published with MATLAB® R2018a

EXECUTE_EXPERIMENT.m

```

##### EXECUTION OF EXPERIMENT #####

% make sure robot is not at a non-desirable position
CHECK_HOME(robot, q,T,dt,Home, Rot_Input,BaseJ1,BaseJ2, Joint1,
Joint2,EE,Grip1,Grip2, Input_Pose );

##### EXECUTION OF EXPERIMENT #####
for i=1:length(machine)

rot_m= Rot_machine(i,1);

if strcmp (machine{i,1}, 'Opentrons')

PLATE (robot, q,T,dt,Plate_frame,Base_frame,Home, BaseJ1, BaseJ2, Joint1,
Joint2,EE, Grip1, Grip2, Turn);
MACHINES(robot, q, T,dt,i, Machine_Position, MachSafe_Pose, rot_m,
BaseJ1,BaseJ2, Joint1, Joint2,EE, Grip1, Grip2, Home);
PLATE (robot, q,T,dt,Plate_frame,Base_frame,Home, BaseJ1, BaseJ2, Joint1,
Joint2,EE, Grip1, Grip2, Turn);

else

MACHINES(robot, q, T,dt,i, Machine_Position, MachSafe_Pose, rot_m,
BaseJ1,BaseJ2, Joint1, Joint2,EE, Grip1, Grip2, Home);

end
%
i=i+1;
end

%Plate returns to technician-output
OUTPUT (robot, q,T,dt, Rot_Output,Output_Pose,BaseJ1,BaseJ2, Joint1,
Joint2,EE, Grip1, Grip2, Home);

```

Published with MATLAB® R2018a

CHECK_HOME.m

```

function CHECK_HOME(robot, q,T,dt,Home, Rot_Input,BaseJ1,BaseJ2, Joint1,
Joint2,EE,Grip1,Grip2, Input_Pose )
%%%%%CHECK HOME%%%%%
%checks if robot is in home position
%if yes user is notified
%if not it is commanded to go to home position before the start of the
experiment

%connect to VREP
    % vrep=remApi('remoteApi','extApi.h'); % using the header (requires a
compiler)
    vrep=remApi('remoteApi'); % using the prototype file (remoteApiProto.m)
    vrep.simxFinish(-1); % just in case, close all opened connections
    clientID =vrep.simxStart('127.0.0.1',19999,true,true,5000,5);

    if (clientID>-1)
        disp('')
    else
        % close the connection to V-REP and notify user
        vrep.simxFinish(clientID);
    end

if q(1)==0 && q(2)== 1 && q(3)==-1.0472 && q(4)==2.5 && q(5)==0

    printf('Robot is in Home Position-Ready to start experiment')
else
    %return robot to home joint configuration
    q_f= Home;
    q= Joint_Trajall(robot,q,T,dt,q_f,BaseJ1,BaseJ2, Joint1, Joint2, EE);
end

prompt='Do you wish to continue to experiment? Y/N [Y]:';
str = input(prompt,'s');
if isempty(str) || str=='Y'
    str = 'Y';

    %start with experiment and notify user
    fprintf('Experiment started \n')
    pause(1);

    %first step is to take plate from technician-input

    %set joint configuration above input window
    q_f= [1.6;1;0.4; 1.3;0];
    q= Joint_Trajall(robot,q,T,dt,q_f,BaseJ1,BaseJ2, Joint1, Joint2, EE);

    % move to grab plate
    OPEN_GRIPPER(Grip1, Grip2);

    rot_m= Rot_Input;
    P_f= (Input_Pose)';

```

```
q= SCARAextraj(robot,q,T,dt,P_f,rot_m,BaseJ1,BaseJ2, Joint1, Joint2,EE);

CLOSE_GRIPPER(Grip1, Grip2);

% move again to safe configuration above input window
%return to home configuration before proceeding
q_f= [1.6;1;0.4; 1.3;0];
q= Joint_Trajall(robot,q,T,dt,q_f,BaseJ1,BaseJ2, Joint1, Joint2,
EE);
q_f= Home;
q= Joint_Trajall(robot,q,T,dt,q_f,BaseJ1,BaseJ2, Joint1, Joint2,
EE);;

else

error('Experiment interrupted by user')

end

% call the destructor!
vrep.simxFinish(clientID);
vrep.delete();

end
```

Published with MATLAB® R2018a

Joint_Trajall.m

```

function q= Joint_Trajall(robot,q,T,dt,q_f,BaseJ1,BaseJ2, Joint1, Joint2,
EE)
%connect to VREP
    % vrep=remApi('remoteApi','extApi.h'); % using the header (requires a
compiler)
    vrep=remApi('remoteApi'); % using the prototype file (remoteApiProto.m)
    vrep.simxFinish(-1); % just in case, close all opened connections
    clientID =vrep.simxStart('127.0.0.1',19999,true,true,5000,5);

    if (clientID>-1)
        disp('Connected ');
    else
        disp('Failed connecting to remote API server');
    end

%Retrieve current joint configuration
q_i= [ q(1); q(2); q(3); q(4); q(5)];

%offset between visual EE and actual EE
T_dummy_e=[1 0 0 0.071004;0 1 0 0.029014 ; 0 0 1 0 ;0 0 0 1];

%parameters for trajectory
% T=1; %set time T
x= TrajParam(T);
% dt= 0.01; %set time step, usually 10ms-1ms
t=0;

c=1;
while t<= T

%homogenous transformation for robot chain
T_e= getTransform(robot,double(q),'ee_link');

%transformation from visual EE to actual EE
T_final= T_e* T_dummy_e;
P_i= T_final(1:3,4);

%get path between initial and desired configuration
[q_d,qdot]=Joint_Traj(q_i,q_f,t,x);

%joint position at t+dt
q= q+qdot*dt;

    for j=3:5
        q(j)=atan2(sin(q(j)),cos(q(j)));
    end

    %%%%%%%%%%%%%%%%%%%%%%%%%%%%%%%%%%%%%%%%%%%%%%%%%%%%%%%%%%%%%%%%%%%%%%%%%
%save the values for position and velocity for later plotting
timeV(c)= t;
X_act(c,:)= P_i(1);
Y_act(c,:)=P_i(2);
Z_act(c,:)= P_i(3);

```

```

q1(c,:) = q(1);
q2(c,:) = q(2);
q3(c,:) = q(3);
q4(c,:) = q(4);
q5(c,:) = q(5);

qd1(c,:) = qdot(1);
qd2(c,:) = qdot(2);
qd3(c,:) = qdot(3);
qd4(c,:) = qdot(4);
qd5(c,:) = qdot(5);
c=c+1 ;
%%%%%%%%%%%%%%%%%%%%%%%%%%%%%%%%%%%%%%%%%%%%%%%%%%%%%%%%%%%%%%%%%%%%%%%%

t=t+dt;

% update visual robot configuration
[~]=vrep.simxPauseCommunication(clientID,1);
[J1]=vrep.simxSetJointPosition(clientID,BaseJ1,q(1),vrep.simx_opmode_oneshot);
[J2]=vrep.simxSetJointPosition(clientID,BaseJ2,q(2),vrep.simx_opmode_oneshot);
[J3]=vrep.simxSetJointPosition(clientID,Joint1,q(3),vrep.simx_opmode_oneshot);
[J4]=vrep.simxSetJointPosition(clientID,Joint2,q(4),vrep.simx_opmode_oneshot);
[J5]=vrep.simxSetJointPosition(clientID,EE,q(5),vrep.simx_opmode_oneshot);
[~]=vrep.simxPauseCommunication(clientID,0);

pause(dt);

end

%%% POSITION PLOTS %%%
figure()
%plot x,y,z of trajectory
subplot(3,1,1);
hold on
plot (timeV,X_act)
title('Actual End-Effector Displacement (FK)' , 'FontSize',14)
ylabel('x-coordinate [m]','FontWeight','Bold')
xlabel('time [s]','FontWeight','Bold')

subplot(3,1,2);
hold on
plot (timeV,Y_act)
ylabel('y-coordinate [m]','FontWeight','Bold')
xlabel('time [s]','FontWeight','Bold')

subplot(3,1,3);
hold on
plot (timeV,Z_act)
hold off
ylabel('z-coordinate [m]','FontWeight','Bold')
xlabel('time [s]','FontWeight','Bold')

```

```

##### JOINT PLOTS #####
figure()
subplot(5,1,1);
hold on
plot (timeV,q1)
title('Joint angles (FK)' , 'FontSize',14)

ylabel('Joint 1 [rad]','FontWeight','Bold')
xlabel('time [s]','FontWeight','Bold')

subplot(5,1,2);
hold on
plot (timeV,q2)
ylabel('Joint 2 [rad]','FontWeight','Bold')
xlabel('time [s]','FontWeight','Bold')

subplot(5,1,3);
hold on
plot (timeV,q3)
ylabel('Joint 3 [rad]','FontWeight','Bold')
xlabel('time [s]','FontWeight','Bold')

subplot(5,1,4);
hold on
plot (timeV,q4)
ylabel('Joint 4 [rad]','FontWeight','Bold')
xlabel('time [s]','FontWeight','Bold')

subplot(5,1,5);
hold on
plot (timeV,q5)
ylabel('Joint 5 [rad]','FontWeight','Bold')
xlabel('time [s]','FontWeight','Bold')

hold off

##### VELOCITY PLOTS #####
figure()
subplot(5,1,1);
hold on
plot (timeV,qd1)
title('Joint velocities (FK)' , 'FontSize',14)
ylabel('Joint 1 [rad/s]','FontWeight','Bold')
xlabel('time [s]','FontWeight','Bold')

subplot(5,1,2);
hold on
plot (timeV,qd2)
ylabel('Joint 2 [rad/s]','FontWeight','Bold')
xlabel('time [s]','FontWeight','Bold')

subplot(5,1,3);
hold on
plot (timeV,qd3)
ylabel('Joint 3 [rad/s]','FontWeight','Bold')

```

```
xlabel('time [s]', 'FontWeight', 'Bold')

subplot(5,1,4);
hold on
plot (timeV, qd4)
ylabel('Joint 4 [rad/s]', 'FontWeight', 'Bold')
xlabel('time [s]', 'FontWeight', 'Bold')

subplot(5,1,5);
hold on
plot (timeV, qd5)
ylabel('Joint 5 [rad/s]', 'FontWeight', 'Bold')
xlabel('time [s]', 'FontWeight', 'Bold')
hold off

    % call the destructor!
    vrep.simxFinish(clientID);
    vrep.delete();

end
```

Published with MATLAB® R2018a

SCARAexetraj.m

```

function q= SCARAexetraj(robot,q,T,dt,P_f,rot_m,BaseJ1,BaseJ2, Joint1,
Joint2,EE)
%start simulation
%connect to VREP

    % vrep=remApi('remoteApi','extApi.h'); % using the header (requires a
compiler)
vrep=remApi('remoteApi'); % using the prototype file (remoteApiProto.m)
vrep.simxFinish(-1); % just in case, close all opened connections
clientID =vrep.simxStart('127.0.0.1',19999,true,true,5000,5);

if (clientID>-1)
    disp('')
else
    % close the connection to V-REP and notify user
vrep.simxFinish(clientID);
end

%offset between visual EE and actual EE
T_dummy_e=[1 0 0 0.071004;0 1 0 0.029014 ; 0 0 1 0 ;0 0 0 1];

%homogenous transformation for robot chain
Trans= getTransform(robot,double(q), 'ee_link');

%Transformation from visual EE to actual EE
T_fi= Trans* T_dummy_e;
P_o= T_fi(1:3,4);

%parameters for trajectory
% T=1; %set time T
x= TrajParam(T);
% dt= 0.01; %set time step, usually 10ms-1ms
t=0;

c=1;
%%%%% Follow Trajectory %%%%%%
while t<= T

%homogenous transformation for robot chain
T_e= getTransform(robot,double(q), 'ee_link');

%transformation from visual EE to actual EE
T_final= T_e* T_dummy_e;
P_i= T_final(1:3,4);

%rotation matrix of EE wrt to base frame
Rot_EE= T_final(1:3,1:3);

%%%%% ORIENTATION ERROR %%%%%%
%angle-axis representation (Sicilliano et.al)

```



```

R_err =transpose(Rot_EE)* (rot_m);
r_theta =rotm2axang(R_err);
r= r_theta(1, 1:3); %r wrt Rot_init
theta_f= r_theta(1, 4);
r= (Rot_EE)* transpose(r); %r wrt base frame
theta_i=0;

%elements (vectors) for Re(Rot_EE)computed from joint variables
ne= Rot_EE(:,1);
se= Rot_EE(:,2);
ae= Rot_EE(:,3);

%elements (vectors) for Rd(rot_m)
nd= rot_m(:,1);
sd= rot_m(:,2);
ad= rot_m(:,3);

%after differentiating eo wrt time
L= (-
0.5)*((nd/dt)*(nd')*(ne/dt)*(ne')+(sd/dt)*(sd')*(se/dt)*(se')+(ad/dt)*(ad')*(ae/dt)*(ae'));

%get trajectory between initial and desired ending point
[P, v, theta, thetad]=Cartesian_Traj(P_o,P_f,theta_i, theta_f,t,x);
w= thetad*r;
wd=(L\((L')*w));
eoo= r*sin(theta);

%positive values Ko, Kp
Ko=(1/dt-10);
Kp=(1/dt-10);

%%% ERRORS %%%
eo= L\((Ko*eoo); %orientation error (only around z)
ep= Kp*(P-P_i); %position error
e= [ep ; eo(3)];

%%%% JACOBIAN %%%%
%calculate geometric jacobian
Jac_rev = geometricJacobian(robot,double(q), 'ee_link');

%reverse rows
%Matlab default (first rotation, second transaltion)
Jac= [Jac_rev(4:6,:);Jac_rev(1:3,:)] ;

%linear velocity, keep x,y,z
%orientation in z axis
J= [Jac(1:3,:) ; Jac(6,:)];

%damping factor λ via SVD
[~,S,~] = svd(J);
diagS=diag(S);
sigma=min(diagS);
lamdamax=0.04;
eps= 10e-4;

```

```

if sigma >= eps
    lamda = 0;
else
    lamda= sqrt((1- ((sigma/eps)^2)*(lamdamax^2)));
end

%%%%% QUADRATIC PROGRAMMING %%%%%
%set lower-upper bounds for quadprog
q_min=[-1.9;0;-2.1;-2.5;0];
q_max= [1.8;1.9;2.1;2.5;0];
lb=(q_min-q)/dt;
ub=(q_max-q)/dt;

%Solving IK
%quadratic programming
H=(J'*J + ((lamda)^2)*eye(5,5));
b=( [v;wd(3)]+ e);
f=- (b')*J ;
options = optimset('Display', 'off');
qd = quadprog(double(H),double(f), [], [], [], [], double(lb),double(ub), [],
options);

ve= J*qd;
q= q+qd*dt; %joint position at t+dt

    for j=3:5
        q(j)=atan2(sin(q(j)),cos(q(j)));
    end

%%%%%%%%%%%%%%%%%%%%%%%%%%%%%%%%%%%%%%%%%%%%%%%%%%%%%%%%%%%%%%%%%%%%%%%%
%save the values for position and velocity for later plotting
timeV(c)= t;
X_des(c,:)= P(1);
Y_des(c,:)= P(2);
Z_des(c,:)= P(3);
X_act(c,:)= P_i(1);
Y_act(c,:)= P_i(2);
Z_act(c,:)= P_i(3);
% v1_des(c,:)= v(1);
% v2_des(c,:)= v(2);
v3_des(c,:)= v(3);
% v1_act(c,:)= ve(1);
% v2_act(c,:)= ve(2);
v3_act(c,:)= ve(3);

q1(c,:)= q(1);
q2(c,:)= q(2);
q3(c,:)= q(3);
q4(c,:)= q(4);
q5(c,:)= q(5);

c=c+1 ;
%%%%%%%%%%%%%%%%%%%%%%%%%%%%%%%%%%%%%%%%%%%%%%%%%%%%%%%%%%%%%%%%%%%%%%%%
    t=t+dt;

```

```

% update visual robot configuration
[~]=vrep.simxPauseCommunication(clientID,1);
[J1]=vrep.simxSetJointPosition(clientID,BaseJ1,q(1),vrep.simx_opmode_oneshot);
[J2]=vrep.simxSetJointPosition(clientID,BaseJ2,q(2),vrep.simx_opmode_oneshot);
[J3]=vrep.simxSetJointPosition(clientID,Joint1,q(3),vrep.simx_opmode_oneshot);
[J4]=vrep.simxSetJointPosition(clientID,Joint2,q(4),vrep.simx_opmode_oneshot);
[J5]=vrep.simxSetJointPosition(clientID,EE,q(5),vrep.simx_opmode_oneshot);
[~]=vrep.simxPauseCommunication(clientID,0);

pause(dt);

end

%%%%% PLOTS %%%%%%%%%%

%%%% JOINT PLOTS
figure()
subplot(5,1,1);
hold on
plot (timeV,q1)
title('Joint angles ' , 'FontSize',14)

ylabel('Joint 1 [rad]','FontWeight','Bold')
xlabel('time [s]','FontWeight','Bold')

subplot(5,1,2);
hold on
plot (timeV,q2)
ylabel('Joint 2 [rad]','FontWeight','Bold')
xlabel('time [s]','FontWeight','Bold')

subplot(5,1,3);
hold on
plot (timeV,q3)
ylabel('Joint 3 [rad]','FontWeight','Bold')
xlabel('time [s]','FontWeight','Bold')

subplot(5,1,4);
hold on
plot (timeV,q4)
ylabel('Joint 4 [rad]','FontWeight','Bold')
xlabel('time [s]','FontWeight','Bold')

subplot(5,1,5);
hold on
plot (timeV,q5)
ylabel('Joint 5 [rad]','FontWeight','Bold')
xlabel('time [s]','FontWeight','Bold')

hold off

```

```

##### VELOCITY PLOTS
figure()

hold on
plot (timeV,v3_des, '.r')
plot (timeV,v3_act, '.b')
% ylim(ax3,[-1 1 ])
title('End-effector Velocity' , 'FontSize',14)
xlabel('time [s]','FontWeight','Bold')
ylabel('velocity [m/s]','FontWeight','Bold')
hold off

##### POSITION PLOTS
figure()
%plot x,y,z of trajectory
ax1=subplot(3,1,1);
hold on
plot (timeV,X_des, '.r')
plot (timeV,X_act, '.b')
% ylim(ax1,[-2 2 ])
title('Displacement' , 'FontSize',14)
ylabel('x-coordinate [m]','FontWeight','Bold')
xlabel('time [s]','FontWeight','Bold')

ax2=subplot(3,1,2);
hold on
plot (timeV,Y_des, '.r')
plot (timeV,Y_act, '.b')
% ylim(ax2,[-1 1 ])
ylabel('y-coordinate [m]','FontWeight','Bold')
xlabel('time [s]','FontWeight','Bold')

ax3=subplot(3,1,3);
hold on
plot (timeV,Z_des, '.r')
plot (timeV,Z_act, '.b')
% ylim(ax3,[-1 1 ])
ylabel('z-coordinate [m]','FontWeight','Bold')
xlabel('time [s]','FontWeight','Bold')

hold off

    % call the destructor!
    vrep.simxFinish(clientID);
    vrep.delete();

end

```

Published with MATLAB® R2018a

SCARAplatetraj.m

```

function q= SCARAplatetraj(robot,q,T,dt,P_f,Base_frame, BaseJ2, Joint1,
Joint2,EE)

%start simulation
%connect to VREP
    % vrep=remApi('remoteApi','extApi.h'); % using the header (requires a
compiler)
    vrep=remApi('remoteApi'); % using the prototype file (remoteApiProto.m)
    vrep.simxFinish(-1); % just in case, close all opened connections
    clientID =vrep.simxStart('127.0.0.1',19999,true,true,5000,5);

    if (clientID>-1)
        disp('')
    else
        % close the connection to V-REP and notify user
        vrep.simxFinish(clientID);
    end

%offset between visual EE and actual EE
T_dummy_e=[1 0 0 0.071004;0 1 0 0.029014 ; 0 0 1 0 ;0 0 0 1];

%homogenous transformation for robot chain
Trans= getTransform(robot,double(q), 'ee_link');

%Transformation from visual EE to actual EE
T_fi= Trans* T_dummy_e;
P_o= T_fi(1:3,4);

[~,Plate_frame]=vrep.simxGetObjectHandle(clientID, 'Plate_frame',vrep.simx_op
mode_blocking);

%parameters for trajectory
x= TrajParam(T);
t=0;

c=1;
    %%%%% IK %%%%%%%
while t<= T
%homogenous transformation for robot chain
T_e= getTransform(robot,double(q), 'ee_link');

%transformation from visual EE to actual EE
T_final= T_e* T_dummy_e;
P_i= T_final(1:3,4);

%rotation matrix of EE wrt to base frame
Rot_EE= T_final(1:3,1:3);

%calculation of orientation of plate

```

```

%it moves around so position & orientation are not fixed
[~,Plate_Orient]=vrep.simxGetObjectOrientation(clientID,Plate_frame,Base_fra
me,vrep.simx_opmode_blocking);
Rot_Plate = eul2rotm(Plate_Orient,'XYZ');

%%%%% ORIENTATION ERROR %%%%%
%angle-axis representation (Sicilliano et.al)
R_err =transpose(Rot_EE)* (Rot_Plate);
r_theta =rotm2axang(R_err);
r= r_theta(1, 1:3); %r wrt Rot_init
theta_f= r_theta(1, 4);
r= (Rot_EE)* transpose(r); %r wrt base frame
theta_i=0;

%elements (vectors) for Re(Rot_EE)computed from joint variables
ne= Rot_EE(:,1);
se= Rot_EE(:,2);
ae= Rot_EE(:,3);

%elements (vectors) for Rd(rot_m)
nd= Rot_Plate(:,1);
sd= Rot_Plate(:,2);
ad= Rot_Plate(:,3);

%after differentiating eo wrt time
L= (-
0.5)*((nd/dt)*(nd')*(ne/dt)*(ne')+(sd/dt)*(sd')*(se/dt)*(se')+(ad/dt)*(ad')*(
ae/dt)*(ae'));

%get trajectory between initial and desired ending point
[P, v, theta, thetad]=Cartesian_Traj(P_o,P_f,theta_i, theta_f,t,x);
w= thetad*r;
wd=(L\((L')*w));
eoo= r*sin(theta);

%positive values Ko, Kp
Ko=(1/dt-10);
Kp=(1/dt-10);

%%%%% ERRORS %%%%%
eo= L\ (Ko*eoo); %orientation error (only around z)
ep= Kp*(P-P_i); %position error
e= [ep ; eo(3)];

%%%%% JACOBIAN %%%%%
%calculate geometric jacobian
Jac_rev = geometricJacobian(robot,double(q), 'ee_link');

%reverse rows
%Matlab default (first rotation, second transaltion)
Jac= [Jac_rev(4:6,:);Jac_rev(1:3,:)] ;

%linear velocity, keep x,y,z
%orientation in z axis
J= [Jac(1:3,:) ; Jac(6,:)];

```

```

%damping factor  $\lambda$  via SVD
[~,S,~] = svd(J);
diagS=diag(S);
sigma=min(diagS);
lamdamax=0.04;
eps= 10e-4;

if sigma >= eps
    lamda = 0;
else
    lamda= sqrt((1- ((sigma/eps)^2)*(lamdamax^2)));
end

%%%% QUADRATIC PROGRAMMING %%%%
%set lower-upper bounds for quadprog
q_min=[0;0;-2.1;-2.5;0];
q_max= [0;1.9;2.1;2.5;0];
lb=(q_min-q)/dt;
ub=(q_max-q)/dt;

%Solving IK
%quadratic programming
H=(J'*J +(lamda^2)*eye(5,5));
b=( [v;wd(3)]+ e);
f=- (b')*J ;
options = optimset('Display', 'off');
qd = quadprog(double(H),double(f), [], [], [], [], double(lb),double(ub), [],
options);

ve= J*qd;
q= q+qd*dt; %joint position at t+dt

    for j=3:5
        q(j)=atan2(sin(q(j)),cos(q(j)));
    end

    %%%%%%%%%%%%%%%%%%%%%%%%%%%%%%%%%%%%%%%%%%%%%%%%%%%%%%%%%%%%%%%%%%%%%%%%%
%save the values for position and velocity for later plotting
timeV(c)= t;
X_des(c,:)= P(1);
Y_des(c,:)= P(2);
Z_des(c,:)= P(3);
X_act(c,:)= P_i(1);
Y_act(c,:)= P_i(2);
Z_act(c,:)= P_i(3);
v3_des(c,:)= v(3);
v3_act(c,:)= ve(3);

q2(c,:)= q(2);
q3(c,:)= q(3);
q4(c,:)= q(4);
q5(c,:)= q(5);

c=c+1 ;
%%%%%%%%%%%%%%%%%%%%%%%%%%%%%%%%%%%%%%%%%%%%%%%%%%%%%%%%%%%%%%%%%%%%%%%%
    t=t+dt;

```

```

% update visual robot configuration
[~]=vrep.simxPauseCommunication(clientID,1);
[J2]=vrep.simxSetJointPosition(clientID,BaseJ2,q(2),vrep.simx_opmode_oneshot);
[J3]=vrep.simxSetJointPosition(clientID,Joint1,q(3),vrep.simx_opmode_oneshot);
[J4]=vrep.simxSetJointPosition(clientID,Joint2,q(4),vrep.simx_opmode_oneshot);
[J5]=vrep.simxSetJointPosition(clientID,EE,q(5),vrep.simx_opmode_oneshot);
[~]=vrep.simxPauseCommunication(clientID,0);
pause(dt);

end

%%% JOINT PLOTS

subplot(4,1,1);
hold on
plot (timeV,q2)
title('Joint angles ', 'FontSize',14)
ylabel('Joint 2 [rad]','FontWeight','Bold')
xlabel('time [s]','FontWeight','Bold')

subplot(4,1,2);
hold on
plot (timeV,q3)
ylabel('Joint 3 [rad]','FontWeight','Bold')
xlabel('time [s]','FontWeight','Bold')

subplot(4,1,3);
hold on
plot (timeV,q4)
ylabel('Joint 4 [rad]','FontWeight','Bold')
xlabel('time [s]','FontWeight','Bold')

subplot(4,1,4);
hold on
plot (timeV,q5)
ylabel('Joint 5 [rad]','FontWeight','Bold')
xlabel('time [s]','FontWeight','Bold')

hold off

%%% VELOCITY PLOTS
figure()

hold on
plot (timeV,v3_des, '.r')
plot (timeV,v3_act, '.b')
% ylim(ax3,[-1 1 ])
title('End-effector Velocity', 'FontSize',14)
xlabel('time [s]','FontWeight','Bold')
ylabel('velocity [m/s]','FontWeight','Bold')
hold off

```



```

%%%% POSITION PLOTS
figure()
%plot x,y,z of trajectory
ax1=subplot(3,1,1);
hold on
plot (timeV,X_des, '.r')
plot (timeV,X_act, '.b')
% ylim(ax1,[-2 2 ])
title('Displacement' , 'FontSize',14)
ylabel('x-coordinate [m]','FontWeight','Bold')
xlabel('time [s]','FontWeight','Bold')

ax2=subplot(3,1,2);
hold on
plot (timeV,Y_des, '.r')
plot (timeV,Y_act, '.b')
% ylim(ax2,[-1 1 ])
ylabel('y-coordinate [m]','FontWeight','Bold')
xlabel('time [s]','FontWeight','Bold')

ax3=subplot(3,1,3);
hold on
plot (timeV,Z_des, '.r')
plot (timeV,Z_act, '.b')
% ylim(ax3,[-1 1 ])
ylabel('z-coordinate [m]','FontWeight','Bold')
xlabel('time [s]','FontWeight','Bold')

hold off

        % call the destructor!
vrep.simxFinish(clientID);
vrep.delete();

end

```

Published with MATLAB® R2018a

OPEN_GRIPPER.m

```

function OPEN_GRIPPER ( Grip1,Grip2)
%%%%%%%%%%%%%%%%%%%%%%%%%%%%%%%%%%%%%%%%%%%%%%%%%%%%%%%%%%%%%%%%%%%%%%%%
%start simulation

    vrep=remApi('remoteApi'); % using the prototype file (remoteApiProto.m)
    vrep.simxFinish(-1); % just in case, close all opened connections
    clientID =vrep.simxStart('127.0.0.1',19999,true,true,5000,5);

    if (clientID>-1)
        disp('')
    else
        % close the connection to V-REP and notify user
        vrep.simxFinish(clientID);
    end

    %gripper opens

    k=0;
    while k <= 0.05

        [~,GripR]=vrep.simxGetJointPosition(clientID,Grip1,vrep.simx_opmode_blocking
        );

        [~,GripL]=vrep.simxGetJointPosition(clientID,Grip2,vrep.simx_opmode_blocking
        );

        GripL_n= GripL+ k;
        GripR_n= GripR- k;

        [~,]=vrep.simxPauseCommunication(clientID,1);

        [~,]=vrep.simxSetJointPosition(clientID,Grip1,GripR_n,vrep.simx_opmode_onesho
        t);

        [~,]=vrep.simxSetJointPosition(clientID,Grip2,GripL_n,vrep.simx_opmode_onesho
        t);
        [~,]=vrep.simxPauseCommunication(clientID,0);

        k=k+0.001;
    end

        % call the destructor!
    vrep.simxFinish(clientID);
    vrep.delete();

end

```

Published with MATLAB® R2018a

CLOSE_GRIPPER.m

```

function CLOSE_GRIPPER ( Grip1,Grip2)
%%%%%%%%%%%%%%%%%%%%%%%%%%%%%%%%%%%%%%%%%%%%%%%%%%%%%%%%%%%%%%%%%%%%%%%%
%start simulation
    vrep=remApi('remoteApi'); % using the prototype file (remoteApiProto.m)
    vrep.simxFinish(-1); % just in case, close all opened connections
    clientID =vrep.simxStart('127.0.0.1',19999,true,true,5000,5);

    if (clientID>-1)
        disp('')
    else
        % close the connection to V-REP and notify user
        vrep.simxFinish(clientID);
    end

    %gripper closes

k=0;
    while k < 0.009

[~,GripR]=vrep.simxGetJointPosition(clientID,Grip1,vrep.simx_opmode_blocking
);

[~,GripL]=vrep.simxGetJointPosition(clientID,Grip2,vrep.simx_opmode_blocking
);

        GripL_n= GripL-k;
        GripR_n= GripR+ k;

        [~,]=vrep.simxPauseCommunication(clientID,1);

[~]=vrep.simxSetJointPosition(clientID,Grip1,GripR_n,vrep.simx_opmode_onesho
t);

[~]=vrep.simxSetJointPosition(clientID,Grip2,GripL_n,vrep.simx_opmode_onesho
t);
        [~,]=vrep.simxPauseCommunication(clientID,0);

        k=k+0.001;

    end

        % call the destructor!
    vrep.simxFinish(clientID);
    vrep.delete();

end

```

Published with MATLAB® R2018a

PLATE.m

```

function PLATE (robot, q,T,dt,Plate_frame,Base_frame,Home, BaseJ1, BaseJ2,
Joint1, Joint2,EE, Grip1, Grip2, Turn)
%%Rotation of the Plate for grabbing%%
%ONLY NECESSARY WHEN WE WANT DEFFERENT ORIENTATION OF PLATE

vrep=remApi('remoteApi'); % using the prototype file (remoteApiProto.m)
vrep.simxFinish(-1); % just in case, close all opened connections
clientID =vrep.simxStart('127.0.0.1',19999,true,true,5000,5);

if (clientID>-1)
    disp('')
else
    % close the connection to V-REP and notify user
    vrep.simxFinish(clientID);
end

%Plate can move in the scene, calculation of position every time
[~,Plate_Pose]=vrep.simxGetObjectPosition(clientID,Plate_frame,Base_frame,vr
ep.simx_opmode_blocking);

%make sure robot is at home configuartion before proceeding
q_f= Home;
q= Joint_Trajall(robot,q,T,dt,q_f,BaseJ1,BaseJ2, Joint1, Joint2, EE);

%%Create intermediate points for grabbing the plate
%%If done directly there is danger for collision
Go_to_Plate(:,1)= [Plate_Pose(1); Plate_Pose(2) ; (Plate_Pose(3)+0.8)];
Go_to_Plate(:,2) = [Plate_Pose(1);Plate_Pose(2);Plate_Pose(3)];

Safe_Plate(:,1) = [Plate_Pose(1); Plate_Pose(2) ; (Plate_Pose(3)+0.1)];
Return_from_Plate(:,1)= [Plate_Pose(1); Plate_Pose(2) ; (Plate_Pose(3))];
Return_from_Plate(:,2) = Go_to_Plate(:,1);

for x=1: 2
    P_f= Go_to_Plate(:,x);
    q= SCARApplatetraj(robot,q,T,dt,P_f,Base_frame, BaseJ2, Joint1,
Joint2,EE);
end

OPEN_GRIPPER (Grip1, Grip2);

%rise above plate to leave plate change orientation
P_f = Safe_Plate(:,1);
q= SCARApplatetraj(robot,q,T,dt,P_f,Base_frame, BaseJ2, Joint1, Joint2,EE);

%change plate orientation
TURN_PLATE (Turn);

%Go back in to grab plate
P_f = Return_from_Plate(:,1);
q= SCARApplatetraj(robot,q,T,dt,P_f,Base_frame, BaseJ2, Joint1, Joint2,EE);

```

```

CLOSE_GRIPPER( Grip1,Grip2);
P_f = Return_from_Plate(:,2);
q= SCARAplatetraaj(robot,q,T,dt,P_f,Base_frame, BaseJ2, Joint1, Joint2,EE);

%Return to home configuration
q_f= Home;
q= Joint_Trajall(robot,q,T,dt,q_f,BaseJ1,BaseJ2, Joint1, Joint2, EE);

    % call the destructor!
    vrep.simxFinish(clientID);
    vrep.delete();

end

```

Published with MATLAB® R2018a

TURN_PLATE.m

```

function TURN_PLATE ( Turn)
%%%%%% GRIPPER ACTIVITY %%%%%%%%%%
%start simulation
    vrep=remApi('remoteApi'); % using the prototype file (remoteApiProto.m)
    vrep.simxFinish(-1); % just in case, close all opened connections
    clientID =vrep.simxStart('127.0.0.1',19999,true,true,5000,5);

    if (clientID>-1)
        disp('')
    else
        % close the connection to V-REP and notify user
        vrep.simxFinish(clientID);
        end

%gripper opens
    jj=0;
    while jj <= 3.14

[~,RotPlate]=vrep.simxGetJointPosition(clientID,Turn,vrep.simx_opmode_blocking);
        RotPlate_n= RotPlate+jj;

[~]=vrep.simxSetJointPosition(clientID,Turn,RotPlate_n,vrep.simx_opmode_blocking);

        jj=jj+0.2;
        end

        % call the destructor!
        vrep.simxFinish(clientID);
        vrep.delete();

end

```

Published with MATLAB® R2018a

MACHINES.m

```

function MACHINES(robot, q, T, dt, i, Machine_Position, MachSafe_Pose, rot_m,
BaseJ1, BaseJ2, Joint1, Joint2, EE, Gripl, Grip2, Home)
%%%%% MACHINES%%%%%%%%%
%%%intermediate points are set for robot to follow
%%%safer way to avoid collisions

vrep=remApi('remoteApi'); % using the prototype file (remoteApiProto.m)
vrep.simxFinish(-1); % just in case, close all opened connections
clientID =vrep.simxStart('127.0.0.1',19999,true,true,5000,5);

if (clientID>-1)
    disp('');
else
    % Now close the connection to V-REP:
    vrep.simxFinish(clientID);
end

%move to machine position to leave plate
Move_Machine(:,1)= MachSafe_Pose{i,1};
Move_Machine(:,2)=Machine_Position{i,1};

Safe_Machine(:,1)=MachSafe_Pose{i,1};
Safe_Machine(:,2)=Machine_Position{i,1};

for x=1: 2
    P_f= Move_Machine(:,x);
    q= SCARAexetraj(robot,q,T,dt,P_f,rot_m,BaseJ1,BaseJ2, Joint1, Joint2,EE);
end

OPEN_GRIPPER (Gripl,Grip2);

for x=1: 2
    P_f= Safe_Machine(:,x);
    q= SCARAexetraj(robot,q,T,dt,P_f,rot_m,BaseJ1,BaseJ2, Joint1, Joint2,EE);
end

CLOSE_GRIPPER (Gripl,Grip2);

P_f= Safe_Machine(:,1);
q= SCARAexetraj(robot,q,T,dt,P_f,rot_m,BaseJ1,BaseJ2, Joint1, Joint2,EE);

%Return to home joint configuration
q_f= Home;
q= Joint_Trajall(robot,q,T,dt,q_f,BaseJ1,BaseJ2, Joint1, Joint2, EE);

    % call the destructor!
    vrep.simxFinish(clientID);
    vrep.delete();

end

```

Published with MATLAB® R2018a

OUTPUT.m

```

function OUTPUT (robot, q,T,dt, Rot_Output,Output_Pose,BaseJ1,BaseJ2,
Joint1, Joint2,EE, Gripl, Grip2, Home)
%%%%OUTPUT%%%%
% last thing after any experiment is to give well-plate back to
% technician

    vrep=remApi('remoteApi'); % using the prototype file (remoteApiProto.m)
    vrep.simxFinish(-1); % just in case, close all opened connections
    clientID =vrep.simxStart('127.0.0.1',19999,true,true,5000,5);

if (clientID>-1)
    disp('');
else
    % Now close the connection to V-REP:
    vrep.simxFinish(clientID);
end

%set joint configuration above input window
q_f= [-1.6;1;-0.4; -1.3;0];
q= Joint_Trajall(robot,q,T,dt,q_f,BaseJ1,BaseJ2, Joint1, Joint2, EE);

rot_m= Rot_Output;
P_f= (Output_Pose)';
q= SCARAexetraj(robot,q,T,dt,P_f,rot_m,BaseJ1,BaseJ2, Joint1, Joint2,EE);

    OPEN_GRIPPER(Gripl, Grip2);

% move again to safe configuration above input window
%return to home configuration before proceeding
q_f= [-1.6;1;-0.4; -1.3;0];
q= Joint_Trajall(robot,q,T,dt,q_f,BaseJ1,BaseJ2, Joint1, Joint2, EE);

    CLOSE_GRIPPER (Gripl, Grip2);

q_f= Home;
q= Joint_Trajall(robot,q,T,dt,q_f,BaseJ1,BaseJ2, Joint1, Joint2, EE);

% call the destructor!
vrep.simxFinish(clientID);
vrep.delete();
end

```

Published with MATLAB® R2018a

STAUBLI FILES

main_STAUBLI.m.....	43
USER_INPUT.m.....	44
TrajecParam.m.....	44
Cartesian_Traj_STAUBLI.m.....	45
Joint_Traj_STAUBLI.m.....	45
SCENE_ELEMENTS_STAUBLI.m.....	45
EXECUTE_EXPERIMENT_STAUBLI.m.....	48
CHECK_HOME_STAUBLI.m.....	48
Joint_Trajall_TX90.m.....	50
STAUBLIextraj.m.....	54
MACHINES_STAUBLI.m.....	60
OUTPUT_STAUBLI.m.....	61

main_STAUBLI.m

```

function main_STAUBLI()

%import URDF file of arm- define kinematic matrix and show details
robot= importrobot('STAB.urdf');
showdetails(robot);
robot.DataFormat='column';

%start simulation
%connect to VREP
disp('Program started');
    % vrep=remApi('remoteApi','extApi.h'); % using the header (requires a
compiler)
vrep=remApi('remoteApi'); % using the prototype file (remoteApiProto.m)
vrep.simxFinish(-1); % just in case, close all opened connections
clientID =vrep.simxStart('127.0.0.1',19999,true,true,5000,5);

    if (clientID>-1)
        disp('Connected ');
    else
        disp('Failed connecting to remote API server');
    end

%User defines experiment protocol
USER_INPUT;

%retrieve important info from VREP
SCENE_ELEMENTS_STAUBLI;

T=1; %set time T
dt= 0.01; %set time step, usually 10ms-1ms

%Execution of experiment according to protocol
EXECUTE_EXPERIMENT_STAUBLI;

%Notify user that experiment was completed successfully
fprintf('Experiment successfully completed \n')

    % call the destructor!
vrep.simxFinish(clientID);
vrep.delete();

end

```

Published with MATLAB® R2018a

USER_INPUT.m

```

%%%%%%%%% USER INPUT %%%%%%%%%%%%%%
%ask user for machine input- experiment protocol
machine={};
    i=1;
while (1)
    prompt=input('Input working station \n', 's');

    if strcmp (prompt, 'stop')
        break
    end

    machine{i,1}=prompt;
    i=i+1;
end

```

Published with MATLAB® R2018a

TrajecParam.m

```

function [x] = TrajecParam(T)
% find time-law (5th order polynomial), [a b c d e f] only need one time
computation
% s= a*t^5+ b*t^4+ c*t^3+d*t^2+e*t+f
% sd= 5*a*t^4+ 4*b*t^3+3*c*t^2+ 2*d*t+e
%sdd= 20*a*t^3+12*b*t^2+6*c*t+2*d

%define constraints
% s(0)=0 ; s(T)= 1;
% sd(0)= 0 ; sd(T)=0;
%sdd(0)=0; sdd(T)=0;

%x= [a b c d e f]
%Ax=b

A= [0 0 0 0 0 1;
    T^5 T^4 T^3 T^2 T 1;
    0 0 0 0 1 0;
    5*T^4 4*T^3 3*T^2 2*T 1 0;
    0 0 0 1 0 0;
    20*T^3 12*T^2 6*T 2 0 0];

B = [0; 1; 0; 0; 0;0];

x= pinv(A)* B ;

end

```

Published with MATLAB® R2018a

Cartesian_Traj_STAUBLI.m

```
function [P,v, theta, thetad]=Cartesian_Traj_STAUBLI(P_o,P_f,theta_f,
theta_i,t,x)

%calculate cartesian trajectory

s= x(1)*t^5+ x(2)*t^4+ x(3)*t^3+x(4)*t^2+x(5)*t+x(6);
sd= 5*x(1)*t^4+ 4*x(2)*t^3+3*x(3)*t^2+ 2*x(4)*t+x(5);
sdd= 20*x(1)*t^3+12*x(2)*t^2+6*x(3)*t+2*x(4);

P= (P_f-P_o)*s+P_o ;
v=(P_f-P_o)*sd ;

theta= (theta_f-theta_i)*s+theta_i ;
thetad=(theta_f-theta_i)*sd ;
end
```

Published with MATLAB® R2018a

Joint_Traj_STAUBLI.m

```
function [q_d,qdot]=Joint_Traj_STAUBLI(q_i,q_f,t,x)

%calculate joint trajectory

s= x(1)*t^5+ x(2)*t^4+ x(3)*t^3+x(4)*t^2+x(5)*t+x(6);
sd= 5*x(1)*t^4+ 4*x(2)*t^3+3*x(3)*t^2+ 2*x(4)*t+x(5);
sdd= 20*x(1)*t^3+12*x(2)*t^2+6*x(3)*t+2*x(4);

q_d= (q_f-q_i)*s+q_i ;
qdot=(q_f-q_i)*sd ;

end
```

Published with MATLAB® R2018a

SCENE_ELEMENTS_STAUBLI.m

```
%%%%%%%%%% HANDLES %%%%%%%%%%%
%get handle for world frame-all machines are relative to this frame
[~,Base_frame]=vrep.simxGetObjectHandle(clientID,'world_visual',vrep.simx_op
mode_blocking);

%get handles for other necessary components of simulation
[~,Plate_frame]=vrep.simxGetObjectHandle(clientID,'Plate_frame',vrep.simx_op
mode_blocking);

[~,EE]=vrep.simxGetObjectHandle(clientID,'ee_link_dummy',vrep.simx_opmode_b
locking);
```

```

[~,ee]=vrep.simxGetObjectHandle(clientID,'ee_link_visual',vrep.simx_opmode_blocking);
[~,Input_Tech]=vrep.simxGetObjectHandle(clientID,'Input_Tech',vrep.simx_opmode_blocking);
[~,Output_Tech]=vrep.simxGetObjectHandle(clientID,'Output_Tech',vrep.simx_opmode_blocking);

%get handles joints
[~,Joint1]=vrep.simxGetObjectHandle(clientID,'joint1',vrep.simx_opmode_blocking);

[~,Joint2]=vrep.simxGetObjectHandle(clientID,'joint2',vrep.simx_opmode_blocking);

[~,Joint3]=vrep.simxGetObjectHandle(clientID,'joint3',vrep.simx_opmode_blocking);

[~,Joint4]=vrep.simxGetObjectHandle(clientID,'joint4',vrep.simx_opmode_blocking);

[~,Joint5]=vrep.simxGetObjectHandle(clientID,'joint5',vrep.simx_opmode_blocking);

[~,Joint6]=vrep.simxGetObjectHandle(clientID,'joint6',vrep.simx_opmode_blocking);

%get joint values from VREP, update position every time
[~,J1]=vrep.simxGetJointPosition(clientID,Joint1,vrep.simx_opmode_blocking);

[~,J2]=vrep.simxGetJointPosition(clientID,Joint2,vrep.simx_opmode_blocking);

[~,J3]=vrep.simxGetJointPosition(clientID,Joint3,vrep.simx_opmode_blocking);

[~,J4]=vrep.simxGetJointPosition(clientID,Joint4,vrep.simx_opmode_blocking);

[~,J5]=vrep.simxGetJointPosition(clientID,Joint5,vrep.simx_opmode_blocking);

[~,J6]=vrep.simxGetJointPosition(clientID,Joint6,vrep.simx_opmode_blocking);

q= [J1; J2;J3;J4;J5;J6];

%set home configuration
Home=[ 0;-0.5000;1.3000;0;-0.7854;0];

%%%%%%%%%% POSITION %%%%%%%%%%%
%position of components
[~,Plate_Pose]=vrep.simxGetObjectPosition(clientID,Plate_frame,Base_frame,vrep.simx_opmode_blocking);
[~,BaseFrame_Pose]=vrep.simxGetObjectPosition(clientID,Base_frame,Base_frame,vrep.simx_opmode_blocking);
[~,Input_Pose]=vrep.simxGetObjectPosition(clientID,Input_Tech,Base_frame,vrep.simx_opmode_blocking);

```

```

[~,Output_Pose]=vrep.simxGetObjectPosition(clientID,Output_Tech,Base_frame,v
rep.simx_opmode_blocking);

%%%%%%%%% ORIENTATION %%%%%%%%%%%%%%%
%orientation of components
[~,Plate_Orient]=vrep.simxGetObjectOrientation(clientID,Plate_frame,Base_fr
ame,vrep.simx_opmode_blocking);
[~,BaseFrame_Orient]=vrep.simxGetObjectOrientation(clientID,Base_frame,Base_
frame,vrep.simx_opmode_blocking);
[~,Input_Orient]=vrep.simxGetObjectOrientation(clientID,Input_Tech,Base_fram
e,vrep.simx_opmode_blocking);
[~,Output_Orient]=vrep.simxGetObjectOrientation(clientID,Output_Tech,Base_fr
ame,vrep.simx_opmode_blocking);

%rotation matrices of components
Rot_Input= eul2rotm(Input_Orient,'XYZ');
Rot_Output= eul2rotm(Output_Orient,'XYZ');

%%%%%%%%% MACHINES USED IN EXPERIMENT ONLY %%%%%%%%%%%%%%%
for i=1:length(machine)

    [~,Handles{i,1}] =
vrep.simxGetObjectHandle(clientID,machine{i,1},vrep.simx_opmode_blocking);

    [~,ObjPos{i,1}]=vrep.simxGetObjectPosition(clientID,Handles{i,1},Base_frame,
vrep.simx_opmode_blocking);

    [~,ObjOr{i,1}]=vrep.simxGetObjectOrientation(clientID,Handles{i,1},Base_fram
e,vrep.simx_opmode_blocking);
    Rot_machine{i,1} = eul2rotm(ObjOr{i,1},'XYZ');

    %set positions where robot will go
    Machine_Position{i,1}= ObjPos{i,1}' ;
    MachSafe_Pose{i,1}= [(ObjPos{i,1}(1,1));
(ObjPos{i,1}(1,2)+0.4);ObjPos{i,1}(1,3)];

end

```

Published with MATLAB® R2018a

EXECUTE_EXPERIMENT_STAUBLI.m

```

CHECK_HOME_STAUBLI(robot, q,T, dt, Home, Rot_Input,Joint1, Joint2, Joint3,
Joint4, Joint5, Joint6 ,Input_Pose );

    %executing trajectory
    for i=1:length(machine)
        rot_m= Rot_machine{i,1}; % rotation matrix of machine-remains same always-
does not move

MACHINES_STAUBLI(robot, q, T,dt, i, Machine_Position,MachSafe_Pose, rot_m,
Joint1, Joint2,Joint3, Joint4,Joint5,Joint6 , Home);

        i=i+1;
    end

OUTPUT_STAUBLI (robot, q, T, dt,Rot_Output,Output_Pose,Joint1,
Joint2,Joint3, Joint4,Joint5,Joint6, Home);

```

Published with MATLAB® R2018a

CHECK_HOME_STAUBLI.m

```

function CHECK_HOME_STAUBLI(robot, q,T, dt,Home, Rot_Input,Joint1, Joint2,
Joint3, Joint4, Joint5, Joint6 ,Input_Pose )
%%CHECK HOME%%
%checks if robot is in home position
%if yes user is notified
%if not it is commanded to go to home position before the start of the
experiment

    vrep=remApi('remoteApi'); % using the prototype file (remoteApiProto.m)
    vrep.simxFinish(-1); % just in case, close all opened connections
    clientID =vrep.simxStart('127.0.0.1',19999,true,true,5000,5);

    if (clientID>-1)
        disp('')
    else
        % close the connection to V-REP and notify user
        vrep.simxFinish(clientID);
    end

    if q(1)==0 && q(2)== -0.5000 && q(3)==1.3000 && q(4)==0 && q(5)==0 &&
q(6)==0
        printf('Robot is in Home Position-Ready to start experiment')
    else
        %return robot to home joint configuration
        q_f= Home;
    end

```

```

    q= Joint_Trajall_TX90(robot,q,T, dt,q_f,Joint1, Joint2, Joint3, Joint4,
Joint5, Joint6);
end

prompt='Do you wish to continue to experiment? Y/N [Y]:';
str = input(prompt,'s');
    if isempty(str) || str=='Y'
        str = 'Y';

        %start with experiment and notify user
        fprintf('Experiment started \n')
        pause(1);

        %first step is to take plate from technician-input

        rot_m= Rot_Input;
        P_f=(Input_Pose)';
        q= STAUBLIexetraj(q,robot,T, dt, P_f,rot_m, Joint1, Joint2,Joint3,
Joint4,Joint5,Joint6 );

        q_f= Home;
        q= Joint_Trajall_STAUBLI(robot,q,T, dt,q_f,Joint1, Joint2, Joint3,
Joint4, Joint5, Joint6);

    else

        error('Experiment interrupted by user')

    end

        % call the destructor!
vrep.simxFinish(clientID);
vrep.delete();

end

```

Published with MATLAB® R2018a

Joint_Trajall_TX90.m

```

function q= Joint_Trajall_TX90(robot,q,T, dt,q_f,Joint1, Joint2, Joint3,
Joint4, Joint5, Joint6)
%start simulation
%connect to VREP
    % vrep=remApi('remoteApi','extApi.h'); % using the header (requires a
compiler)
    vrep=remApi('remoteApi'); % using the prototype file (remoteApiProto.m)
    vrep.simxFinish(-1); % just in case, close all opened connections
    clientID =vrep.simxStart('127.0.0.1',19999,true,true,5000,5);

    if (clientID>-1)
        disp('');
    else
        % close the connection to V-REP and notify user
        vrep.simxFinish(clientID);
    end

%Retrieve current joint configuration
q_i= [ q(1); q(2); q(3); q(4); q(5); q(6)];

%offset between visual EE and actual EE
T_dummy_e=[1 0 0 0;0 1 0 -0.162 ; 0 0 1 0 ;0 0 0 1];

%parameters for trajectory
x= TrajecParam(T);
t=0;

c=1;
while t<= T
%homogenous transformation for robot chain
T_e= getTransform(robot,double(q), 'ee_link');

%transformation from visual EE to actual EE
T_final= T_e* T_dummy_e;
P_i= T_final(1:3,4);

%get path between initial and desired configuration
[q_d,qdot]=Joint_Traj_STAUBLI(q_i,q_f,t,x);

%joint position at t+dt
q= q+qdot*dt;

    for j=1:6
        q(j)=atan2(sin(q(j)),cos(q(j)));
    end

    %%%%%%%%%%%%%%%%%%%%%%%%%%%%%%%%%%%%%%%%%%%%%%%%%%%%%%%%%%%%%%%%%%%%%%%%%
%save the values for position and velocity for later plotting

```



```

timeV(c)= t;
X_act(c,:)= P_i(1);
Y_act(c,:)=P_i(2);
Z_act(c,:)= P_i(3);

q1(c,:)= q(1);
q2(c,:)= q(2);
q3(c,:)= q(3);
q4(c,:)= q(4);
q5(c,:)= q(5);
q6(c,:)= q(6);

qd1(c,:)= qdot(1);
qd2(c,:)= qdot(2);
qd3(c,:)= qdot(3);
qd4(c,:)= qdot(4);
qd5(c,:)= qdot(5);
qd6(c,:)= qdot(6);

q_d1(c,:)= q_d(1);
q_d2(c,:)= q_d(2);
q_d3(c,:)= q_d(3);
q_d4(c,:)= q_d(4);
q_d5(c,:)= q_d(5);
q_d6(c,:)= q_d(6);

c=c+1 ;
%%%%%%%%%%%%%%%%%%%%%%%%%%%%%%%%%%%%%%%%%%%%%%%%%%%%%%%%%%%%%%%%%%%%%%%%
t=t+dt;

% update visual robot configuration
[~]=vrep.simxPauseCommunication(clientID,1);
[J1]=vrep.simxSetJointPosition(clientID,Joint1,q(1),vrep.simx_opmode_oneshot);
[J2]=vrep.simxSetJointPosition(clientID,Joint2,q(2),vrep.simx_opmode_oneshot);
[J3]=vrep.simxSetJointPosition(clientID,Joint3,q(3),vrep.simx_opmode_oneshot);
[J4]=vrep.simxSetJointPosition(clientID,Joint4,q(4),vrep.simx_opmode_oneshot);
[J5]=vrep.simxSetJointPosition(clientID,Joint5,q(5),vrep.simx_opmode_oneshot);
[J6]=vrep.simxSetJointPosition(clientID,Joint6,q(6),vrep.simx_opmode_oneshot);
[~]=vrep.simxPauseCommunication(clientID,0);
pause(dt);

end

%%% POSITION PLOTS
figure()

%plot x,y,z of trajectory
subplot(3,1,1);
hold on
plot (timeV,X_act)

```

```

title('Actual End-Effector Displacement (FK)' , 'FontSize',14)
ylabel('x-coordinate [m]','FontWeight','Bold')
xlabel('time [s]','FontWeight','Bold')

subplot(3,1,2);
hold on
plot (timeV,Y_act)
ylabel('y-coordinate [m]','FontWeight','Bold')
xlabel('time [s]','FontWeight','Bold')

subplot(3,1,3);
hold on
plot (timeV,Z_act)
hold off
ylabel('z-coordinate [m]','FontWeight','Bold')
xlabel('time [s]','FontWeight','Bold')

%%% JOINT PLOTS
figure()
subplot(6,1,1);
hold on
plot (timeV,q1, '.b')
% plot(timeV, q_d1, '.r')
title('Joint angles (FK)' , 'FontSize',14)

ylabel('Joint 1 [rad]','FontWeight','Bold')
xlabel('time [s]','FontWeight','Bold')

subplot(6,1,2);
hold on
plot (timeV,q2, '.b')
% plot(timeV, q_d2, '.r')
ylabel('Joint 2 [rad]','FontWeight','Bold')
xlabel('time [s]','FontWeight','Bold')

subplot(6,1,3);
hold on
plot (timeV,q3, '.b')
% plot(timeV, q_d3, '.r')
ylabel('Joint 3 [rad]','FontWeight','Bold')
xlabel('time [s]','FontWeight','Bold')

subplot(6,1,4);
hold on
plot (timeV,q4, '.b')
% plot(timeV, q_d4, '.r')
ylabel('Joint 4 [rad]','FontWeight','Bold')
xlabel('time [s]','FontWeight','Bold')

subplot(6,1,5);
hold on
plot (timeV,q5, '.b')
% plot(timeV, q_d5, '.r')
ylabel('Joint 5 [rad]','FontWeight','Bold')
xlabel('time [s]','FontWeight','Bold')

```

```

subplot(6,1,6);
hold on
plot (timeV,q6, '.b')
% plot(timeV, q_d6, '.r')
ylabel('Joint 6 [rad]','FontWeight','Bold')
xlabel('time [s]','FontWeight','Bold')

hold off

%%% VELOCITY PLOTS
figure()
subplot(6,1,1);
hold on
plot (timeV,qd1)
title('Joint velocities (FK)' , 'FontSize',14)
ylabel('Joint 1 [rad/s]','FontWeight','Bold')
xlabel('time [s]','FontWeight','Bold')

subplot(6,1,2);
hold on
plot (timeV,qd2)
ylabel('Joint 2 [rad/s]','FontWeight','Bold')
xlabel('time [s]','FontWeight','Bold')

subplot(6,1,3);
hold on
plot (timeV,qd3)
ylabel('Joint 3 [rad/s]','FontWeight','Bold')
xlabel('time [s]','FontWeight','Bold')

subplot(6,1,4);
hold on
plot (timeV,qd4)
ylabel('Joint 4 [rad/s]','FontWeight','Bold')
xlabel('time [s]','FontWeight','Bold')

subplot(6,1,5);
hold on
plot (timeV,qd5)
ylabel('Joint 5 [rad/s]','FontWeight','Bold')
xlabel('time [s]','FontWeight','Bold')

subplot(6,1,6);
hold on
plot (timeV,qd5)
ylabel('Joint 6 [rad/s]','FontWeight','Bold')
xlabel('time [s]','FontWeight','Bold')
hold off

    % call the destructor!
    vrep.simxFinish(clientID);
    vrep.delete();

end

```

Published with MATLAB® R2018a

STAUBLIexetraj.m

```

function q= STAUBLIexetraj(q,robot,T, dt, P_f,rot_m, Joint1, Joint2,Joint3,
Joint4,Joint5,Joint6 )
%start simulation
%connect to VREP

    % vrep=remApi('remoteApi','extApi.h'); % using the header (requires a
compiler)
    vrep=remApi('remoteApi'); % using the prototype file (remoteApiProto.m)
    vrep.simxFinish(-1); % just in case, close all opened connections
    clientID =vrep.simxStart('127.0.0.1',19999,true,true,5000,5);

if (clientID>-1)
    disp('')
else
    % close the connection to V-REP and notify user
    vrep.simxFinish(clientID);
end

%offset between visual EE and actual EE
T_dummy_e=[1 0 0 0;0 1 0 -0.162 ; 0 0 1 0 ;0 0 0 1];

%homogenous transformation for robot chain
Trans= getTransform(robot,double(q), 'ee_link');

%Transformation from visual EE to actual EE
T_fi= Trans* T_dummy_e;
P_o= T_fi(1:3,4);

%parameters for trajectory
x = TrajecParam(T);
t=0;

c=1;
%%%%% Follow Trajectory %%%%%%
while t<= T

%homogenous transformation for robot chain
T_e= getTransform(robot,double(q), 'ee_link');

%transformation from visual EE to actual EE
T_final= T_e* T_dummy_e;
P_i= T_final(1:3,4);

%rotation matrix of EE wrt to base frame
Rot_EE= T_final(1:3,1:3);

%%%%% ORIENTATION ERROR %%%%%%
%angle-axis representation (Sicilliano et.al)

```

```

R_err =transpose(Rot_EE)*(rot_m);
r_theta =rotm2axang(R_err);
r= r_theta(1, 1:3); %r wrt Rot_init
theta_f= r_theta(1, 4);
r= (Rot_EE)* transpose(r); %r wrt base frame
theta_i=0;

%elements (vectors) for Re(Rot_EE)computed from joint variables
ne= Rot_EE(:,1);
se= Rot_EE(:,2);
ae= Rot_EE(:,3);

%elements (vectors) for Rd(rot_m)
nd= rot_m(:,1);
sd= rot_m(:,2);
ad= rot_m(:,3);

%after differentiating eo wrt time
L= (-
0.5)*((nd/dt)*(nd')*(ne/dt)*(ne')+(sd/dt)*(sd')*(se/dt)*(se')+(ad/dt)*(ad')*(ae/dt)*(ae'));

%get trajectory between initial and desired ending point
[P,v, theta, thetad]=Cartesian_Traj_STAUBLI(P_o,P_f,theta_f, theta_i,t,x);
w= thetad*r;
wd=(L\((L')*w));
eoo= r*sin(theta);

%positive values Ko, Kp
Ko=(1/dt-10);
Kp=(1/dt-10);

%%% ERRORS %%%
eo= L\((Ko*eoo); %orientation error (only around z)
ep= Kp*(P-P_i); %position error
e= [ep ; eo] ;

%%%%% JACOBIAN %%%%%
%calculate geometric jacobian
Jac_rev = geometricJacobian(robot,double(q), 'ee_link');

%reverse rows
%Matlab default (first rotation, second transaltion)
Jac= [Jac_rev(4:6,:);Jac_rev(1:3,:)] ;

%linear velocity, keep x,y,z
%orientation in x,y,z axis
J= [Jac(1:3,:) ; Jac(4:6,:)];

%damping factor λ via SVD
[~,S,~] = svd(J);
diagS=diag(S);
sigma=min(diagS);
lamdamax=0.04;
eps= 10e-4;

```

```

if sigma >= eps
    lamda = 0;
else
    lamda= sqrt((1- ((sigma/eps)^2)*(lamdamax^2)));
end

%%%%% QUADRATIC PROGRAMMING %%%%%
%set lower-upper bounds for quadprog
% q_min=[-2.8;-3.97;-0.91;-4.7;-1.5;-4.5];
% q_max= [2.8;0.83;4.06;4.7;1.5;4.5];
q_min=[-3.14;-2.27;-2.53;-4.7;-2.01;-4.7];
q_max= [3.14;2.57;2.53;4.7;2.44;4.7];

lb=(q_min-q)/dt;
ub=(q_max-q)/dt;

%Solving IK
%quadratic programming
H=(J'*J + ((lamda)^2)*eye(6,6));
b=( [v;wd]+ e);
f=- (b')*J ;
options = optimset('Display', 'off');
qd = quadprog(double(H),double(f), [], [], [], [], double(lb), double(ub), [],
options);

ve= J*qd;
q= q+qd*dt; %joint position at t+dt

    for j=1:6
        q(j)=atan2(sin(q(j)), cos(q(j)));
    end

    %%%%%%%%%%%%%%%%%%%%%%%%%%%%%%%%%%%%%%%%%%%%%%%%%%%%%%%%%%%%%%%%%%%%%%%%%
%save the values for position and velocity for later plotting
timeV(c)= t;
X_des(c,:)= P(1);
Y_des(c,:)= P(2);
Z_des(c,:)= P(3);
X_act(c,:)= P_i(1);
Y_act(c,:)= P_i(2);
Z_act(c,:)= P_i(3);
v1_des(c,:)= v(1);
v2_des(c,:)= v(2);
v3_des(c,:)= v(3);
v1_act(c,:)= ve(1);
v2_act(c,:)= ve(2);
v3_act(c,:)= ve(3);

q1(c,:)= q(1);
q2(c,:)= q(2);
q3(c,:)= q(3);
q4(c,:)= q(4);
q5(c,:)= q(5);
q6(c,:)= q(6);

c=c+1 ;

```

```

%%%%%%%%%%%%%%%%%%%%%%%%%%%%%%%%%%%%%%%%%%%%%%%%%%%%%%%%%%%%%%%%%%%%%%%%
    t=t+dt;

% update visual robot configuration
[~]=vrep.simxPauseCommunication(clientID,1);
[J1]=vrep.simxSetJointPosition(clientID,Joint1,q(1),vrep.simx_opmode_oneshot
);
[J2]=vrep.simxSetJointPosition(clientID,Joint2,q(2),vrep.simx_opmode_oneshot
);
[J3]=vrep.simxSetJointPosition(clientID,Joint3,q(3),vrep.simx_opmode_oneshot
);
[J4]=vrep.simxSetJointPosition(clientID,Joint4,q(4),vrep.simx_opmode_oneshot
);
[J5]=vrep.simxSetJointPosition(clientID,Joint5,q(5),vrep.simx_opmode_oneshot
);
[J6]=vrep.simxSetJointPosition(clientID,Joint6,q(6),vrep.simx_opmode_oneshot
);
[~]=vrep.simxPauseCommunication(clientID,0);

pause(dt);

end

%%%%%%%%%%%%%%%%%%%%%%%%%%%%%%%%%%%%%%%%%%%%%%%%%%%%%%%%%%%%%%%%%%%%%%%%

%%% JOINT PLOTS
figure()
subplot(6,1,1);
hold on
plot (timeV,q1)
title('Joint angles ' , 'FontSize',14)

ylabel('Joint 1 [rad]','FontWeight','Bold')
xlabel('time [s]','FontWeight','Bold')

subplot(6,1,2);
hold on
plot (timeV,q2)
ylabel('Joint 2 [rad]','FontWeight','Bold')
xlabel('time [s]','FontWeight','Bold')

subplot(6,1,3);
hold on
plot (timeV,q3)
ylabel('Joint 3 [rad]','FontWeight','Bold')
xlabel('time [s]','FontWeight','Bold')

subplot(6,1,4);
hold on
plot (timeV,q4)
ylabel('Joint 4 [rad]','FontWeight','Bold')
xlabel('time [s]','FontWeight','Bold')

subplot(6,1,5);

```

```

hold on
plot (timeV,q5)
ylabel('Joint 5 [rad]','FontWeight','Bold')
xlabel('time [s]','FontWeight','Bold')

subplot(6,1,6);
hold on
plot (timeV,q6)
ylabel('Joint 6 [rad]','FontWeight','Bold')
xlabel('time [s]','FontWeight','Bold')

hold off

%%% VELOCITY PLOTS
figure()
axv1=subplot(3,1,1);

hold on
plot (timeV,v1_des, '.r')
plot (timeV,v1_act, '.b')
ylim(axv1,[-2 2 ])
title('End-effector Velocity' , 'FontSize',14)
xlabel('time [s]','FontWeight','Bold')
ylabel('velocity [m/s]','FontWeight','Bold')

axv2=subplot(3,1,2);
hold on
plot (timeV,v2_des, '.r')
plot (timeV,v2_act, '.b')
ylim(axv2,[-2 2 ])
xlabel('time [s]','FontWeight','Bold')
ylabel('velocity [m/s]','FontWeight','Bold')

axv3=subplot(3,1,3);
hold on
plot (timeV,v3_des, '.r')
plot (timeV,v3_act, '.b')
ylim(axv3,[-2 2 ])
xlabel('time [s]','FontWeight','Bold')
ylabel('velocity [m/s]','FontWeight','Bold')

hold off

%%% POSITION PLOTS
figure()
%plot x,y,z of trajectory
ax1=subplot(3,1,1);
hold on
plot (timeV,X_des, '.r')
plot (timeV,X_act, '.b')
% ylim(ax1,[-2 2 ])
title('Displacement' , 'FontSize',14)
ylabel('x-coordinate [m]','FontWeight','Bold')
xlabel('time [s]','FontWeight','Bold')

```



```
ax2=subplot(3,1,2);
hold on
plot (timeV,Y_des, '.r')
plot (timeV,Y_act, '.b')
% ylim(ax2,[-1 1 ])
ylabel('y-coordinate [m]','FontWeight','Bold')
xlabel('time [s]','FontWeight','Bold')

ax3=subplot(3,1,3);
hold on
plot (timeV,Z_des, '.r')
plot (timeV,Z_act, '.b')
% ylim(ax3,[-1 1 ])
ylabel('z-coordinate [m]','FontWeight','Bold')
xlabel('time [s]','FontWeight','Bold')

hold off

    % call the destructor!
vrep.simxFinish(clientID);
vrep.delete();

end
```

Published with MATLAB® R2018a

MACHINES_STAUBLI.m

```

function MACHINES_STAUBLI(robot, q, T,dt, i, Machine_Position,MachSafe_Pose,
rot_m, Joint1, Joint2,Joint3, Joint4,Joint5,Joint6 , Home)
%%%%% MACHINES%%%%%%%%%
%%intermediate points are set for robot to follow
%%safer way to avoid collisions

vrep=remApi('remoteApi'); % using the prototype file (remoteApiProto.m)
vrep.simxFinish(-1); % just in case, close all opened connections
clientID =vrep.simxStart('127.0.0.1',19999,true,true,5000,5);

if (clientID>-1)
    disp('');
else
    % Now close the connection to V-REP:
    vrep.simxFinish(clientID);
end

%move to machine position to leave plate
Move_Machine(:,1)= MachSafe_Pose{i,1};
Move_Machine(:,2)=Machine_Position{i,1};
Move_Machine(:,3)= Move_Machine(:,1);

for x=1:3
    P_f= Move_Machine(:,x);
    q= STAUBLIextraj(q,robot,T, dt, P_f,rot_m, Joint1, Joint2,Joint3,
Joint4,Joint5,Joint6 );
end

pause(1);

for x=2:3
    P_f= Move_Machine(:,x);
    q= STAUBLIextraj(q,robot,T, dt, P_f,rot_m, Joint1, Joint2,Joint3,
Joint4,Joint5,Joint6 );
end

q_f= Home;
q= Joint_Trajall_STAUBLI (robot,q,T, dt, q_f,Joint1, Joint2, Joint3,
Joint4, Joint5, Joint6);

% call the destructor!
vrep.simxFinish(clientID);
vrep.delete();
end

```

Published with MATLAB® R2018a

OUTPUT_STAUBLI.m

```

function OUTPUT_STAUBLI (robot, q, T, dt, Rot_Output, Output_Pose, Joint1,
Joint2, Joint3, Joint4, Joint5, Joint6, Home)
%%%%%OUTPUT%%%%%
% last thing after any experiment is to give well-plate back to
% technician

%connect to VREP
    % vrep=remApi('remoteApi','extApi.h'); % using the header (requires a
compiler)
    vrep=remApi('remoteApi'); % using the prototype file (remoteApiProto.m)
    vrep.simxFinish(-1); % just in case, close all opened connections
    clientID =vrep.simxStart('127.0.0.1',19999,true,true,5000,5);

if (clientID>-1)
    disp('');
else
    % Now close the connection to V-REP:
    vrep.simxFinish(clientID);
end

    %set joint configuration above output window
    rot_m= Rot_Output;
    P_f= (Output_Pose)';
    q= STAUBLIextraj(q,robot,T, dt, P_f,rot_m, Joint1, Joint2,Joint3,
Joint4,Joint5,Joint6 );

    %return to home joint configuration
    q_f= Home;
    q= Joint_Trajall_RX90(robot,q,T, dt, q_f,Joint1, Joint2, Joint3,
Joint4, Joint5, Joint6);

    % call the destructor!
    vrep.simxFinish(clientID);
    vrep.delete();
end

```

Published with MATLAB® R2018a



ΕΘΝΙΚΟ ΜΕΤΣΟΒΙΟ ΠΟΛΥΤΕΧΝΕΙΟ
Σχολή Μηχανολόγων Μηχανικών
Τομέας Τεχνολογίας των Κατεργασιών

Διπλωματική εργασία

Σχεδιασμός και Προσομοίωση Ευέλικτου
Ρομποτικού Συστήματος Παραγωγής Πειραμάτων
Βιοτεχνολογίας

Αγγελίδου Χαρίκλεια

Επιβλέποντες

Γ. - Χ. Βοσνιάκος
Καθηγητής ΕΜΠ

Π. Μπενάρδος
Επίκουρος Καθηγητής ΕΜΠ

Αθήνα, Οκτώβριος 2019

“Η καλύτερη προετοιμασία για το αύριο είναι να βάζεις τα δυνατά σου σήμερα”

H. Jackson Brown Jr, (b. 1941)

ΕΥΧΑΡΙΣΤΙΕΣ

Η παρούσα εργασία δεν θα είχε πραγματοποιηθεί χωρίς την υποστήριξη και την καθοδήγηση πολλών σημαντικών ανθρώπων.

Πρώτα απ' όλα θα ήθελα να ευχαριστήσω τον καθηγητή μου και επιβλέποντα της εργασίας, Γεώργιο Χ. Βοσνιάκο, ο οποίος μου έδωσε την ευκαιρία να συμμετάσχω στην ομάδα του και μετέτρεψε αυτή την εμπειρία σε κάτι παραπάνω από μία απλή ακαδημαϊκή εργασία. Δίνοντάς μου την ευκαιρία να συνεργαστώ άμεσα με τη βιομηχανία, απέκτησα πολύτιμες γνώσεις και δεξιότητες. Το ενδιαφέρον και η εμπιστοσύνη εκ μέρους του ήταν καταλυτικοί παράγοντες για την εκπόνηση της παρούσας διπλωματικής εργασίας. Η καθοδήγηση και οι συμβουλές που μου παρείχε υπήρξαν πολύ σημαντικές για μένα και το εκτιμώ ιδιαίτερα.

Επιπλέον, είμαι ευγνώμων που γνώρισα και δούλεψα με τον επίκουρο καθηγητή Πανώριο Μπενάρδο, ο οποίος πάντα ήταν πρόθυμος να με βοηθήσει να ξεπεράσω τις δυσκολίες που είχα καθ' όλη τη διάρκεια της εργασίας. Η ενέργειά του υπήρξε πολύ ευχάριστη και η «φρέσκια ματιά» του ιδιαίτερα διαφωτιστική.

Θα ήθελα επίσης να απευθύνω μια ειλικρινή ευχαριστία προς τους ανθρώπους της start-up experiment, μια ομάδα νέων πρωτοπόρων, που με εμπιστεύτηκαν να δουλέψω πάνω στο project τους. Ιδιαίτερα θα ήθελα να ευχαριστήσω τον υποψήφιο διδάκτορα του Imperial College, Francesco Cursi, για το χρόνο που αφιέρωσε, βοηθώντας, συμβουλευόντας και υποστηρίζοντάς με κατά την εκπόνηση της διπλωματικής εργασίας, παρόλο που δεν είχε καμία υποχρέωση.

Εκτός από τους ανθρώπους στον ακαδημαϊκό χώρο, θα ήθελα να ευχαριστήσω ολόψυχα τους φίλους μου για την υποστήριξή τους και τη βοήθεια που μου παρείχαν, ο καθένας με τον δικό του μοναδικό τρόπο. Δεν θα ήμουν ο άνθρωπος που είμαι χωρίς αυτούς.

Τέλος, θα ήθελα να εκφράσω την ευγνωμοσύνη μου στους γονείς μου, οι οποίοι δεν έπαψαν ποτέ να πιστεύουν σε μένα και να μου παρέχουν την πολύτιμη υποστήριξη και αγάπη τους καθ' όλη τη διάρκεια των σπουδών μου, καθώς και στα αδέρφια μου, που είναι πάντα εκεί για μένα, παρόλο που η απόσταση μας κρατάει μακριά· αυτή η διπλωματική εργασία είναι αφιερωμένη στα αδέρφια μου.

ΠΕΡΙΛΗΨΗ

Η πρόθεση να επιταχυνθεί η επιστημονική έρευνα στη βιοτεχνολογία έχει αυξηθεί δραστικά τις τελευταίες δεκαετίες. Η επένδυση σε νέους τρόπους προώθησης αυτού του τομέα, χρησιμοποιώντας τον πλέον σύγχρονο τεχνολογικό εξοπλισμό, βρίσκεται στο επίκεντρο της προσοχής. Αυτός είναι ο λόγος για τον οποίο οι ερευνητές και οι εταιρείες έχουν αρχίσει να κατευθύνουν την προσοχή τους στην αυτοματοποίηση και τα παρακλάδια της. Τα ρομποτικά συστήματα με εφαρμογές όπως είναι τα cloud εργαστήρια βιοτεχνολογίας αποτελούν έναν από τους κλάδους αυτούς, που στοχεύουν στην αλλαγή του τρόπου με τον οποίο γίνεται η έρευνα, ιδιαίτερα στον φαρμακευτικό κλάδο. Επιτυγχάνουν την αντιστάθμιση του συνεχώς αυξανόμενου κόστους των κλινικών δοκιμών και την αυτοματοποίηση του κουραστικού εργαστηριακού έργου, ενώ επιταχύνουν την έρευνα διενεργώντας παράλληλα πειράματα. Έτσι, η πειραματική διαδικασία γίνεται πιο αποδοτική και ευχάριστη για όλους. Μια επισκόπηση του σχεδιασμού και της λειτουργίας ενός τέτοιου ρομποτικού συστήματος είναι το κεντρικό θέμα της τρέχουσας εργασίας.

Στην παρούσα εργασία μελετάται η μεθοδολογία και τα εργαλεία για την ανάπτυξη του εικονικού ισοδύναμου ενός πραγματικού εργαστηρίου βιοτεχνολογίας για φαρμακευτικά πειράματα. Συγκεκριμένα, ένα ρομπότ τύπου SCARA, ο ρομποτικός βραχίονας Stäubli TX2-90XL καθώς και το εργαστηριακό περιβάλλον, διαμορφώνονται χρησιμοποιώντας το λογισμικό ανάπτυξης 3D εφαρμογών VREP από την Coppelia Robotics. Ο στόχος είναι να διερευνηθεί ο προγραμματισμός του βραχίονα εκτός σύνδεσης σε περιβάλλον εικονικής πραγματικότητας, καθώς και να σχεδιαστεί μια πλήρως εξοπλισμένη εργαστηριακή διάταξη που να μπορεί να μεταφερθεί σε πραγματικά δεδομένα και σε φυσικό επίπεδο.

Ως μέρος του σχεδιασμού εισάγονται οι γεωμετρίες για τη δημιουργία του εργαστηρίου, συμπεριλαμβανομένου του εξοπλισμού και των αναλωσίμων. Στη συνέχεια δημιουργούνται και συγκρίνονται διάφορες εργαστηριακές διατάξεις, καταλήγοντας σε δύο, που τελικά προσομοιώνονται.

Για τη μοντελοποίηση και την προσομοίωση, εισάγονται τα μοντέλα ρομπότ και αναπτύσσονται οι αντίστοιχες κινηματικές τους αλυσίδες. Η εμπρόσθια και αντίστροφη κινηματική του βραχίονα αναλύεται και αναπτύσσεται στη Matlab, χρησιμοποιώντας διαφορετικές προσεγγίσεις και αλγορίθμους, όπως η αντίστροφη και ψευδο-αντίστροφη Ιακωβιανή, καθώς και η μέθοδος αποσβενύμενων ελαχίστων τετραγώνων. Η τροχιά και των δύο ρομποτικών βραχιόνων σχεδιάζεται, έτσι ώστε να δημιουργηθεί ένα σχέδιο κίνησης που μπορεί να χρησιμοποιηθεί για οποιοδήποτε πείραμα στο εργαστήριο. Επιπλέον, δημιουργείται μια διεπαφή για την επικοινωνία των πειραματικών πρωτοκόλλων μεταξύ του ερευνητή και των ρομποτικών βραχιόνων.

ΠΕΡΙΕΧΟΜΕΝΑ

1	ΕΙΣΑΓΩΓΗ	1
1.1	Τι είναι ένα Ρομποτικό Cloud Εργαστήριο Βιοτεχνολογίας;	1
1.2	Τεχνολογία Digital Factory	2
1.3	Προσπάθειες για την ανάπτυξη αυτοματοποιημένων εργαστηρίων βιοτεχνολογίας	3
1.4	Υπάρχουσες ρομποτικές cloud πλατφόρμες βιοτεχνολογίας.....	4
1.5	Αντικείμενο και στόχοι της διπλωματικής εργασίας	5
2	ΠΡΟΣΟΜΟΙΩΣΗ	7
2.1	Ψηφιακό Μοντέλο Προσομοίωσης.....	7
2.1.1	Ρομπότ.....	7
2.1.2	Εργαστηριακός Εξοπλισμός.....	8
2.1.3	Ασφαλείς Θέσεις	9
2.1.4	Παραμετροποίηση του προβλήματος.....	10
2.2	Πειραματικά πρωτόκολλα.....	10
2.3	Διεπαφή χρήστη-ρομπότ.....	11
2.4	Προσομοίωση πειραμάτων με τους ρομποτικούς βραχίονες SCARA και STAUBLI	13
2.4.1	SCARA	13
2.4.2	STAUBLI TX2-90XL.....	15
3	ΑΠΟΤΕΛΕΣΜΑΤΑ	17
3.1	Σχολιασμός	17
3.1.1	SCARA	18
3.1.2	STAUBLI TX2-90XL.....	25
4	ΣΥΜΠΕΡΑΣΜΑΤΑ	30
4.1	Συνεισφορά	30
4.2	Πλεονεκτήματα περιβάλλοντος εικονικής πραγματικότητας.....	30
4.3	Προτάσεις για μελλοντική έρευνα	31
5	ΒΙΒΛΙΟΓΡΑΦΙΑ	33

Ευρετήριο Εικόνων

Εικόνα 1: Τμήμα από την ηλεκτρονική σελίδα της εταιρίας experoment	4
Εικόνα 2: Το ee_link_dummy για την περίπτωση του SCARA (πάνω) και του STAUBLI (κάτω)8	
Εικόνα 3: Σημεία φόρτωσης-εκφόρτωσης των εργαστηριακών μηχανών.....	9
Εικόνα 4: Παραδείγματα πεοραματικών πρωτοκόλλων	11
Εικόνα 5: Διαγραμματική απεικόνιση διεπαφής χρήστη- περιβάλλοντος εργασίας.....	13
Εικόνα 6: Αρχική θέση του ρομπότ SCARA	13
Εικόνα 7: Το ρομπότ SCARA παίρνει το μικροπλακίδιο από τον τεχνικό του εργαστηρίου (θέση input)	13
Εικόνα 8: Μετακίνηση ρομπότ SCARA πάνω από μικροπλακίδιο σε περιστρεφόμενη	14
Εικόνα 9: Ασφαλής απόσταση SCARA από εξοπλισμό εργαστηρίου	14
Εικόνα 10: Η αρπάγη του SCARA είναι έτοιμη να αφήσει/παραλάβει πλακίδιο.....	14
Εικόνα 11: Ρομπότ SCARA επιστρέφει μικροπλακίδιο σε τεχνικό εργαστηρίου (θέση output)	14
Εικόνα 12: Επιστροφή SCARA σε αρχική θέση	14
Εικόνα 13: Αρχική θέση του ρομπότ STAUBLI.....	13
Εικόνα 14: Το ρομπότ STAUBLI παίρνει το μικροπλακίδιο από τον τεχνικό του εργαστηρίου (θέση input).....	15
Εικόνα 15: Ασφαλής απόσταση STAUBLI από εξοπλισμό εργαστηρίου	15
Εικόνα 16: Η αρπάγη του STAUBLI είναι έτοιμη να αφήσει/παραλάβει πλακίδιο	15
Εικόνα 17: Το ρομπότ STAUBLI επιστρέφει το μικροπλακίδιο στον τεχνικό του εργαστηρίου (θέση output)	16
Εικόνα 18: Επιστροφή STAUBLI σε αρχική θέση.....	16

Ευρετήριο Διαγραμμάτων

Διάγραμμα 1: : Θέση ΤΣΔ του SCARA με EK- Αρχική σε Ασφαλή θέση	18
Διάγραμμα 2: Γωνιακές ταχύτητες αρθρώσεων του SCARA με EK- Αρχική σε Ασφαλή θέση	18
Διάγραμμα 3: Γωνίες αρθρώσεων του SCARA με EK- Αρχική σε Ασφαλή θέση	19
Διάγραμμα 4: Επιθυμητή vs Πραγματική θέση ΤΣΔ του SCARA με AK- Ασφαλής σε θέση Input	19
Διάγραμμα 5: Γωνίες αρθρώσεων του SCARA με AK- Ασφαλής σε θέση Input.....	19
Διάγραμμα 6: Επιθυμητή vs Πραγματική ταχύτητα ΤΣΔ του SCARA με AK- Ασφαλής σε θέση Input	20
Διάγραμμα 7: Επιθυμητή vs Πραγματική θέση ΤΣΔ του SCARA με AK- Αρχική σε Ασφαλή θέση	20
Διάγραμμα 8: Γωνίες αρθρώσεων του SCARA με AK- Αρχική σε Ασφαλή θέση.....	20
Διάγραμμα 9: Ταχύτητα ΤΣΔ του SCARA με AK- Αρχική σε Ασφαλή θέση.....	21
Διάγραμμα 10: Επιθυμητή vs Πραγματική θέση ΤΣΔ του SCARA με AK- Ασφαλής θέση σε Πλακίδιο	21
Διάγραμμα 11: Γωνίες αρθρώσεων του SCARA με AK- Ασφαλής θέση σε Πλακίδιο	21
Διάγραμμα 12: Επιθυμητή vs Πραγματική ταχύτητα ΤΣΔ του SCARA με AK- Ασφαλής θέση σε Πλακίδιο	22
Διάγραμμα 13: Επιθυμητή vs Πραγματική θέση ΤΣΔ του SCARA με AK – Μηχάνημα 1 σε Μηχάνημα 2	22
Διάγραμμα 14: Γωνίες αρθρώσεων του SCARA με AK – Μηχάνημα 1 σε Μηχάνημα 2	22
Διάγραμμα 15: Επιθυμητή vs Πραγματική ταχύτητα ΤΣΔ του SCARA με AK – Μηχάνημα 1 σε Μηχάνημα 2	23
Διάγραμμα 16: Θέση ΤΣΔ του SCARA με EK- Αρχική σε Ασφαλή θέση	23
Διάγραμμα 17: Γωνίες αρθρώσεων SCARA με EK- Αρχική σε Ασφαλή θέση.....	23
Διάγραμμα 18: Γωνιακές ταχύτητες αρθρώσεων του SCARA με EK- Αρχική σε Ασφαλή θέση	24
Διάγραμμα 19: Επιθυμητή vs Πραγματική θέση ΤΣΔ του SCARA με AK – Ασφαλής σε θέση Output	24
Διάγραμμα 20: Γωνίες αρθρώσεων SCARA με AK- Ασφαλής σε θέση Output	24
Διάγραμμα 21: Επιθυμητή vs Πραγματική ταχύτητα ΤΣΔ του SCARA με AK – Ασφαλής σε θέση Output	25

Διάγραμμα 22: Επιθυμητή vs Πραγματική θέση ΤΣΔ του STAUBLI με AK- Αρχική σε θέση Input	25
Διάγραμμα 23: Γωνίες αρθρώσεων του STAUBLI με AK - Αρχική σε θέση Input.....	25
Διάγραμμα 24: Επιθυμητή vs Πραγματική ταχύτητα ΤΣΔ του STAUBLI με AK- Αρχική σε θέση Input	26
Διάγραμμα 25: Επιθυμητή vs Πραγματική θέση ΤΣΔ του STAUBLI με AK – Ασφαλής θέση σε Μηχάνημα 1	26
Διάγραμμα 26: Γωνίες αρθρώσεων του STAUBLI με AK – Ασφαλής θέση σε Μηχάνημα 1 ..	26
Διάγραμμα 27: Επιθυμητή vs Πραγματική ταχύτητα ΤΣΔ του STAUBLI με AK – Ασφαλής θέση σε Μηχάνημα 1	27
Διάγραμμα 28: Θέση ΤΣΔ του STAUBLI με EK- Μηχάνημα 1 σε Αρχική θέση.....	27
Διάγραμμα 29: Γωνίες αρθρώσεων του STAUBLI με EK- Μηχάνημα 1 σε Αρχική θέση.....	27
Διάγραμμα 30: Γωνιακές ταχύτητες αρθρώσεων το STAUBLI με EK- Μηχάνημα 1 σε Αρχική θέση.....	28
Διάγραμμα 31: Επιθυμητή vs Πραγματική θέση ΤΣΔ του STAUBLI με AK – Αρχική σε θέση Output	28
Διάγραμμα 32: Γωνίες αρθρώσεων του STAUBLI με AK – Αρχική σε θέση Output.....	28
Διάγραμμα 33: Επιθυμητή vs Πραγματική ταχύτητα ΤΣΔ του STAUBLI με AK – Αρχική σε θέση Output	29

1

ΕΙΣΑΓΩΓΗ

1.1 Τι είναι ένα Ρομποτικό Cloud Εργαστήριο Βιοτεχνολογίας;

Όταν σκεφτόμαστε βελτιώσεις αυτοματισμού και παραγωγικότητας, τα βιομηχανικά ρομπότ βαρέας παραγωγής είναι ίσως τα πρώτα πράγματα που μας έρχονται στο μυαλό. Ωστόσο, υπάρχουν πολλά περισσότερα σε αυτό. Οι περισσότεροι ερευνητές, τόσο στον ακαδημαϊκό χώρο όσο και στη βιομηχανία, χρησιμοποιούν ακόμα χειρόγραφες σημειώσεις εργαστηρίου και υπολογιστικά φύλλα του Excel για να καταγράψουν τα ευρήματά τους. Για πολλά από αυτά τα εργαστήρια που εισέρχονται στον 21ο αιώνα αυτοματοποίησης, οι αισθητήρες και το Internet of Things (IoT) είναι σχεδόν αδύνατο χωρίς σημαντικές οικονομικές επενδύσεις για την πρόσληψη ειδικευμένου προσωπικού και την αγορά εξοπλισμού.

Ένας από τους πιο αναπτυσσόμενους, από την άποψη αυτή, τομείς είναι η βιοτεχνολογία. Ωστόσο, η καινοτομία στη βιοτεχνολογία παρεμποδίζεται από την έλλειψη δύο σημαντικών παραγόντων. Το πρώτο είναι η αναπαραγωγικότητα. Τα περισσότερα από τα πειράματα σε επιστημονικές δημοσιεύσεις είναι δύσκολο να αναπαραχθούν. Το δεύτερο είναι η προσβασιμότητα. Πολύ λίγοι άνθρωποι έχουν πρόσβαση στον εξοπλισμό ή τα κεφάλαια που απαιτούνται για την έναρξη ενός εργαστηρίου. Ακόμα κι αν κάποιος το κάνει, μπορεί να χρειαστούν πολλοί μήνες ή και χρόνια έρευνας πριν να έχει καν ένα μόνο προϊόν στη γραμμή.

Η κύρια έννοια που κρύβεται πίσω από το εργαστήριο ρομποτικής βιοτεχνολογίας, είναι μια ερευνητική μονάδα μοριακής και κυτταρικής βιολογίας που λειτουργεί με ρομπότ και ελέγχεται μέσω API (Application Programming Interface). Η χρήση του; Να επιτραπεί σε επιστήμονες να διαχειρίζονται πλήρως και εξ αποστάσεως μια ολοκληρωμένη βιοτεχνολογική εγκατάσταση, όπως ένα εργαστήριο. Η μεταφορά υγρών μεταξύ μηχανών αντί για τη χρήση πιπέτας γίνεται αυτοματοποιημένα, ενώ οι ρομποτικοί βραχίονες έχουν τον κύριο ρόλο για την εκτέλεση πειραμάτων με μικρή ανθρώπινη παρέμβαση. Οι πελάτες υποβάλλουν παραγγελίες μέσω μιας διεπαφής και λαμβάνουν ανατροφοδότηση δεδομένων σε κάθε βήμα του πειράματος. Η βασική ιδέα είναι ότι πολλά πειράματα στη βιολογία χρησιμοποιούν τις ίδιες βασικές λειτουργίες με διαφορετικό υλικό και σε διαφορετική ακολουθία. Ένα τυπικό πείραμα περιλαμβάνει τη φυγοκέντρηση, την ανάγνωση δειγμάτων με φωτομετρία και ένα μικρό αριθμό άλλων λειτουργιών που μπορούν να αντιμετωπιστούν ακολουθιακά και να αυτοματοποιηθούν πλήρως. [1]

Ο στόχος είναι να αλλάξει ο τρόπος με τον οποίο γίνεται η έρευνα, αντισταθμίζοντας δραματικά το συνεχώς αυξανόμενο κόστος των κλινικών δοκιμών, αυτοματοποιώντας την κουραστική εργαστηριακή εργασία και επιταχύνοντας την έρευνα με την διεξαγωγή παράλληλων πειραμάτων. Συγκεκριμένα, αυτή η νέα προσέγγιση ανοίγει τη δυνατότητα

φτηνής και αποτελεσματικής αναπαραγωγής παλαιότερων επιστημονικών πειραμάτων, γεγονός που αποτελεί περίπλοκο πρόβλημα του τομέα. Επίσης, υπόσχεται να μειώσει δραστικά το χρόνο και το κόστος απόκτησης νέων φαρμάκων στην αγορά. Συγκεκριμένα, ο αριθμός των νέων φαρμάκων που εγκρίνονται ανά δισεκατομμύριο δολάρια δαπανών μειώνεται έως και κατά το ήμισυ κάθε εννέα χρόνια. Οι ρυθμοί αυτοί διασφαλίζουν ότι η ανάπτυξη φαρμάκων θα παραμένει ζήτημα των μεγάλων πολυεθνικών εταιρειών και ότι τα περισσότερα φάρμακα που σώζουν ζωές θα παραμένουν απρόσιτα για την πλειοψηφία των ανθρώπων στον κόσμο. Κρίνεται λοιπόν αναγκαίο να ακολουθηθεί μια πιο δημοκρατική προσέγγιση για την προώθηση του σημερινού μοντέλου ανάπτυξης φαρμάκων. [2] Αυτός είναι και ένας βασικός λόγος για τον οποίο οι cloud και open source πλατφόρμες κρύβουν τόσες πολλές υποσχέσεις. Τα ρομποτικά cloud εργαστήρια αφαιρούν την απαίτηση για μεγάλες δαπάνες στη διαδικασία ανάπτυξης φαρμάκων και έτσι επιτρέπουν σε ένα ευρύτερο φάσμα ανθρώπων να σχεδιάσουν και να δοκιμάσουν νέες επιστημονικές ιδέες.

Επίσης, πιθανόν να αλλάξει τον τρόπο με τον οποίο οι επιστήμονες σχεδιάζουν τα πειράματά τους, δεδομένου ότι με την ανθρώπινη επιστημονική έρευνα κάθε πρόσθετο βήμα σε μια εργαστηριακή διαδικασία συνεπάγεται εκθετική αύξηση του κόστους και αυξάνει την πιθανότητα ανθρώπινου σφάλματος και απόκλισης από το πρωτόκολλο, γεγονότα που προλαμβάνονται μέσω μιας πλήρως αυτοματοποιημένης προσέγγισης .

Με άλλα λόγια, υπάρχουν πολλαπλά πλεονεκτήματα με τα cloud lab, με την απομακρυσμένη πρόσβαση σε πραγματικό χρόνο να είναι μόνο ένα από αυτά. Τα εργαστήρια επιτρέπουν στους ερευνητές να αναπαράγουν ευκολότερα τα αποτελέσματα. Κάνουν πιο εύκολη την τυποποίηση της πειραματικής διαδικασίας. Οι ερευνητές μπορούν να αναλύσουν αποτελεσματικότερα τα δεδομένα από όλα τα πειράματα που αποθηκεύονται στο «σύννεφο». Όλα αυτά μπορούν να μεταφραστούν σε μαζικά αυξανόμενη παραγωγικότητα.

1.2 Τεχνολογία Digital Factory

Η βιομηχανία 4.0 επικεντρώνεται στην υιοθέτηση νέων τεχνολογιών πληροφορικής και διαδικτύου, συμπεριλαμβανομένου του διαδικτύου των πραγμάτων, της κατασκευής σύννεφων, της ψηφιακής / εικονικής πραγματικότητας κλπ. ως βασικές τεχνολογίες για την αντιμετώπιση νέων προκλήσεων. [3], [4]. Τα κύρια χαρακτηριστικά του Industry 4.0 είναι η διαλειτουργικότητα, η αποκέντρωση, η ικανότητα δράσης σε πραγματικό χρόνο, ο προσανατολισμός των υπηρεσιών και η εικονικοποίηση, δηλαδή η σύνδεση των πραγματικών εργοστασιακών δεδομένων με τα μοντέλα εικονικών εγκαταστάσεων και τα μοντέλα προσομοίωσης για τη δημιουργία ενός εικονικού αντιγράφου του Smart Factory. Σκοπός του είναι η αυξημένη ευελιξία στην παραγωγή, π.χ. μέσω της χρήσης διαμορφωμένων ρομπότ και μηχανημάτων που μπορεί να παράγουν μια ποικιλία διαφορετικών προϊόντων, προσαρμογή μαζών, π.χ. επιτρέποντας την παραγωγή ακόμη και μικρών παρτίδων, προσαρμοσμένων στις προδιαγραφές των πελατών λόγω της δυνατότητας ταχείας διαμόρφωσης των μηχανών και της ταχύτητας επεξεργασίας, δεδομένου ότι ο ψηφιακός σχεδιασμός και η εικονική μοντελοποίηση των διαδικασιών παραγωγής και συστημάτων μπορούν να μειώσουν το χρόνο μεταξύ σχεδιασμού και έναρξης παραγωγής,

που απαιτούνται για την παράδοση των παραγγελιών και το χρόνο για να τεθούν τα προϊόντα στην αγορά. [5]

Συνεπώς, η τέταρτη βιομηχανική επανάσταση δεν αντιπροσωπεύεται μόνο από την αλληλεπίδραση μεταξύ μηχανών, ρομπότ, ηλεκτρονικών υπολογιστών και δεδομένων μέσω του Διαδικτύου, αλλά και από την αυξημένη χρήση ψηφιακών μέσων παραγωγής και λογισμικού, επιτρέποντας την ψηφιακή αναπαράσταση του πραγματικού περιβάλλοντος παραγωγής, όλα τα επίπεδα από το σύνολο του εργοστασίου παραγωγής, από ένα μόνο μηχάνημα, από μια συγκεκριμένη διαδικασία ή από μια επιχείρηση ή από τον σχεδιασμό και την ανάπτυξη νέων προϊόντων. [6] Σε αυτό το πλαίσιο, οι τεχνολογίες Digital Factory βασίζονται στην αξιοποίηση ψηφιακών μεθόδων και εργαλείων, όπως η αριθμητική προσομοίωση, η τρισδιάστατη μοντελοποίηση και η εικονική πραγματικότητα για την εξέταση ενός σύνθετου κατασκευαστικού συστήματος και την αξιολόγηση διαφορετικών διαμορφώσεων για βέλτιστη λήψη αποφάσεων με σχετικά χαμηλό κόστος. [4], [7] Οι τεχνολογίες που βασίζονται στην προσομοίωση είναι κεντρικά στοιχεία στην προσέγγιση Digital Factory, καθώς επιτρέπουν τον πειραματισμό και την επικύρωση διαφόρων διαμορφώσεων συστημάτων προϊόντων, διαδικασιών και κατασκευών. [8]

Τα κοινά ψηφιακά δεδομένα και μοντέλα στο Smart Factory θα πρέπει να είναι προσαρμοσμένα, με την έννοια ότι πρέπει πάντα να αντιπροσωπεύουν την τρέχουσα κατάσταση του φυσικού συστήματος παραγωγής. Για το λόγο αυτό, θα πρέπει να ενημερώνονται τακτικά με πληροφορίες που προέρχονται από το φυσικό σύστημα παραγωγής καθώς και με βάση τις εισόδους των χρηστών. Δεδομένου ότι τα μοντέλα είναι ενημερωμένα και έγκυρα, μπορούν να χρησιμοποιηθούν αποτελεσματικά για τη λήψη αποφάσεων μέσω της χρήσης έγκυρων μεθόδων βελτιστοποίησης. Ως εκ τούτου, ένα θεμελιώδες ζήτημα αποτελεί η προσαρμογή των κοινών δεδομένων και των μοντέλων που πραγματοποιούν μια στενή σύνδεση μεταξύ του φυσικού και του ψηφιακού κόσμου [4].

Από την άποψη αυτή, είναι εμφανής η σημασία της ανάπτυξης μεθόδων παραγωγής αιχμής για φαρμακευτικά προϊόντα που χρησιμοποιούν τεχνολογίες ψηφιακού εργοστασίου. Τις νεοφυείς εταιρίες, μεταξύ άλλων, μπορεί να βοηθήσει η ανάπτυξη αυτών των τεχνολογιών, δεδομένου ότι το κόστος και ο κίνδυνος για την κατασκευή, στην περίπτωσή μας, ενός βιοτεχνολογικού εργαστηρίου, ελαχιστοποιούνται χάρη στις τεχνολογίες προσομοίωσης, στις οποίες η τρέχουσα εργασία βασίζεται επίσης σε μεγάλο βαθμό.

1.3 Προσπάθειες για την ανάπτυξη αυτοματοποιημένων εργαστηρίων βιοτεχνολογίας

Οι περισσότερες εταιρίες φαρμακευτικών και βιοτεχνολογικών προϊόντων, και εν μέρει και ακαδημαϊκά εργαστήρια, διαθέτουν αυτοματοποιημένα τμήματα των διαδικασιών τους και χρησιμοποιούν συστήματα διαχείρισης υγρών, ενώ οι πρώτες εργαστηριακές εφαρμογές API είναι διαθέσιμες. Οι εταιρίες Science-As-a-Service (SciAAS) άρχισαν να εμφανίζονται, με πρόθεση να επιταχύνουν την επιστημονική έρευνα και τη βελτίωση της βιοτεχνολογίας. Επιτρέποντας στους ερευνητές να αναθέτουν το ακριβό έργο της διεξαγωγής πειραμάτων σε εξωτερικούς συνεργάτες, οι ομάδες εξοικονομούν χρόνο και χρήματα χωρίς να διακυβεύουν την ποιότητα της επιστημονικής έρευνας, μειώνοντας έτσι τα εμπόδια που εμφανίζονται

κατά την ανάπτυξη νέων επιχειρήσεων βιοτεχνολογίας. Η προγραμματιζόμενη και αυτοματοποιημένη πειραματική διαδικασία θα δώσει τη δυνατότητα σε όσους έχουν τις ανάγκες και τις ιδέες, αλλά δεν διαθέτουν τους πόρους, να μετατρέψουν τα πειράματά τους σε πραγματικότητα.

Τα API θα απελευθερώσουν τους ερευνητές από παράγοντες, όπως είναι το ανθρώπινο λάθος και η έλλειψη αναπαραγωγιμότητας, και θα οδηγήσουν σε πολλά περισσότερα πειράματα.

1.4 Υπάρχουσες ρομποτικές cloud πλατφόρμες βιοτεχνολογίας

Το πρώτο ρομποτικό cloud εργαστήριο για έρευνα σχετικά με βιολογικές επιστήμες αναπτύχθηκε από μια start-up εταιρεία με την επωνυμία Transcriptic. Ιδρύθηκε το 2012 και υποστηρίζεται από την Google Ventures και τους ιδρυτές πίσω από την Pay Pal. Η εταιρεία αριθμεί 40 άτομα και καταλαμβάνει εγκαταστάσεις 22.000 τετραγωνικών στην καρδιά της Silicon Valley. Η εταιρεία κατασκευάζει και διαχειρίζεται ρομποτικά εργαστήρια βιοτεχνολογίας, κλεισμένα από πλεξιγκλάς ή αλλιώς «κύτταρα» που φιλοξενούν περίπου 20 συσκευές η κάθε μία. Τα κύτταρα λειτουργούν με ηλεκτρονικούς υπολογιστές, οι οποίοι λαμβάνουν πρωτόκολλα πειραμάτων και τα εκτελούν. Ένα ρομπότ κρεμασμένο σε ράγα διατρέχει το μήκος του κυττάρου, μεταφέροντας μικροπλακίδια από μηχανήμα σε μηχανήμα για την διεκπεραίωση των πειραμάτων. [Πηγή: [Transcriptic](#)]

Έχουν πραγματοποιηθεί διάφορες προσπάθειες προς αυτή την κατεύθυνση, μεταξύ των οποίων και η προσπάθεια της start-up experoment, σε συνεργασία με την οποία πραγματοποιήθηκε η διπλωματική αυτή εργασία. Η experoment στοχεύει κυρίως σε πειράματα ανοσο-ογκολογίας, μερικά από τα οποία θα αναδημιουργηθούν και θα προσομοιωθούν για τους σκοπούς της τρέχουσας εργασίας.

experoment
[ɪkˈsperom(ə)nt] (noun)
Your Cloud Lab for on-demand R&D

- Experiment as software**
 Programming languages are unambiguous and explicit. Describe your experiments in our visual programming language and ensure on-demand reproducibility of results, anywhere in the world.
- Robotic facilities**
 Take advantage of high performance automation and robotics to speed up your results with zero human error.
- Data digitalisation**
 Unlock the full potential of your research. Enable next-generation AI and data analytics with high quality standardized digital data.

Εικόνα 1: Τμήμα από την ηλεκτρονική σελίδα της εταιρίας experoment

1.5 Αντικείμενο και στόχοι της διπλωματικής εργασίας

Το αντικείμενο της τρέχουσας έρευνας είναι ο προγραμματισμός της τροχιάς και η απομακρυσμένη λειτουργία ενός ρομποτικού βραχίονα σε ένα εργαστήριο βιοτεχνολογίας, χρησιμοποιώντας ένα περιβάλλον εικονικής προσομοίωσης, καθώς και ο σχεδιασμός ενός Ευέλικτου Συστήματος Παραγωγής, με στόχο την εισαγωγή νέων αντικειμένων με χαμηλή επιβάρυνση και την αύξηση της παραγωγικότητας του κυττάρου. Το σύστημα θα πρέπει να είναι σε θέση να επεξεργάζεται οποιοδήποτε συνδυασμό πειραμάτων ή συνεχών παρτίδων πειραμάτων ανά πάσα στιγμή.

Η τεχνολογία που μελετάται αποτελείται από μια διεπαφή λογισμικού που συνδέει υλικό και εξοπλισμό σε ένα εργαστήριο ρομποτικής βιοτεχνολογίας για να αυτοματοποιήσει τις απλές ροές εργασίας του πειραματισμού. Επιτρέπει σε έναν ερευνητή να δημιουργήσει ένα πρωτόκολλο και στη συνέχεια να το κοινοποιήσει στον εργαστηριακό εξοπλισμό του. Οι ερευνητές έχουν πρόσβαση σε αυτές μέσω μιας πλατφόρμας cloud, προκειμένου να εκτελούν εξ αποστάσεως πειράματα χωρίς να χρειάζεται φυσική πρόσβαση στο εργαστήριο. Ο χρήστης επιλέγει το πείραμα για εκτέλεση από την σχεδιασμένη πλατφόρμα και έχει την ελευθερία να αλλάξει μερικές παραμέτρους, σε σχέση με τα πειράματα που πρόκειται να διεξαχθούν. Τα πειράματα μπορούν να κατηγοριοποιηθούν σε:

I. προ-βελτιστοποιημένα πειράματα και

II. ειδικά σχεδιασμένα πειράματα

Οι ερευνητές περιγράφουν τις παραμέτρους του πειράματος σε μια φιλική προς το χρήστη οπτική γλώσσα και στη συνέχεια το σχέδιο μεταφορτώνεται στο εργαστήριο, προσφέροντας διαφάνεια εκτέλεσης καθώς οι ερευνητές έχουν συνεχή εποπτεία εξ αποστάσεως, ενώ ο χρήστης μπορεί να κατεβάσει τα αποτελέσματα των πειραμάτων μετά την ολοκλήρωσή τους.

Συγκεκριμένα, στα πλαίσια αυτής της μελέτης, επιχειρήθηκε:

- Μοντελοποίηση ενός ρομποτικού βραχίονα τύπου SCARA και του ρομποτικού βραχίονα Stäubli TX2-90XL, καθώς και του περιβάλλοντος του εργαστηρίου, χρησιμοποιώντας την πλατφόρμα Virtual Robot Experimentation Platform (V-REP).
- Ανάπτυξη της κινηματικής αλυσίδας μεταξύ των συνδέσμων των ρομπότ και της αντίστροφης κινηματικής τους.
- Προγραμματισμός της τροχιάς του ρομπότ για την εξαγωγή πλάνου κίνησης των ρομποτικών βραχιόνων.
- Επιλογή μηχανικών διεπαφών μεταξύ των ρομπότ και των οργάνων και εισαγωγή τους στο μοντέλο προσομοίωσης.
- Προσομοίωση πειραμάτων και αξιολόγηση της συμπεριφοράς του κάθε ρομπότ σε διαφορετικές διατάξεις εργαστηρίου.

Οι στόχοι της παραπάνω μελέτης είναι:

- Απλοποίηση της διαδικασίας προγραμματισμού τροχιάς του ρομπότ, αν ο χειριστής ελέγχει το σημείο τερματισμού και οι τιμές των γωνιών άρθρωσης προέρχονται από την αντίστροφη κινηματική.
- Μείωση των σφαλμάτων στη φυσική παραγωγή, καθώς τα σφάλματα σε ένα εικονικό περιβάλλον δεν έχουν φυσικές συνέπειες και μπορούν να διορθωθούν, εξοικονομώντας χρόνο και αποτρέποντας ζημιές στη μηχανή ή δαπανηρές αποτυχίες κατά τη διάρκεια της παραγωγής.
- Ικανότητα παρακολούθησης και τροποποίησης της λειτουργίας του ρομποτικού βραχίονα χωρίς να απαιτείται άτομο στο χώρο του εργαστηρίου. Το τελευταίο εξαλείφει τη δυνατότητα τραυματισμού του ανθρώπινου παράγοντα με τη μετακίνηση εξαρτημάτων.
- Προσφορά μιας εναλλακτικής λύσης χαμηλού κόστους στον οπτικό έλεγχο (visual servoing) του ρομπότ ή σε ακριβό ρομπότ υψηλής ακρίβειας, ειδικά επειδή στην περίπτωση αυτή όλα τα αναλώσιμα στοιχεία μετακινούνται μεταξύ γνωστών προκαθορισμένων θέσεων και προσανατολισμών και ο ρομποτικός βραχίονας είναι υπεύθυνος για τη μεταφορά αντικειμένων προκαθορισμένων διαστάσεων από ένα σταθμό εργασίας σε άλλο.

2

ΠΡΟΣΟΜΟΙΩΣΗ

2.1 Ψηφιακό Μοντέλο Προσομοίωσης

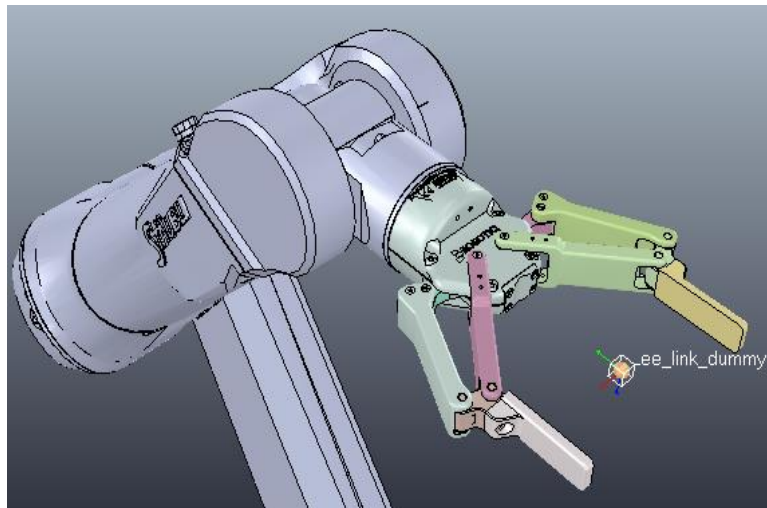
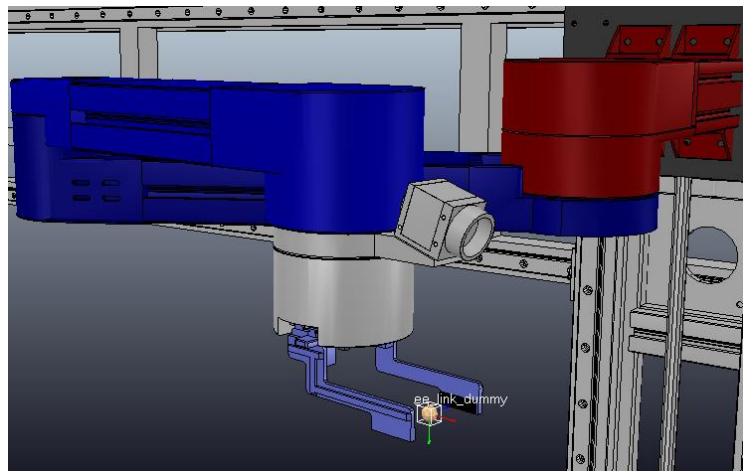
Ο σημαντικότερος παράγοντας της προσομοίωσης που έχει υπογραμμιστεί καθ' όλη τη διάρκεια της τρέχουσας εργασίας, είναι η παροχή ευελιξίας στον ερευνητή και η παραμετροποίηση της πειραματικής διαδικασίας, κατά τρόπο τέτοιο ώστε να μπορεί να ολοκληρωθεί οποιοδήποτε πρωτόκολλο πειράματος, ανεξάρτητα από τον αριθμό ή τον τύπο μηχανών, τη σειρά της χρήση τους κατά τη διάρκεια ενός πειράματος ή ακόμα και ανεξάρτητα από τις γνώσεις του χρήστη σχετικά με ρομποτικά συστήματα.

2.1.1 Ρομπότ

Μετά την έκφραση της κινηματικής αλυσίδας κάθε ρομπότ ως αρχείο URDF, τα μοντέλα εισάγονται στη σκηνή προσομοίωσης. Κάθε ρομπότ αποτελείται από δικούς του συνδέσμους και αρθρώσεις, ενώ στα αρχεία URDF προστέθηκαν δύο επιπλέον οντότητες, συγκεκριμένα τα `ee_link` και `world`.

Ο ρόλος του `world`, που θα αναφέρεται ως `world frame` του ρομπότ και δεν πρέπει να συγχέεται με το `global frame` του VREP, είναι να παράσχει ένα σημείο αναφοράς για όλα όσα συμβαίνουν στη σκηνή προσομοίωσης. Δεδομένου ότι οι ρομποτικοί βραχίονες αποτελούν το κεντρικό θέμα της λειτουργίας των ρομποτικών συστημάτων, είναι λογικό να εκφράζονται ως προς το `world frame`, όχι μόνο η θέση και ο προσανατολισμός των συνδέσμων και των αρθρώσεων του ρομπότ, αλλά και η θέση και ο προσανατολισμός όλων των συνιστωσών μιας σκηνής.

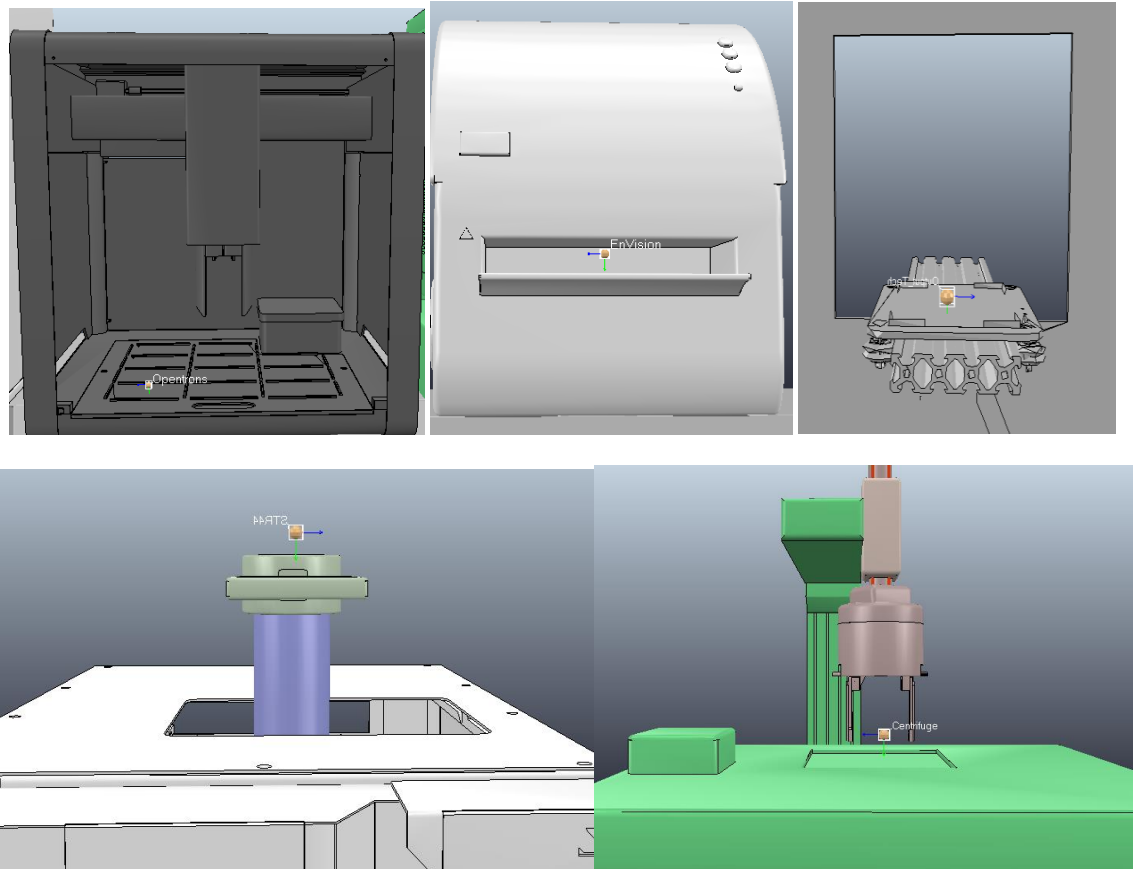
Αντίστοιχα, το `ee_link` αντιπροσωπεύει την πραγματική τελική θέση του τελικού σημείου δράσης, η οποία είναι πάντα περίπου στη μέση της αρπάγης, αντιπροσωπεύοντας το σημείο όπου θα προσαρτηθεί το μικροπλακίδιο. Ωστόσο, είναι πιθανό το `ee_link` του αρχείου URDF να μην συμπίπτει με το πραγματικό σημείο πιασίματος, αλλά να συμπίπτει μονάχα με τη βάση της αρπάγης ή την τελική άρθρωση ενός ρομπότ. Σε αυτή την περίπτωση, ένα `ee_link_dummy` προστίθεται στη σκηνή VREP. Το `ee_link_dummy` εκφράζεται στη συνέχεια σε σχέση με το `ee_link` του URDF, μέσω ενός κατάλληλου `offset` και αυτό αργότερα εκφράζεται σε σχέση με τον κόσμο. Η διατήρηση της ομοιογενούς έκφρασης της θέσης και του προσανατολισμού ως προς ένα σημείο αναφοράς είναι το κλειδί για μια επιτυχημένη και με ακρίβεια προσομοίωση.



Εικόνα 2: Το ee_link_dummy για την περίπτωση του SCARA (πάνω) και του STAUBLI (κάτω)

2.1.2 Εργαστηριακός Εξοπλισμός

Ο εργαστηριακός εξοπλισμός, συμπεριλαμβανομένων των μηχανών και των αναλώσιμων εισάγονται στη σκηνή σύμφωνα με την επιθυμητή διάταξη. Ο στόχος είναι να δημιουργηθεί ένα περιβάλλον όπου το ρομπότ θα μπορεί να εντοπίζει τα σημεία φόρτωσης και εκφόρτωσης κάθε μηχανής σε σχέση με το world frame του, όπως αυτό αναλύθηκε προηγουμένως. Προκειμένου το ρομπότ να καταλάβει ποια μηχανήματα θα πρέπει να επισκεφθεί κατά τη διάρκεια ενός πειράματος, dummies από το VREP τοποθετούνται στις θέσεις φόρτωσης-εκφόρτωσης κάθε μηχανής και ονομάζονται με βάση την ονομασία της μηχανής στην οποία ανήκουν. Είναι σημαντικό ο προσανατολισμός των dummies να είναι ο ίδιος με τον προσανατολισμό του ee_link_dummy στο τελικό σημείο δράσης, έτσι ώστε ο ρομποτικός βραχίονας να μπορεί να προσεγγίσει τη σωστή θέση με τον σωστό προσανατολισμό. Οι θέσεις των μηχανών και του περιβάλλοντος του εργαστηρίου όπου οι ρομποτικοί βραχίονες πρέπει να φορτώνουν και να εκφορτώνουν τα μικροπλακίδια παρουσιάζονται στην **Εικόνα 3**.



Εικόνα 3: Σημεία φόρτωσης-εκφόρτωσης των εργαστηριακών μηχανών

2.1.3 Ασφαλείς Θέσεις

Τα dummies δεν χρησιμοποιούνται μόνο για να εκφράσουν τη θέση και τον προσανατολισμό ενός αντικειμένου σε σχέση με το world frame του ρομπότ, αλλά χρησιμοποιούνται επίσης ως σημεία αναφοράς για να περιγράψουν κάποιες άλλες θέσεις στον χώρο, οι οποίες είναι απαραίτητες για την πραγματοποίηση ομαλής τροχιάς του ρομπότ.

Για παράδειγμα, συνιστάται ιδιαίτερα να χρησιμοποιούνται ενδιάμεσα σημεία μεταξύ της αρχικής θέσης ρομπότ και οποιασδήποτε θέσης μηχανής. Ο καθορισμός μιας ασφαλούς θέσης μηχανής βοηθά στην εξάλειψη των συγκρούσεων του ρομπότ με τον εργαστηριακό εξοπλισμό. Μια τέτοια θέση μηχανής μπορεί να οριστεί ως η θέση μηχανής +/- μια μετατόπιση. Η μετατόπιση μπορεί να αντιπροσωπεύει μια απόσταση από την πραγματική θέση φόρτωσης-εκφόρτωσης που θεωρείται ασφαλής για να προσεγγίσει το ρομπότ, πριν ολοκληρώσει την κίνησή του.

Οι ασφαλείς θέσεις στα πειράματα που ακολουθούνται καθορίζονται για τις ακόλουθες περιπτώσεις:

- Πριν ο ρομποτικός βραχίονας SCARA πλησιάσει την περιστροφική βάση στην οποία αλλάζουν οι προσανατολισμοί των μικροπλακών για να αποφευχθεί η σύγκρουση με τα μηχανήματα κατά την αναδίπλωση / ξεδίπλωση του βραχίονα

- Πριν ο ρομποτικός βραχίονας SCARA προσεγγίσει τις θέσεις εισόδου / εξόδου (input/output) για να αποφευχθούν συγκρούσεις με το πλαίσιο του εργαστηρίου
- Προτού οι ρομποτικοί βραχίονες SCARA και STAUBLI πλησιάσουν τις θέσεις φόρτωσης / εκφόρτωσης κάθε μηχανής για να αποφευχθούν ακανόνιστες κινήσεις του βραχίονα και συγκρούσεις με τα μηχανήματα

2.1.4 Παραμετροποίηση του προβλήματος

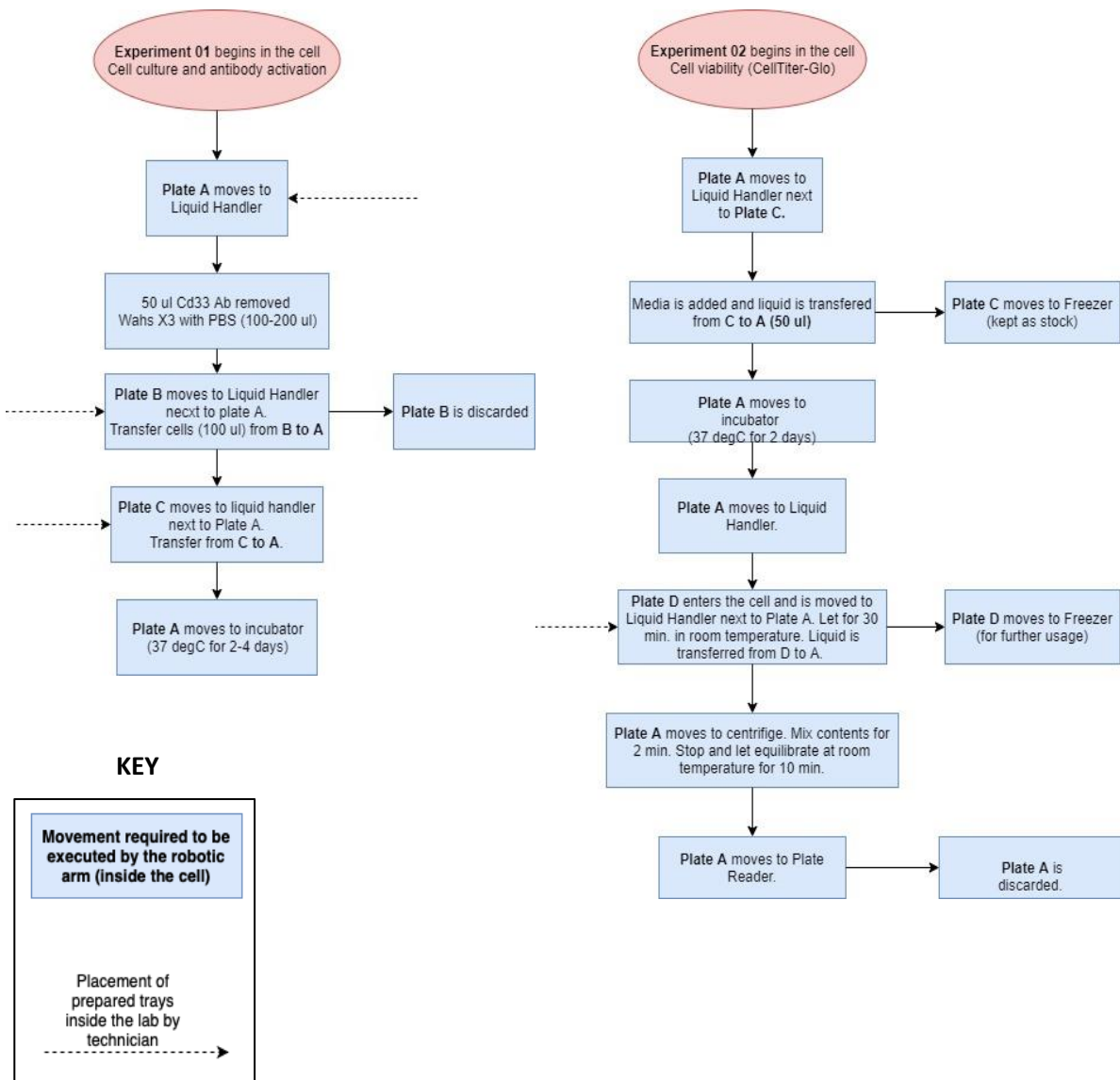
Στην περίπτωση μας, μόλις καθοριστεί το περιβάλλον προσομοίωσης και οριστούν τα *dummies*, το VREP αποθηκεύει αυτές τις πληροφορίες και τις μεταδίδει στη Matlab. Έτσι, για παράδειγμα, δίδοντας εντολή μέσω Matlab να φτάσει το ρομπότ στον φυγόκεντρο, το VREP έχοντας αποθηκεύσει τη θέση και τον προσανατολισμό του μηχανήματος, μπορεί να μεταδώσει αυτές τις πληροφορίες στη Matlab, όπου έχει γραφτεί κώδικας υπεύθυνος για τα υπόλοιπα. Επομένως, η παραμετροποίηση του προβλήματος είναι εύκολη.

Η ύπαρξη πολλαπλών ενδιάμεσων σημείων καθιστά απαραίτητη τον εκ νέου υπολογισμό της τροχιάς μεταξύ δύο διαφορετικών σημείων. Πιο συγκεκριμένα, η τροχιά υπολογίζεται κάθε φορά που το ρομπότ χρειάζεται να μετακινηθεί μεταξύ δύο σημείων A και B. Η Matlab ζητά από το VREP τη θέση και τον προσανατολισμό του σημείου A, που είναι η αρχική τρέχουσα θέση P_o του τελικού σημείου δράσης, καθώς και τη θέση και προσανατολισμό του σημείου B, η οποία είναι η τελική επιθυμητή θέση P_f που το τελικό σημείο δράσης πρέπει να φτάσει. Αφού το ρομπότ μετακινηθεί από το A στο B, τότε η νέα θέση A' είναι βασικά η θέση B της προηγούμενης τροχιάς. Προκειμένου το ρομπότ να ξεκινήσει μια νέα κίνηση μεταξύ των A' και του νέου σημείου Γ, πρέπει να υπολογιστεί εκ νέου μια τροχιά με τις ανανεωμένες θέσεις. Η τροχιά ακολουθείται από το κάθε ρομπότ σύμφωνα με προγραμματισμό της αντίστροφης κινηματικής του, ενώ η θέση του τελικού σημείου δράσης ενημερώνεται στο VREP σε κάθε βήμα dt .

Μεταξύ άλλων παραμέτρων που μπορούν να προσαρμοστούν από τον ίδιο τον χρήστη είναι η ανάλυση των αποτελεσμάτων και η ομαλότητα των κινήσεων του ρομπότ. Είναι προφανές ότι όσο μικρότερο είναι το χρονικό βήμα dt , τόσο πιο ακριβής και ομαλή είναι η κίνηση του ρομπότ, αφού ο αριθμός παρεμβολής είναι υψηλότερος και υπολογίζονται περισσότερα σημεία της τροχιάς.

2.2 Πειραματικά πρωτόκολλα

Ένα πρωτόκολλο πειράματος περιγράφει τις απαραίτητες ενέργειες για ένα πείραμα που θα διεξαχθεί, από την αρχή μέχρι το τέλος του. Παραδείγματα πειραματικών πρωτοκόλλων παρέχονται παρακάτω για δύο πειράματα, τα οποία εξαρτώνται το ένα από το άλλο, αφού το Πείραμα 02 χρειάζεται υλικό από το Πείραμα 01.



Εικόνα 4: Παραδείγματα πειραματικών πρωτοκόλλων

2.3 Διεπαφή χρήστη-ρομπότ

Η διευκόλυνση της επικοινωνίας μεταξύ του χρήστη (ερευνητή) και του περιβάλλοντος προσομοίωσης έχει μεγάλη σημασία, καθώς η πλατφόρμα πρέπει να είναι προσβάσιμη σε ανθρώπους που δεν έχουν βαθιά γνώση ρομποτικής. Ο στόχος είναι απλά ο χρήστης να είναι σε θέση να επικοινωνήσει στο ρομποτικό σύστημα ένα πρωτόκολλο πειράματος όπως παρουσιάστηκε παραπάνω, με την ελάχιστη δυνατή προσπάθεια. Για αυτό το σκοπό σκόπιμη κρίνεται η δημιουργία μιας διεπιφάνειας φιλικής προς τον χρήστη.

Με την έναρξη των προγραμμάτων `main_SCARA.m` και `main_STAUBLI.m`, τα οποία είναι τα δύο προγράμματα Matlab υπεύθυνα για όλα όσα συμβαίνουν σε κάθε εργαστήριο, ο χρήστης καλείται να εισάγει σταθμούς εργασίας στο κύτταρο:

Input working station:

Σε αυτό το σημείο, ο χρήστης μπορεί να εισάγει το όνομα των σταθμών εργασίας - εργαστηριακές μηχανές - που περιλαμβάνονται στο πείραμα και με τη σειρά που ο χρήστης επιθυμεί να χρησιμοποιηθεί κάθε μηχανή, μαζί με το χρόνο που ο χρήστης επιθυμεί για το κάθε δείγμα να παραμένει σε κάθε μηχανή. Κάθε μηχανή μπορεί να χρησιμοποιηθεί περισσότερες από μία φορές, εάν το πείραμα απαιτεί την επίσκεψη συγκεκριμένου σταθμού εργασίας πολλαπλές φορές. Αφού συμπεριληφθούν όλες οι μηχανές και οι αντίστοιχοι χρόνοι με τη σωστή σειρά, ο χρήστης μπορεί να πληκτρολογήσει `stop` για να υποδείξει ότι το πρωτόκολλο πειράματος είναι πλήρες και ότι όλος ο απαραίτητος εξοπλισμός έχει ήδη αναφερθεί.

Για τις ανάγκες της τρέχουσας μελέτης, οι χρόνοι δεν έχουν ληφθεί υπόψη, αφού μπορούν να φτάσουν ακόμα και σε δύο ημέρες αναμονής σε μια συγκεκριμένη μηχανή. Έτσι, αυτή η διαδικασία αντιπροσωπεύεται από τη διακοπή των κινήσεων βραχίονα για μερικά δευτερόλεπτα.

Αφού εισαχθεί το πρωτόκολλο στην πλατφόρμα, το πρόγραμμα ελέγχει αν το ρομπότ βρίσκεται στην αρχική του θέση, η οποία είναι μια ασφαλής θέση για το ρομπότ να ξεκινήσει οποιοδήποτε πείραμα. Εάν υπάρχει, ο χρήστης θα σας ζητήσει την ειδοποίηση:

Robot is in Home Position-Ready to start experiment

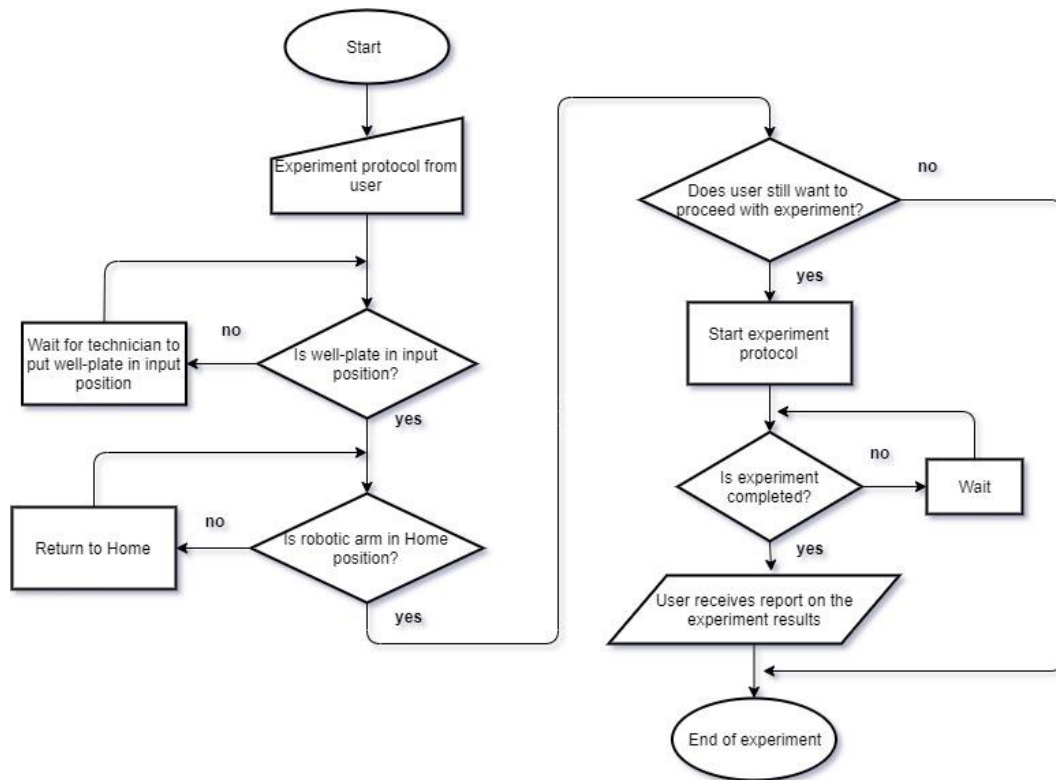
Διαφορετικά, το ρομπότ μετακινείται στην αρχική του θέση και στη συνέχεια ο χρήστης καλείται για τελευταία φορά αν επιθυμεί να προχωρήσει με το πείραμα. Η προεπιλεγμένη απάντηση είναι NAI.

Do you wish to continue to experiment? Y/N [Y]:

Εάν ο χρήστης πληκτρολογήσει N, τότε το πείραμα διακόπτεται. Εάν ο χρήστης πληκτρολογήσει Y, το πείραμα ξεκινά σύμφωνα με το πρωτόκολλό του.

Εάν ο χρήστης έχει κάποια γνώση σχετικά με τη ρομποτική, μπορεί επίσης να τροποποιήσει το χρόνο T και το βήμα dt που χρησιμοποιείται για τον προγραμματισμό της τροχιάς και την κίνηση των όπλων.

Παρακάτω παρέχεται ένα διάγραμμα ροής, το οποίο αντιπροσωπεύει την αλληλεπίδραση του χρήστη με την πλατφόρμα.

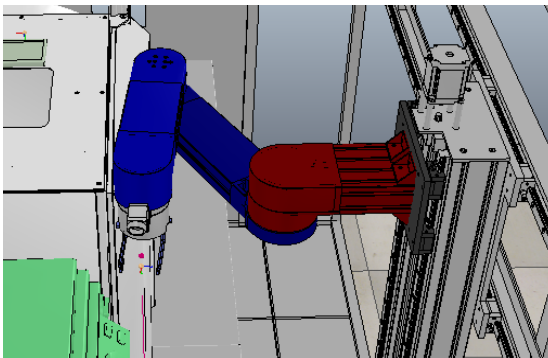


Εικόνα 5: Διαγραμματική απεικόνιση διεπαφής χρήστη- περιβάλλοντος εργασίας

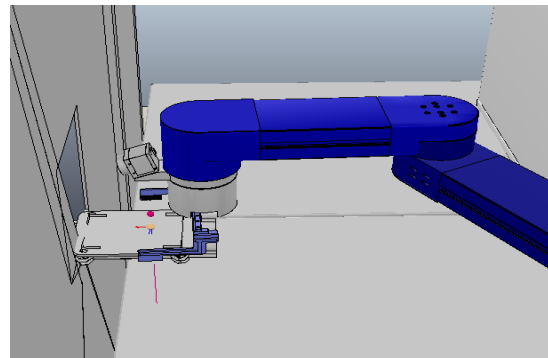
2.4 Προσομοίωση πειραμάτων με τους ρομποτικούς βραχίονες SCARA και STAUBLI

Μετά την έναρξη του πειράματος, το ρομπότ αποκτά διαφορετικές θέσεις και διαμορφώσεις στο διάστημα, οι οποίες εξαρτώνται από τον τελικό του προορισμό και τους περιορισμούς που επιβάλλονται. Παρακάτω παρουσιάζεται μια σειρά εικόνων που δείχνουν αυτές τις πληροφορίες τόσο για το ρομπότ SCARA όσο και για το STAUBLI.

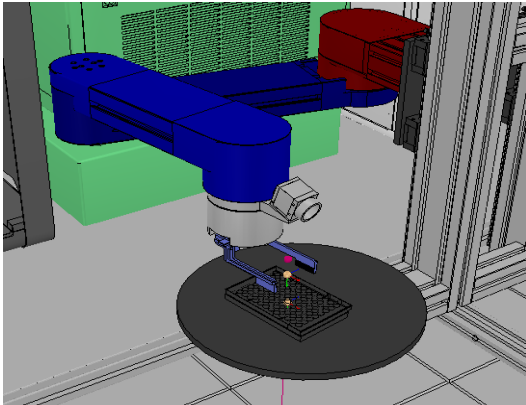
2.4.1 SCARA



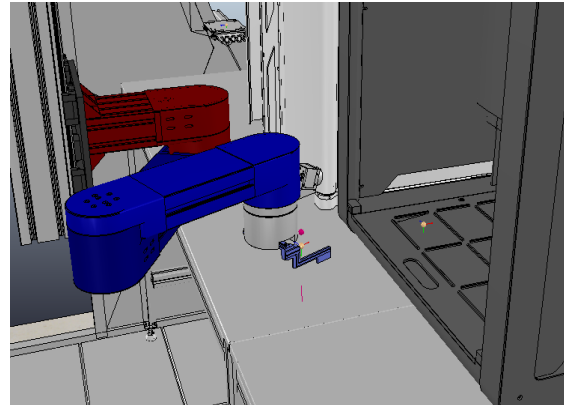
Εικόνα 6: Αρχική θέση του ρομπότ SCARA



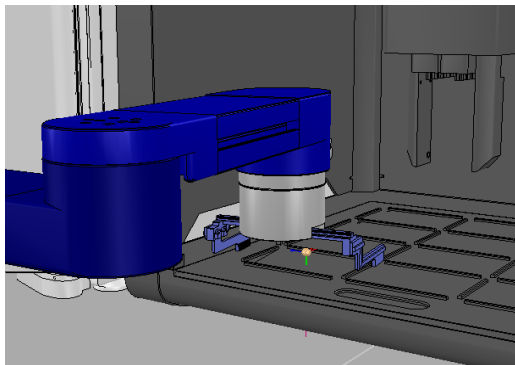
Εικόνα 7: Το ρομπότ SCARA παίρνει το μικροπλακίδιο από τον τεχνικό του εργαστηρίου (θέση input)



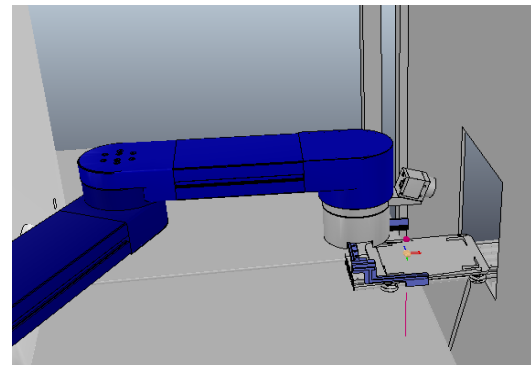
Εικόνα 8: Μετακίνηση ρομπότ SCARA πάνω από μικροπλακίδιο σε περιστρεφόμενη



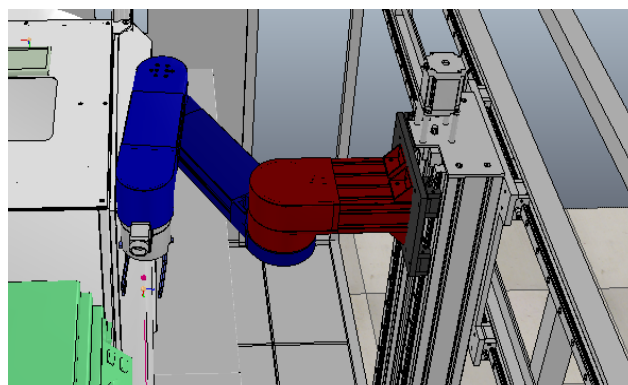
Εικόνα 9: Ασφαλής απόσταση SCARA από εξοπλισμό εργαστηρίου



Εικόνα 10: Η αρπάγη του SCARA είναι έτοιμη να αφήσει/παραλάβει πλακίδιο

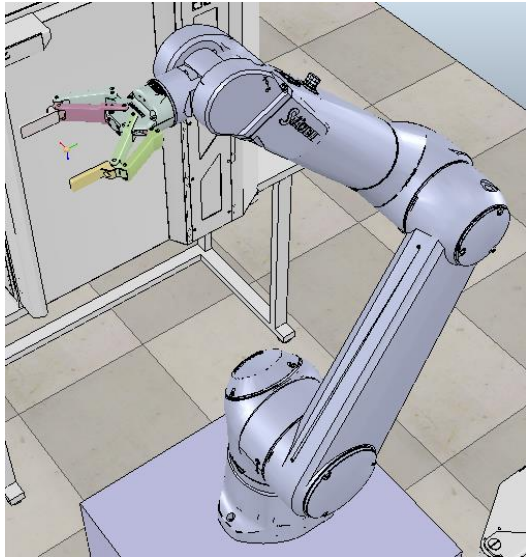


Εικόνα 11: Ρομπότ SCARA επιστρέφει μικροπλακίδιο σε τεχνικό εργαστήριο (θέση output)

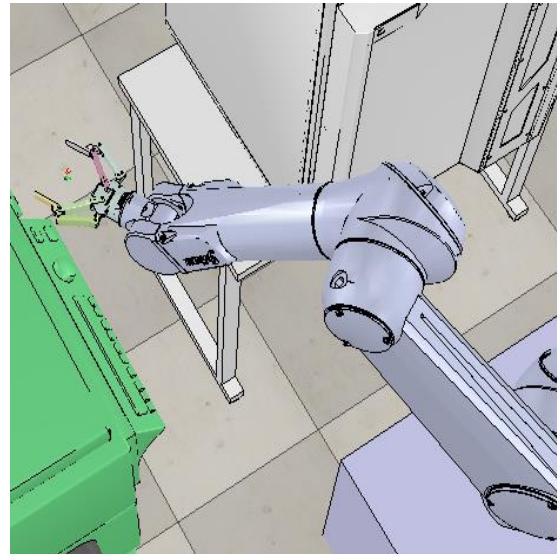


Εικόνα 12: Επιστροφή SCARA σε αρχική θέση

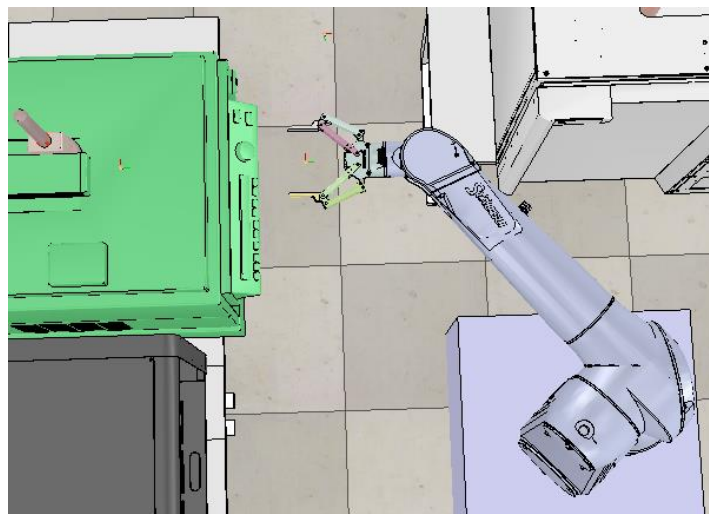
2.4.2 STAUBLI TX2-90XL



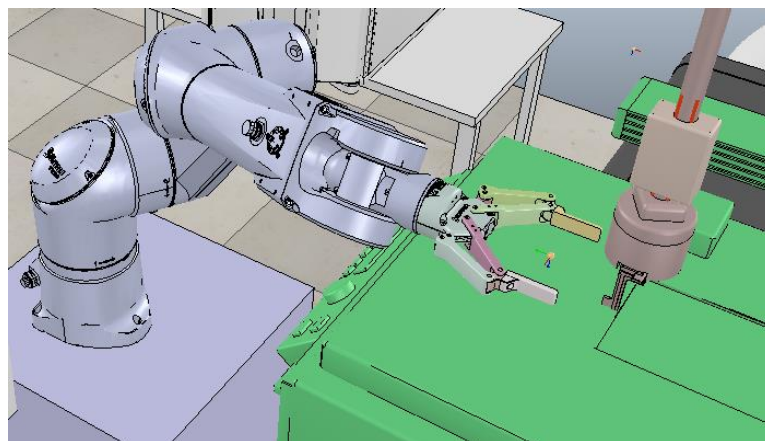
Εικόνα 13: Αρχική θέση του ρομπότ STAUBLI



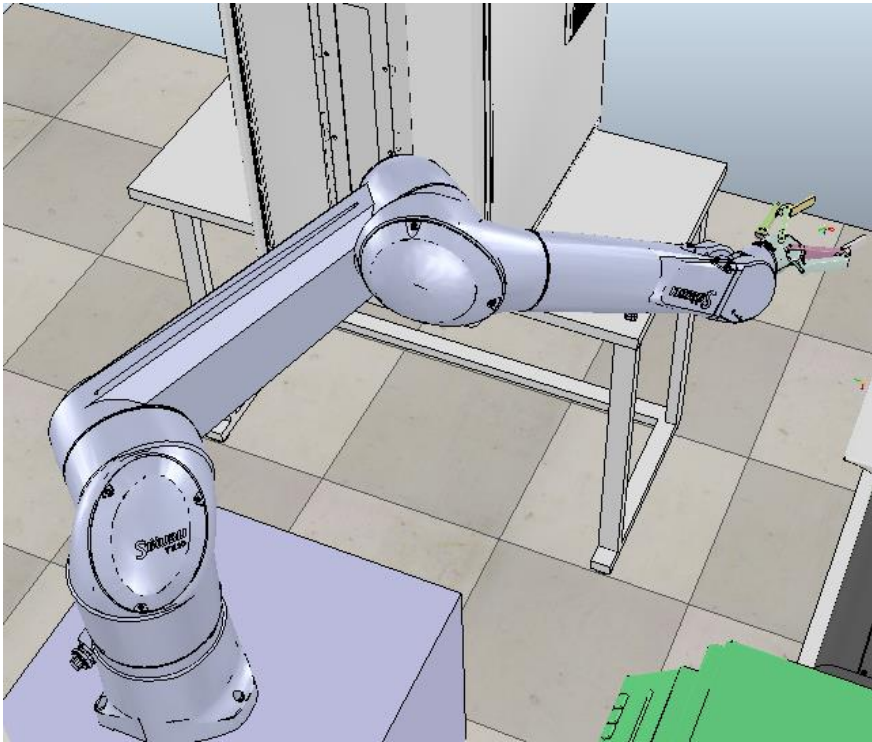
Εικόνα 14: Το ρομπότ STAUBLI παίρνει το μικροπλακίδιο από τον τεχνικό του εργαστηρίου (θέση input)



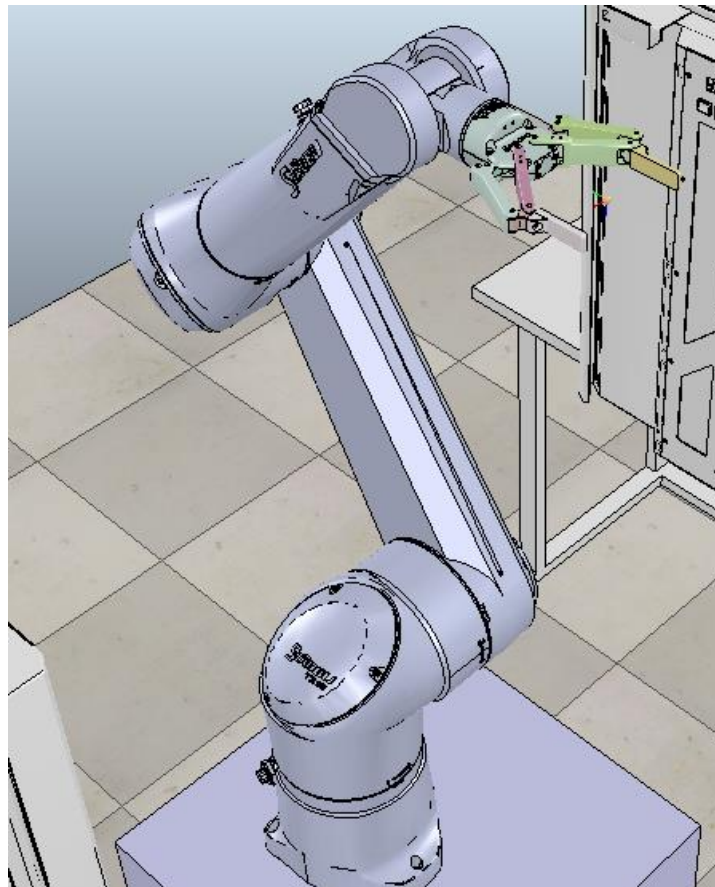
Εικόνα 15: Ασφαλής απόσταση STAUBLI από εξοπλισμό εργαστηρίου



Εικόνα 16: Η αρπάγη του STAUBLI είναι έτοιμη να αφήσει/παραλάβει πλακίδιο



Εικόνα 17: Το ρομπότ STAUPLI επιστρέφει το μικροπλακίδιο στον τεχνικό του εργαστηρίου (θέση output)



Εικόνα 18: Επιστροφή STAUPLI σε αρχική θέση

3

ΑΠΟΤΕΛΕΣΜΑΤΑ

3.1 Σχολιασμός

Τα παρακάτω διαγράμματα είναι τα αποτελέσματα των προσομοιώσεων που έγιναν σύμφωνα με τα πρωτόκολλα πειράματος που αναφέρθηκαν προηγουμένως. Μόνο οι πιο βασικές κινήσεις κάθε ρομπότ περιλαμβάνονται σε αυτά τα διαγράμματα για λόγους συντομίας, ωστόσο οι συμπεριφορές των ρομπότ δεν αλλάζουν σημαντικά μεταξύ των κινήσεων. Είναι σημαντικό να σημειωθεί και να δοθεί προσοχή στην κλίμακα του άξονα κάθε διαγράμματος. Συγκεκριμένα, σε ορισμένες περιπτώσεις τα γραφήματα μπορεί να φαίνεται ότι αποκλίνουν ή ότι παρουσιάζουν σημαντικά σφάλματα, αλλά αυτό οφείλεται συνήθως στην κλίμακα του άξονα του οποίου το μέγεθος μπορεί να αντιπροσωπεύει αλλαγές στο 10^{-3} του αντίστοιχου μεγέθους. Τα αποτελέσματα του SCARA και του STAUBLI παρουσιάζονται χωριστά.

Για το SCARA αξίζει να σημειωθεί ότι η 5η άρθρωση, δηλαδή η άρθρωση της αρπάγης, η οποία την περιστρέφει, έχει οριστεί ως 0 για όλες τις προσομοιώσεις που υπάρχουν. Αυτό οφείλεται στο γεγονός ότι, δεδομένου ότι όλα τα μηχανήματα είναι στη σειρά, δεν χρειάζεται να περιστρέφεται η λαβή. Αν αυτό είναι απαραίτητο, τότε η αντίστοιχη άρθρωση μπορεί να «ενεργοποιηθεί» θέτοντας τα ανώτερα και κατώτερα όριά της στο πρόγραμμα SCARAp1atetraj.m. Η ίδια προσέγγιση μπορεί επίσης να χρησιμοποιηθεί για το ρομπότ STAUBLI.

Στα αποτελέσματα των προσομοιώσεων που παρατίθενται, όλες οι αρθρώσεις του ρομπότ είναι «ενεργοποιημένες» και λειτουργούν σύμφωνα με τα αντίστοιχα όριά τους, όπως καθορίζονται από την εταιρεία και όπως αυτά αναφέρονται σε προηγούμενα κεφάλαια. Αν όμως το ρομπότ συμπεριφέρεται απροσδόκητα και όχι σύμφωνα με τον επιθυμητό τρόπο, με την έννοια ότι δεν κρατάει τα μικροπλακίδια παράλληλα προς το έδαφος, η 4η και η 6η άρθρωση μπορούν να τεθούν ως 0, δηλαδή να μην πραγματοποιούν περιστροφικές κινήσεις. Η τέταρτη άρθρωση ελέγχει την περιστροφή του αντιβραχίου, ενώ η έκτη ελέγχει την περιστροφή της φλάντζας του εργαλείου. Κρατώντας αυτά τα δύο ακίνητα, τότε το πρόβλημα μπορεί να αντιμετωπιστεί ανάλογα.

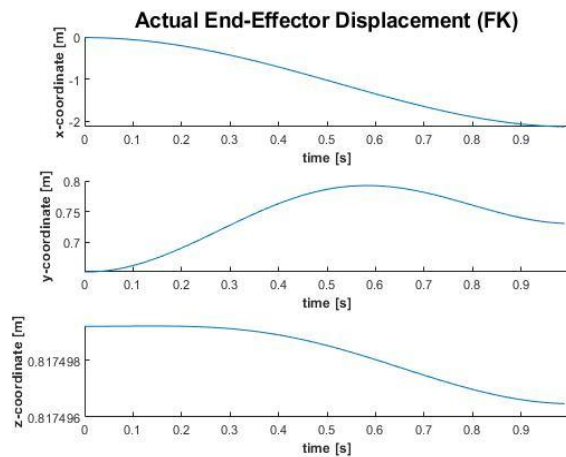
Συνολικά, τα προκύπτοντα γραφήματα είναι πολύ ικανοποιητικά, δείχνοντας ότι οι χρησιμοποιούμενες μέθοδοι και οι αλγόριθμοι πέτυχαν τον αρχικό στόχο, που ήταν ο έλεγχος των ρομποτικών βραχιόνων, σύμφωνα όχι μόνο με τις δικές τους αλλά και με αυτές του περιβάλλοντός τους. Πιο συγκεκριμένα:

- ✓ Οι αρθρώσεις των ρομπότ παραμένουν πάντοτε εντός των προκαθορισμένων ορίων τους και δεν τα υπερβαίνουν, όπως αντιπροσωπεύουν τα διαγράμματα των γωνιών των αρθρώσεων «Joint angles»
- ✓ Οι ταχύτητες έχουν την αναμενόμενη καμπύλη και στις δύο περιπτώσεις της προσομοίωσης.
- ✓ Το σφάλμα θέσης εξαλείφεται στις περισσότερες περιπτώσεις, εκτός από την κίνηση Home-Plate του SCARA. Αυτό πιθανότατα συμβαίνει επειδή η πρώτη άρθρωση του SCARA, που ευθύνεται για την κατά μήκος μετακίνηση του ρομπότ στο εργαστήριο, είναι ανενεργή. Ταυτόχρονα, τα σημεία που τροφοδοτούνται στον ρομποτικό βραχίονα πιθανώς να μην είναι πλήρως γραμμικά, γεγονός που καθιστά πιο δύσκολο το να τα ακολουθήσει ο βραχίονας. Αυτός είναι και ο λόγος για τον οποίο παρατηρούνται σφάλματα, αλλά δεν είναι αρκετά μεγάλα για να διαταράξουν το πείραμα και να επηρεάσουν την ακρίβειά του.

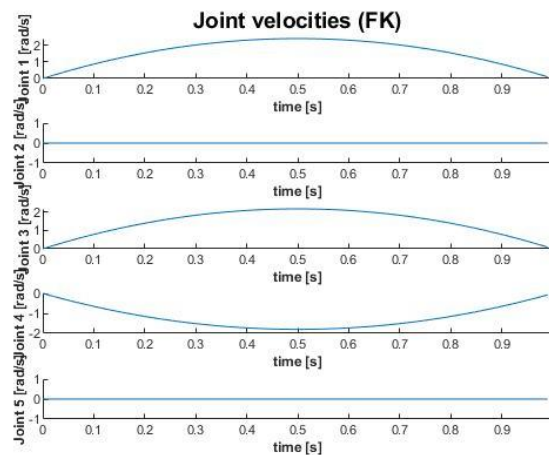
Τα διαγράμματα έχουν ληφθεί για τιμές $T=1$ και $dt=0,01$.

3.1.1 SCARA

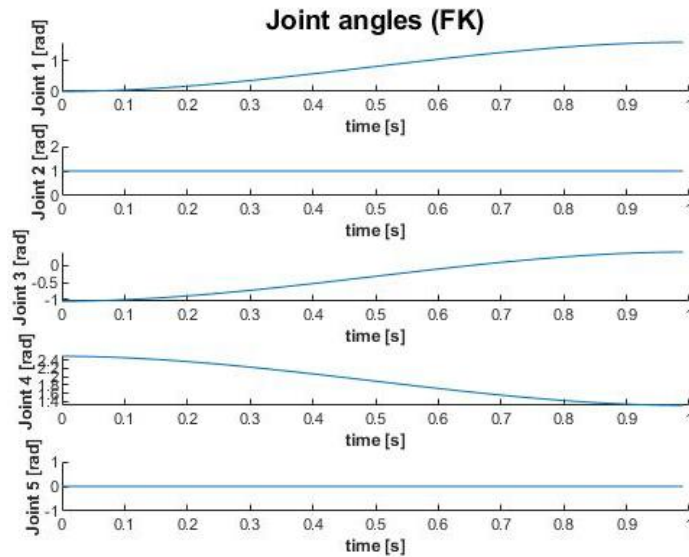
- A. Από Αρχική θέση σε Ασφαλή θέση πριν από θέση Input μέσω EK (Ευθείας Κινηματικής)



Διάγραμμα 34 : Θέση ΤΣΔ του SCARA με EK- Αρχική σε Ασφαλή θέση

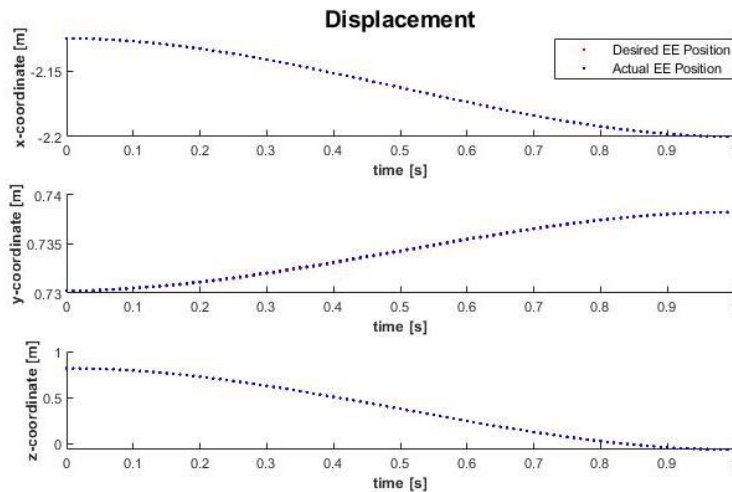


Διάγραμμα 35: Γωνιακές ταχύτητες αρθρώσεων του SCARA με EK- Αρχική σε Ασφαλή θέση

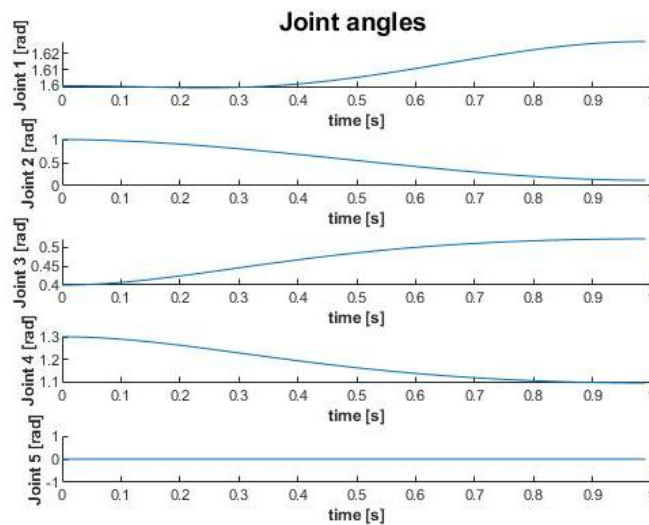


Διάγραμμα 36: Γωνίες αρθρώσεων του SCARA με EK- Αρχική σε Ασφαλή θέση

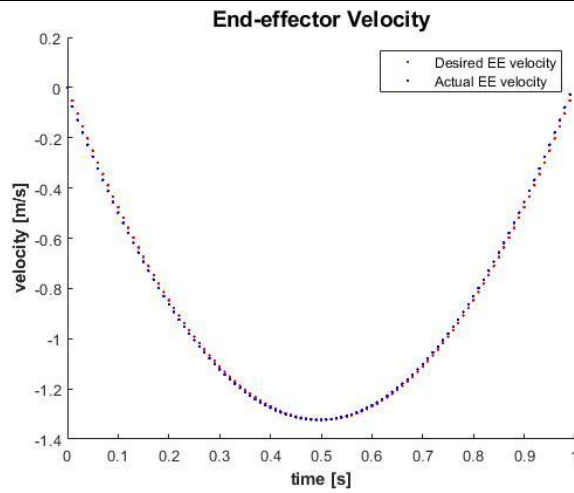
B. Από **Ασφαλή** θέση πριν από θέση **Input** σε θέση **Input** μέσω AK (αντίστροφης κινηματικής)



Διάγραμμα 37: Επιθυμητή vs Πραγματική θέση ΤΣΔ του SCARA με AK- Ασφαλής σε θέση Input

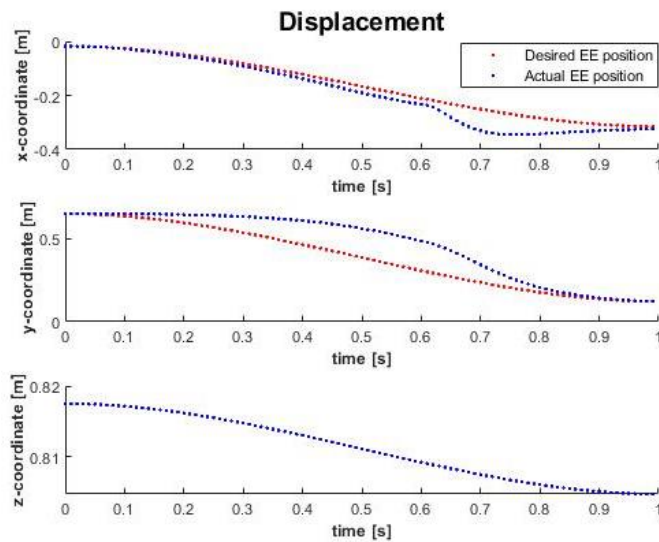


Διάγραμμα 38: Γωνίες αρθρώσεων του SCARA με AK- Ασφαλής σε θέση Input

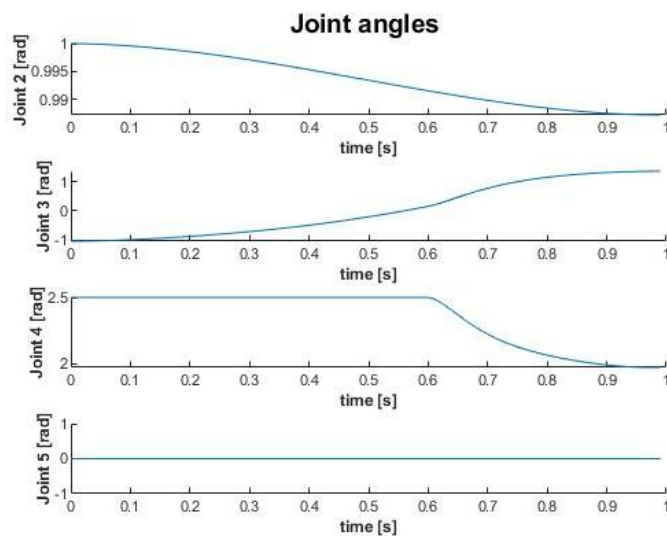


Διάγραμμα 39: Επιθυμητή vs Πραγματική ταχύτητα ΤΣΔ του SCARA με ΑΚ- Ασφαλής σε θέση Input

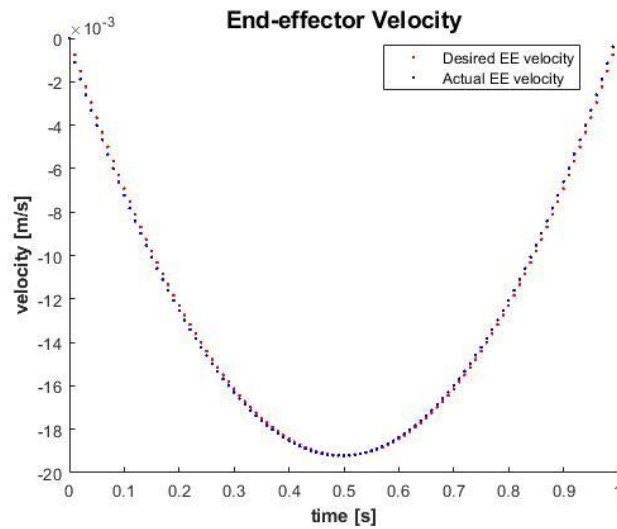
C. Από Αρχική θέση σε Ασφαλή θέση πάνω από πλακίδιο σε περιστρεφόμενη βάση με ΑΚ



Διάγραμμα 40: Επιθυμητή vs Πραγματική θέση ΤΣΔ του SCARA με ΑΚ- Αρχική σε Ασφαλή θέση

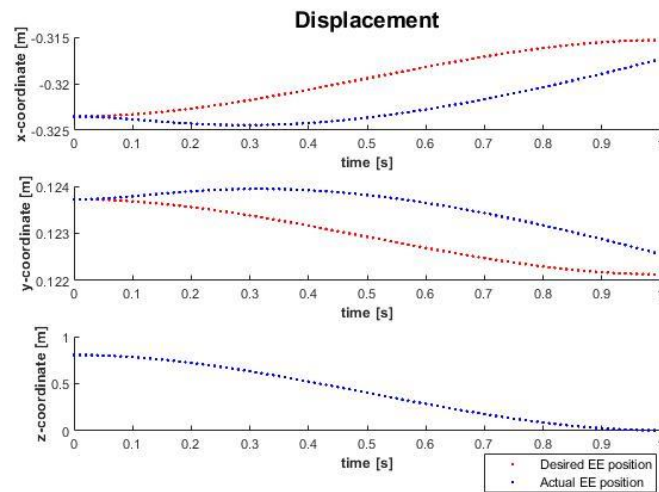


Διάγραμμα 41: Γωνίες αρθρώσεων του SCARA με ΑΚ- Αρχική σε Ασφαλή θέση

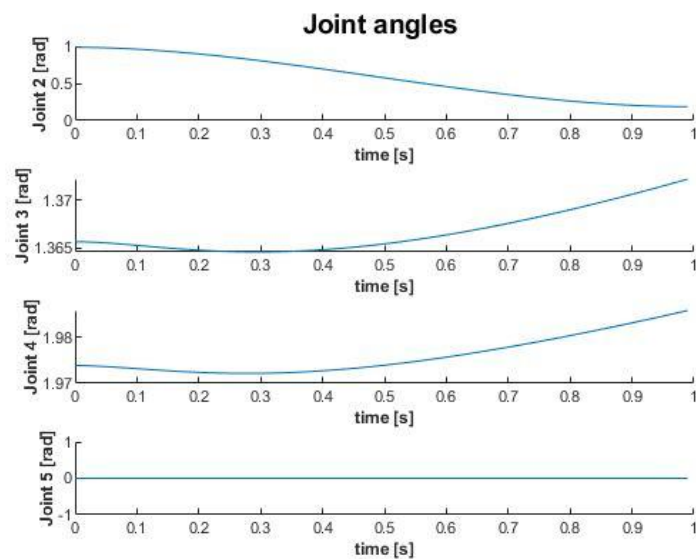


Διάγραμμα 42: Ταχύτητα ΤΣΔ του SCARA με ΑΚ- Αρχική σε Ασφαλή θέση

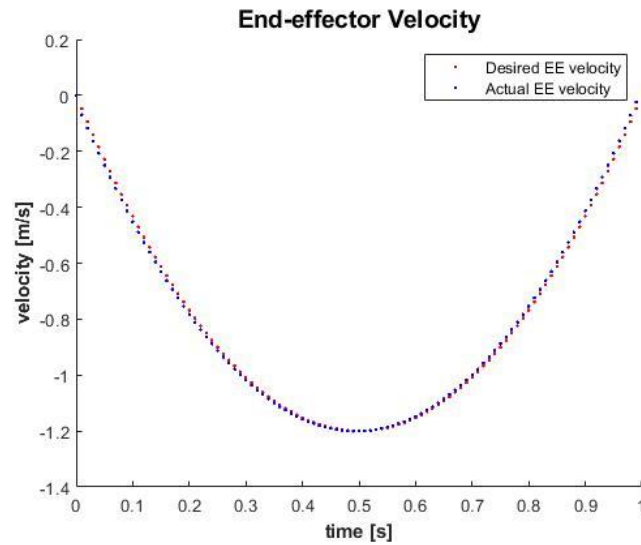
D. Από Ασφαλή θέση πάνω από πλακίδιο σε Πλακίδιο σε περιστρεφόμενη βάση με ΑΚ



Διάγραμμα 43: Επιθυμητή vs Πραγματική θέση ΤΣΔ του SCARA με ΑΚ- Ασφαλής θέση σε Πλακίδιο

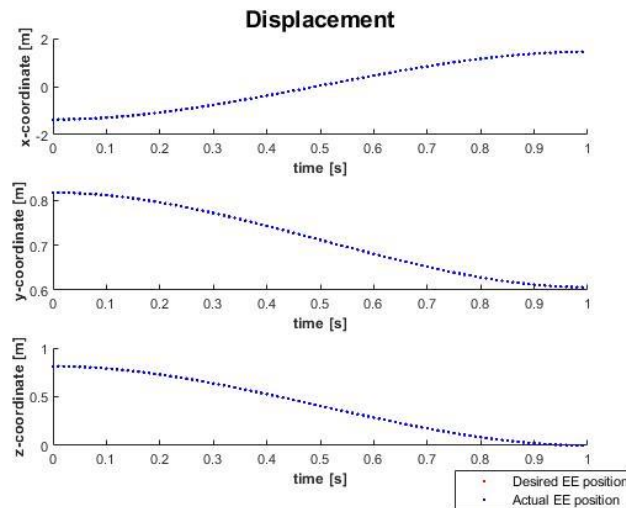


Διάγραμμα 44: Γωνίες αρθρώσεων του SCARA με ΑΚ- Ασφαλής θέση σε Πλακίδιο

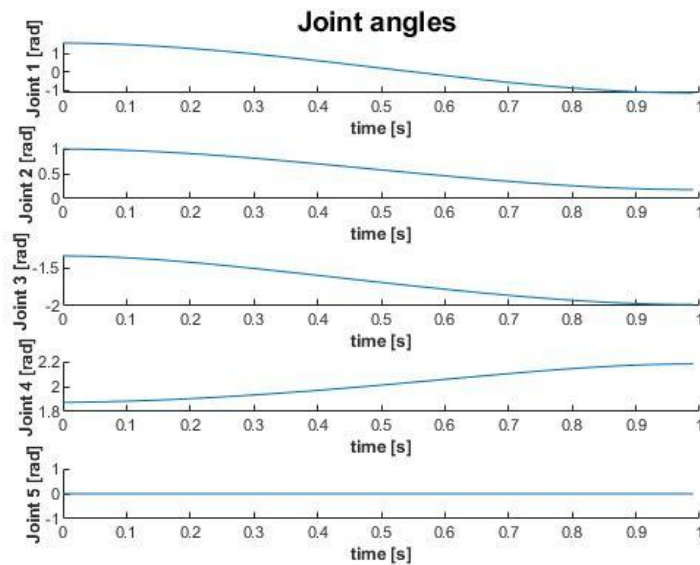


Διάγραμμα 45: Επιθυμητή vs Πραγματική ταχύτητα ΤΣΔ του SCARA με ΑΚ- Ασφαλής θέση σε Πλακίδιο

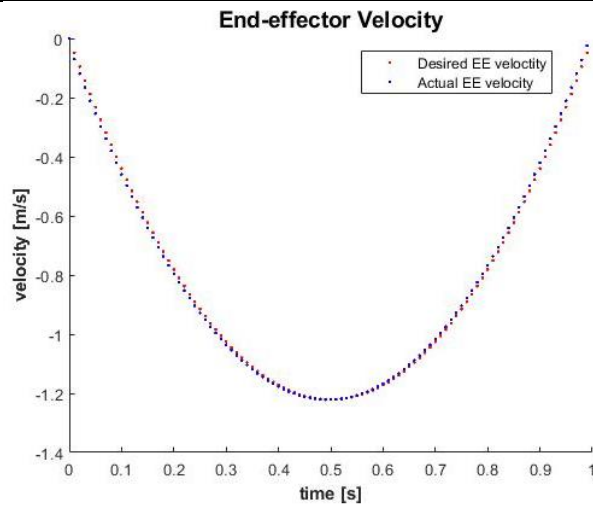
Ε. Από Μηχάνημα 1 σε Μηχάνημα 2 μέσω ΑΚ



Διάγραμμα 46: Επιθυμητή vs Πραγματική θέση ΤΣΔ του SCARA με ΑΚ – Μηχάνημα 1 σε Μηχάνημα 2

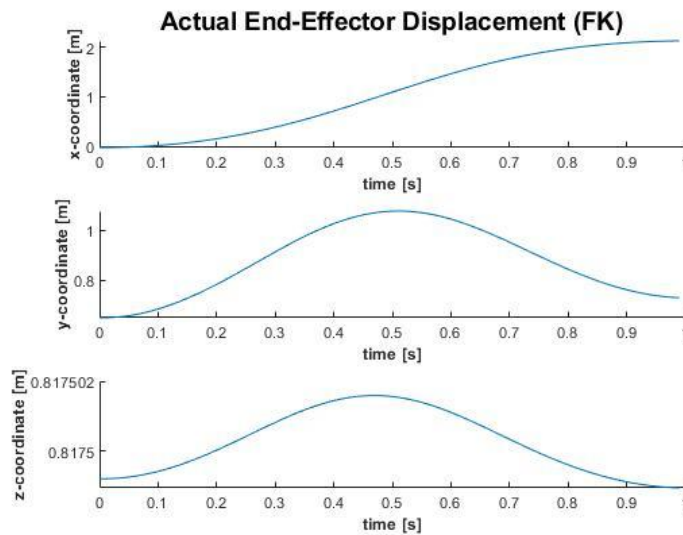


Διάγραμμα 47: Γωνίες αρθρώσεων του SCARA με ΑΚ – Μηχάνημα 1 σε Μηχάνημα 2

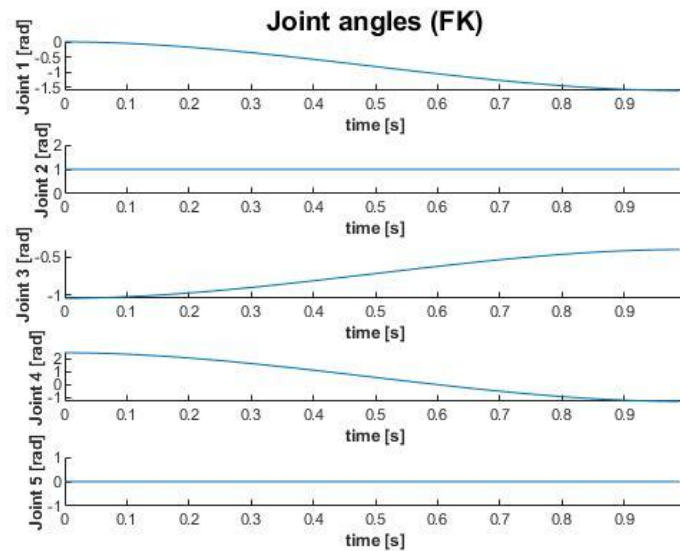


Διάγραμμα 48: Επιθυμητή vs Πραγματική ταχύτητα ΤΣΔ του SCARA με ΑΚ – Μηχάνημα 1 σε Μηχάνημα 2

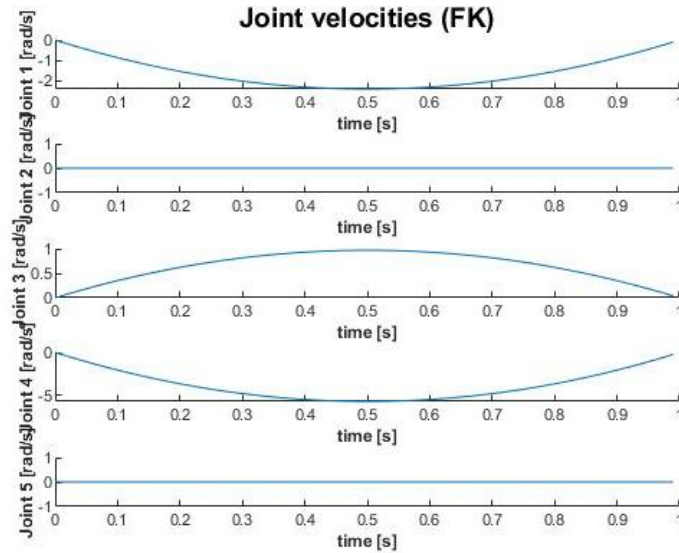
Φ. Από Αρχική θέση σε Ασφαλή θέση πριν τη θέση Output μέσω ΕΚ



Διάγραμμα 49: Θέση ΤΣΔ του SCARA με ΕΚ- Αρχική σε Ασφαλή θέση

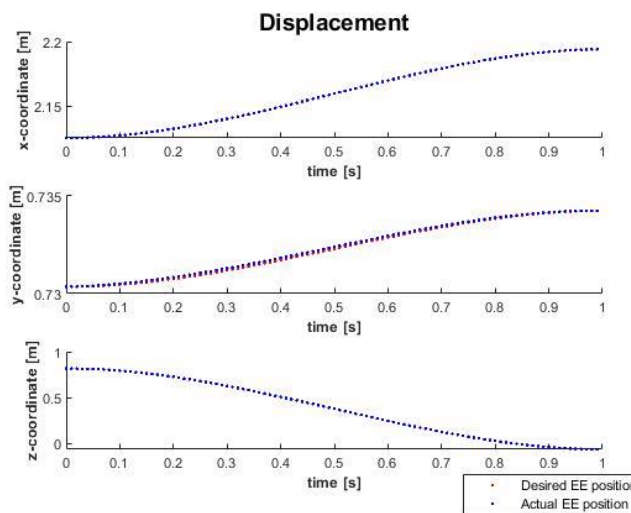


Διάγραμμα 50: Γωνίες αρθρώσεων SCARA με ΕΚ- Αρχική σε Ασφαλή θέση

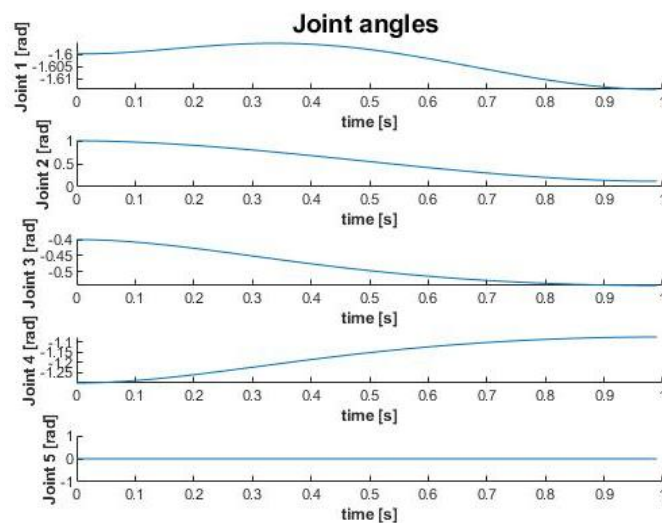


Διάγραμμα 51: Γωνιακές ταχύτητες αρθρώσεων του SCARA με EK- Αρχική σε Ασφαλή θέση

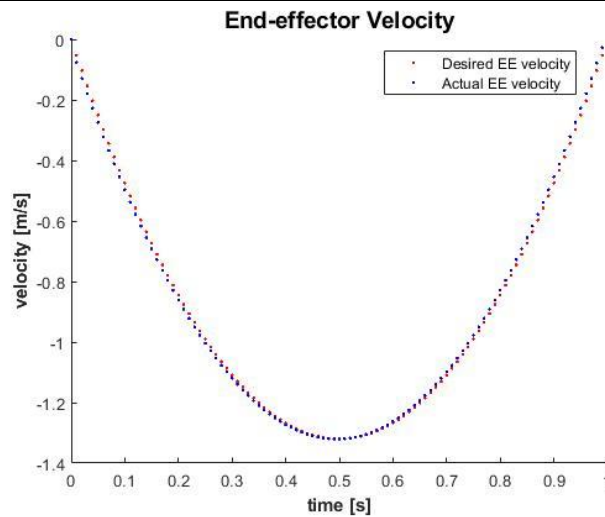
G. Από Ασφαλή θέση πριν θέση Output σε θέση Output μέσω AK



Διάγραμμα 52: Επιθυμητή vs Πραγματική θέση ΤΣΔ του SCARA με AK – Ασφαλής σε θέση Output



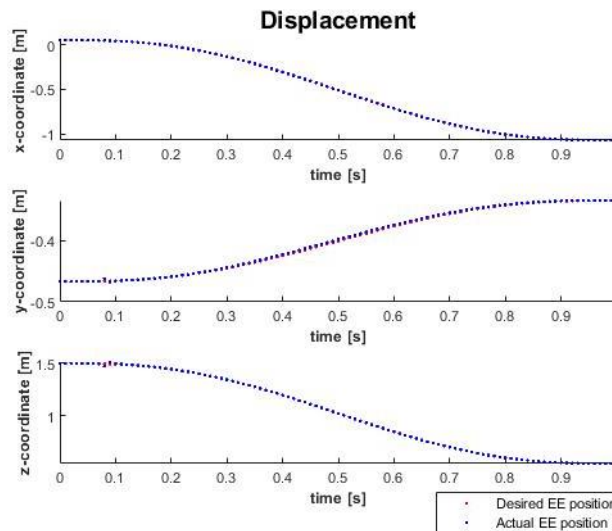
Διάγραμμα 53: Γωνίες αρθρώσεων SCARA με AK- Ασφαλής σε θέση Output



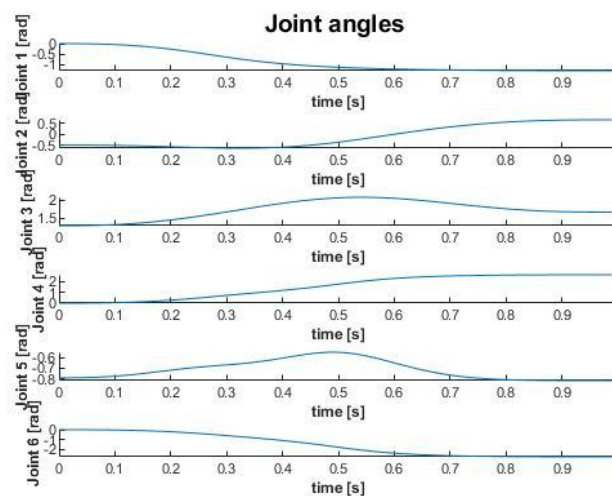
Διάγραμμα 54: Επιθυμητή vs Πραγματική ταχύτητα ΤΣΔ του SCARA με ΑΚ – Ασφαλής σε θέση Output

3.1.2 STAUBLI TX2-90XL

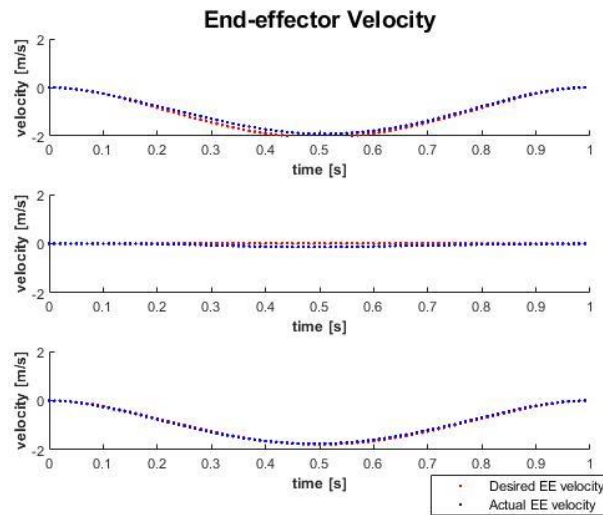
A. Από Αρχική θέση σε θέση Input μέσω ΑΚ



Διάγραμμα 55: Επιθυμητή vs Πραγματική θέση ΤΣΔ του STAUBLI με ΑΚ- Αρχική σε θέση Input

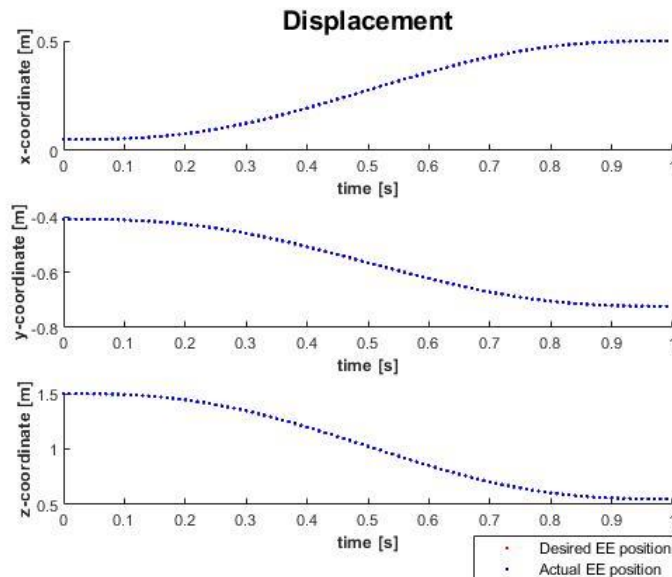


Διάγραμμα 56: Γωνίες αρθρώσεων του STAUBLI με ΑΚ - Αρχική σε θέση Input

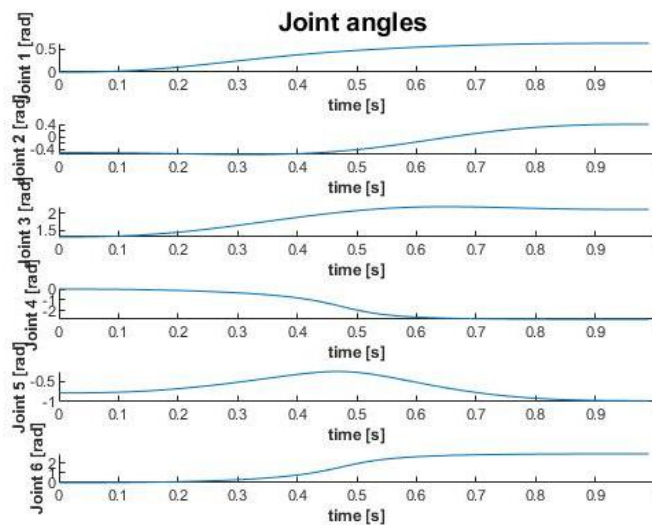


Διάγραμμα 57: Επιθυμητή vs Πραγματική ταχύτητα ΤΣΔ του STAUBLI με ΑΚ- Αρχική σε θέση Input

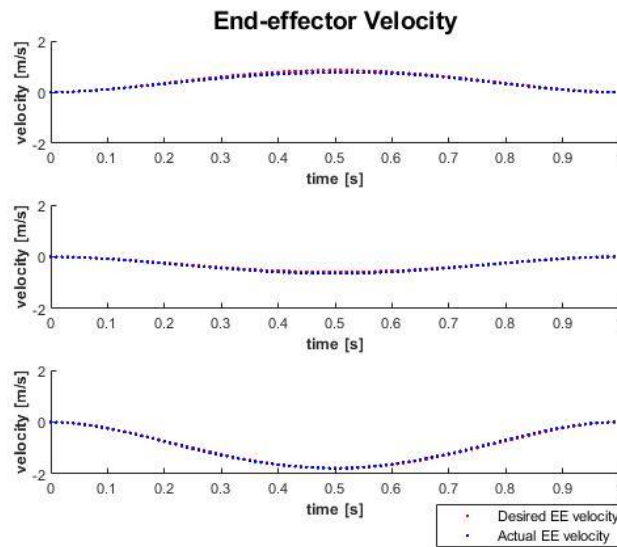
B. Από Αρχική θέση σε Μηχάνημα 1 με ΑΚ



Διάγραμμα 58: Επιθυμητή vs Πραγματική θέση ΤΣΔ του STAUBLI με ΑΚ – Ασφαλής θέση σε Μηχάνημα 1

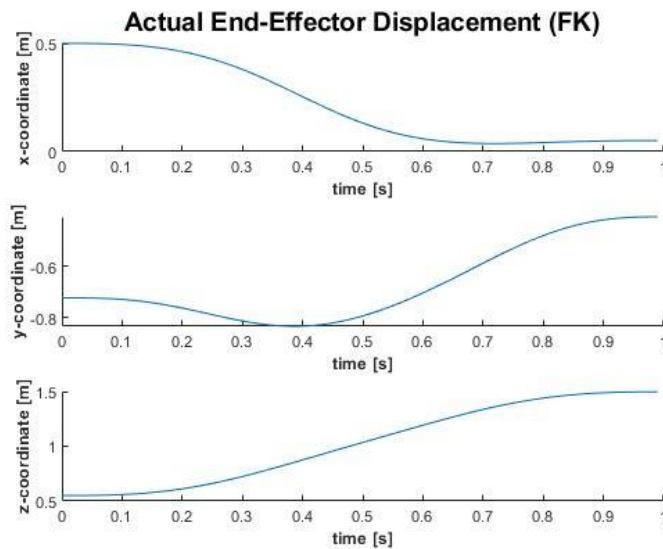


Διάγραμμα 59: Γωνίες αρθρώσεων του STAUBLI με ΑΚ – Ασφαλής θέση σε Μηχάνημα 1

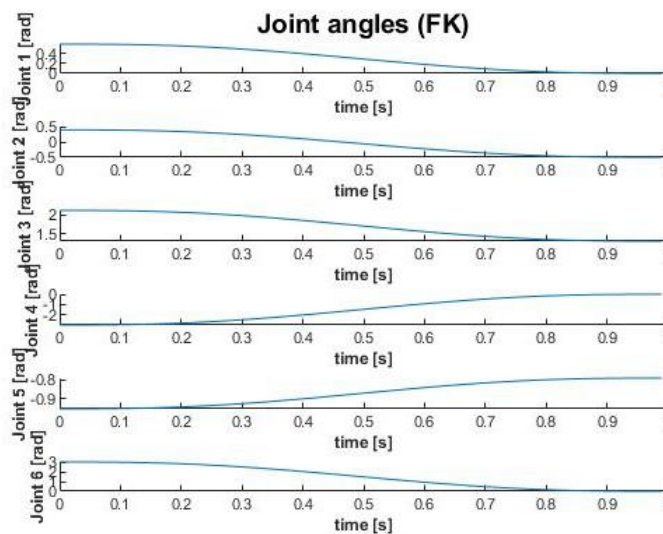


Διάγραμμα 60: Επιθυμητή vs Πραγματική ταχύτητα ΤΣΔ του STAUBLI με ΑΚ – Ασφαλής θέση σε Μηχάνημα 1

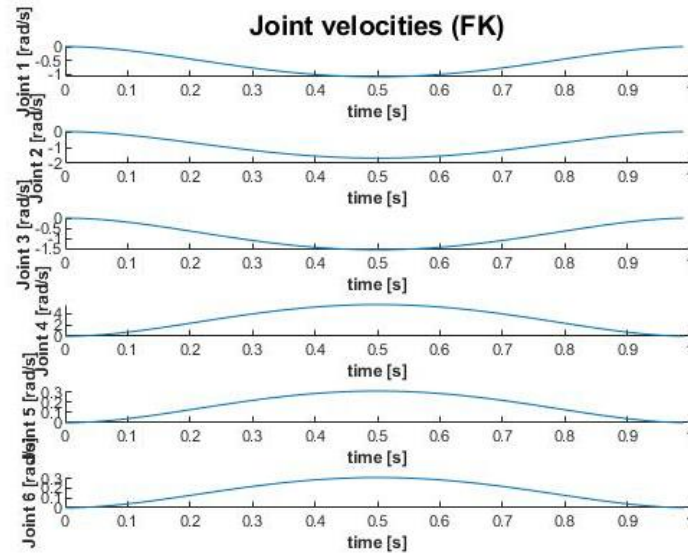
C. Μηχάνημα 1 σε Αρχική Θέση με ΕΚ



Διάγραμμα 61: Θέση ΤΣΔ του STAUBLI με ΕΚ- Μηχάνημα 1 σε Αρχική θέση

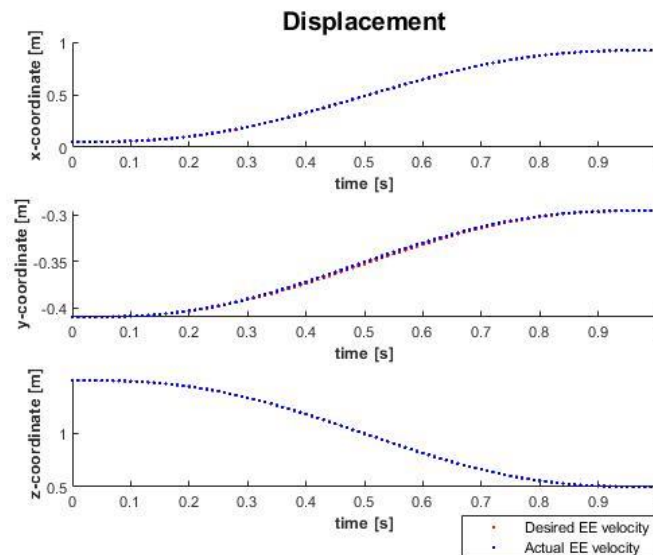


Διάγραμμα 62: Γωνίες αρθρώσεων του STAUBLI με ΕΚ- Μηχάνημα 1 σε Αρχική θέση

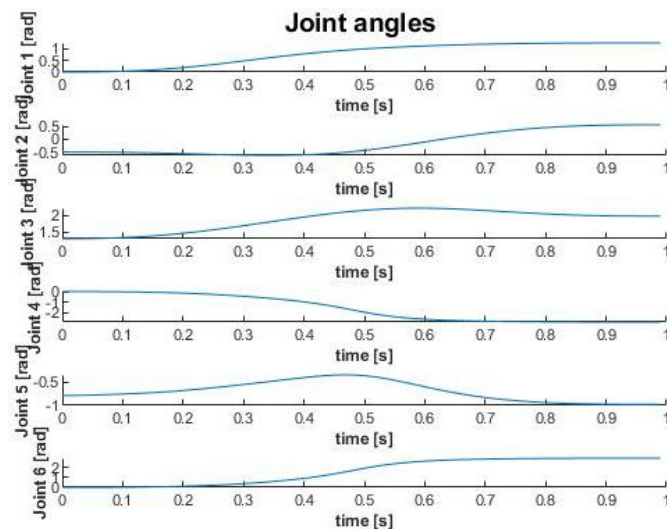


Διάγραμμα 63: Γωνιακές ταχύτητες αρθρώσεων του STAUBLI με EK- Μηχάνημα 1 σε Αρχική θέση

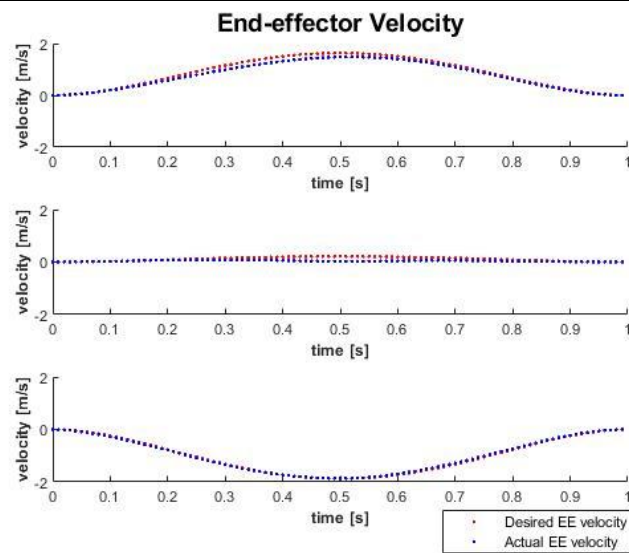
D. Από Αρχική θέση σε θέση Output με AK



Διάγραμμα 64: Επιθυμητή vs Πραγματική θέση ΤΣΔ του STAUBLI με AK – Αρχική σε θέση Output



Διάγραμμα 65: Γωνίες αρθρώσεων του STAUBLI με AK – Αρχική σε θέση Output



Διάγραμμα 66: Επιθυμητή vs Πραγματική ταχύτητα ΤΣΔ του STAUBLI με ΑΚ – Αρχική σε θέση Output

4

ΣΥΜΠΕΡΑΣΜΑΤΑ

4.1 Συνεισφορά

Στην παρούσα εργασία αναπτύχθηκε μια μεθοδολογία ανάπτυξης του μοντέλου ενός εργαστηριακού χώρου βιοτεχνολογίας σε περιβάλλον εικονικής πραγματικότητας. Η διαδικασία περιλάμβανε τόσο την εισαγωγή των 3D μοντέλων για την αναπαράσταση του φυσικού χώρου, όσο και τον προγραμματισμό τους ώστε τα ρομπότ να αποκτήσουν «ζωή» και να αλληλεπιδρούν με τα υπόλοιπα μέρη της σκηνής.

Η κύρια συμβολή αυτής της εργασίας είναι η ανάπτυξη μεθοδολογίας για τον κινηματικό έλεγχο δύο διαφορετικών ρομπότ και δύο διαφορετικών εργαστηριακών διατάξεων, τα οποία μπορούν να χρησιμοποιηθούν ως εναλλακτική λύση χαμηλού κόστους στον οπτικό έλεγχο ή στα ακριβά -υψηλής ακρίβειας- ρομπότ. Η εργασία αυτή μπορεί να αποτελέσει υπόβαθρο για την επέκταση ή ακόμα και την ανάπτυξη άλλων σχετικών μεθοδολογιών.

Συγκεκριμένα παρέχονται:

1. Μοντέλο ενός προσαρμοσμένου στις ανάγκες της εργασίας ρομποτικού βραχίονα τύπου SCARA με πλήρως ανεπτυγμένη κινηματική αλυσίδα μεταξύ των συνδέσμων.
2. Μοντέλο του ρομποτικού βραχίονα Stäubli TX2-90XL με πλήρως ανεπτυγμένη κινηματική αλυσίδα μεταξύ των συνδέσμων.
3. Μοντέλο πραγματικών διαστάσεων του χώρου του εργαστηρίου βιοτεχνολογίας.
4. Ευθεία και αντίστροφη κινηματική ανάλυση των ρομποτικών βραχιόνων.
5. Προσομοίωση ολοκληρωμένων πειραματικών πρωτοκόλλων στην πλατφόρμα VREP.

4.2 Πλεονεκτήματα περιβάλλοντος εικονικής πραγματικότητας

Ο συμβατικός προγραμματισμός εργασιών ενός ρομπότ, στηριζόταν ανέκαθεν στην εμπειρία του χειριστή, ο οποίος προγραμματίζε την τροχιά του ενώ βρισκόταν σε λειτουργία. Ο τρόπος αυτός εκτός από το ότι ήταν χρονοβόρος, εγκυμονούσε τον κίνδυνο του λάθους, θέτοντας σε κίνδυνο την ακεραιότητα του χειριστή, του βιομηχανικού εξοπλισμού καθώς και της εργασίας.

Στη σημερινή εποχή, νέοι μηχανικοί καλούνται να εκτελέσουν την διαδικασία του προγραμματισμού. Λόγω της εξοικείωσής τους με τις τεχνολογίες εικονικής πραγματικότητας, η χρήση της τελευταίας στην εργασία αυτή δίνει γρήγορα, αξιόπιστα και ασφαλή αποτελέσματα.

Όφελος υπάρχει προφανώς και από οικονομικής άποψης. Χρηματικοί πόροι εξοικονομούνται λόγω της μείωσης των απαιτούμενων εργατοωρών, των αποτυχημένων προσπαθειών καθώς και των ζημιών που προκαλούν οι συγκρούσεις. Επίσης, ένα τέτοιο σύστημα μπορεί να χρησιμοποιηθεί για την σωστή μελέτη τοποθέτησης πρόσθετου εξοπλισμού σε ένα ήδη υπάρχον περιβάλλον.

4.3 Προτάσεις για μελλοντική έρευνα

Η ανάπτυξη του εργαστηρίου και ο σχεδιασμός των τροχιών ήταν επιτυχημένα, αλλά υπάρχει ακόμα περιθώριο βελτίωσης.

Όσον αφορά στο εργαστηριακό περιβάλλον που έχει δημιουργηθεί:

- Τα σενάρια του πειράματος που δοκιμάστηκαν για τους σκοπούς της παρούσας εργασίας περιελάμβαναν μόνο 5 μηχανές - σταθμούς εργασίας μέσα στις εργαστηριακές διατάξεις. Αυτά τα μηχανήματα είναι τα πιο συνηθισμένα που μπορεί να υπάρξουν σε ένα εργαστήριο βιοτεχνολογίας και χρησιμοποιούνται συχνά για τη διεξαγωγή πειραμάτων. Μια πιθανή επέκταση θα μπορούσε να είναι η εισαγωγή πιο εξειδικευμένων μηχανών στις ίδιες εργαστηριακές εγκαταστάσεις για την πραγματοποίηση πειραμάτων.
- Στην παρούσα διπλωματική εργασία προσομοιώνεται ένα πείραμα σε κάθε τρέξιμο του προγράμματος, γεγονός που σημαίνει ότι ένα νέο πείραμα προβλέπεται να ξεκινήσει αμέσως μετά την ολοκλήρωση του προηγούμενου πειράματος και όχι παράλληλα με αυτό. Μελέτη αλγορίθμων σχετικά με τον προγραμματισμό του ευέλικτου συστήματος παραγωγής θα μπορούσε να οδηγήσει σε πραγματοποίηση πολλαπλών πειραμάτων στο εργαστήριο ταυτόχρονα. Ενσωματώνοντας συστήματα όρασης για την αναγνώριση των μηχανών και των μικροπλακιδίων που βρίσκονται στο εργαστήριο κάθε στιγμή, το ρομπότ θα μπορούσε να λάβει πολλαπλά πρωτόκολλα πειράματος και να τα ολοκληρώσει ταυτόχρονα. Με αυτόν τον τρόπο, η παραγωγικότητα στο κύτταρο μπορεί να αυξηθεί ριζικά.

Όσον αφορά τον έλεγχο των ρομποτικών βραχιόνων:

- Η έρευνα εστίασε στην κινηματική ανάλυση των ρομποτικών βραχιόνων, αγνοώντας εντελώς τη δυναμική τους. Μια δυναμική προσομοίωση θα μπορούσε να επιχειρηθεί για να αναλύσει τις ταλαντώσεις των ρομπότ ενώ αυτά βρίσκονται σε λειτουργία, καθώς και την επίδρασή τους στην ακρίβεια της τροχιάς.
- Μπορεί να εφαρμοστεί ένα ζωντανό σύστημα εντοπισμού με την προσθήκη κάμερας για την εξασφάλιση της ακρίβειας. Μια κάμερα πάνω στον βραχίονα θα μπορούσε να χρησιμοποιηθεί για την ευθυγράμμιση αυτού με τα σημεία εισόδου του κάθε μηχανήματος, καθώς και την θέση των μικροπλακιδίων με μεγαλύτερη ακρίβεια. Αυτές οι κάμερες μπορούν να χρησιμοποιηθούν για να διορθώσουν τα σφάλματα θέσης και να δώσουν ζωντανή ανατροφοδότηση.

- Τα πειραματικά αποτελέσματα από τον έλεγχο του ρομποτικού βραχίονα Stäubli TX2-90XL θα μπορούσαν να μεταφερθούν σε φυσικό επίπεδο με τις πληροφορίες που παρέχονται από το εικονικό περιβάλλον μέσω της γλώσσας V+. Τα αρχεία εξόδου Matlab-VREP που παρέχουν πληροφορίες σχετικά με τη θέση του τελικού τελεστή ή τις τιμές των γωνιών άρθρωσης του βραχίονα, μπορούν να περάσουν μέσω ενός controller V+ στο πραγματικό μοντέλο του Stäubli TX2-90XL.

5

ΒΙΒΛΙΟΓΡΑΦΙΑ

- [1] R. Pauwels, H. Azijn, M. P. de Béthune, C. Claeys, and K. Hertogs, “Automated techniques in biotechnology,” *Curr. Opin. Biotechnol.*, vol. 6, no. 1, pp. 111–117, 1995.
- [2] A. Sertkaya, H. H. Wong, A. Jessup, and T. Beleche, “Key cost drivers of pharmaceutical clinical trials in the United States,” *Clin. Trials*, vol. 13, no. 2, pp. 117–126, Apr. 2016.
- [3] L. Monostori, “Cyber-physical production systems: Roots, expectations and R&D challenges,” in *Procedia CIRP*, 2014, vol. 17, pp. 9–13.
- [4] L. Monostori *et al.*, “Cyber-physical systems in manufacturing,” *CIRP Ann.*, vol. 65, no. 2, pp. 621–641, 2016.
- [5] M. Smith, J., Kreutzer, S., Moeller, C., & Carlberg, “Industry 4.0. Study for the ITRE committee,” 2016.
- [6] N. Shariatzadeh, T. Lundholm, L. Lindberg, and G. Sivard, “Integration of Digital Factory with Smart Factory Based on Internet of Things,” in *Procedia CIRP*, 2016, vol. 50, pp. 512–517.
- [7] U. Bracht and T. Masurat, “The Digital Factory between vision and reality,” *Comput. Ind.*, vol. 56, no. 4, pp. 325–333, May 2005.
- [8] D. Mourtzis, N. Papakostas, D. Mavrikios, and S. Makris, “Det 2011,” no. November 2017, 2011.
- [9] V. Bottazzi and J. Fonseca, “Off-line Programming Industrial Robots Based in the Information Extracted From Neutral Files Generated by the Commercial CAD Tools,” *Ind. Robot. Program. Simul. Appl.*, 2006.
- [10] Coppelia Robotics, “V-REP User Manual.” [Online]. Available: <http://www.coppeliarobotics.com/helpFiles/index.html>.
- [11] Wikipedia, “SCARA.” [Online]. Available: <https://en.wikipedia.org/wiki/SCARA>. [Accessed: 08-Aug-2019].
- [12] Cyan-Tec, “When to use a SCARA Robot.” [Online]. Available: <https://cyan-tec.com/laser-systems/when-to-use-a-scara-robot>.
- [13] Γ. Χ. Βοσνιάκος, *Συστήματα Κατεργασιών Ι, Πρόχειρες σημειώσεις*. .
- [14] H. Fleischer and K. Thurow, “Automation Solutions for Analytical Measurements: Concepts and Applications.” [Online]. Available: https://books.google.gr/books?id=Mlw6DwAAQBAJ&pg=PA171&lpg=PA171&dq=gripper+fingers+for+microplate&source=bl&ots=WlkBUNulqG&sig=ACfU3U24QXQ_rKo_7Q8UWz5Uj_ikVcCC_A&hl=el&sa=X&ved=2ahUKEwiotebAyrLIAhVOecAKHQI1D_oQ6AEwEXoECAgQAQ#v=onepage&q=gripper+fingers+f. [Accessed: 23-Oct-2019].

- [15] "PTM-Präzisionstechnik." [Online]. Available: <http://www.ptm-automation.de/HomePTMPräzisionstechnik/OurCompany/Products/ServoGripperLaboratoryAutomation.aspx>.
- [16] "PatentSwarm." [Online]. Available: <https://patentswarm.com/patents/US7670555B2>.
- [17] P. Kosky, R. Balmer, W. Keat, and G. Wise, "Manufacturing Engineering," in *Exploring Engineering*, Elsevier, 2013, pp. 205–235.
- [18] V. Manthou and M. Vlachopoulou, "Agile Manufacturing Strategic Options," in *Agile Manufacturing: The 21st Century Competitive Strategy*, Elsevier, 2001, pp. 685–702.
- [19] T. Yang, B. A. Peters, and M. Tu, "Layout design for flexible manufacturing systems considering single-loop directional flow patterns," *Eur. J. Oper. Res.*, vol. 164, no. 2, pp. 440–455, Jul. 2005.
- [20] J. J. Craig, *Introduction to ROBOTICS mechanics and control*, 3rd ed. Pearson Education International, 2005.
- [21] B. Siciliano, L. Sciavicco, L. Villani, and G. Oriolo, *Robotics : modelling, planning and control*. Springer, 2009.
- [22] S. Chiaverini, B. Siciliano, and O. Egeland, "Review of the Damped Least-Squares Inverse Kinematics with Experiments on an Industrial Robot Manipulator," *IEEE Trans. Control Syst. Technol.*, vol. 2, no. 2, pp. 123–134, 1994.
- [23] R. Krasňanský, P. Valach, D. Soós, and J. Zorbakhsh, "Reference trajectory tracking for a multi-DOF robot arm," *Arch. Control Sci.*, vol. 25, no. 4, pp. 513–527, 2015.
- [24] D. Di Vito, C. Natale, and G. Antonelli, "A Comparison of Damped Least Squares Algorithms for Inverse Kinematics of Robot Manipulators," *IFAC-PapersOnLine*, vol. 50, no. 1, pp. 6869–6874, 2017.
- [25] X. Zhao, M. Wang, N. Liu, and Y. Tang, "Trajectory Planning for 6-DOF Robotic Arm Based on Quintic Polynormial," vol. 134, no. Caai, pp. 115–118, 2017.
- [26] C. Feng, G. Gao, and Y. Cao, "Kinematic modeling and verification for a SCARA robot," no. Icmemtc, pp. 918–921, 2016.
- [27] "ROS URDF." [Online]. Available: <https://wiki.ros.org/urdf>.

